ISSN 2307-8960 (online)

World Journal of *Clinical Cases*

World J Clin Cases 2023 November 26; 11(33): 7940-8093

Published by Baishideng Publishing Group Inc

World Journal of Clinical Cases

Contents Thrice Monthly Volume 11 Number 33 November 26, 2023

World Journal of Clinical Cases

Thrice Monthly Volume 11 Number 33 November 26, 2023

Contents

CASE REPORT

World Journal of Clinical Cases

Thrice Monthly Volume 11 Number 33 November 26, 2023

Contents

NAME OF JOURNAL
World Journal of Clinical Cases

ISSN
ISSN 2307-8960 (online)

LAUNCH DATE
April 16, 2013

FREQUENCY
Thrice Monthly

EDITORS-IN-CHIEF
Bao-Gan Peng, Salim Surani, Jerzy Tadeusz Chudek, George Kontogeorgos, Maurizio Serati

EDITORIAL BOARD MEMBERS
https://www.wjgnet.com/2307-8960/editorialboard.htm

PUBLICATION DATE
November 26, 2023

COPYRIGHT
© 2023 Baishideng Publishing Group Inc

INSTRUCTIONS TO AUTHORS
https://www.wjgnet.com/bpg/gerinfo/204

GUIDELINES FOR ETHICS DOCUMENTS
https://www.wjgnet.com/bpg/GerInfo/287

GUIDELINES FOR NON-NATIVE SPEAKERS OF ENGLISH
https://www.wjgnet.com/bpg/gerinfo/240

PUBLICATION ETHICS
https://www.wjgnet.com/bpg/GerInfo/288

PUBLICATION MISCONDUCT
https://www.wjgnet.com/bpg/gerinfo/208

ARTICLE PROCESSING CHARGE
https://www.wjgnet.com/bpg/gerinfo/242

STEPS FOR SUBMITTING MANUSCRIPTS
https://www.wjgnet.com/bpg/GerInfo/239

ONLINE SUBMISSION
https://www.f6publishing.com

© 2023 Baishideng Publishing Group Inc. All rights reserved. 7041 Koll Center Parkway, Suite 160, Pleasanton, CA 94566, USA
E-mail: bpgoffice@wjgnet.com https://www.wjgnet.com

World Journal of Clinical Cases

Submit a Manuscript: https://www.f6publishing.com

World J Clin Cases 2023 November 26; 11(33): 7940-7942

DOI: 10.12998/wjcc.v11.i33.7940

ISSN 2307-8960 (online)

EDITORIAL

Glimpse into the future of prosthodontics: The synergy of artificial intelligence

Artak Heboyan, Nazia Yazdanie, Naseer Ahmed

Specialty type: Medicine, research and experimental

Provenance and peer review: Invited article; Externally peer reviewed.

Peer-review model: Single blind

Peer-review report's scientific quality classification
Grade A (Excellent): 0
Grade B (Very good): 0
Grade C (Good): C
Grade D (Fair): 0
Grade E (Poor): 0

P-Reviewer: Corte-Real A, Portugal

Received: September 21, 2023
Peer-review started: September 21, 2023
First decision: October 24, 2023
Revised: October 26, 2023
Accepted: November 17, 2023
Article in press: November 17, 2023
Published online: November 26, 2023

Artak Heboyan, Department of Prosthodontics, Yerevan State Medical University after Mkhitar Heratsi, Yerevan 0025, Armenia

Nazia Yazdanie, Department of Prosthodontics, FMH College of Medicine and Dentistry, Lahore 54000, Pakistan

Naseer Ahmed, Department of Prosthodontics, Altammash Institute of Dental Medicine, Karachi 75500, Pakistan

Corresponding author: Artak Heboyan, DDS, MD, MSc, PhD, Associate Professor, Department of Prosthodontics, Yerevan State Medical University after Mkhitar Heratsi, No. 2 Koryun Street, Yerevan 0025, Armenia. heboyan.artak@gmail.com

Abstract

Prosthodontics, deals in the restoration and replacement of missing and structurally compromised teeth, this field has been remarkably transformed in the last two decades. Through the integration of digital imaging and three-dimensional printing, prosthodontics has evolved to provide more durable, precise, and patient-centric outcome. However, as we stand at the convergence of technology and healthcare, a new era is emerging, one that holds immense promise for the field and that is artificial intelligence (AI). In this paper, we explored the fascinating challenges and prospects associated with the future of prosthodontics in the era of AI.

Key Words: Artificial intelligence; Prosthodontics; Treatment planning; Patient-centric care; Three-dimensional printing

©The Author(s) 2023. Published by Baishideng Publishing Group Inc. All rights reserved.

Core Tip: Prosthodontics and artificial intelligence working together will raise the standard of dental care in the twenty-first century and improve the quality of life for many people who require dental replacements.

Citation: Heboyan A, Yazdanie N, Ahmed N. Glimpse into the future of prosthodontics: The synergy of artificial intelligence. *World J Clin Cases* 2023; 11(33): 7940-7942
URL: https://www.wjgnet.com/2307-8960/full/v11/i33/7940.htm
DOI: https://dx.doi.org/10.12998/wjcc.v11.i33.7940

INTRODUCTION

Artificial intelligence (AI) has transformed diagnoses in healthcare, including the prosthodontics field[1-3]. Machine learning (ML) algorithms can evaluate exponential patient data, such as patient interviews, radiographs, and intraoral scans to detect oral diseases early with a high accuracy[4]. AI can help prosthodontists discover oral conditions earlier, allowing them to intervene rapidly and deliver highly effective treatments[5]. Furthermore, AI-powered treatment planning can improve decision-making in prosthodontic procedures. AI can offer customized treatment plans by analyzing patient-specific data, ensuring that prosthetic solutions are matched to the individual needs. This improves not just patient satisfaction but also treatment efficacy[3,6].

While AI generally involves the application of advanced algorithms and ML technologies to complete tasks that would typically require human intelligence. ML in medicine particularly refers to the use of algorithms that can acquire information from data to improve performance on a certain task. This maybe acquired from huge datasets involve teaching models, patient histories or medical photographs to recognize configurations and associations that would be challenging for individuals to distinguish. ML can be applied for a variety of healthcare applications including treatment outcomes prediction, patients' possible medical conditions identification, or treatment plans optimization[7,8].

The future of prosthodontics will be characterized by a shift towards greater customization[2]. AI algorithms can analyze a patient's unique oral anatomy and recommend the most suitable materials, designs, and manufacturing techniques for prosthetic devices. This level of personalization ensures that patients receive prostheses that fit seamlessly, enhancing comfort and functionality[9]. Furthermore, the integration of AI with three-dimensional printing technology allows for the rapid fabrication of complex dental prosthesis. This combination enables the fabrication of precise crowns, bridges and dentures. As a result, prosthodontists would provide rapid, cost-effective, and aesthetically acceptable solutions to their patients[10].

The chatbots and virtual assistants driven by AI are already revolutionizing patient interaction in healthcare. These technologies in prosthodontics can give patients with information, support, and appointment reminders. AI-powered tele-prosthodontics services can offer remote consultations and follow-ups, increasing access to dental treatment for people living in distant or underserved areas[11,12]. Furthermore, AI can improve the patient experience by anticipating and resolving potential issues before they arise. Prosthodontists can offer pro-active interventions and recommendations by continuously monitoring and analyzing patient data, assuring the long-term success of prosthetic treatment[13].

While the future of prosthodontics with AI holds immense promise, it also presents several challenges and ethical considerations. Ensuring data privacy, security, and informed consent are crucial aspects of integrating AI into healthcare [14]. Taking into consideration that patient records are mostly confidential, there is an expected disagreement among organizations to exchange patients` medical data and personal information. AI systems raise some significant concerns regarding data safety and privacy. Since health-related data are significant and vulnerable, hackers sometimes can target them, thus, preserving the privacy of medical data is crucial. Patient informed consent is another key factor for data confidentiality since healthcare specialists may permit widespread usage of patient medical data for AI research without demanding patient consent[15,16]. Moreover, there is a need for rigorous training and education to equip prosthodontists with the skills required to harness the power of AI effectively.

Finally, there are possible threats to healthcare providers and humans connected to potential misuse of AI-systems. Limitations in the use of AI in dentistry may be related to lack of transparency and accountability as well as bias and discrimination. AI-based systems may be inadequate in their understanding of the context of human oral health and disease. Nowadays, job displacement is not a significant shortcoming of AI application in dentistry, especially for prosthodontics, but it is likely that some procedures could be replaced by AI devices. However, AI systems may not be available or affordable to all human beings and communities, which may lead to discriminations in access to healthcare [16,17].

CONCLUSION

AI will open up new possibilities for prosthodontics and take it into unexplored landscape. Dental prosthetic solutions will soon be more precise and available than ever due to AI-powered diagnostics, treatment planning, customization and patient-centered care. It is crucial to keep an eye out for emerging ethical and regulatory issues as we proceed along this transformational route. Prosthodontics and AI working together will raise the standard of dental care in the twenty-first century and improve the quality of life for many people who require dental replacement and rehabilitation.

FOOTNOTES

Author contributions: Heboyan A, Yazdanie N, and Ahmed N contributed to this paper; Yazdanie N and Ahmed N designed the overall concept and outline of the manuscript; Heboyan A contributed to the discussion and design of the manuscript; Heboyan A, Yazdanie N, and Ahmed N contributed to the writing, and editing the manuscript and review of literature.

Conflict-of-interest statement: The authors declare no conflict of interest.

Open-Access: This article is an open-access article that was selected by an in-house editor and fully peer-reviewed by external reviewers. It is distributed in accordance with the Creative Commons Attribution NonCommercial (CC BY-NC 4.0) license, which permits others to distribute, remix, adapt, build upon this work non-commercially, and license their derivative works on different terms, provided the original work is properly cited and the use is non-commercial. See: https://creativecommons.org/Licenses/by-nc/4.0/

Country/Territory of origin: Armenia

ORCID number: Artak Heboyan 0000-0001-8329-3205.

S-Editor: Qu XL
L-Editor: A
P-Editor: Qu XL

REFERENCES

1 **Fatima A**, Shafi I, Afzal H, Díez IT, Lourdes DRM, Breñosa J, Espinosa JCM, Ashraf I. Advancements in Dentistry with Artificial Intelligence: Current Clinical Applications and Future Perspectives. *Healthcare (Basel)* 2022; **10** [PMID: 36360529 DOI: 10.3390/healthcare10112188]
2 **Chadha U**, Abrol A, Vora NP, Tiwari A, Shanker SK, Selvaraj SK. Performance evaluation of 3D printing technologies: a review, recent advances, current challenges, and future directions. *Progress in Additive Manufacturing* 2022 [DOI: 10.1007/s40964-021-00257-4]
3 **Ritushree T**, Dhaded S, Konin P. Future of prosthodontics together with artificial intelligence and robotics. *Guident* 2022; 16
4 **Zhang X**, Liang Y, Li W, Liu C, Gu D, Sun W, Miao L. Development and evaluation of deep learning for screening dental caries from oral photographs. *Oral Dis* 2022; **28**: 173-181 [PMID: 33244805 DOI: 10.1111/odi.13735]
5 **Singi SR**, Sathe S, Reche AR, Sibal A, Mantri N. Extended Arm of Precision in Prosthodontics: Artificial Intelligence. *Cureus* 2022; **14**: e30962 [PMID: 36465202 DOI: 10.7759/cureus.30962]
6 **Chau RCW**, Chong M, Thu KM, Chu NSP, Koohi-Moghadam M, Hsung RT, McGrath C, Lam WYH. Artificial intelligence-designed single molar dental prostheses: A protocol of prospective experimental study. *PLoS One* 2022; **17**: e0268535 [PMID: 35653388 DOI: 10.1371/journal.pone.0268535]
7 **Marino R**, Uribe S, Chen R, Schwendicke F, Giraudeau N, Scheerman J. Terminology of e-Oral Health: Consensus Report of the IADR's e-Oral Health Network Terminology Task Force. 2023 Preprint [DOI: 10.21203/rs.3.rs-2802188/v1]
8 **Mohammad-Rahimi H**, Rokhshad R, Bencharit S, Krois J, Schwendicke F. Deep learning: A primer for dentists and dental researchers. *J Dent* 2023; **130**: 104430 [PMID: 36682721 DOI: 10.1016/j.jdent.2023.104430]
9 **Alammar A**, Kois JC, Revilla-León M, Att W. Additive Manufacturing Technologies: Current Status and Future Perspectives. *J Prosthodont* 2022; **31**: 4-12 [PMID: 35313022 DOI: 10.1111/jopr.13477]
10 **Rokaya D**, Kongkiatkamon S, Heboyan A, Dam VV, Amornvit P, Khurshid Z, Srimaneepong V, Zafar MS. 3D-Printed Biomaterials in Biomedical Application. *Functional biomaterials: Drug delivery and biomedical applications* 2022; 319-339 [DOI: 10.1007/978-981-16-7152-4_12]
11 **Mariño R**, Ghanim A. Definition of Teledentistry, e-Health Care in Dentistry and Oral Medicine: A Clinician's Guide. 2018; 3-14
12 **Chen YW**, Stanley K, Att W. Artificial intelligence in dentistry: current applications and future perspectives. *Quintessence Int* 2020; **51**: 248-257 [PMID: 32020135 DOI: 10.3290/j.qi.a43952]
13 **Khan B**, Fatima H, Qureshi A, Kumar S, Hanan A, Hussain J, Abdullah S. Drawbacks of Artificial Intelligence and Their Potential Solutions in the Healthcare Sector. *Biomed Mater Devices* 2023; 1-8 [PMID: 36785697 DOI: 10.1007/s44174-023-00063-2]
14 **Kim CS**, Samaniego CS, Sousa Melo SL, Brachvogel WA, Baskaran K, Rulli D. Artificial intelligence (A.I.) in dental curricula: Ethics and responsible integration. *J Dent Educ* 2023 [PMID: 37489621 DOI: 10.1002/jdd.13337]
15 **Schwendicke F**, Büttner M. Artificial intelligence: advances and pitfalls. *Br Dent J* 2023; **234**: 749-750 [PMID: 37237204 DOI: 10.1038/s41415-023-5855-0]
16 **Ayad N**, Schwendicke F, Krois J, van den Bosch S, Bergé S, Bohner L, Hanisch M, Vinayahalingam S. Patients' perspectives on the use of artificial intelligence in dentistry: a regional survey. *Head Face Med* 2023; **19**: 23 [PMID: 37349791 DOI: 10.1186/s13005-023-00368-z]
17 **Kelly CJ**, Karthikesalingam A, Suleyman M, Corrado G, King D. Key challenges for delivering clinical impact with artificial intelligence. *BMC Med* 2019 [DOI: 10.1186/s12916-019-1426-2]

World Journal of Clinical Cases

Submit a Manuscript: https://www.f6publishing.com

World J Clin Cases 2023 November 26; 11(33): 7943-7950

DOI: 10.12998/wjcc.v11.i33.7943

ISSN 2307-8960 (online)

MINIREVIEWS

Application progress of nursing intervention in cardiac surgery

Si-Ru Wang, Ke Zhou, Wei Zhang

Specialty type: Medicine, research and experimental

Provenance and peer review: Unsolicited article; Externally peer reviewed.

Peer-review model: Single blind

Peer-review report's scientific quality classification

Grade A (Excellent): 0
Grade B (Very good): B
Grade C (Good): C
Grade D (Fair): 0
Grade E (Poor): 0

P-Reviewer: Leker RR, Israel; Lerner A, Israel

Received: September 7, 2023
Peer-review started: September 7, 2023
First decision: September 20, 2023
Revised: September 27, 2023
Accepted: November 16, 2023
Article in press: November 16, 2023
Published online: November 26, 2023

Si-Ru Wang, Wei Zhang, Department of Nursing, Shengjing Hospital of China Medical University, Shenyang 110004, Liaoning Province, China

Ke Zhou, Department of Cardiac Surgery, Shengjing Hospital of China Medical University, Shenyang 110004, Liaoning Province, China

Corresponding author: Wei Zhang, RN, Nurse, Department of Nursing, Shengjing Hospital of China Medical University, No. 36 Sanhao Street, Heping District, Shenyang 110004, Liaoning Province, China. m18940256213@163.com

Abstract

As a stressor, cardiac surgery affects the physiology and psychology of patients, as well as their postoperative recovery. Patients tend to worry about cognitive deficiency, pain, discomfort, the risk of death, sleep, complications, and other factors, resulting in stress and anxiety. Moreover, serious adverse events, such as circulatory and respiratory dysfunction and infection, tend to occur after cardiac surgery and increase the economic burden on patients. Therefore, appropriate nursing interventions should be selected to strengthen patients' cognitive levels, compliance, and postoperative practices to accelerate their recovery, reduce complications, and shorten hospital stays so as to contribute to patients' lives and health.

Key Words: Cardiac surgery; Nursing intervention; Rehabilitation; Nursing

©The Author(s) 2023. Published by Baishideng Publishing Group Inc. All rights reserved.

Core Tip: Surgery can extend the life of patients with heart diseases (such as congenital and coronary heart diseases) and improve their quality of life. However, it can trigger emotional, cognitive, and physiological responses in patients, leading to fear and anxiety regarding mortality and even depression. Through nursing interventions, we can strengthen patients' cognitive abilities, compliance, and postoperative recovery, thereby reducing complications, shortening hospital stays, and providing importance for patients' overall health and well-being.

Citation: Wang SR, Zhou K, Zhang W. Application progress of nursing intervention in cardiac surgery. *World J Clin Cases* 2023; 11(33): 7943-7950
URL: https://www.wjgnet.com/2307-8960/full/v11/i33/7943.htm
DOI: https://dx.doi.org/10.12998/wjcc.v11.i33.7943

INTRODUCTION

Cardiovascular disease (CVD) is the world's deadliest disease. According to a report by the World Health Organization, more than 23 million people will die of CVD every year by 2030. This situation is not optimistic, and surgical treatment plays an important role in prolonging and improving the quality of life of patients with heart disease[1,2]. Cardiac surgery is often used to treat valvular heart disease, congenital heart disease, coronary heart disease, and other heart diseases. It is characterized by complicated steps, high risk, great difficulty, and a lengthy postoperative recovery period [3], all of which can cause emotional, cognitive, and physiological reactions. Patients undergoing surgery often experience anxiety and even depression from fears regarding permanent disability, loss of physical control, loss of the ability to work, pain, loss of sexual ability, the inability to awaken from anesthesia, and death[2,4-6]. One study reported that 34% of patients undergoing cardiac surgery experienced preoperative anxiety, 24.7% experienced postoperative anxiety, and 16.5% experienced both preoperative and postoperative anxiety[7].

Postoperative complications can easily occur, with an incidence rate ranging from 15% to 30%. Possible complications include the following: Stroke, renal failure, prolonged intubation time, sternal wound infection[8,9], and postoperative pulmonary infections (*e.g.*, atelectasis, pleural effusion, pneumonia, pulmonary edema, cardiogenic pulmonary edema, acute respiratory distress syndrome, pulmonary embolism, phrenic nerve injury, pneumothorax, and mediastinitis)[10]. In view of the serious nature of cardiac surgery, the study objective was to summarize applicable preoperative, intraoperative, postoperative, and perioperative nursing intervention methods to provide a reference for clinical practice. The information conveyed is vitally important for improving the health and quality of life of patients (Figure 1).

PREOPERATIVE NURSING

Predictive nursing

Postoperative pneumonia is one of the most common complications after cardiac surgery and it can increase the morbidity, mortality, and health care burden of patients. Bardia *et al*[11] guided 1125 patients undergoing cardiac surgery to use a chlorhexidine mouthwash before surgery and found that the risk of postoperative pneumonia was reduced by approximately half[11].

Individualized education

Individualized care is defined as reducing patients' anxiety according to their beliefs, values, emotions, thoughts, preferences, personal experiences, and opinions[12]. Ertürk and Ünlü[13] identified the source of anxiety in 300 patients undergoing cardiac surgery and provided preoperative individualized care for 30-90 min. They found that the main sources of preoperative anxiety were a lack of knowledge, distance from family, the risk of death, and pain. A total of 95.4% of patients were satisfied with the preoperative education, and they could quickly adapt to the intensive care unit (ICU) environment and perform guided breathing and coughing exercises following surgery.

Inspiratory muscle training

In their study, Chen *et al*[14] selected 197 patients over age 50 who had undergone cardiac surgery and received five days of respiratory muscle training before surgery. The results of the training showed that the postoperative respiratory muscle strength of these patients was substantially enhanced, and the incidence of postoperative pulmonary complications and a lengthy hospital stay were reduced[14].

Orientation tour

For their study, Niknejad *et al*[15] selected 70 patients scheduled for coronary artery bypass grafting. They learned about the procedure one day before surgery and were shown around the hospital for 40 min by an anesthesia technician, a nurse, and a researcher. The tour included a 10-min visit to an unattended operating room during the night shift, a 5-min visit to an ICU, a 10-min visit to an operating room to familiarize themselves with personnel who could answer questions about surgery, and a 15-min conversation with inpatients. Findings showed that the anxiety levels of the patients decreased after the orientation tour.

INTRAOPERATIVE NURSING

Plan-Do-Check-Act cycle intervention

The operating room is the most important place for patients, as it is the location where they undergo surgery. Owing to the variability and high risk of the work in this environment, operating rooms have higher requirements for nursing quality[16]. Du *et al*[17] adopted the Plan-Do-Check-Act (PDCA) cycle management method to continuously improve the quality of cardiac surgery preparation time by identifying the causes of illness, developing countermeasures, eliminating hidden dangers, and optimizing workflow to ensure smooth Surgeries.

Holistic nursing

Khajian Gelogahi *et al*[18] selected 80 patients undergoing coronary artery bypass surgery and provided each one with

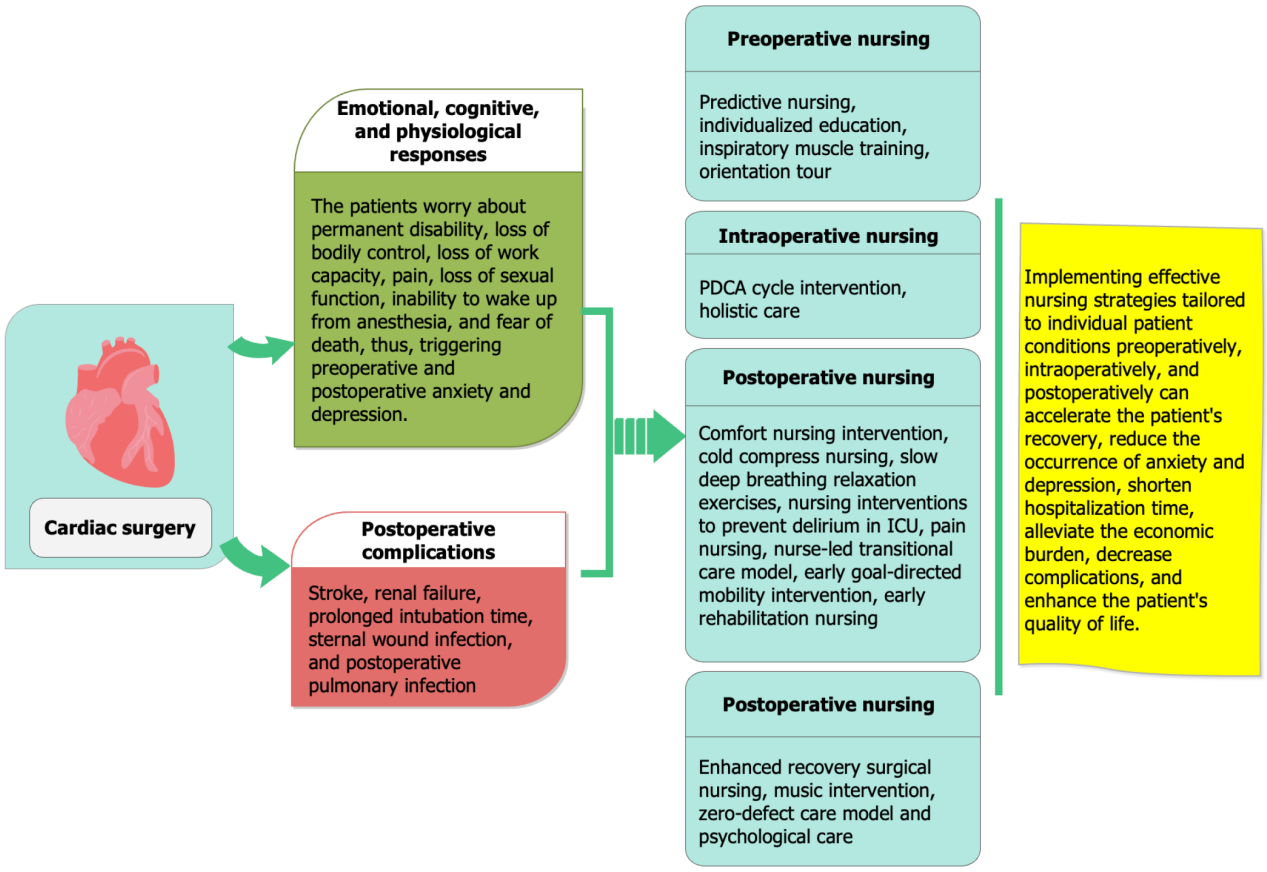

DOI: 10.12998/wjcc.v11.i33.7943 **Copyright** ©The Author(s) 2023.

Figure 1 Nursing intervention methods in cardiac surgery. ICU: Intensive care unit; PDCA: Plan-Do-Check-Act.

four 30- to 45-min individual sessions of intentional nursing presence during surgery. The results showed that conscious nursing arrangements were an effective way to relieve depression, stress, and anxiety in patients undergoing surgery.

POSTOPERATIVE NURSING

Comfort nursing intervention

Complications after cardiac surgery, such as pain, mental distress, and hemodynamic instability, have multiple negative effects on children and surgical outcomes. Comfort theory is a comprehensive, descriptive nursing theory that can be used as a guide for patients requiring holistic care. Nurses implement three levels of comfort measures (relief, ease, and transcendence) from four dimensions: Body, psychology, social culture, and the environment. Khaleghi *et al*[19] selected 60 infants aged 28 d to 2 years and collected demographic details, information regarding comfort behavior, hemodynamic parameters, and other data, and carried out a comfort nursing intervention. This approach can significantly improve a patient's postoperative pain, as well as respiration and heart rate.

Cold compress nursing

Chest tube placement is necessary in all types of cardiac surgery to maintain cardiopulmonary function and prevent pneumothorax, hemothorax, and pleural effusion. Generally, the tube should be removed within 24-48 h after cardiac surgery, but removal of the chest tube can cause patients to experience considerable pain. Mohammadi *et al*[20] used cold compresses to relieve the pain caused by chest tube removal after cardiac surgery and found that their use could significantly reduce the pain severity score. However, the effect was not significant 15 min after removal[20].

Slow deep breathing relaxation exercise

Jarrah *et al*[21] guided 25 patients undergoing coronary artery bypass transplantation to perform slow deep breathing relaxation exercises before chest tube extraction (after surgery) and found that their pain levels decreased significantly 5 and 15 min after extubation. Thus, slow deep breathing relaxation exercises can be used effectively to relieve pain during chest tube extubation and minimize related side effects and the need for analgesics.

Nursing interventions to prevent delirium in ICU

Postoperative delirium is a state of acute brain dysfunction following anesthesia and surgery[22]; it occurs in 25%-52% of patients undergoing cardiac surgery and is associated with increased mortality, a prolonged hospital stay, and long-term cognitive decline[23]. From a literature review, Pieri *et al*[24] concluded that the most commonly used strategies for preventing postoperative delirium are therapies involving dexmedetomidine, ketamine, antipsychotics, glucocorticoids, propofol, opioids, volatile anesthetics, local anesthetics, and remote ischemic preconditioning, among which dexmedetomidine is the most promising measure. The nUrsiNg DEliRium Preventive INterventions in the ICU (UNDERPIN-ICU) is a nurse-oriented intervention to prevent delirium developed for the main risk factors, such as visual and auditory disorders, sleep disorders, cognitive disorders, and activity disorders[25]. Song *et al*[26] established a delirium research group to develop UNDERPIN-ICU for cardiac surgery and trained nurses for two months to implement it with patients undergoing cardiac surgery. The results pointed to the effectiveness of this program in preventing or reducing the incidence of postoperative delirium following cardiac surgery and shortening the duration of mechanical ventilation and length of the ICU stay.

Pain nursing

Doğan and Saritaş[27] applied the new behavioral formation technique of neuro-linguistic programming (NLP) and the guided imagination relaxation technique using a 30-min audio CD for patients undergoing cardiac surgery. Consequently, the postoperative pain level of patients in the NLP group decreased significantly, and the comfort level of patients in the guided imagination group increased substantially. Luque Oliveros and Morilla Romero de la Osa[28] applied 0.5% bupivacaine to 69 patients in order to infiltrate their surgical wounds within 12 h after cardiac surgery, and the results showed that this practice could relieve pain considerably and effectively.

Nurse-led transitional care model

Coskun and Duygulu[29] adopted a nurse-led transitional care model to carry out a transitional nursing program nine weeks after 33 elderly patients were discharged following cardiac surgery. The authors found that the functional autonomous measurement system and quality of life scores of these patients improved significantly, and readmission and rehospitalization rates decreased substantially.

Early goal-directed therapy intervention

In Early goal-directed therapy (EGDT), a team of medical staff and rehabilitation technicians develops a humanized, feasible, and progressive rehabilitation plan for patients undergoing cardiac surgery. Lin *et al*[30] evaluated 60 cardiac surgery patients attended to by an EGDT team and formulated and implemented an accurate and effective personalized EGDT plan. They found that this method could shorten the indwelling time of endotracheal intubation and the length of stay in the ICU, reduce the occurrence of complications, and improve patient satisfaction[30].

Early rehabilitation nursing

Cardiac surgery is a risky and challenging procedure. The rapid recovery of motor function and mental health is challenging in the field of post-nursing care. Ge *et al*[31] searched cardiac surgery-related vocabulary through a database, extracted and summarized the evidence related to early postoperative rehabilitation exercise, and concluded that early cardiac rehabilitation should be implemented in a planned and procedural manner based on the concept of multidisciplinary team collaboration and nursing orientation. Further, psychological nursing and health education should be implemented throughout the entire rehabilitation training process[31]. Long *et al*[32] implemented rehabilitation process management for 127 patients who had undergone cardiac surgery. By establishing a rehabilitation nursing quality control group, they formulated and implemented a progressive graded activity process for patients in the early postoperative period and controlled for quality in the implementation process. The results showed that this method could improve the cognitive level of nurses' early related knowledge, increase the efficiency of team cooperation, accelerate the recovery of patients, and shorten the length of the hospital stay.

PERIOPERATIVE NURSING INTERVENTION

Enhanced recovery surgical nursing

Enhanced recovery after surgery (ERAS) is a multimodel, interdisciplinary nursing improvement program designed to promote the recovery of patients undergoing surgery throughout the perioperative period[33]. Interventions cover the entire surgical process, including preoperative, intraoperative, and postoperative periods[34]. The idea is that patients perform better when emotional and physical stress is minimized during surgery. The goal is to return them to normal functioning as soon as possible[35]. Li *et al*[36] selected 104 patients undergoing cardiac valve surgery for ERAS protocol optimization nursing, and the results showed that this method could reduce ICU and hospital stays, postoperative complications, and costs for cardiac surgery patients.

Music intervention

Kakar *et al*[37] conducted a database search for a review and meta-analysis of music intervention during cardiac surgery and found that it significantly reduced postoperative anxiety and pain during surgery. Furthermore, no side effects were observed.

The zero-defect nursing model and psychological nursing

The zero-defect nursing theory is a personalized and creative holistic nursing model based on zero defects, with the goal of minimizing patients' physical pain and psychological unhappiness. Nursing staff should receive professional training in zero-defect theoretical knowledge before carrying out nursing practices. Preoperative health education and psychological counseling for patients can improve their cognitive and psychological stress responses to surgery. Wang *et al*[38] adopted zero-defect and psychological nursing models to provide perioperative nursing care for 30 patients undergoing cardiac surgery and found that the operative time, intraoperative blood loss, and length of hospital stay decreased significantly. Moreover, the sleep quality and mental and psychological status of patients improved significantly, indicating clinical value.

CONCLUSION

Cardiac surgery is the most effective method for treating heart disease, especially valvular disease. However, patients' conditions are complicated, the operations are difficult, and many urgent conditions arise during surgery. In recent years, with the development of science and technology, the mortality rate of patients after cardiac surgery has declined. However, the surgical procedure still has a negative impact on patients' lives. Adverse effects include post-traumatic stress reactions, decreased postoperative activity, and a reduced quality of life. Most studies have focused on patients' postoperative health status and functional symptoms. An increasing number of studies have found that the disease burden, functional status, and psychological feelings of patients throughout the perioperative period affect postoperative rehabilitation. Therefore, reasonable and feasible treatment and nursing modes should be formulated according to a patient's status and psychological state to improve the treatment effect and promote recovery[39]. In summary (Table 1), effective nursing methods can be implemented before, during, and after surgery according to the individual situations of patients to accelerate their recovery, shorten the length of the hospital stay, reduce the economic burden and complications, and provide a reference for clinical practice.

Table 1 Approaches and outcomes of nursing for patients undergoing cardiac surgery

Item	Nursing approach	Nursing measures	Nursing outcomes
Preoperative nursing	Predictive nursing [11]	Guiding the patient to use Betadine mouthwash before surgery	Postoperative pneumonia risk reduced by approximately 50%
	Individualized education[12,13]	Providing individualized preoperative care for 30-90 min based on the patient's sources of anxiety	Patients quickly adapt to the ICU environment, with a satisfaction rate of 94% given for preoperative education
	Inspiratory muscle training[14]	Instructing the patient to undergo respiratory muscle training for 5 d	Marked improvement in postoperative respiratory muscle strength, reducing the incidence of complications and hospital stay
	Orientation tour[15]	One day before surgery, healthcare personnel visit the patient to explain the surgical process (15 min) and accompany them to visit an unattended operating room at night (10 min), the ICU (5 min), an operating room (10 min)	Decreased levels of anxiety
Intraoperative nursing	PDCA cycle intervention[16,17]	Using the PDCA cycle management method, continuous quality improvement is implemented in the preparation phrase for cardiac surgery by the methods of identifying the causes, formulating countermeasures, eliminating potential risks, optimizing workflow, and so on	Reduces the variability and risks of operating room work to ensure smooth surgical procedures
	Holistic care[18]	Four 30- to 45-min sessions of nursing intentional presence were conducted for each patient individually in the intervention group	Effectively reduce depression, stress, and anxiety in surgical patients
Postoperative nursing	Comfort nursing intervention[19]	Collecting demographic details, comfort behaviors, hemodynamic parameters, and other data and implementing comfort care interventions	Majorly improve indicators of postoperative pain, discomfort, respiration, and heart rate in pediatric patients
	Cold compress nursing[20]	Using cold compresses to alleviate pain caused by chest tube removal after cardiac surgery	Cold compress during chest tube removal significantly reduces the severity of pain scores, but the effect is not significant after 15 min of removal
	Slow, deep breathing relaxation exercises [21]	Instructing 25 patients undergoing coronary artery bypass graft surgery to perform slow deep breathing relaxation exercises before chest tube removal	Pain levels are significantly reduced at 5 min and 15 min after extubation
	Nursing interventions to prevent delirium in ICU[22-25]	Nurse-led preventive nursing interventions targeting patients with visual and auditory impairments, sleep disorders, cognitive impairments, and mobility impairments, among	Prevents postoperative delirium, reduces its incidence, and shortens mechanical ventilation time and ICU stay

		other major risk factors for delirium	
	Pain nursing[27,28]	Patients are provided with a 30-min continuous NLP technique and guided imagery relaxation technique using audio CDs to promote behavior formation. Additionally, 0.5% bupivacaine wound infiltration is administered within 12 h after surgery to alleviate pain	Comfort levels markedly improve, reducing postoperative pain and enhancing patient comfort in patients undergoing cardiac surgery
	Nurse-led transitional care model[29]	Transitional care is provided for 9 wk after patient discharge, to facilitate their gradual adjustment, along with provision of necessary support	The self-measurement system and quality of life scale scores both significantly improved, and readmission rates were significantly reduced
	EGDT	An EGDT team is established to develop personalized, feasible, and progressive rehabilitation plans for patients	EGDT can shorten the duration of endotracheal intubation and ICU stay for patients, reduce the occurrence of complications, and enhance patient satisfaction
	Early rehabilitation nursing[30]	A rehabilitation nursing quality control group is created to develop and implement postoperative early progressive graded activity protocols and ensure quality control throughout the implementation process	Early rehabilitation nursing has enhanced nurses' awareness of early interventions and improved team collaboration efficiency, which can accelerate patient recovery and shorten hospital stay
Perioperative nursing intervention	Enhanced recovery surgical nursing[31, 32]	A multimodal and interdisciplinary approach is implemented to optimize nursing care throughout the entire surgical process, including preoperative, intraoperative, and postoperative phases	Reduce ICU and hospital stay, postoperative complications, and costs for patients undergoing cardiac surgery
	Music intervention [37]	Music interventions are utilized for patients during the surgical procedure	Significantly reduce postoperative anxiety and pain in patients undergoing cardiac surgery without any side effects
	Zero-defect care model and psychological care[38]	Nursing staff undergo specialized training on the theory of zero defects to enhance their professional competence. They also provide preoperative health education and psychological counseling for patients	Significantly decrease surgical time, intraoperative bleeding, and hospital stay and improve sleep quality, mental well-being, and psychological condition

ICU: Intensive care unit; PDCA: Plan-Do-Check-Act; NLP: Neuro-linguistic programming; EGDT: Early goal-directed therapy.

FOOTNOTES

Author contributions: Wang SR proposed concept for review, collected data, wrote and revised the manuscript with critical revisions; Zhou K collected data, helped write manuscript; Zhang W edited the article, critical revision of the article, and final approval.

Conflict-of-interest statement: All the authors report no relevant conflicts of interest for this article.

Open-Access: This article is an open-access article that was selected by an in-house editor and fully peer-reviewed by external reviewers. It is distributed in accordance with the Creative Commons Attribution NonCommercial (CC BY-NC 4.0) license, which permits others to distribute, remix, adapt, build upon this work non-commercially, and license their derivative works on different terms, provided the original work is properly cited and the use is non-commercial. See: https://creativecommons.org/Licenses/by-nc/4.0/

Country/Territory of origin: China

ORCID number: Wei Zhang 0009-0005-5967-4936.

S-Editor: Fan JR
L-Editor: A
P-Editor: Zhang XD

REFERENCES

1 **Erdil F**, Elbaş NÖ. Surgical Nursing. 6th ed. Ankara: Tasarım Offset; 2012: 322–328
2 **Xue J**, Li J, Sun D, Sheng L, Gong Y, Wang D, Zhang S, Zou Y, Shi J, Xu W, An M, Dai C, Li W, Zheng L, Vinograd A, Liu G, Kong Y, Li Y. Functional Evaluation of Intermediate Coronary Lesions with Integrated Computed Tomography Angiography and Invasive Angiography in Patients with Stable Coronary Artery Disease. *J Transl Int Med* 2022; **10**: 255-263 [PMID: 36776233 DOI: 10.2478/jtim-2022-0018]
3 **Zhao J**. [Effect of continuous nursing on cardiac rehabilitation in patients with cardiac surgery]. *Dangdai Linchuang Yikan* 2022; **35**: 117-119
4 **Prado-Olivares J**, Chover-Sierra E. Preoperatory Anxiety in Patients Undergoing Cardiac Surgery. *Diseases* 2019; **7** [PMID: 31248177 DOI: 10.3390/diseases7020046]

5 **Guo P**, East L, Arthur A. A preoperative education intervention to reduce anxiety and improve recovery among Chinese cardiac patients: a randomized controlled trial. *Int J Nurs Stud* 2012; **49**: 129-137 [PMID: 21943828 DOI: 10.1016/j.ijnurstu.2011.08.008]

6 **Guo P**. Preoperative education interventions to reduce anxiety and improve recovery among cardiac surgery patients: a review of randomised controlled trials. *J Clin Nurs* 2015; **24**: 34-46 [PMID: 24894181 DOI: 10.1111/jocn.12618]

7 **Vencloviene J**, Beresnevaite M, Cerkauskaite S, Lopatiene K, Grizas V, Benetis R. The effects of weather on depressive symptoms in patients after cardiac surgery. *Psychol Health Med* 2023; **28**: 682-692 [PMID: 36203385 DOI: 10.1080/13548506.2022.2132411]

8 **Song X**, Wang H, Kashani KB, Wang C. Extracorporeal Membrane Oxygenation using a Modified Cardiopulmonary Bypass System. *J Transl Int Med* 2022; **10**: 175-177 [PMID: 35959450 DOI: 10.2478/jtim-2022-0015]

9 **Ball L**, Costantino F, Pelosi P. Postoperative complications of patients undergoing cardiac surgery. *Curr Opin Crit Care* 2016; **22**: 386-392 [PMID: 27309972 DOI: 10.1097/MCC.0000000000000319]

10 **Mali S**, Haghaninejad H. Pulmonary complications following cardiac surgery. *Arch Med Sci Atheroscler Dis* 2019; **4**: e280-e285 [PMID: 32368683 DOI: 10.5114/amsad.2019.91432]

11 **Bardia A**, Blitz D, Dai F, Hersey D, Jinadasa S, Tickoo M, Schonberger RB. Preoperative chlorhexidine mouthwash to reduce pneumonia after cardiac surgery: A systematic review and meta-analysis. *J Thorac Cardiovasc Surg* 2019; **158**: 1094-1100 [PMID: 30826096 DOI: 10.1016/j.jtcvs.2019.01.014]

12 **Suhonen R**, Leino-Kilpi H, Välimäki M. Development and psychometric properties of the Individualized Care Scale. *J Eval Clin Pract* 2005; **11**: 7-20 [PMID: 15660532 DOI: 10.1111/j.1365-2753.2003.00481.x]

13 **Ertürk EB**, Ünlü H. Effects of pre-operative individualized education on anxiety and pain severity in patients following open-heart surgery. *Int J Health Sci (Qassim)* 2018; **12**: 26-34 [PMID: 30022900]

14 **Chen X**, Hou L, Zhang Y, Liu X, Shao B, Yuan B, Li J, Li M, Cheng H, Teng L, Guo M, Wang Z, Chen T, Liu J, Liu Y, Liu Z, Guo Q. The effects of five days of intensive preoperative inspiratory muscle training on postoperative complications and outcome in patients having cardiac surgery: a randomized controlled trial. *Clin Rehabil* 2019; **33**: 913-922 [PMID: 30722696 DOI: 10.1177/0269215519828212]

15 **Niknejad R**, Mirmohammad-Sadeghi M, Akbari M, Ghadami A. Effects of an orientation tour on preoperative anxiety in candidates for coronary artery bypass grafting: A randomized clinical trial. *ARYA Atheroscler* 2019; **15**: 154-160 [PMID: 31819748 DOI: 10.22122/arya.v15i4.1806]

16 **Yao X**, Zhu H, Wang Y, Xiang Y, Chen Y. Study on the Effect of PDCA Circulation Method on Nursing Quality Management in the Day Operating Room. *Contrast Media Mol Imaging* 2022; **2022**: 3503095 [PMID: 35652037 DOI: 10.1155/2022/3503095]

17 **Du J**, Yang J, Sun S, Zhi H. [Application Effect of PDCA Cycle in Shortening Preparation Time Management in Compound Operating Room]. *Zhongwai Yixue Yanjiu* 2022; **20**: 169-173 [DOI: 10.14033/j.cnki.cfmr.2022.04.047]

18 **Khajian Gelogahi Z**, Aghebati N, Mazloum SR, Mohajer S. Effectiveness of Nurse's Intentional Presence as a Holistic Modality on Depression, Anxiety, and Stress of Cardiac Surgery Patients. *Holist Nurs Pract* 2018; **32**: 296-306 [PMID: 30320654 DOI: 10.1097/HNP.0000000000000294]

19 **Khaleghi M**, Fomani F, Hoseini A. The effect of the comfort care model on distress, pain, and hemodynamic parameters in infants after congenital heart defect surgery. *J Neonatal Nurs* 2022; **29**: 108-116 [DOI: 10.1016/j.jnn.2022.03.004]

20 **Mohammadi N**, Pooria A, Yarahmadi S, Tarrahi MJ, Najafizadeh H, Abbasi P, Moradi B. Effects of Cold Application on Chest Tube Removal Pain in Heart Surgery Patients. *Tanaffos* 2018; **17**: 29-36 [PMID: 30116276]

21 **Jarrah MI**, Hweidi IM, Al-Dolat SA, Alhawatmeh HN, Al-Obeisat SM, Hweidi LI, Hweidi AI, Alkouri OA. The effect of slow deep breathing relaxation exercise on pain levels during and post chest tube removal after coronary artery bypass graft surgery. *Int J Nurs Sci* 2022; **9**: 155-161 [PMID: 35509699 DOI: 10.1016/j.ijnss.2022.03.001]

22 **Pantzaris ND**, Platanaki C, Tsiotsios K, Koniari I, Velissaris D. The Use of Electroencephalography in Patients with Sepsis: a Review of The Literature. *J Transl Int Med* 2021; **9**: 12-16 [PMID: 33850796 DOI: 10.2478/jtim-2021-0007]

23 **Lopez MG**, Hughes CG, DeMatteo A, O'Neal JB, McNeil JB, Shotwell MS, Morse J, Petracek MR, Shah AS, Brown NJ, Billings FT 4th. Intraoperative Oxidative Damage and Delirium after Cardiac Surgery. *Anesthesiology* 2020; **132**: 551-561 [PMID: 31770146 DOI: 10.1097/ALN.0000000000003016]

24 **Pieri M**, De Simone A, Rose S, De Domenico P, Lembo R, Denaro G, Landoni G, Monaco F. Trials Focusing on Prevention and Treatment of Delirium After Cardiac Surgery: A systematic Review of Randomized Evidence. *J Cardiothorac Vasc Anesth* 2020; **34**: 1641-1654 [PMID: 31668634 DOI: 10.1053/j.jvca.2019.09.028]

25 **Wassenaar A**, Rood P, Schoonhoven L, Teerenstra S, Zegers M, Pickkers P, van den Boogaard M. The impact of nUrsiNg DEliRium Preventive INnterventions in the Intensive Care Unit (UNDERPIN-ICU): A study protocol for a multi-centre, stepped wedge randomized controlled trial. *Int J Nurs Stud* 2017; **68**: 1-8 [PMID: 28013104 DOI: 10.1016/j.ijnurstu.2016.11.018]

26 **Song Y**, Yang M, Ling Y, Lin Q. [Effects of nursing delirium preventive interventions in the intensive care unit on delirium management in patients after cardiac surgery]. *Zhongguo Huli Guanli* 2022; **22**: 507-511

27 **Doğan A**, Saritaş S. The effects of neuro-linguistic programming and guided imagery on the pain and comfort after open-heart surgery. *J Card Surg* 2021; **36**: 2389-2397 [PMID: 33760270 DOI: 10.1111/jocs.15505]

28 **Luque Oliveros M**, Morilla Romero de la Osa R. Bupivacaine infiltration for acute postoperative pain management after cardiac surgery. *Nurs Crit Care* 2022; **27**: 223-232 [PMID: 33641253 DOI: 10.1111/nicc.12614]

29 **Coskun S**, Duygulu S. The effects of Nurse Led Transitional Care Model on elderly patients undergoing open heart surgery: a randomized controlled trial. *Eur J Cardiovasc Nurs* 2022; **21**: 46-55 [PMID: 33821999 DOI: 10.1093/eurjcn/zvab005]

30 **Lin Y**, Li S, Xie B. [Nursing effect analysis of intervention based on early goal-directed activities in the rehabilitation of patients after cardiac surgery]. *Xinxueguanbing Fangzhi Zhishi* 2021; **11**: 82-84

31 **Ge W**, Liu F, Yao H. [Summary of best evidence on early rehabilitation exercise for patients after cardiac surgery]. *Hulixue Zazhi* 2021; **36**: 85-89

32 **Long H**, Yang J, Li S, Zhong X, Huang Z, Wu L. [Early rehabilitation nursing process management for ICU patients after cardiac surgery]. *Hulixue Zazhi* 2020; **35**: 1-4

33 **Ljungqvist O**, Scott M, Fearon KC. Enhanced Recovery After Surgery: A Review. *JAMA Surg* 2017; **152**: 292-298 [PMID: 28097305 DOI: 10.1001/jamasurg.2016.4952]

34 **Varadhan KK**, Lobo DN, Ljungqvist O. Enhanced recovery after surgery: the future of improving surgical care. *Crit Care Clin* 2010; **26**: 527-547, x [PMID: 20643305 DOI: 10.1016/j.ccc.2010.04.003]

35 **Salenger R**, Morton-Bailey V, Grant M, Gregory A, Williams JB, Engelman DT. Cardiac Enhanced Recovery After Surgery: A Guide to Team Building and Successful Implementation. *Semin Thorac Cardiovasc Surg* 2020; **32**: 187-196 [PMID: 32120008 DOI: 10.1053/j.semtcvs.2020.02.029]

36 **Li M**, Zhang J, Gan TJ, Qin G, Wang L, Zhu M, Zhang Z, Pan Y, Ye Z, Zhang F, Chen X, Lin G, Huang L, Luo W, Guo Q, Wang E. Enhanced recovery after surgery pathway for patients undergoing cardiac surgery: a randomized clinical trial. *Eur J Cardiothorac Surg* 2018; **54**: 491-497 [PMID: 29514224 DOI: 10.1093/ejcts/ezy100]

37 **Kakar E**, Billar RJ, van Rosmalen J, Klimek M, Takkenberg JJM, Jeekel J. Music intervention to relieve anxiety and pain in adults undergoing cardiac surgery: a systematic review and meta-analysis. *Open Heart* 2021; **8** [PMID: 33495383 DOI: 10.1136/openhrt-2020-001474]

38 **Wang H**, Zhao X, Liu L, Zhang L. [Application of zero defect nursing model and psychological nursing in operating room in the practice of heart surgery]. *Xinli Yuekan* 2020; **15**: 152-153

39 **Guo H**, Chen X, Zheng J. [Application progress of patient-reported outcomes assessment tools for patients undergoing cardiac surgery]. *Huli Yanjiu* 2021; **35**: 1027-1030

World Journal of Clinical Cases

Submit a Manuscript: https://www.f6publishing.com

World J Clin Cases 2023 November 26; 11(33): 7951-7964

DOI: 10.12998/wjcc.v11.i33.7951

ISSN 2307-8960 (online)

ORIGINAL ARTICLE

Retrospective Cohort Study

Comparison between multiple logistic regression and machine learning methods in prediction of abnormal thallium scans in type 2 diabetes

Chung-Chi Yang, Chung-Hsin Peng, Li-Ying Huang, Fang Yu Chen, Chun-Heng Kuo, Chung-Ze Wu, Te-Lin Hsia, Chung-Yu Lin

Specialty type: Endocrinology & metabolism

Provenance and peer review: Unsolicited article; Externally peer reviewed.

Peer-review model: Single blind

Peer-review report's scientific quality classification

Grade A (Excellent): 0
Grade B (Very good): 0
Grade C (Good): C, C
Grade D (Fair): 0
Grade E (Poor): 0

P-Reviewer: Zhang W, China; Surani S, United States

Received: August 4, 2023
Peer-review started: August 4, 2023
First decision: October 9, 2023
Revised: October 23, 2023
Accepted: November 13, 2023
Article in press: November 13, 2023
Published online: November 26, 2023

Chung-Chi Yang, Division of Cardiovascular Medicine, Taoyuan Armed Forces General Hospital, Taoyuan City 32551, Taiwan

Chung-Chi Yang, Division of Cardiovascular, Tri-service General Hospital, Taipei City 114202, Taiwan

Chung-Hsin Peng, Department of Urology, Cardinal Tien Hospital, New Taipei City 23148, Taiwan

Chung-Hsin Peng, School of Medicine, Fu-Jen Catholic University, New Taipei City 242062, Taiwan

Li-Ying Huang, Department of Internal Medicine, Department of Medical Education, School of Medicine, Fu Jen Catholic University Hospital, New Taipei City 243, Taiwan

Li-Ying Huang, Chun-Heng Kuo, School of Medicine, College of Medicine, Fu Jen Catholic University, New Taipei City 243, Taiwan

Fang Yu Chen, Department of Endocrinology, Fu Jen Catholic University Hospital, New Taipei City 243, Taiwan

Chun-Heng Kuo, Division of Endocrinology and Metabolism, Department of Internal Medicine, Fu Jen Catholic University Hospital, New Taipei City 243, Taiwan

Chung-Ze Wu, Division of Endocrinology, Shuang Ho Hospital, New Taipei City 23561, Taiwan

Chung-Ze Wu, School of Medicine, Taipei Medical University, Taipei City 11031, Taiwan

Te-Lin Hsia, Department of Internal Medicine, Cardinal Tien Hospital, New Taipei City 23148, Taiwan

Chung-Yu Lin, Department of Cardiology, Fu Jen Catholic University Hospital, New Taipei City 24352, Taiwan

Chung-Yu Lin, Graduate Institute of Business Administration, Fu Jen Catholic University, New Taipei City 242062, Taiwan

Corresponding author: Chung-Yu Lin, MD, Doctor, Department of Cardiology, Fu Jen Catholic University Hospital, No. 69 Guizi Road, Taishan District, New Taipei City 24352, Taiwan. a02076@mail.fjuh.fju.edu.tw

Abstract

BACKGROUND

The prevalence of type 2 diabetes (T2D) has been increasing dramatically in recent decades, and 47.5% of T2D patients will die of cardiovascular disease. Thallium-201 myocardial perfusion scan (MPS) is a precise and non-invasive method to detect coronary artery disease (CAD). Most previous studies used traditional logistic regression (LGR) to evaluate the risks for abnormal CAD. Rapidly developing machine learning (Mach-L) techniques could potentially outperform LGR in capturing non-linear relationships.

AIM

To aims were: (1) Compare the accuracy of Mach-L methods and LGR; and (2) Found the most important factors for abnormal TMPS.

METHODS

556 T2D were enrolled in the study (287 men and 269 women). Demographic and biochemistry data were used as independent variables and the sum of stressed score derived from MPS scan was the dependent variable. Subjects with a MPS score ≥ 9 were defined as abnormal. In addition to traditional LGR, classification and regression tree (CART), random forest, Naïve Bayes, and eXtreme gradient boosting were also applied. Sensitivity, specificity, accuracy and area under the receiver operation curve were used to evaluate the respective accuracy of LGR and Mach-L methods.

RESULTS

Except for CART, the other Mach-L methods outperformed LGR, with gender, body mass index, age, low-density lipoprotein cholesterol, glycated hemoglobin and smoking emerging as the most important factors to predict abnormal MPS.

CONCLUSION

Four Mach-L methods are found to outperform LGR in predicting abnormal TMPS in Chinese T2D, with the most important risk factors being gender, body mass index, age, low-density lipoprotein cholesterol, glycated hemoglobin and smoking.

Key Words: Myocardial perfusion scintigraphy; Machine learning; Type 2 diabetes; Thallium-201

©The Author(s) 2023. Published by Baishideng Publishing Group Inc. All rights reserved.

Core Tip: This is a retrospective study to use four machine learning methods to evaluate the impacts of demographic and biochemistry data to identify subjects with abnormal myocardial perfusion scan in Chinese type 2 diabetes. Our results showed that gender was the most important factor, followed by body mass index, age, LDL-cholesterol, glycated hemoglobin and smoking accordingly.

Citation: Yang CC, Peng CH, Huang LY, Chen FY, Kuo CH, Wu CZ, Hsia TL, Lin CY. Comparison between multiple logistic regression and machine learning methods in prediction of abnormal thallium scans in type 2 diabetes. *World J Clin Cases* 2023; 11(33): 7951-7964

URL: https://www.wjgnet.com/2307-8960/full/v11/i33/7951.htm

DOI: https://dx.doi.org/10.12998/wjcc.v11.i33.7951

INTRODUCTION

The International Diabetes Federation reported a global diabetic population of 415 million people in 2018 [of which 91% were type 2 diabetes (T2D)] and this is expected to increase to 642 million by 2040[1]. In Taiwan, the diabetic population rose from 8.5% in 2008 to 12.3% in 2015[2]. As of 2019, T2D treatment accounted for 4.4% of the entire budget for Taiwan's national health insurance program (equivalent to USD238 million), making it the second highest treatment category after dialysis[3]

Several micro- and macrovascular diseases are related to T2D, namely stroke, myocardial infarction, diabetic retinopathy, nephropathy and diabetic foot. According to World Health Organization, 50.3% of T2D patients die from cardiovascular diseases, and the disease typically shortens lifespans by 6 years[4,5]. Avogaro *et al*[6] reported that subjects

with T2D bear 70% higher risk for acute myocardial infarction and the risk for the first-time myocardial infarction is higher than 20% 10 years after the diagnosis of diabetes. Asian patients have even higher mortality rate than those in Western countries[7]. Thus, early detection of coronary artery disease (CAD) in these patients is of great importance.

Methods for diagnosing CAD including coronary angiography, computed tomography coronary angiography, exercise electrocardiogram and myocardial perfusion scintigraphy (MPS). While coronary angiography provides the most detailed information for artery stenosis, it is an invasive procedure and is unsuited for routine application in subjects with mild symptoms. Tomography coronary angiography is expensive and not covered by Taiwan's National Insurance Program, thus making it inappropriate for routine screening. Exercise electrocardiogram is relatively less expensive but requires a certain amount of treadmill exercise loading to increase the heart rate, making it inappropriate for patients already suffering from debility[8,9]. Lastly, MPS uses Thallium as a tracer to evaluate the perfusion of blood in myocardium. At the same time, dipyridamole is injected to increase the heart rate, thus allowing comparison between fast and slow heart rate. Giri *et al*[10] note MPS is widely used to reliably diagnose significant CAD and to stratify those at higher risk levels. Thus, MPS could also be used as a surrogate. Scholte *et al*[7] found that current smoker status, long duration of diabetes and high cholesterol/HDL ratio contribute to abnormal MPS. It should be noted that all the aforementioned studies used traditional multiple logistic regression (MLR) to analyze categorical data (i.e., the dependent variable).

Recently, artificial intelligence using machine learning (Mach-L) techniques have developed rapidly and are increasingly used in medical research. Mach-L is the use of computer algorithms that learn automatically without explicit programming through experience and data application[11]. Mach-L has emerged as a new mainstream modality for data analysis competitive with traditional MLR[12,13]. Since Mach-L could capture nonlinear relationships in the data and complex interactions among multiple predictors, it has the potential to outperform conventional logistic regression in disease prediction[14].

Our group previously explored the relationships between risks and MPS score in a group of T2D Chinese[15]. We applied traditional linear regression and treated the MPS score as the dependent variable. In the present study, we categorize subjects by MPS status (normal and abnormal) as a dependent variable, and compare the performance of traditional linear regression against multiple Mach-L methods for the first time, seeking to determine the relative importance of various risk factors.

MATERIALS AND METHODS

Subjects

This study recruited T2D patients, aged between 30 and 95 years old, who had undergone Thallium-201 MPS at Taiwan's Cardinal Tien Hospital from 1999 to 2008. All study subjects were anonymous, and informed consent was obtained prior to participation. The study proposal was reviewed and approved by the institutional review board of the Cardinal Tien Hospital (Approval No. CTH-102-2-5-024) before the study began. The diagnostic criteria for T2DM were based on the 2012 American Diabetes Association criteria[16]. A total of 928 T2DM patients were initially recruited. Following exclusions for various causes, the final sample included 556 T2D patients (287 men and 269 women). Figure 1 shows the flowchart for subject selection. Since the patients were randomly selected and they were relatively stable at the time of the study, the bias should be minimun.

The inclusion criteria of the study participants are: Age between 30-70 years old; Body mass index (BMI) between 20-30 kg/m^2; Without dialysis at the time of the study; Without major medical diseases such as myocardial infarction, stroke and diabetic foot.

BMI was calculated as body weight (kg)/height (m)^2. Systolic and diastolic blood pressure (SBP and DBP) were measured on the right arm of seated subjects using a standard mercury sphygmomanometer. Blood samples were drawn from the antecubital vein for biochemical analysis.

MPS

On the day of testing, patients fasted for 4 h and avoided dipyridamole, b-blockers, calcium channel blockers, long-acting nitrates, xanthine-containing medications, caffeinated beverages. Dipyridamole was infused intravenously over 4 minutes at a concentration of 0.56 mg/kg in 20 mL of normal saline (an infusion rate of 0.14 mg/kg/min), followed 3 to 4 min later by Th-201 administration. The scan was conducted 5 to 8 min after radiopharmaceutical administration (stress scan) and 3 h later (rest).

The myocardial region was classified into 17 parts, each of which was evaluated by nuclear medicine experts based on a 5-point scoring system as follows[17]: 0, normal; 1, slight decrease of tracer uptake; 2, moderate decrease of tracer uptake; 3, severe decrease of tracer uptake; 4, absence of tracer uptake. The stress score and rest score of single vessels was initially counted into individual vessel scores. The sums of individual vessel stress scores (after injection of dipyridamole) were recognized as the presentative of the MPS results since some studies have shown that SSS provides important information to detect CAD and its outcome[18-20]. In the present study, an SSS score ≥ 9 was considered to be abnormal[21].

Laboratory evaluation

Following 10 h overnight fast, blood specimens were collected from each subject for further analysis. Plasma was separated from the whole blood within one hour and stored at -70 °C. A glucose oxidase method (YSI 203 glucose analyzer; Scientific Division, Yellow Springs Instruments, Yellow Springs, OH, United States) was used to determine

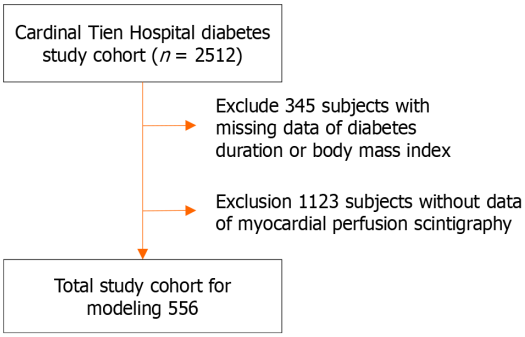

DOI: 10.12998/wjcc.v11.i33.7951 **Copyright** ©The Author(s) 2023.

Figure 1 Flowchart of sample selection from the Cardinal Tien Hospital Diabetes Study Cohort.

fasting plasma glucose levels. The dry, multilayer analytical slide method in the Fuji Dri-Chem 3000 analyzer (Fuji Photo Film, Minato-Ku, Tokyo, Japan) was used to determine total cholesterol and triglyceride (TG) levels. An enzymatic cholesterol assay following dextran sulfate precipitation was used to determine serum high density lipoprotein (HDL-C) and low-density lipoprotein cholesterol (LDL-C) levels. The HbA1c level was measured using the Bio-Rad Variant II automatic analyzer (Bio-Rad Diagnostic Group, Los Angeles, CA, United States). Plasma insulin was assayed using a commercial solid phase radioimmunoassay technique (Coat-A-Count insulin kit, Diagnostic Products Corporation, Los Angeles, CA, United States) with intra- and inter-assay coefficients of variance of 3.3% and 2.5%, respectively.

Statistical analysis

The data were tested for normal distribution using the Kolmogorov–Smirnov test and for homogeneity of variances using the Levene's test. Continuous variables were expressed as mean ± standard deviation.

Tables 1 and 2 lists the seventeen clinical variables (independent variables) used in this study: Sex, age, smoking, BMI, duration of diabetes, SBP, DBP, hemoglobin (Hb), TG, glycated hemoglobin (GA), HDL-C, LDL-C, homeostasis assessment insulin resistance (HOMA-IR), homeostasis assessment insulin secretion (HOMA-IS). As previously mentioned, the SSS derived from the Th-201 scan is the dependent variable, while the remaining 15 variables are used as predictor variables.

Machine learning methods and proposed scheme

The following methods were designed and published by our group in another recent study[22]. This research proposed a scheme based on four Mach-L methods, namely classification and regression tree (CART), random forest (RF), eXtreme gradient boosting (XGBoost) and naïve Byes (NB) to construct predictive models for determining abnormal MPS, and to identify the importance of these risk factors. These Mach-L methods have been widely applied in various healthcare and/or medical informatics applications and do not have prior assumptions about data distributions[23-31]. MLR is a used as a benchmark for comparison.

For the first method, CART is a tree structure method[32] composed of root nodes, branches, and leaf nodes based the recursive growth of trees from root nodes, splitting at each node based on the Gini index to produce branches and leaf nodes. A pruning node is applied to overgrown trees to produce optimal tree size by using a cost-complexity criterion, finally generating different decision rules to compose a complete tree structure[33,34].

RF is an ensemble learning decision tree algorithm that combines bootstrap resampling and bagging[35]. RF randomly generates many different and unpruned CART decision trees in which the decrease Gini impurity is regarded as the splitting criterion, and combining all generating trees into a forest. All the trees in the forest are then averaged or voted to generate output probabilities and a robust final model[36].

NB's Classifier is widely used for classification tasks. This algorithm can sort objects according to specific characteristics and variables based on the Bayes theorem. It calculates the probability of hypotheses on presumed groups[37].

XGBoost is a gradient boosting technique based on the stochastic gradient boosting method optimized extension[38]. It sequentially trains and integrates many weak models using the gradient boosting method of outputs, thus improving prediction performance. The Taylor binomial expansion is used to approximate the objective function and determine arbitrary differentiable loss functions to accelerate model construction and convergence[39]. XGBoost then applies a regularized boosting technique to penalize model complexity and correct overfitting, thereby increasing model accuracy [38].

Figure 2 presents a flowchart of the proposed scheme combining the four Mach-L methods. The proposed scheme first collects patients to prepare the dataset for model construction. The dataset is then randomly split into a training dataset for model building (80%) and a testing dataset (20%) for out of sample testing. In the training process, each Mach-L method has its own hyperparameters to be tuned to construct a model with relatively good performance. We use a 10-fold cross-validation technique for hyperparameter tuning, in which the training dataset was randomly divided into a training dataset to build the model with different sets of hyperparameters and a validation dataset. All possible combinations of hyperparameters were investigated by grid search. The model with the highest accuracy, sensitivity, specificity and area under the receiver operation characteristic curve (AUROC) on the validation dataset was viewed as the best model for each Mach-L method. The turned best model CART, RF, XGBoost and NB are generated and the corresponding

Table 1 Participant demographics

Variables	mean ± SD	*N*
Age	67.38 ± 9.69	556
Body mass index	26.16 ± 3.9	556
Duration of diabetes	13.69 ± 7.94	556
Systolic blood pressure	131.14 ± 15.42	493
Diastolic blood pressure	73.32 ± 10.15	493
Hemoglobin	12.92 ± 1.68	444
Triglyceride	153.74 ± 45.85	539
Glycated hemoglobin	7.79 ± 1.36	538
High density lipoprotein cholesterol	122.65 ± 74.34	535
Low density lipoprotein cholesterol	49.65 ± 14.75	498
Alanine aminotransferase	23.87 ± 13.94	537
Creatinine	1.16 ± 1	536
Microalbumin creatinine ratio	194.18 ± 733.73	526
Homeostasis assessment-insulin resistance	0.63 ± 0.34	366
Homeostasis assessment-insulin secretion	1.71 ± 0.37	366

Table 2 Participant demographics – sex, smoking and sum stressed score

	N (%)	*N*
Sex		556
0	287 (51.62)	
1	269 (48.38)	
Smoking		310
0	202 (65.16)	
1	108 (34.84)	
Sum stressed score		556
0	180 (32.37)	
1	376 (67.63)	

variable impact rankings can be obtained.

To provide a more robust comparison, the training and testing process mentioned above is randomly repeated 10 times, taking the average accuracy, sensitivity, specificity and AUROC values of the Mach-L methods as the performance benchmark for the MLR model using the same training and testing dataset as that used for the Mach-L methods. A Mach-L model with a higher AUROC is considered to be the convincing model.

All the Mach-L methods used can produce an impact ranking of each predictor variable, and these rankings may differ among the various Mach-L methods due to differences in their modeling characteristics. We therefore integrated the variable importance rankings of the convincing Mach-L models to enhance model stability and integrity in terms of the relative risk factor impacts. Below we summarize and discuss our significant findings about convincing Mach-L models and the related impact factors.

According to the proposed scheme, for modeling effective RF, stellate ganglion block (SGB), NB, and XGBoost models, use 10-fold cross-validation hyperparameters of each method are tuned and evaluated. The MLR method without hyperparameter tuning, the baseline method, was constructed by using the proposed scheme. The values of hyperparameters which generate the best RF, SGB, NB, and XGBoost models are listed in the following (Table 3).

All methods used R software version 4.0.5 and RStudio version 1.1.453 with the required packages installed (http://www.R-project.org; https://www.rstudio.com/products/rstudio/). The implementations of RF, NB, CART, and XGBoost are respectively "randomForest" R package version 4.6-14[40], "gbm" R package version 2.1.8[41], "rpart" R package version 4.1-15[42], and "XGBoost" R package version 1.5.0.2.[43]. To optimize the hyperparameter set for the developed CART, RF, NB, XGBoost methods, the "caret" R package version 6.0-90 was used[44]. The MLR was

Table 3 Summary of the values of the hyperparameters for the best random forest, classification and regression tree, Naïve Byer's classifier, eXtreme gradient boosting

Methods	Hyperparameters	Best value	Meaning
RF	Mtry	8	The number of random features used in each tree
	Ntree	500	The number of trees in forest
CART	Minispilt	20	The minimum number of observations required to attempt a split in a node
	Minibucket	7	The minimum number of observations in a terminal node
	Maxdepth	10	The maximum depth of any node in the final tree
	Xval	10	Number of cross-validations
	Cp	0.03588	Complexity parameter: The minimum improvement required in the model at each node
XGBoost	Nrounds	100	The number of tree model iterations
	Max_depth	3	The maximum depth of a tree
	Eta	0.4	Shrinkage coefficient of tree
	Gamma	0	The minimum loss reduction
	Subsample	0.75	Subsample ratio of columns when building each tree
	Colsample_bytree	0.8	Subsample ratio of columns when constructing each tree
	Rate_drop	0.5	Rate of trees dropped
	Skip_drop	0.05	Probability of skipping the dropout procedure during a boosting iteration
	Min_child_weight	1	The minimum sum of instance weight
NB	Fl	0	Adjustment of Laplace smoother
	Usekernel	TRUE	Using kernel density estimate for continuous variable versus a Gaussian density estimate
	Adjust	1	Adjust the bandwidth of the kernel density

CART: Classification and regression tree; RF: random forest; XGBoost: eXtreme gradient boosting; NB: Naïve Byes.

implemented using the "stats" R package version 4.0.5 using the default settings for model construction.

RESULTS

Tables 1 and 2 summarizes the demographic data of the T2D subjects. Table 4 compares the conventional MLR and four Mach-L methods in terms of accuracy in identifying abnormal MPS. We find that, aside from CART, the other three Mach-L methods outperformed MLR in terms of AUROC performance, suggesting that these three methods are more reliable and accurate than traditional MLR.

The average ranking of each factor created by Mach-L is shown in Table 5. The different Mach-L methods generated different variable impact rankings for each risk factor. The impact ranking is obtained by averaging the variable impact. Note that a darker blue color indicates greater relative importance of a particular risk factor. To identify the overall predictive power of each parameter from all three Mach-L methods, the mean ranking of each risk factor is obtained by averaging the ranking values of each variable in each method.

Figure 3 graphically depicts the orders of risk factors importance. The top 6 risk factors in predicting abnormal MPS scan are sex, BMI, age, LDL-C, GH and smoking.

Finally, Figure 4 shows the AUROC of the LGR and Mach-L. Since CART has poor AUROC results, this method was not included in the analysis.

DISCUSSION

Three out of the four Mach-L methods outperformed multiple logistic regression in identifying abnormal MPS. Also, the most important risk factors for abnormal MPS in T2D Chinese are (in descending order) sex, BMI, age, LDL-C, GH and smoking.

Table 4 The average performance of the LR, random forest, stellate ganglion block, classification and regression tree, and eXtreme gradient boosting methods

	Accuracy	Sensitivity	Specificity	AUC
LGR	0.685 ± 0.072	0.687 ± 0.152	0.683 ± 0.114	0.703 ± 0.057
CART	0.541 ± 0.074	0.546 ± 0.078	0.529 ± 0.670	0.540 ± 0.070
RF	0.707 ± 0.047	0.711 ± 0.100	0.678 ± 0.099	0.707 ± 0.037
XGBoost	0.712 ± 0.072	0.727 ± 0.139	0.674 ± 0.088	0.719 ± 0.062
NB	0.692 ± 0.059	0.702 ± 0.116	0.669 ± 0.090	0.704 ± 0.056

AUC: Area under the curve; LGR: Logistic regression; CART: Classification and regression tree; RF: Random forest; XGBoost: eXtreme gradient boosting; NB: Naïve Byes.

Table 5 The variable importance and rank of the importance of the risk factors derived from machine learning methods

Variables	RF	XGBoost	NB	Average	Rank
Sex	100.0 ± 0	100.0 ± 0	100.0 ± 0	100.0	1.0
Body mass index	54.2 ± 6.6	61.1 ± 14.7	86.2 ± 6.8	67.1	2.0
Age	13.1 ± 7.6	78.3 ± 13.2	67.9 ± 6.5	53.1	3.0
Low density lipoprotein cholesterol	30.4 ± 3.1	8.4 ± 12.8	71.0 ± 7.8	36.6	4.0
Glycated hemoglobin	15.4 ± 5.9	12.8 ± 11.9	48.0 ± 8.3	25.4	5.0
Smoking	12.2 ± 2.7	28.8 ± 9.2	34.5 ± 6.6	25.2	6.0
Creatinine	10.1 ± 2.3	5.3 ± 9.12	53.1 ± 7.3	22.8	7.0
Duration	6.3 ± 4.61	41.5 ± 8.6	10.1 ± 8.9	19.3	8.0
Hemoglobin	8.0 ± 4.16	16.6 ± 8.9	17.0 ± 5.7	13.8	9.0
Blood urine nitrogen	9.0 ± 8.15	6.5 ± 6.79	17.3 ± 9.6	11.0	10.0
Systolic blood pressure	4.2 ± 1.03	21.6 ± 5.1	6.4 ± 2.88	10.7	11.0
Triglyceride	5.4 ± 17.5	15.0 ± 4.4	11.1 ± 12.3	10.5	12.0
Microalbumin	4.3 ± 2.23	3.6 ± 3.83	22.7 ± 6.9	10.2	13.0
Diastolic blood pressure	2.5 ± 5.91	18.9 ± 3.7	5.6 ± 9.33	9.0	14.0
Alainine aminotransferase	3.2 ± 5.96	6.9 ± 3.90	13.0 ± 12.6	7.7	15.0
High density lipoprotein cholesterol	1.3 ± 3.60	9.8 ± 3.29	7.3 ± 8.41	6.1	16.0
HOMA-IR	5.7 ± 2.85	2.2 ± 2.52	10.2 ± 8.1	6.0	17.0
HOMA-B	4.3 ± 2.22	0.0 ± 0.00	7.4 ± 8.831	3.9	18.0

The most important sixth rank. RF: Random forest; XGBoost: eXtreme gradient boosting; NB: Naïve Byes; HOMA-IR: Homeostasis assessment insulin resistance; HOMA-B: homeostasis model assessment of beta-cell function.

Our results suggest that gender is the most important factor selected by Mach-L. However, the role of gender on CAD is still under debate. Zafrir *et al*[45] and Miller *et al*[46] found that men are at greater than women for higher risk of abnormal MPS. Among Chinese subjects, a similar finding was also reported that diabetic men are more prone to CAD than women[47]. However, opposite findings have been reported by Wu *et al*[48] reporting that menopausal women had higher SSS than men of the same age, but their study was based on a relatively small sample of 94 T2D. Both Prior *et al*[49] and Scholte *et al*[7] also found that gender had no impact on MPS score, but these were also based on relatively small samples (133 and 120, respectively). This inconsistency may be due to the sample size, or differences in age and ethnicity of the sample populations. In the present study, sex was identified as the most important variable using three different Mach-L methods, and we believe that gender does play an important role in CAD.

BMI is the second most important factor on MPS score. It is not surprising that T2D patients with higher BMI would have increased susceptibility of CAD[50]. Katzel *et al*[51] also reported that subjects with higher BMI are more prone to having myocardial ischemia detected by MPS and treadmill exercise test (OR=91.7, 95%CI = 1.075-999). However, their study was done on non-diabetic subjects. The impact of BMI on CAD could easily be explained by the derangements

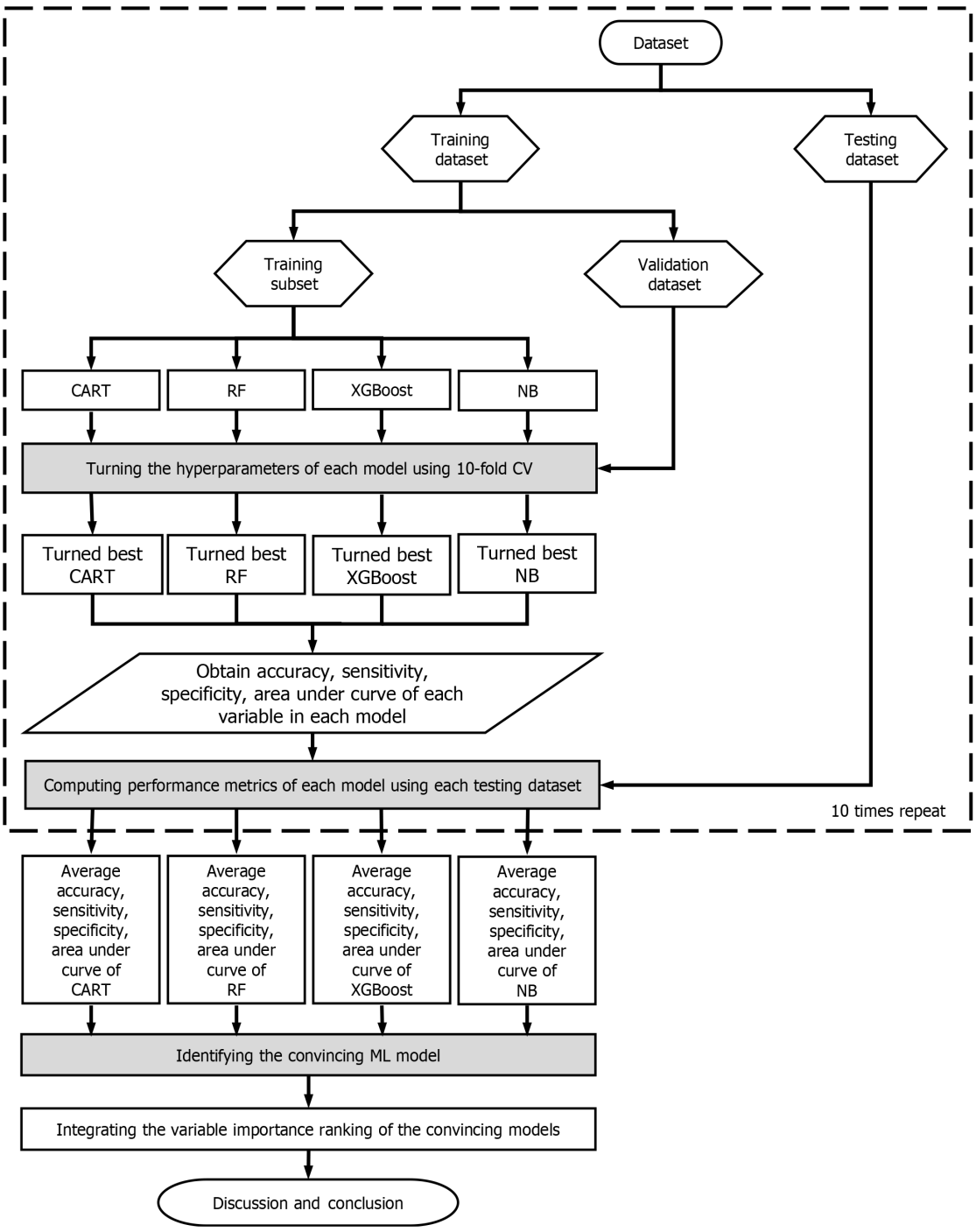

DOI: 10.12998/wjcc.v11.i33.7951 **Copyright** ©The Author(s) 2023.

Figure 2 Proposed scheme for four machine learning methods. CART: Classification and regression tree; RF: random forest; XGBoost: eXtreme gradient boosting; NB: Naïve Byes.

directly induced by obesity itself[52]. Obesity is also the underlying pathophysiology for other metabolic alterations such as hyperglycemia, hypertriglyceridemia, low high density lipoprotein cholesterol, inflammation, hypercoagulation, endothelial dysfunction and oxidative stress. All these factors are well-known contributors to CAD[53]. It is well-known that obesity is also an important contributor for insulin resistance. But in the present study, HOMA-IR was not selected as an important contributor. This interesting finding could be explained by the tight relationship between BMI and CAD. In other words, the significance of the relationship between HOMA-IR and MPS is 'diluted' by the influence of BMI[53]. This finding suggests BMI plays a crucial role in determining the likelihood of developing CAD.

Age is strongly correlated with the occurrence of CAD. Budoff *et al*[54] used the engine proposed by United Kingdom Prospective Study to calculate the CAD in a 7-year longitudinal study of 1087 T2D patients. Another study in Finland followed a much larger cohort (14786 subjects) for 7 years, also finding that total cholesterol level, BP, BMI and diabetes could explain a 30% increase in coronary heart disease in men and 50% in women. Thus, this correlation is confirmed in both Indians and Caucasians, and the present study confirms it in ethnic Chinese. This finding is unsurprising given that

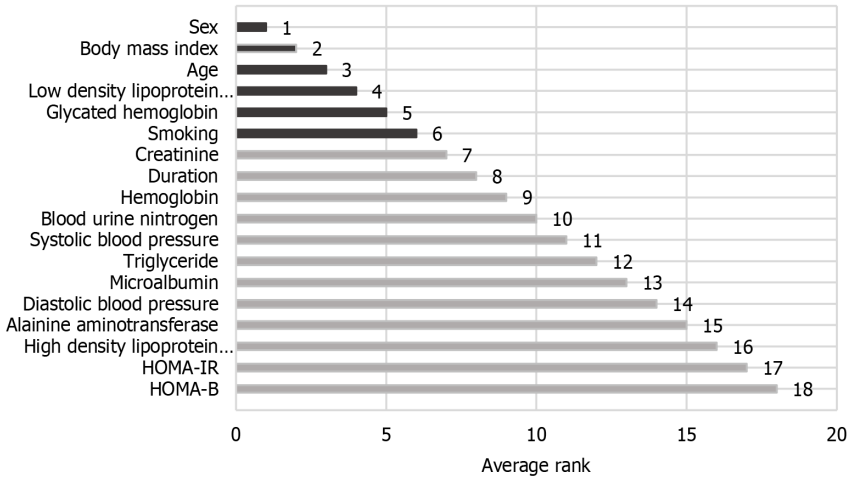

DOI: 10.12998/wjcc.v11.i33.7951 **Copyright** ©The Author(s) 2023.

Figure 3 Integrated importance ranking of all risk factors.

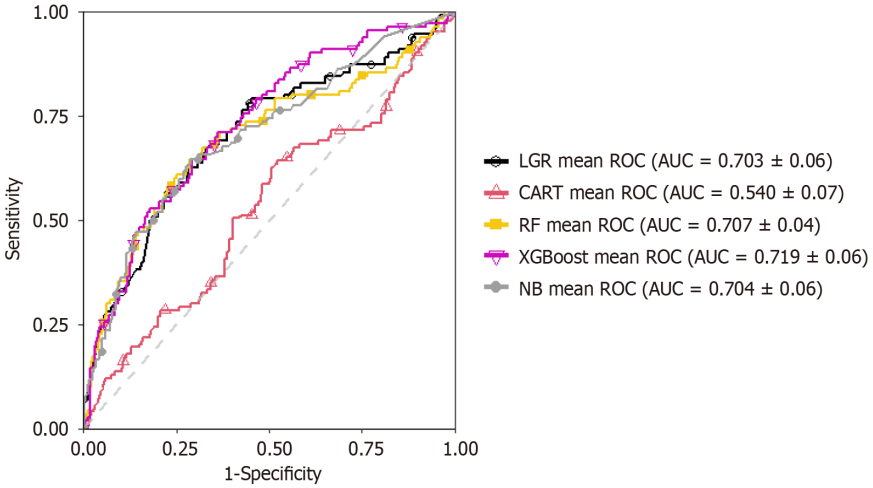

DOI: 10.12998/wjcc.v11.i33.7951 **Copyright** ©The Author(s) 2023.

Figure 4 Receiver operation curve of logistic regression and other four different machine learning methods. LGR: Logistic regression; CART: Classification and regression tree; RF: Random forest; XGBoost: eXtreme gradient boosting; NB: Naïve Byes.

aging causes hypertrophy of left ventricle, arrythmia, ischemic tissue, fibrosis of cardiac muscle and the appearance of apoptotic/necrotic cells[55].

According to the results of United Kingdom Prospective Diabetes Study, LDL-C was one of the many risk factors for CAD[56]. Our results show that LDL-C is the fourth most important factor. Similar to the previously discussed factors, the role of LDL-C on the CAD has long been recognized. As early as 2001, the Third Report of the National Cholesterol Education Program, Expert Panel on Detection, Evaluation, and Treatment of High Blood Cholesterol in Adults published guidelines for the diagnosis and treatment of dyslipidemia[57]. In this version, LDL-C was suggested as the most important factor for future occurrence of coronary heart disease. Colantonio *et al*[58] studied 370763 subjects in three different cohorts, finding that the hazard ratio and 95% confidence interval for having coronary heart disease in the highest *vs* lowest LDL-C level (≥ 146 mg/dL *vs* ≤ 102 mg/dL) ranged from 1.89 (1.42–2.51) to 1.25 (0.81–1.92). Hosokawa *et al*[59] showed that reducing total cholesterol in patients with either angina or old myocardial infarction by 22% resulted in myocardial perfusion improvement detectable by MPS. However, this study only included there were only 40 participants enrolled (15 patients, 25 controls). The mechanisms for LDL-C to increase CAD were comprehensively explained: The most crucial steps for artherosclerosis are the retention and accumulation of LDL-C and ApoB lipoprotein in the intima of coronary artery which leads to the appearance of plaque[60-62]. This is because these two particles are both smaller than 70 nm in diameters[62,63]. Interestingly, plaque formation is also dose-dependent to the LDL-C concentration[64].

To our knowledge, the earliest large cohort study exploring the relationship between glucose control and risks for CAD was UKPDS 33, published in 1998. This study included 3867 T2D patients, followed up for 20 years, and found that despite a 16% decrease of myocardial infarction in the intensive control group, the result did not reach the level of statistical significance[65]. However, at the end of 30 years, the same cohort was followed up again, finding a significant

15% decrease of myocardial infarction. This is the famous 'legacy effect' of the glucose control. Other large-scale studies followed the UKPDS. For instance, the Intensive Blood Glucose Control and Vascular Outcomes in Patients with Type 2 Diabetes (ADVANCE) study enrolled 11140 T2D patients and verified a significant decrease in combined major macrovascular disease[66]. The results of the present study are consistent with these cornerstone studies. The conjunctions between hyperglycemia and CAD are multi-faceted and include increased oxidative stress, advanced glycation end products and protein kinases C signaling. All these derangements lead to endothelial dysfunction of the coronary artery[67].

As early as in 1960, the Framingham Heart Study pointed out that smoking increases the risk for CAD[68], and also affects CAD severity and development pattern[69]. Smoking damages the epithelium of the coronary artery through oxidation of LDL-C, nicotine effects, increased sympathetic tone and myocardial necrosis[70-74]. Our findings are similar to those of other major studies but shows smoking at the sixth most important factor.

While our study verifies the most important factors for abnormal MPS using Mach-L methods which is naïve and informative, the present work is still subject to certain limitations. First, this is a cross-sectional study which is less convincing that a longitudinal one. Secondly, our sample size is smaller than several other previous works. However, since MPS is an expensive tool for detecting coronary artery perfusion, to increase the number of participants would be practically difficult. In the same time, by using four Mach-L methods, the bias could be reduced. Further longitudinal studies with larger samples are needed to further consolidate the present findings.

CONCLUSION

Three machine learning methods are found to outperform traditional logistic regression in predicting abnormal MPS in T2D Chinese subjects, with the most important risk factors identified (in descending order) as gender, BMI, age, LDL-C, GH and smoking.

ARTICLE HIGHLIGHTS

Research background

The prevalence of type 2 diabetes (T2D) has been increasing dramatically in recent decades, and 47.5% of T2D patients will die of cardiovascular disease. Thallium-201 myocardial perfusion scan (MPS) is a precise and non-invasive method to detect coronary artery disease (CAD). Most previous studies used traditional logistic regression (LGR) to evaluate the risks for abnormal CAD. Rapidly developing machine learning (Mach-L) techniques could potentially outperform LGR in capturing non-linear relationships.

Research motivation

To compare the accuracy of LGR and Mach-L. To rank importance of risk factors for abnormal TMPS scan.

Research objectives

The present study enrolled 556 T2D patients, using four different Mach-L methods to analyze risk factors for abnormal MPS. Our goals are: (1) To compare the accuracy of LGR and Mach-L; and (2) To rank importance of risk factors for abnormal TMPS scan.

Research methods

556 T2D were enrolled in the study (287 men and 269 women). Demographic and biochemistry data were used as independent variables and the sum of stressed score derived from MPS scan was the dependent variable. Subjects with a MPS score ≥ 9 were defined as abnormal. In addition to traditional LGR, classification and regression tree (CART), random forest, Naïve Bayes, and eXtreme gradient boosting were also applied. Sensitivity, specificity, accuracy and area under the receiver operation curve were used to evaluate the respective accuracy of LGR and Mach-L methods.

Research results

Except for CART, the other Mach-L methods outperformed LGR, with gender, body mass index, age, LDL-cholesterol, glycated hemoglobin and smoking emerging as the most important factors to predict abnormal MPS.

Research conclusions

Four Mach-L methods are found to outperform LGR in predicting abnormal TMPS in Chinese T2D, with the most important risk factors being gender, body mass index, age, LDL-cholesterol, glycated hemoglobin and smoking.

Research perspectives

Mach-L methods outperformed LGR in this kind of study. Body mass index, age, LDL-cholesterol, glycated hemoglobin and smoking were most relevant to abnormal MPS.

FOOTNOTES

Author contributions: Yang CC, Lin CY designed the research study; Huang LY, Chen FY and Hsia TL performed the research; Kuo CH and Wu CZ contributed new reagents and analytic tools; Yang CC, Peng CH and Lin CY analyzed the data and wrote the manuscript; All authors have read and approve the final manuscript.

Institutional review board statement: The study was reviewed and approved by the Cardinal Tien Hospital Institutional Review Board (Approval No. CTH-102-2-5-024).

Informed consent statement: Since this is a retrospective cohort study and we collected our data from the medical records of the hospital. Therefore, no informed consent was needed. This was approved by the IRB of the hospital.

Conflict-of-interest statement: There is no conflict of Interest in the current study.

Data sharing statement: The datasets generated and/or analyzed during the current study are not publicly available because they include other valuable information which could be used to produce additional papers, but are available from the corresponding author on reasonable request.

STROBE statement: The authors have read the STROBE Statement—checklist of items, and the manuscript was prepared and revised according to the STROBE Statement—checklist of items.

Open-Access: This article is an open-access article that was selected by an in-house editor and fully peer-reviewed by external reviewers. It is distributed in accordance with the Creative Commons Attribution NonCommercial (CC BY-NC 4.0) license, which permits others to distribute, remix, adapt, build upon this work non-commercially, and license their derivative works on different terms, provided the original work is properly cited and the use is non-commercial. See: https://creativecommons.org/Licenses/by-nc/4.0/

Country/Territory of origin: Taiwan

ORCID number: Chung-Chi Yang 0009-0000-8271-2885; Chung-Hsin Peng 0000-0002-7080-2602; Li-Ying Huang 0000-0002-0593-6428; Fang Yu Chen 0000-0002-5590-2744; Chun-Heng Kuo 0000-0001-7673-3567; Chung-Ze Wu 0000-0001-6118-6070; Te-Lin Hsia 0009-0000-9822-1570; Chung-Yu Lin 0009-0003-1209-3603.

S-Editor: Liu JH
L-Editor: A
P-Editor: Zhao S

REFERENCES

1 International Diabetes Federation. idf diabetes atlas. 7th ed. Brussels: International Diabetes Federation; 2015
2 **Health Promotion Administration**, Ministry of Health and Welfare Statistical Yearbook of Health Promotion. [(accessed on 17 February 2020)];2015 Available from: https://www.hpa.gov.tw/Pages/Detail.aspx?nodeid=268&pid=8535
3 **National Health Insurance Administration**. Statistics of Medical Care, National Health Insurance; 2020. Available from: https://www.nhi.gov.tw/Content_List.aspx?n=86ACD5A48FA3B1A1&topn=23C660CAACAA159D
4 **Federation ID**. IDF Diabetes Atlas. 7th edn. 2015 2017 [cited 2017]. Available from: www.idf.org/diabetesatlas
5 **Morrish NJ**, Wang SL, Stevens LK, Fuller JH, Keen H. Mortality and causes of death in the WHO Multinational Study of Vascular Disease in Diabetes. *Diabetologia* 2001; **44** Suppl 2: S14-S21 [PMID: 11587045 DOI: 10.1007/pl00002934]
6 **Avogaro A**, Bonora E, Consoli A, Del Prato S, Genovese S, Giorgino F. Glucose-lowering therapy and cardiovascular outcomes in patients with type 2 diabetes mellitus and acute coronary syndrome. *Diab Vasc Dis Res* 2019; **16**: 399-414 [PMID: 31044622 DOI: 10.1177/1479164119845612]
7 **Scholte AJ**, Schuijf JD, Kharagjitsingh AV, Dibbets-Schneider P, Stokkel MP, van der Wall EE, Bax JJ. Prevalence and predictors of an abnormal stress myocardial perfusion study in asymptomatic patients with type 2 diabetes mellitus. *Eur J Nucl Med Mol Imaging* 2009; **36**: 567-575 [PMID: 18985347 DOI: 10.1007/s00259-008-0967-y]
8 **Mark DB**, Hlatky MA, Harrell FE Jr, Lee KL, Califf RM, Pryor DB. Exercise treadmill score for predicting prognosis in coronary artery disease. *Ann Intern Med* 1987; **106**: 793-800 [PMID: 3579066 DOI: 10.7326/0003-4819-106-6-793]
9 **Mark DB**, Shaw L, Harrell FE Jr, Hlatky MA, Lee KL, Bengtson JR, McCants CB, Califf RM, Pryor DB. Prognostic value of a treadmill exercise score in outpatients with suspected coronary artery disease. *N Engl J Med* 1991; **325**: 849-853 [PMID: 1875969 DOI: 10.1056/NEJM199109193251204]
10 **Giri S**, Shaw LJ, Murthy DR, Travin MI, Miller DD, Hachamovitch R, Borges-Neto S, Berman DS, Waters DD, Heller GV. Impact of diabetes on the risk stratification using stress single-photon emission computed tomography myocardial perfusion imaging in patients with symptoms suggestive of coronary artery disease. *Circulation* 2002; **105**: 32-40 [PMID: 11772873 DOI: 10.1161/hc5001.100528]
11 **Koopaie M**, Ghafourian M, Manifar S, Younespour S, Davoudi M, Kolahdooz S, Shirkhoda M. Evaluation of CSTB and DMBT1 expression in saliva of gastric cancer patients and controls. *BMC Cancer* 2022; **22**: 473 [PMID: 35488257 DOI: 10.1186/s12885-022-09570-9]
12 **Wang C**, Li Y, Tsuboshita Y, Sakurai T, Goto T, Yamaguchi H, Yamashita Y, Sekiguchi A, Tachimori H; Alzheimer's Disease Neuroimaging Initiative. A high-generalizability machine learning framework for predicting the progression of Alzheimer's disease using limited data. *NPJ Digit Med* 2022; **5**: 43 [PMID: 35414651 DOI: 10.1038/s41746-022-00577-x]
13 **Xu S**, Arnetz JE, Arnetz BB. Applying machine learning to explore the association between biological stress and near misses in emergency

medicine residents. *PLoS One* 2022; **17**: e0264957 [PMID: 35259166 DOI: 10.1371/journal.pone.0264957]
14 **Lin Z**, Chou WC, Cheng YH, He C, Monteiro-Riviere NA, Riviere JE. Predicting Nanoparticle Delivery to Tumors Using Machine Learning and Artificial Intelligence Approaches. *Int J Nanomedicine* 2022; **17**: 1365-1379 [PMID: 35360005 DOI: 10.2147/IJN.S344208]
15 **Lin JD**, Pei D, Chen FY, Wu CZ, Lu CH, Huang LY, Kuo CH, Kuo SW, Chen YL. Comparison between Machine Learning and Multiple Linear Regression to Identify Abnormal Thallium Myocardial Perfusion Scan in Chinese Type 2 Diabetes. *Diagnostics (Basel)* 2022; **12** [PMID: 35885524 DOI: 10.3390/diagnostics12071619]
16 **Mitchell TM**. Machine Learning; New York McGraw Hill: New York, NY, USA, 1997
17 **Saquib N**, Saquib J, Ahmed T, Khanam MA, Cullen MR. Cardiovascular diseases and type 2 diabetes in Bangladesh: a systematic review and meta-analysis of studies between 1995 and 2010. *BMC Public Health* 2012; **12**: 434 [PMID: 22694854 DOI: 10.1186/1471-2458-12-434]
18 **Ye Y**, Xiong Y, Zhou Q, Wu J, Li X, Xiao X. Comparison of Machine Learning Methods and Conventional Logistic Regressions for Predicting Gestational Diabetes Using Routine Clinical Data: A Retrospective Cohort Study. *J Diabetes Res* 2020; **2020**: 4168340 [PMID: 32626780 DOI: 10.1155/2020/4168340]
19 **Marateb HR**, Mansourian M, Faghihimani E, Amini M, Farina D. A hybrid intelligent system for diagnosing microalbuminuria in type 2 diabetes patients without having to measure urinary albumin. *Comput Biol Med* 2014; **45**: 34-42 [PMID: 24480161 DOI: 10.1016/j.compbiomed.2013.11.006]
20 **Nusinovici S**, Tham YC, Chak Yan MY, Wei Ting DS, Li J, Sabanayagam C, Wong TY, Cheng CY. Logistic regression was as good as machine learning for predicting major chronic diseases. *J Clin Epidemiol* 2020; **122**: 56-69 [PMID: 32169597 DOI: 10.1016/j.jclinepi.2020.03.002]
21 2006 Astellas Pharma US, Inc. ADS10257 9/06
22 **Wu CZ**, Huang LY, Chen FY, Kuo CH, Yeih DF. Using Machine Learning to Predict Abnormal Carotid Intima-Media Thickness in Type 2 Diabetes. *Diagnostics (Basel)* 2023; **13** [PMID: 37296685 DOI: 10.3390/diagnostics13111834]
23 **Miller DD**, Brown EW. Artificial Intelligence in Medical Practice: The Question to the Answer? *Am J Med* 2018; **131**: 129-133 [PMID: 29126825 DOI: 10.1016/j.amjmed.2017.10.035]
24 Introduction: The American Diabetes Association's (ADA) evidence-based practice guidelines, standards, and related recommendations and documents for diabetes care. *Diabetes Care* 2012; **35** Suppl 1: S1-S2 [PMID: 22187466 DOI: 10.2337/dc12-s001]
25 **Hachamovitch R**, Berman DS, Shaw LJ, Kiat H, Cohen I, Cabico JA, Friedman J, Diamond GA. Incremental prognostic value of myocardial perfusion single photon emission computed tomography for the prediction of cardiac death: differential stratification for risk of cardiac death and myocardial infarction. *Circulation* 1998; **97**: 535-543 [PMID: 9494023 DOI: 10.1161/01.cir.97.6.535]
26 **Gimelli A**, Rossi G, Landi P, Marzullo P, Iervasi G, L'abbate A, Rovai D. Stress/Rest Myocardial Perfusion Abnormalities by Gated SPECT: Still the Best Predictor of Cardiac Events in Stable Ischemic Heart Disease. *J Nucl Med* 2009; **50**: 546-553 [PMID: 19289433 DOI: 10.2967/jnumed.108.055954]
27 **Nakajima K**, Yamasaki Y, Kusuoka H, Izumi T, Kashiwagi A, Kawamori R, Shimamoto K, Yamada N, Nishimura T. Cardiovascular events in Japanese asymptomatic patients with type 2 diabetes: a 1-year interim report of a J-ACCESS 2 investigation using myocardial perfusion imaging. *Eur J Nucl Med Mol Imaging* 2009; **36**: 2049-2057 [PMID: 19593560 DOI: 10.1007/s00259-009-1207-9]
28 **Tseng CJ**, Lu CJ, Chang CC, Chen GD, Cheewakriangkrai C. Integration of data mining classification techniques and ensemble learning to identify risk factors and diagnose ovarian cancer recurrence. *Artif Intell Med* 2017; **78**: 47-54 [PMID: 28764872 DOI: 10.1016/j.artmed.2017.06.003]
29 **Shih CC**, Lu CJ, Chen GD, Chang CC. Risk Prediction for Early Chronic Kidney Disease: Results from an Adult Health Examination Program of 19,270 Individuals. *Int J Environ Res Public Health* 2020; **17** [PMID: 32664271 DOI: 10.3390/ijerph17144973]
30 **Chang CC**, Chen SH. Developing a Novel Machine Learning-Based Classification Scheme for Predicting SPCs in Breast Cancer Survivors. *Front Genet* 2019; **10**: 848 [PMID: 31620166 DOI: 10.3389/fgene.2019.00848]
31 **Lee TS**, Chen IF, Chang TJ, Lu CJ. Forecasting Weekly Influenza Outpatient Visits Using a Two-Dimensional Hierarchical Decision Tree Scheme. *Int J Environ Res Public Health* 2020; **17** [PMID: 32630311 DOI: 10.3390/ijerph17134743]
32 **Chang CC**, Yeh JH, Chen YM, Jhou MJ, Lu CJ. Clinical Predictors of Prolonged Hospital Stay in Patients with Myasthenia Gravis: A Study Using Machine Learning Algorithms. *J Clin Med* 2021; **10** [PMID: 34640412 DOI: 10.3390/jcm10194393]
33 **Chiu YL**, Jhou MJ, Lee TS, Lu CJ, Chen MS. Health Data-Driven Machine Learning Algorithms Applied to Risk Indicators Assessment for Chronic Kidney Disease. *Risk Manag Healthc Policy* 2021; **14**: 4401-4412 [PMID: 34737657 DOI: 10.2147/RMHP.S319405]
34 **Wu CW**, Shen HL, Lu CJ, Chen SH, Chen HY. Comparison of Different Machine Learning Classifiers for Glaucoma Diagnosis Based on Spectralis OCT. *Diagnostics (Basel)* 2021; **11** [PMID: 34574059 DOI: 10.3390/diagnostics11091718]
35 **Wu TE**, Chen HA, Jhou MJ, Chen YN, Chang TJ, Lu CJ. Evaluating the Effect of Topical Atropine Use for Myopia Control on Intraocular Pressure by Using Machine Learning. *J Clin Med* 2020; **10** [PMID: 33396943 DOI: 10.3390/jcm10010111]
36 **Chang CC**, Yeh JH, Chiu HC, Chen YM, Jhou MJ, Liu TC, Lu CJ. Utilization of Decision Tree Algorithms for Supporting the Prediction of Intensive Care Unit Admission of Myasthenia Gravis: A Machine Learning-Based Approach. *J Pers Med* 2022; **12** [PMID: 35055347 DOI: 10.3390/jpm12010032]
37 **Huang YC**, Cheng YC, Jhou MJ, Chen M, Lu CJ. Important Risk Factors in Patients with Nonvalvular Atrial Fibrillation Taking Dabigatran Using Integrated Machine Learning Scheme-A Post Hoc Analysis. *J Pers Med* 2022; **12** [PMID: 35629177 DOI: 10.3390/jpm12050756]
38 **Tierney NJ**, Harden FA, Harden MJ, Mengersen KL. Using decision trees to understand structure in missing data. *BMJ Open* 2015; **5**: e007450 [PMID: 26124509 DOI: 10.1136/bmjopen-2014-007450]
39 **Breiman L**. Random Forests. Machine Learning. 2001; 45: 5-32 [DOI: 10.1023/A:1010933404324
40 **Calle ML**, Urrea V. Letter to the editor: Stability of Random Forest importance measures. *Brief Bioinform* 2011; **12**: 86-89 [PMID: 20360022 DOI: 10.1093/bib/bbq011]
41 **Friedman JH**. Greedy function approximation: A gradient boosting machine. *Ann Statist* 2001; **29**: 189-1232 [DOI: 10.1214/aos/1013203451]
42 **Friedman JH**. Stochastic gradient boosting. *Comput Stat Data Anal* 2002; **38**: 367-78 [DOI: 10.1016/S0167-9473(01)00065-2]
43 **Chen T**, Guestrin C. XGBoost: A Scalable Tree Boosting System. In Proceedings of the 22nd ACM SIGKDD International Conference on Knowledge Discovery and Data Mining; ACM: New York, NY, USA, 2016 [DOI: 10.1145/2939672.2939785]
44 **Torlay L**, Perrone-Bertolotti M, Thomas E, Baciu M. Machine learning-XGBoost analysis of language networks to classify patients with epilepsy. *Brain Inform* 2017; **4**: 159-169 [PMID: 28434153 DOI: 10.1007/s40708-017-0065-7]
45 **Zafrir N**, Mats I, Solodky A, Ben-Gal T, Battler A. Characteristics and outcome of octogenarian population referred for myocardial perfusion

imaging: comparison with non-octogenarian population with reference to gender. *Clin Cardiol* 2006; **29**: 117-120 [PMID: 16596834 DOI: 10.1002/clc.4960290307]

46 **Miller TD**, Roger VL, Hodge DO, Hopfenspirger MR, Bailey KR, Gibbons RJ. Gender differences and temporal trends in clinical characteristics, stress test results and use of invasive procedures in patients undergoing evaluation for coronary artery disease. *J Am Coll Cardiol* 2001; **38**: 690-697 [PMID: 11527619 DOI: 10.1016/s0735-1097(01)01413-9]

47 **Yao MF**, He J, Sun X, Ji XL, Ding Y, Zhao YM, Lou HY, Song XX, Shan LZ, Kang YX, Zhang SZ, Shan PF. Gender Differences in Risks of Coronary Heart Disease and Stroke in Patients with Type 2 Diabetes Mellitus and Their Association with Metabolic Syndrome in China. *Int J Endocrinol* 2016; **2016**: 8483405 [PMID: 28042294 DOI: 10.1155/2016/8483405]

48 **Wu YT**, Chien CL, Wang SY, Yang WS, Wu YW. Gender differences in myocardial perfusion defect in asymptomatic postmenopausal women and men with and without diabetes mellitus. *J Womens Health (Larchmt)* 2013; **22**: 439-444 [PMID: 23600438 DOI: 10.1089/jwh.2012.4055]

49 **Prior JO**, Monbaron D, Koehli M, Calcagni ML, Ruiz J, Bischof Delaloye A. Prevalence of symptomatic and silent stress-induced perfusion defects in diabetic patients with suspected coronary artery disease referred for myocardial perfusion scintigraphy. *Eur J Nucl Med Mol Imaging* 2005; **32**: 60-69 [PMID: 15309331 DOI: 10.1007/s00259-004-1591-0]

50 **Dilmanian H**, Aronow WS, Kaplan S, Pucillo AL, Weiss MB, Kalapatapu K, Monsen CE. Comparison of age, body mass index, and frequency of systemic hypertension and diabetes mellitus in patients having coronary angioplasty in 1996 versus in 2006. *Am J Cardiol* 2007; **100**: 1224-1226 [PMID: 17920361 DOI: 10.1016/j.amjcard.2007.05.052]

51 **Katzel LI**, Sorkin KD, Colman E, Goldberg AP, Busby-Whitehead MJ, Lakatta LE, Becker LC, Lakatta EG, Fleg JL. Risk factors for exercise-induced silent myocardial ischemia in healthy volunteers. *Am J Cardiol* 1994; **74**: 869-874 [PMID: 7977116 DOI: 10.1016/0002-9149(94)90578-9]

52 **Powell-Wiley TM**, Poirier P, Burke LE, Després JP, Gordon-Larsen P, Lavie CJ, Lear SA, Ndumele CE, Neeland IJ, Sanders P, St-Onge MP; American Heart Association Council on Lifestyle and Cardiometabolic Health; Council on Cardiovascular and Stroke Nursing; Council on Clinical Cardiology; Council on Epidemiology and Prevention; and Stroke Council. Obesity and Cardiovascular Disease: A Scientific Statement From the American Heart Association. *Circulation* 2021; **143**: e984-e1010 [PMID: 33882682 DOI: 10.1161/CIR.0000000000000973]

53 **Poirier P**, Giles TD, Bray GA, Hong Y, Stern JS, Pi-Sunyer FX, Eckel RH; American Heart Association; Obesity Committee of the Council on Nutrition, Physical Activity, and Metabolism. Obesity and cardiovascular disease: pathophysiology, evaluation, and effect of weight loss: an update of the 1997 American Heart Association Scientific Statement on Obesity and Heart Disease from the Obesity Committee of the Council on Nutrition, Physical Activity, and Metabolism. *Circulation* 2006; **113**: 898-918 [PMID: 16380542 DOI: 10.1161/CIRCULATIONAHA.106.171016]

54 **Budoff MJ**, Raggi P, Beller GA, Berman DS, Druz RS, Malik S, Rigolin VH, Weigold WG, Soman P; Imaging Council of the American College of Cardiology. Noninvasive Cardiovascular Risk Assessment of the Asymptomatic Diabetic Patient: The Imaging Council of the American College of Cardiology. *JACC Cardiovasc Imaging* 2016; **9**: 176-192 [PMID: 26846937 DOI: 10.1016/j.jcmg.2015.11.011.]

55 **Boorse C**. A rebuttal on health. In What is Disease?, ed. Humber JM, and Almeder RF, 3–134. Totowa, New Jersey: Humana Press 1997 [DOI: 10.1007/978-1-59259-451-1_1]

56 **Chew P**, Yuen DY, Stefanovic N, Pete J, Coughlan MT, Jandeleit-Dahm KA, Thomas MC, Rosenfeldt F, Cooper ME, de Haan JB. Antiatherosclerotic and renoprotective effects of ebselen in the diabetic apolipoprotein E/GPx1-double knockout mouse. *Diabetes* 2010; **59**: 3198-3207 [PMID: 20823099 DOI: 10.2337/db10-0195]

57 **Expert Panel on Detection**, Evaluation, and Treatment of High Blood Cholesterol in Adults. Executive Summary of The Third Report of The National Cholesterol Education Program (NCEP) Expert Panel on Detection, Evaluation, And Treatment of High Blood Cholesterol In Adults (Adult Treatment Panel III). *JAMA* 2001; **285**: 2486-2497 [PMID: 11368702 DOI: 10.1001/jama.285.19.2486]

58 **Colantonio LD**, Bittner V, Reynolds K, Levitan EB, Rosenson RS, Banach M, Kent ST, Derose SF, Zhou H, Safford MM, Muntner P. Association of Serum Lipids and Coronary Heart Disease in Contemporary Observational Studies. *Circulation* 2016; **133**: 256-264 [PMID: 26659948 DOI: 10.1161/CIRCULATIONAHA.115.011646]

59 **Hosokawa S**, Hiasa Y, Tomokane T, Ogura R, Miyajima H, Ohara Y, Ogata T, Yuba K, Suzuki N, Takahashi T, Kishi K, Ohtani R. The effects of atorvastatin on coronary endothelial function in patients with recent myocardial infarction. *Clin Cardiol* 2006; **29**: 357-362 [PMID: 16933577 DOI: 10.1002/clc.4960290808]

60 **Schwenke DC**, Carew TE. Initiation of atherosclerotic lesions in cholesterol-fed rabbits. II. Selective retention of LDL vs. selective increases in LDL permeability in susceptible sites of arteries. *Arteriosclerosis* 1989; **9**: 908-918 [PMID: 2590068 DOI: 10.1161/01.atv.9.6.908]

61 **Frank JS**, Fogelman AM. Ultrastructure of the intima in WHHL and cholesterol-fed rabbit aortas prepared by ultra-rapid freezing and freeze-etching. *J Lipid Res* 1989; **30**: 967-978 [PMID: 2794795]

62 **Tabas I**, Williams KJ, Borén J. Subendothelial lipoprotein retention as the initiating process in atherosclerosis: update and therapeutic implications. *Circulation* 2007; **116**: 1832-1844 [PMID: 17938300 DOI: 10.1161/CIRCULATIONAHA.106.676890]

63 **Nordestgaard BG**, Zilversmit DB. Large lipoproteins are excluded from the arterial wall in diabetic cholesterol-fed rabbits. *J Lipid Res* 1988; **29**: 1491-1500 [PMID: 3241125]

64 **Goldstein JL**, Brown MS. A century of cholesterol and coronaries: from plaques to genes to statins. *Cell* 2015; **161**: 161-172 [PMID: 25815993 DOI: 10.1016/j.cell.2015.01.036]

65 Effect of intensive blood-glucose control with metformin on complications in overweight patients with type 2 diabetes (UKPDS 34). UK Prospective Diabetes Study (UKPDS) Group. *Lancet* 1998; **352**: 854-865 [PMID: 9742977]

66 **ADVANCE Collaborative Group**, Patel A, MacMahon S, Chalmers J, Neal B, Billot L, Woodward M, Marre M, Cooper M, Glasziou P, Grobbee D, Hamet P, Harrap S, Heller S, Liu L, Mancia G, Mogensen CE, Pan C, Poulter N, Rodgers A, Williams B, Bompoint S, de Galan BE, Joshi R, Travert F. Intensive blood glucose control and vascular outcomes in patients with type 2 diabetes. *N Engl J Med* 2008; **358**: 2560-2572 [PMID: 18539916 DOI: 10.1056/NEJMoa0802987]

67 **Poznyak A**, Grechko AV, Poggio P, Myasoedova VA, Alfieri V, Orekhov AN. The Diabetes Mellitus-Atherosclerosis Connection: The Role of Lipid and Glucose Metabolism and Chronic Inflammation. *Int J Mol Sci* 2020; **21** [PMID: 32155866 DOI: 10.3390/ijms21051835]

68 **Kannel WB**, Dawber TR, Friedman GD, Glennon WE, Mcnamara PM. Risk factors in coronary heart disease. An evaluation of several serum lipids as predictors of coronary heart disease; the framingham study. *Ann Intern Med* 1964; **61**: 888-899 [PMID: 14233810 DOI: 10.7326/0003-4819-61-5-888]

69 **Salehi N**, Janjani P, Tadbiri H, Rozbahani M, Jalilian M. Effect of cigarette smoking on coronary arteries and pattern and severity of coronary

artery disease: a review. *J Int Med Res* 2021; **49**: 3000605211059893 [PMID: 34855538 DOI: 10.1177/03000605211059893]

70 **Barua RS**, Ambrose JA, Srivastava S, DeVoe MC, Eales-Reynolds LJ. Reactive oxygen species are involved in smoking-induced dysfunction of nitric oxide biosynthesis and upregulation of endothelial nitric oxide synthase: an in vitro demonstration in human coronary artery endothelial cells. *Circulation* 2003; **107**: 2342-2347 [PMID: 12707237 DOI: 10.1161/01.CIR.0000066691.52789.BE]

71 **Desideri G**, Ferri C. Endothelial activation. Sliding door to atherosclerosis. *Curr Pharm Des* 2005; **11**: 2163-2175 [PMID: 16026286 DOI: 10.2174/1381612054367382]

72 **Separham K**, H. S. Smoking or high blood pressure, which one is more important in premature coronary artery disease? *J Isfahan Med Sch Spring* 2007; **25**: 1-9

73 **Leone A**. Relation between coronary lesions and cigarette smoking of subjects deceased from acute myocardial infarction. A histopathological study. *J Cardiobiol* 2014; **2**: 5

74 **Leone A**, Landini L Jr, Biadi O, Balbarini A. Smoking and cardiovascular system: cellular features of the damage. *Curr Pharm Des* 2008; **14**: 1771-1777 [PMID: 18673180 DOI: 10.2174/138161208784746699]

World Journal of Clinical Cases

Submit a Manuscript: https://www.f6publishing.com

World J Clin Cases 2023 November 26; 11(33): 7965-7971

DOI: 10.12998/wjcc.v11.i33.7965

ISSN 2307-8960 (online)

ORIGINAL ARTICLE

Retrospective Study

Fever glove hand-shake method safe blood collection from children's fingertips in COVID-19 fever clinic

Ling Luo, Wei-Li Qin, Han-Mei Huang, Zhi-Hong Ou, Zhi-Hua Peng

Specialty type: Methodology

Provenance and peer review: Unsolicited article; Externally peer reviewed.

Peer-review model: Single blind

Peer-review report's scientific quality classification

Grade A (Excellent): 0
Grade B (Very good): 0
Grade C (Good): C
Grade D (Fair): 0
Grade E (Poor): 0

P-Reviewer: Annweiler C, France

Received: August 30, 2023
Peer-review started: August 30, 2023
First decision: September 13, 2023
Revised: September 21, 2023
Accepted: November 17, 2023
Article in press: November 17, 2023
Published online: November 26, 2023

Ling Luo, Han-Mei Huang, Department of Infectious Diseases, Guilin Municipal Hospital of Traditional Chinese Medicine, Guilin 541000, Guangxi Zhuang Autonomous Region, China

Wei-Li Qin, Department of Emergency, Guilin Municipal Hospital of Traditional Chinese Medicine, Guilin 541000, Guangxi Zhuang Autonomous Region, China

Zhi-Hong Ou, Laboratory, Guilin Municipal Hospital of Traditional Chinese Medicine, Guilin 541000, Guangxi Zhuang Autonomous Region, China

Zhi-Hua Peng, Department of Nursing, Guilin Traditional Chinese Medicine Hospital, Guilin 541000, Guangxi Zhuang Autonomous Region, China

Corresponding author: Zhi-Hua Peng, MNurs, Director of Nursing Department, Department of Nursing, Guilin Traditional Chinese Medicine Hospital, No. 2 Lingui Road, Xiangshan District, Guilin 541000, Guangxi Zhuang Autonomous Region, China. shiyin202308@163.com

Abstract

BACKGROUND

During the coronavirus disease 2019 (COVID-19) epidemic, the fever clinic is an important link for screening and diagnosing whether a patient is infected with the novel coronavirus. Blood collection from children's fingertips is a commonly used detection method; however, in children, the blood collection process may cause discomfort and resistance. To address this problem, the use of heating gloves combined with hand swinging can be considered for fingertip blood collection in children.

AIM

To explore the application of fever gloves with the handshaking method for fingertip blood collection from children in fever clinics during the COVID-19 epidemic.

METHODS

A total of 100 children were selected for fingertip blood collection at the fever clinic of our hospital from June 2022 to June 2023 and were divided into two groups using a randomized numerical table method, with 50 cases in each group, including the control and observation groups. The patients in the control group followed the doctor's instructions to cooperate with the routine fingertip blood collection method, and the patients in the observation group followed the doctor's

instructions to cooperate with the static fever gloves with the shaking hands method of children's fingertip blood collection. The level of the six blood routine and collection indexes, and the satisfaction of the examination of the patients in the peripheral blood group and the fever gloves with the shaking hands method of the children's fingertip blood collection group were compared.

RESULTS

The red and white blood cell count, hemoglobin, and red blood cell pressure volume in the observation group were higher than those in the control group ($P < 0.05$); the platelet count in the control group was lower than that in the observation group ($P < 0.05$); the number of times of squeezing the fingertip, the average time of blood collection, and the score of puncture pain in the observation group were significantly better than those in the control group ($P < 0.05$); and satisfaction with the routine blood examination in the observation group was greater than that in the control group.

CONCLUSION

The application value of the fever gloves with shaking hands method for children's fingertip blood collection was better, the accuracy of examination indexes was higher, and patient satisfaction with the examination was greater.

Key Words: Fever gloves; Shaking hands method; Peripheral blood; Index; Puncture; Satisfaction

©The Author(s) 2023. Published by Baishideng Publishing Group Inc. All rights reserved.

Core Tip: The research results can evaluate the application effect of heating gloves combined with the hand-swinging method for fingertip blood collection in children. If fever gloves combined with flicking can reduce children's discomfort and resistance and improve the effect of blood collection, they can be applied to fever clinics during the coronavirus disease 2019 epidemic to improve the success rate of children's fingertip blood collection and patient experience.

Citation: Luo L, Qin WL, Huang HM, Ou ZH, Peng ZH. Fever glove hand-shake method safe blood collection from children's fingertips in COVID-19 fever clinic. *World J Clin Cases* 2023; 11(33): 7965-7971
URL: https://www.wjgnet.com/2307-8960/full/v11/i33/7965.htm
DOI: https://dx.doi.org/10.12998/wjcc.v11.i33.7965

INTRODUCTION

Fever clinics play an important role in the diagnosis and screening of patients during the coronavirus disease 2019 (COVID-19) pandemic. Fingertip blood collection is a common but difficult procedure in pediatric patients. Traditional fingertip blood collection methods require the use of a needle to puncture the patient's fingertip, which can be painful and frustrating for children. Therefore, a new method is required to improve the efficiency of blood collection and minimize patient suffering[1-3]. In this study, we proposed a new method for fingertip blood collection in children using a heated glove in conjunction with the hand-shaking method. Heated gloves can be heated to increase the patient's blood circulation and dilate the blood vessels in the fingertips, thus facilitating blood collection. The flutter method increases blood flow by fluttering the arm, which can further improve the efficiency of blood collection. In practice, we found that the use of heated gloves in conjunction with the flap method for fingertip blood collection in children significantly improved the efficiency of blood collection. Compared with the traditional fingertip blood collection method, the use of a heated glove can dilate the blood vessels at the fingertip, making it easier to locate the vessels and collect sufficient blood samples. Simultaneously, the flap method increases blood flow, further improving the efficiency of blood collection.

Shaking fever gloves is a simple but effective method that can be applied to fingertip blood collection from children in fever clinics during the COVID-19 outbreak. This method not only improves the efficiency of blood collection and reduces patient suffering but also reduces the contact time of healthcare workers and decreases the risk of infection[4]. However, further studies are required to evaluate the safety and feasibility of the proposed method. Shaking fever gloves is a promising method that can be applied to fingertip blood collection from children in fever clinics during the COVID-19 outbreak. This method may improve the efficiency of blood collection, reduce patient distress, and reduce the risk of infection. Further studies are needed to validate the safety and feasibility of this method and promote its use in clinical practice.

MATERIALS AND METHODS

General information

Case selection: Between June 2022 and June 2023, 100 children underwent fingertip blood collection at our hospital's fever

clinic. Inclusion criteria: (1) Fever clinic selection of children with fingertip blood collection routine, body temperature of 36 ℃–39 ℃ or less; (2) children aged 7 mo to 6 years; and (3) parents know about the research program and voluntary participation in this study; exclusion criteria: (1) Children with a temperature of 39 ℃ or more and their condition of them being critically ill; and (2) family members of the communication barriers. The children were randomly divided into the control and observation groups according to the single or double serial number of consultations.

Methodology

(1) Control group: 50 patients, routine fingertip blood collection. The family fixes the root of the child's palm with their fingers and places it on the operating table; the blood collector fixes the child's finger, pinches the finger, and disinfects the child's left ring finger with a skin disinfectant (Maokang brand), then takes the disposable peripheral blood collection needle (Huahong) and quickly inserts it to a depth of approximately 2 mm, pulls out the needle, squeezes the child's finger to see the blood flows out, wipes away the first drop of blood with a sterile dry cotton ball, and sucks out the blood with a disposable micro blood collection pipette (Laixu), by repeatedly squeezing. The first drop of blood was dried with a sterile dry cotton ball, and the blood was aspirated using a disposable micro blood collection pipette (Laixu) by repeatedly squeezing the child's finger until the blood reached the area of the blue fine marking line; the micro-blood collection pipette was put into a disposable anticoagulation test tube, the family of the patient was instructed to use a sterile dry cotton ball to hold down the puncture hole, and the pressure was held down for 2–3 min. The nurse immediately pushed all the blood into a disposable anticoagulation test tube by using the red cap, the stopper was tightened on the test tube, and the test tube was placed in a vortex oscillator to mix the blood; and (2) Observation group: 50 cases - Fever gloves with the hand shaking method for fingertip blood collection.

Fever gloves with the hand method of children's fingertip blood collection method: (1) Heat the disposable baby warmer into the cotton half-finger finger gloves in the compartment, the cotton gloves through the baby warmer heated; (2) Warm baby heated to the appropriate temperature, with a digital thermometer to measure the temperature of the heated gloves (37 ± 1) ℃, to the child's hands on the homemade heated gloves. After 5 min, the nurse guided/assisted the child in implementing the hand shaking method. Specific operation of the hand-shaking method: The family members of infants and toddlers hold the child from behind and sit on the lap of the family members; older children take the seated position; the child's arm is naturally lowered to the wrist as the pivot point, and the nurse gently shakes the hand by holding the child's arm 10–15 times. The nurse held the child's arm and gently shakes it 10–15 times; (3) Same as the conventional fingertip blood collection method; and (4) Take off the cotton gloves when there is no bleeding from the finger at the puncture site of the child and put the cotton gloves into the recycling box.

The baby was uniformly sent to the supply room for autoclave sterilization and disinfection, and the warm baby was disposed of in medical waste garbage.

Routine blood specimens from both groups were examined using an XN-350 automatic five-category hematology analyzer, and the reagents, quality control products, and calibration products were imported. The instruments were calibrated, and performance was verified with reference to the "Quality Requirements for Analysis of Routine Clinical Hematology Tests."

Observation indicators

Observe and record the number of times the fingertip is squeezed during blood collection and the aspiration time required to memorize the volume of blood collected (100 UL) using a micro-blood collection pipette. The pass rate of the blood specimen and whether the blood specimen was returned for recollection. Satisfaction with the child's family was assessed using a questionnaire.

Statistical methods

The SPSS19.0 statistical software was used to analyze the data. Measurement data were expressed as mean ± standard deviation using the *t*-test; count data were expressed as rate (%) using the χ^2 test. $P < 0.05$ was considered statistically significant.

RESULTS

Comparison of the levels of blood routine testing indexes between the two groups

There was no difference in the average hemoglobin concentration in red blood cells between the control and observation groups ($P > 0.05$), whereas the red blood cell count, white blood cell count, hemoglobin, and erythrocyte pressure volume were higher in the observation group than in the control group ($P < 0.05$), and the platelet count was lower in the observation group than in the control group ($P < 0.05$) (Table 1).

Comparison of blood collection indexes between the two groups

The number of times the fingertip was squeezed, average blood collection time, and puncture pain score in the observation group were significantly better than those in the control group ($P < 0.05$), as shown in Table 2.

Comparison of satisfaction with routine blood tests between the two groups

Satisfaction with routine blood tests in the observation group was greater than in the control group ($P < 0.05$) (Table 3).

Table 1 Comparison of the levels of blood routine testing indexes between the two groups (mean ± SD)

Groups	Erythrocyte count (× 10^{12}/l)	White blood cell count (× 10^9/l)	Hemoglobin (g/L)	Erythrocyte pressure (%)	Average hemoglobin of red blood cells; white concentration (g/L)	Platelet count (× 10^9 /L)
Control group (n = 50)	3.95 ± 0.76	6.19 ± 1.57	110.03 ± 19.73	31.19 ± 10.89	301.76 ± 39.72	238.97 ± 47.89
Observation group (n = 50)	4.32 ± 0.85	7.03 ± 1.65	119.42 ± 20.65	40.39 ± 12.13	304.23 ± 39.76	207.65 ± 47.86
t	7.865	3.681	3.423	5.865	0.761	4.365
P value	0.001	0.001	0.001	0.001	0.267	0.001

Table 2 Comparison of blood collection indexes between the two groups (mean ± SD)

Groups	Number of fingertip squeezes (times)	Average blood collection time (min)	Puncture pain score (points)
Control group (n = 50)	4.19 ± 0.68	5.00 ± 0.33	0.79 ± 0.10
Observation group (n = 50)	1.36 ± 0.50[b]	2.01 ± 0.28[b]	0.48 ± 0.13[a]
t	8.732	6.281	2.139
P value	0.000	0.000	0.041

[a]P < 0.05 compared with control group.
[b]P < 0.01 compared with control group.

Table 3 Satisfaction with routine blood tests in both groups [n (%)]

Groups	Unsatisfactory	Partially satisfactory	Extremely satisfied	Satisfaction with routine blood tests
Control group (n = 50)	16 (32.00)	25 (50.00)	9 (18.00)	34 (68.00)
Observation group (n = 50)	5 (10.00)	30 (60.00)	15 (30.00)	45 (90.00)
χ^2	-	-	-	6.873
P value	-	-	-	0.001

DISCUSSION

Routine blood tests are the most basic clinical examination. After collecting human blood samples, it identifies and analyzes the substances in the blood, assesses the patient's health, detects the presence of diseases in time, and guides the clinic in carrying out effective treatment. Human blood consists of various types of blood cells and plasma, including white blood cells, red blood cells, and platelets, which have different functions and are used for various purposes in disease diagnosis. Red blood cells are the main component of blood, which bear the important responsibility of transporting oxygen to all parts of the body and can reflect the body's physical strength and mental state. White blood cells are human immune cells that can protect the human body from foreign pathogens and effectively remove cancer cells from the human body, assuming an important defense function[5]. Platelets are an important part of the blood and have a coagulation effect. After the body is damaged, platelets work quickly to promote wound healing. If platelets exceed the standard, they cause damage to the human body, leading to thrombosis, and thrombus dislodgement to form emboli can lead to the death of the host. From the clinical application of routine blood tests, a variety of white blood cell counts, human inflammatory responses, and viral infections, there is a close relationship between hemoglobin, the number of red blood cells, a variety of anemic diseases, and anemia severity. In the early stages of some diseases, abnormalities in routine blood tests are almost invisible. With the prolongation of the course of the disease, the patient's condition gradually worsens, and the abnormalities of routine blood tests become increasingly obvious. Active routine blood tests can assess the number of cells in the blood as well as morphological changes, which can detect disease abnormalities in a timely manner and provide important test data support for clinicians to effectively diagnose, target intervention, and evaluate disease regression. Routine blood tests for a variety of diseases can also play a strong role in assisting the timely clinical detection of the presence of disease and targeted intervention.

Since the outbreak of COVID-19 in Wuhan, Hubei, China, it has rapidly spread to all provinces of the country and is highly contagious and generally susceptible to the population[6]. Children's fever clinics are the first line of defense for virus prevention and control in hospitals, and they are also a high-risk area for cross-infection. Therefore, medical staff

should not neglect their own protection when contacting patients, especially blood collection nurses in fever clinics. Intravenous blood collection is a nursing operation project with close contact with patients, and children generally have a poorer ability to cooperate; peripheral blood vessels are finer than adults. Nurses in the blood collection are very likely due to coughing, sneezing, crying, or swinging too large, resulting in increased difficulty in puncture and prolonged close contact with the child, increasing the risk of contact transmission. Thus, improving the success rate and shortening the time of blood collection are key to reducing the rate of nosocomial infection among nurses and preventing the nosocomial transmission of the virus. Fingertip blood collection for routine blood tests in children is a commonly used clinical blood collection method; it is easier to perform fingertip blood collection, which is also a more adherent blood collection method for children.

Several studies have shown[7-9] that routine blood collection is performed using fever gloves with a shaking hand method of performing fingertip blood collection in children for routine blood tests.

The examination revealed some differences in the levels of these indicators. The results of this study are consistent with the above viewpoints, and the results show that there are sharp differences in the red blood cell count, white blood cell count, hemoglobin, red blood cell pressure volume, and platelet count of the patients in the peripheral blood group and the group of children's fingertip blood collection with fever gloves with the shaking hand method; however, there was no difference in the average hemoglobin concentration of red blood cells and the three puncture indices of the two groups. In addition, the patients in the group of children's fingertip blood collection with the fever gloves with the shaking hand method are more likely to have a greater degree of examination. The degree of intention is greater. From the perspective of blood collection, the peripheral blood source is the capillary, the site of blood flow velocity is relatively slow, platelets are attached to the puncture site and then form clots, and the results of routine blood tests have a direct impact.

CONCLUSION

The blood content of the peripheral site is low, and blood collection alone often fails to collect an adequate blood sample. Therefore, it is necessary to rub the fingertip to engorge it with blood and repeatedly press the puncture site to obtain an adequate blood sample[10]. However, this behavior can lead to other blood components entering the blood specimen, diluting the blood specimen, and ultimately affecting the examination results[11]. From the perspective of blood collection time, the heating gloves with the shaking hands method of children's fingertip blood collection site utilizes the elbow vein of the upper limb; the patient's blood vessels are thicker, more blood is collected, and blood collection speed and stability are higher; therefore, the routine blood examination is more accurate.

ARTICLE HIGHLIGHTS

Research background

During the coronavirus disease 2019 (COVID-19) pandemic, fever clinics have become an important link for screening and diagnosing patients infected with the novel coronavirus. Children's fingertip blood collection is a commonly used detection method, and the use of heated gloves combined with hand swinging can be considered for fingertip blood collection.

Research motivation

Fever gloves can generate heat, which can improve blood circulation in children's fingers, thereby increasing blood flow and blood collection. The hand-swinging method increases blood flow by quickly swinging the arm, which can further promote blood collection.

Research objectives

In applied research, a certain number of pediatric patients can be recruited and were randomly divided into two groups. One group used the traditional fingertip blood collection method, whereas the other group used heating gloves combined with the fingertip blood collection method.

Research methods

The effects of blood collection, discomfort, and resistance were compared between the two groups.

Research results

The research results can be used to evaluate the application of heating gloves combined with the hand-wagging method for fingertip blood collection in children.

Research conclusions

Combining fever gloves with flicking can reduce discomfort and resistance in children.

Research perspectives

It can be applied in fever clinics during the COVID-19 pandemic to improve the success rate of children's fingertip blood

collection and patient experience.

FOOTNOTES

Author contributions: Luo L and Peng ZH contributed equally to this work; Luo L, Qin WL, Huang HM, Ou ZH, and Peng ZH designed the research study; Luo L, Qin WL, Huang HM, Ou ZH, and Peng ZH performed the research; Luo L and Peng ZH analyzed the data and wrote the manuscript; all authors have read and approved the final manuscript.

Supported by Health Commission of Guangxi Zhuang Autonomous Region Application for Self Funded Research Projects, No. Z20210159.

Institutional review board statement: The study was reviewed and approved by the [Guilin Traditional Chinese Medicine Hospital] Institutional Review Board.

Informed consent statement: All study participants or their legal guardian provided informed written consent about personal and medical data collection prior to study enrolment.

Conflict-of-interest statement: All authors have no conflicts of interest.

Data sharing statement: No additional data are available.

Open-Access: This article is an open-access article that was selected by an in-house editor and fully peer-reviewed by external reviewers. It is distributed in accordance with the Creative Commons Attribution NonCommercial (CC BY-NC 4.0) license, which permits others to distribute, remix, adapt, build upon this work non-commercially, and license their derivative works on different terms, provided the original work is properly cited and the use is non-commercial. See: https://creativecommons.org/Licenses/by-nc/4.0/

Country/Territory of origin: China

ORCID number: Ling Luo 0009-0000-9612-0661; Wei-Li Qin 0009-0009-1623-9773; Han-Mei Huang 0009-0002-6543-7927; Zhi-Hua Peng 0009-0004-1716-3874.

S-Editor: Liu JH
L-Editor: A
P-Editor: Liu JH

REFERENCES

1 **Kawasuji H**, Sakamaki I, Kawamura T, Ueno A, Miyajima Y, Matsumoto K, Kawago K, Higashi Y, Yamamoto Y. Proactive infectious disease consultation at the time of blood culture collection is associated with decreased mortality in patients with methicillin-resistant Staphylococcus aureus bacteremia: A retrospective cohort study. *J Infect Chemother* 2020; **26**: 588-595 [PMID: 32085966 DOI: 10.1016/j.jiac.2020.01.017]

2 **Shah EE**, Young RP, Wong SW, Damon LE, Wolf JL, Shah ND, Leavitt AD, Loeffler P, Martin TG 3rd. Impact of Plerixafor Use at Different Peripheral Blood CD34(+) Thresholds on Autologous Stem Cell Collection in Patients with Multiple Myeloma. *Biol Blood Marrow Transplant* 2020; **26**: 876-883 [PMID: 31785375 DOI: 10.1016/j.bbmt.2019.11.024]

3 **Maeng JY**, Kim SY, An BY, Kim S, Lee JL, Oh IH, Kim TG. Comparison and correlation among in vitro and in vivo assays to assess cord blood quality according to delivery temperature and time after collection. *Transfus Apher Sci* 2019; **58**: 475-483 [PMID: 31147270 DOI: 10.1016/j.transci.2019.05.006]

4 **Benakli M**, Ahmed Nacer R, Mehdid F, Belhadj R, Rahmoune N, Baazizi M, Ait Ouali D, Harieche F, Hamladji RM. Peripheral Blood Stem Cell Mobilization and Collection in Pediatric Healthy Sibling Donors Weighing 20 Kilograms or Less; Algerian Experience. *Transfus Apher Sci* 2020; **59**: 102987 [PMID: 33162340 DOI: 10.1016/j.transci.2020.102987]

5 **Nakamura Y**, Okubo M, Furuta Y, Tokida M, Ichikawa K, Ohsaka A. Impact of CD34+ pre-counting and plerixafor on autologous peripheral blood stem cell collection in Japanese university hospitals in eight years. *Transfus Apher Sci* 2019; **58**: 102664 [PMID: 31753774 DOI: 10.1016/j.transci.2019.10.006]

6 **Andreazza AC**, Laksono I, Fernandes BS, Toben C, Lewczuk P, Riederer P, Kennedy SH, Kapogiannis D, Thibaut F, Gerlach M, Gallo C, Kim YK, Grünblatt E, Yatham L, Berk M, Baune BT. Guidelines for the standardized collection of blood-based biomarkers in psychiatry: Steps for laboratory validity - a consensus of the Biomarkers Task Force from the WFSBP. *World J Biol Psychiatry* 2019; **20**: 340-351 [PMID: 30907211 DOI: 10.1080/15622975.2019.1574024]

7 **Evans DL**, Volsko TA, Capellari E, Strickland SL. AARC Clinical Practice Guidelines: Capillary Blood Gas Sampling for Neonatal and Pediatric Patients. *Respir Care* 2022; **67**: 1190-1204 [PMID: 36002161 DOI: 10.4187/respcare.10151]

8 **McGillivray D**, Ducharme FM, Charron Y, Mattimoe C, Treherne S. Clinical decisionmaking based on venous versus capillary blood gas values in the well-perfused child. *Ann Emerg Med* 1999; **34**: 58-63 [PMID: 10381995 DOI: 10.1016/S0196-0644(99)70272-6]

9 **Brierley J**, Carcillo JA, Choong K, Cornell T, Decaen A, Deymann A, Doctor A, Davis A, Duff J, Dugas MA, Duncan A, Evans B, Feldman J, Felmet K, Fisher G, Frankel L, Jeffries H, Greenwald B, Gutierrez J, Hall M, Han YY, Hanson J, Hazelzet J, Hernan L, Kiff J, Kissoon N, Kon A, Irazuzta J, Lin J, Lorts A, Mariscalco M, Mehta R, Nadel S, Nguyen T, Nicholson C, Peters M, Okhuysen-Cawley R, Poulton T, Relves M, Rodriguez A, Rozenfeld R, Schnitzler E, Shanley T, Kache S, Skippen P, Torres A, von Dessauer B, Weingarten J, Yeh T, Zaritsky A,

Stojadinovic B, Zimmerman J, Zuckerberg A. Clinical practice parameters for hemodynamic support of pediatric and neonatal septic shock: 2007 update from the American College of Critical Care Medicine. *Crit Care Med* 2009; **37**: 666-688 [PMID: 19325359 DOI: 10.1097/CCM.0b013e31819323c6]

10 **Dorofaeff T**, Bandini RM, Lipman J, Ballot DE, Roberts JA, Parker SL. Uncertainty in Antibiotic Dosing in Critically Ill Neonate and Pediatric Patients: Can Microsampling Provide the Answers? *Clin Ther* 2016; **38**: 1961-1975 [PMID: 27544661 DOI: 10.1016/j.clinthera.2016.07.093]

11 **Lorenz TK**. Autonomic, endocrine, and psychological stress responses to different forms of blood draw. *PLoS One* 2021; **16**: e0257110 [PMID: 34478481 DOI: 10.1371/journal.pone.0257110]

World Journal of Clinical Cases

Submit a Manuscript: https://www.f6publishing.com

World J Clin Cases 2023 November 26; 11(33): 7972-7979

DOI: 10.12998/wjcc.v11.i33.7972

ISSN 2307-8960 (online)

ORIGINAL ARTICLE

Retrospective Study

Influence of ganglioside combined with methylprednisolone sodium succinate on efficacy and neurological function in patients with acute myelitis

Yu-Fei Sun, Li-Li Liu, Sha-Sha Jiang, Xian-Juan Zhang, Feng-Jun Liu, Wan-Ming Zhang

Specialty type: Medicine, research and experimental

Provenance and peer review: Unsolicited article; Externally peer reviewed.

Peer-review model: Single blind

Peer-review report's scientific quality classification

Grade A (Excellent): 0
Grade B (Very good): 0
Grade C (Good): C, C
Grade D (Fair): 0
Grade E (Poor): 0

P-Reviewer: Konstantinopoulos PA, United States; Kuroda K, Japan

Received: September 13, 2023
Peer-review started: September 13, 2023
First decision: September 28, 2023
Revised: October 11, 2023
Accepted: October 30, 2023
Article in press: October 30, 2023
Published online: November 26, 2023

Yu-Fei Sun, Wan-Ming Zhang, Department of Special Medicine, Basic Medical College of Qingdao University, Qingdao 266071, Shandong Province, China

Li-Li Liu, Sha-Sha Jiang, Department of Medical Microbiology, Basic Medical College of Qingdao University, Qingdao 266075, Shandong Province, China

Xian-Juan Zhang, Department of Clinical Laboratory, The Affiliated Hospital of Qingdao University, Qingdao 266000, Shandong Province, China

Feng-Jun Liu, Department of Special Medicine, School of Basic Medicine, Qingdao University, Qingdao 266000, Shandong Province, China

Corresponding author: Wan-Ming Zhang, MD, Doctor, Department of Special Medicine, Basic Medical College of Qingdao University, No. 821 Ningde Road, Qingdao 266071, Shandong Province, China. zhangwanming0532@126.com

Abstract

BACKGROUND

Acute myelitis (AM) can lead to sudden sensory, motor and autonomic nervous dysfunction, which negatively affects their daily activities and quality of life, so it is necessary to explore optimization from a therapeutic perspective to curb the progression of the disease.

AIM

To investigate the effect of ganglioside (GM) combined with methylprednisolone sodium succinate (MPSS) on the curative effect and neurological function of patients with AM.

METHODS

First, we selected 108 AM patients visited between September 2019 and September 2022 and grouped them based on treatment modality, with 52 patients receiving gamma globulin (GG) + MPSS and 56 patients receiving GM + MPSS, assigned to the control group (Con) and observation group (Obs), respectively. The therapeutic effect, neurological function (sensory and motor function scores), adverse events (AEs), recovery (time to sphincter function recovery, time to limb muscle strength recovery above grade 2, and time to ambulation), inflammatory factors

(IFs) [interleukin (IL)-6, C-reactive protein (CRP), and tumor necrosis factor (TNF)-α] and other data of the two groups were collected for evaluation and comparison.

RESULTS

The Obs had: (1) A significantly higher response rate of treatment than the Con; (2) Higher scores of sensory and motor functions after treatment that were higher than the baseline (before treatment) and higher than the Con levels; (3) Lower incidence rates of skin rash, gastrointestinal discomfort, dyslipidemia, osteoporosis and other AEs; (4) Faster posttreatment recovery of sphincter function, limb muscle strength and ambulation; and (5) Markedly lower posttreatment IL-6, CRP and TNF-α levels than the baseline and the Con levels.

CONCLUSION

From the above, it can be seen that GM + MPSS is highly effective in treating AM, with a favorable safety profile comparable to that of GG + MPSS. It can significantly improve patients' neurological function, speed up their recovery and inhibit serum IFs.

Key Words: Ganglioside; Methylprednisolone sodium succinate; Acute myelitis; Therapeutic effect; Neurological function

©The Author(s) 2023. Published by Baishideng Publishing Group Inc. All rights reserved.

Core Tip: Acute myelitis (AM) is an autoimmune demyelinating disease in which patients may experience clinical symptoms such as difficult defecation, nerve root pain, lower limb paralysis, low-grade fever, and other symptoms that lead to limitations in daily life. This study mainly verified the clinical advantages of ganglioside + methylprednisolone sodium succinate in the treatment of AM, so as to provide timely and effective treatment for patients with AM and improve the condition and prognosis of patients.

Citation: Sun YF, Liu LL, Jiang SS, Zhang XJ, Liu FJ, Zhang WM. Influence of ganglioside combined with methylprednisolone sodium succinate on efficacy and neurological function in patients with acute myelitis. *World J Clin Cases* 2023; 11(33): 7972-7979
URL: https://www.wjgnet.com/2307-8960/full/v11/i33/7972.htm
DOI: https://dx.doi.org/10.12998/wjcc.v11.i33.7972

INTRODUCTION

Acute myelitis (AM), also known as acute transverse myelitis, is an acute focal inflammatory disease occurring in the spinal cord (SC) that can cause sudden sensory, motor and autonomic dysfunction, reducing daily mobility and quality of life[1,2]. The nosogenesis of the disease is complex and diverse, as a variety of autoimmune reactions and infectious agents, such as herpesvirus, enterovirus, and varicella zoster virus, can be contributing factors[3]. According to epidemiological data, the disease mostly occurs in young and middle-aged groups, and its incidence is rising[4,5]. Prompt treatment of AM can help protect neurological function and prevent the disease from further progressing[6]. Our research mainly seeks effective treatment strategies for AM patients, which would carry great clinical implications for improving the condition of these patients and speeding up their recovery.

Ganglioside (GM) is mainly found in the brain tissues of all mammals and can help the molecular recognition of various glycan-binding proteins and mediate the activity of plasma membrane proteins through transverse binding, thus playing a regulatory role in the body's neurodevelopment, differentiation and pathological changes[7,8]. In one animal experiment, intrathecal administration of GM showed significant therapeutic efficacy against bupivacaine-associated nerve injury and torsion dysfunction compared to the intravenously administered route[9]. Methylprednisolone sodium succinate (MPSS) is an anti-inflammatory corticosteroid that is beneficial to the recovery of damaged SCs[10] and can protect SC function by inhibiting lipid peroxidation and avoiding ischemia-induced tissue damage[11]. Research on the effect of GM + MPSS has been limited. This study mainly aimed to fill this research gap, seeking a new clinical exploration for the improvement of the condition and symptom recovery of patients with AM.

MATERIALS AND METHODS

General data

One hundred eight AM patients were selected the Affiliated Hospital of Qingdao University between September 2019 and September 2022 as the research participants, including 52 patients in the control group (the Con) and 56 patients in the observation group (the Obs), who were given gamma globulin (GG) + MPSS and GM + MPSS, respectively. The two patient cohorts showed no differences in age, sex, onset time or other general data ($P > 0.05$).

Eligibility criteria

The eligible patients met all of the following criteria: AM as confirmed by spinal magnetic resonance imaging and cerebrospinal fluid examination[12]; no other treatment measures taken in the past six months; stable vital signs with clear consciousness; complete medical records; and willingness to cooperate with the research.

Patients were excluded if they met any of the following criteria: Heart, lung, or kidney dysfunction/disease; autoimmune deficiency; coagulation dysfunction; malignant tumor; severe mental disorders; systemic fungal infection; and allergy to a research medication.

Medication methods

The medication regimen GG + MPSS was given to the Con group. Patients received intravenous injections of 10 g of GG and 250 mL of 5% glucose once a day. MPSS (1000 mg) and 5% glucose injection (250 mL) were given intravenously for 4 wk. The medication regimen for the Obs was GM + MPSS. Patients were given an intravenous drip of monosialotetrahexosylganglioside sodium for injection (100 mg) and 5% glucose injection (250 mL) once a day; MPSS (1000 mg) and 5% glucose (250 mL) were injected intravenously once daily for 4 wk.

Evaluation indices

Curative effect: The clinical symptoms and recovery of the two groups of patients (before *vs* after treatment) were compared and analyzed, which were used as the evaluation criteria of the treatment effectiveness. Cured: The patients recovered nearly fully in terms of limb sensation and muscle strength and could take care of themselves with complications that disappeared; marked response: The patients had improved limb sensation, muscle strength and sphincter function and mostly controlled complications; response: Limb sensation and muscle strength improved, and the complications were gradually controlled; nonresponse: There was no change or even worsening of limb sensation and symptoms.

Neurological function: The recovery of patients' nerve function was evaluated by referring to the International Standards for Neurological Classification of Spinal Cord Injury (SCI)[13], mainly by calculating the scores of sensory function and motor function, with scores ranging from 0 to 50 that were in direct proportion to the recovery degree of nerve function.

Occurrence of adverse events: The incidence of adverse events (AEs) was counted by observing and recording the cases of skin rash, gastrointestinal discomfort, dyslipidemia (DL), and osteoporosis (OS) in the two groups.

Recovery: Three clinical indices, namely, time to sphincter function recovery, time to recovery of limb muscle strength above grade 2, and time to ambulation, were recorded.

Inflammatory factors: On venous blood drawn from both cohorts before and after treatment, we performed enzyme-linked immunosorbent assay (ELISA)[14] to quantify the levels of inflammatory factors (IFs) such as interleukin (IL)-6, C-reactive protein (CRP) and tumor necrosis factor (TNF)-α.

Statistical processing

The measurement data, statistically described by mean ± SEM, were compared between groups by the independent samples *t* test and within groups before and after treatment by the paired *t* test. The count data are denoted by *n* (%), and the comparison between the two groups of counting data was made by χ^2-test. The collected experimental data were analyzed by SPSS 21.0, and the figures were made in GraphPad Prism 7.0. Differences were significant when $P < 0.05$.

RESULTS

General data

Age, sex, onset time, lower limb muscle strength, marital status and other general data were similar between the two patient cohorts ($P > 0.05$; Table 1).

Curative effect

The Obs had a higher overall response rate (ORR) (calculated as the percentage of the sum of cured, marked response and response in all cases) than the Con (89.29% *vs* 73.08%; $P < 0.05$; Table 2).

Neurological function

By evaluating the scores of sensory and motor functions of AM patients in the two groups, we found that there was no significant difference between them before treatment ($P > 0.05$). Both scores increased in both groups after treatment, with significantly higher scores in the Obs ($P < 0.05$; Figure 1).

Occurrence of AEs

We observed and counted AEs such as rash, gastrointestinal discomfort, DL and OS and found that their total incidence was lower in the Obs group than in the Con group (7.14% *vs* 21.15%; $P < 0.05$; Table 3).

Table 1 General data, *n* (%) or mean ± SEM

Factors	Control group (*n* = 52)	Observation group (*n* = 56)	χ^2/t	*P* value
Age (yr)	43.85 ± 8.23	42.98 ± 8.30	0.546	0.586
Sex (male/female)	28/24	33/23	0.283	0.595
Time of onset (d)	3.06 ± 0.46	3.20 ± 0.62	1.324	0.188
Lower limb muscle strength (grade 0-1/grade 2-3)	26/26	30/26	0.138	0.711
Marital status (married/single)	35/17	29/27	2.691	0.101

Table 2 Therapeutic effect, *n* (%)

Factors	Control group (*n* = 52)	Observation group (*n* = 56)	χ^2	*P* value
Cured	17 (32.69)	24 (42.86)	-	-
Marked response	14 (26.92)	20 (35.71)	-	-
Response	7 (13.46)	6 (10.71)	-	-
Nonresponse	14 (26.92)	6 (10.71)	-	-
Total	38 (73.08)	50 (89.29)	4.695	0.030

Table 3 Occurrence of adverse events, *n* (%)

Factors	Control group (*n* = 52)	Observation group (*n* = 56)	χ^2	*P* value
Rash	2 (3.85)	1 (1.79)	-	-
Gastrointestinal discomfort	2 (3.85)	1 (1.79)	-	-
Dyslipidemia	4 (7.69)	2 (3.57)	-	-
Osteoporosis	3 (5.77)	0 (0.00)	-	-
Total	11 (21.15)	4 (7.14)	4.426	0.035

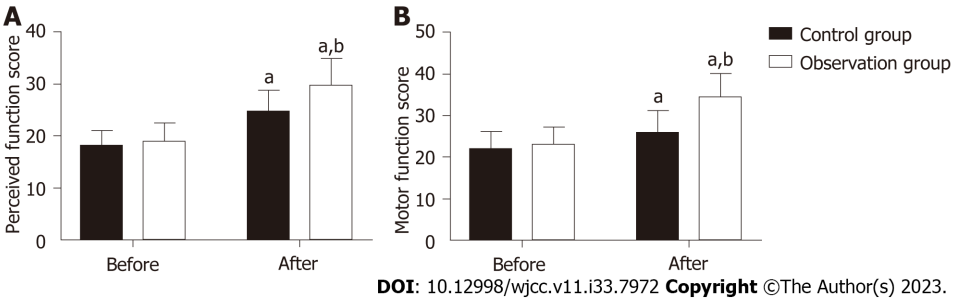

DOI: 10.12998/wjcc.v11.i33.7972 **Copyright** ©The Author(s) 2023.

Figure 1 Neurological function. A: The observation group had statistically higher posttreatment sensory function scores than the control group; B: The observation group had significantly higher posttreatment motor function scores than the control group. [a]*P* < 0.01 *vs* before treatment; [b]*P* < 0.05 *vs* control group.

Recovery

By evaluating the time to sphincter function recovery, time to limb muscle strength recovery above grade 2 and time to ambulation, we found that the recovery time of the above three aspects was significantly shorter in the Obs group than in the Con group ($P < 0.05$; Figure 2).

IFs

Three IFs, namely, IL-6, CRP, and TNF-α, were detected by ELISA in two groups of patients with AM. The three indices were not significantly different before treatment between groups ($P > 0.05$). Their posttreatment levels were markedly reduced in both cohorts, all three being significantly lower in the Obs ($P < 0.05$; Figure 3).

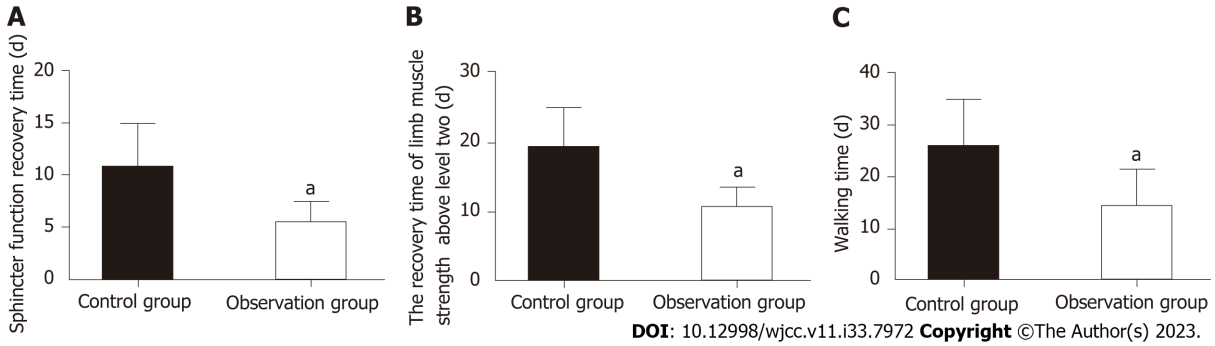

DOI: 10.12998/wjcc.v11.i33.7972 **Copyright** ©The Author(s) 2023.

Figure 2 Recovery. A: The observation group had an obviously shorter sphincter function recovery time than the control group; B: The observation group had an obviously shorter limb muscle strength recovery time than the control group; C: The observation group had obviously earlier ambulation than the control group. [a]*P* < 0.01 *vs* control group.

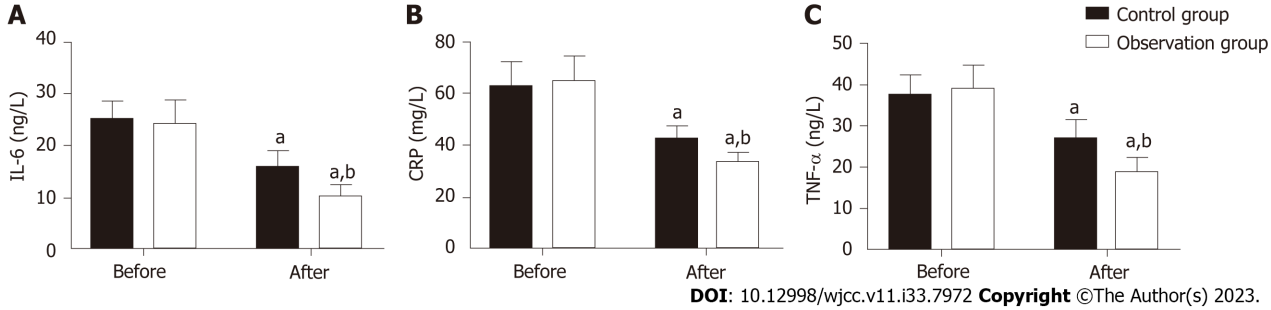

DOI: 10.12998/wjcc.v11.i33.7972 **Copyright** ©The Author(s) 2023.

Figure 3 Inflammatory factors. A: The observation group had evidently lower posttreatment interleukin-6 than the control group; B: The observation group had evidently lower posttreatment C-reactive protein than the control group; C: The observation group had evidently lower posttreatment tumor necrosis factor-α than the control group. [a]*P* < 0.01 *vs* before treatment; [b]*P* < 0.05 *vs* control group. IL-6: Interleukin-6; CRP: C-reactive protein; TNF-α: Tumor necrosis factor-α.

DISCUSSION

AM is a common and rapidly occurring neurological disorder that is essentially an autoimmune demyelinating condition [15]. It can lead to clinical symptoms such as difficulty urinating and defecating, nerve root pain, lower limb paralysis, and low fever, which seriously worsen patients' everyday lives[16,17]. The early pathological changes of AM involve SC shock, increased muscle tone, active tendon reflex, *etc*. In severe cases, complications such as pressure sores and pulmonary and urinary tract infections may occur[18,19]. Therefore, providing timely and effective treatment to AM patients is of great significance to curb disease development and improve patient prognosis.

Our research data showed that the ORRs of Obs and Con were 89.29% and 73.08%, respectively. The significantly higher ORR in the Obs suggests that AM patients receiving GM + MPSS have obvious advantages in symptom recovery, self-care and complication control. GM is a structural component of the human nerve cell membrane that can not only mediate the growth, repair and reconstruction of damaged cranial nerves but also effectively modulate brain nerve conduction and the activities of various enzymes in cell membranes[20]. As a systemic immunosuppressive drug, MPSS can not only inhibit SCI-associated neuroinflammation through its immunomodulatory function but also avoid systemic immune responses, which may help explain its therapeutic mechanism in AM[21]. From the aspects of sensory and motor functions, the neurological function of the two groups was evaluated. The Obs were found to have obviously elevated sensory and motor function scores after treatment that were higher than the baseline and the Con, indicating that GM + MPSS used in the Obs was more beneficial to sensory and motor function recovery. In the study by Shen *et al*[22], the recovery of GM on neurons of SCI rats seemed to be linked to the increased secretion of GM in rat SC after CXCL14 silencing. A clinical study pointed out that MPSS can enhance the neurological function and activities of daily living of patients with acute SCI and cauda equina injury with sensory and motor dysfunction[23]. Our results of three recovery indices revealed that the times to sphincter function recovery, limb muscle strength recovery above grade 2 and ambulation were significantly shorter in the Obs group than in the Con group, suggesting that GM + MPSS was helpful in promoting the functional recovery of sphincters, limb muscle strength and ambulation in AM patients. Zhai *et al*[24] suggested that GM plus systematic rehabilitation training for SC patients is more conducive to limb function rehabilitation. In our safety evaluation, we found that the incidences of AEs such as rash, gastrointestinal discomfort, DL and OS in the Obs group were significantly lower than those in the Con group (7.14% *vs* 21.15%), indicating that GM + MPSS is safer for AM patients. Finally, we used ELISA to detect IFs. The posttreatment IL-6, CRP and TNF-α levels were markedly reduced in the Obs compared with the baseline and Con groups, demonstrating that GM + MPSS can inhibit excessive inflammation in AM patients. As reported by Hu *et al*[25], GM can significantly lower IL-1β, IL-6, TNF-α and other inflammatory proteins in the SC tissue of SCI rats, similar to our results. Consistent with these findings, Schmidt *et al*[26]

found that MPSS can significantly inhibit the secretion of systemic inflammatory cytokines such as CRP and TNF-α in patients undergoing liver resection.

There are several areas in this study that need further improvement. First, since this is a small sample single-center analysis, it is necessary to expand the sample range and sample size in the future to improve the accuracy of the study results and to minimize or even avoid the bias of information collection. Second, the addition of follow-up analysis will enable in-depth evaluation of the long-term efficacy of GM + MPSS in the treatment of AM. Third, basic experiments related to GM + MPSS treatment of AM should be supplemented, which will be conducive to revealing the underlying mechanisms. In the future, we will make improvements based on the above points.

CONCLUSION

GM + MPSS can enhance the curative effect, neurological function, and functional recovery of patients' perception, movement, sphincter function, limb muscle strength and ambulation, with favorable safety and anti-inflammatory action. These findings provide novel insight and clinical reference for the management and treatment of patients with AM.

ARTICLE HIGHLIGHTS

Research background

Acute myelitis (AM) can cause sudden sensory, motor and autonomic nervous dysfunction in patients, which negatively affects their daily activities and quality of life. Therefore, it is necessary to optimize exploration from a therapeutic perspective to curb the progression of the disease.

Research motivation

It is necessary to optimize the therapeutic strategy to improve the clinical outcomes of AM patients.

Research objectives

In this research, the effect of ganglioside (GM) combined with methylprednisolone sodium succinate (MPSS) on the curative effect and neurological function of patients with AM was investigated.

Research methods

Of the 108 AM patients selected, 52 cases were treated with gamma globulin plus MPSS (control group) and 56 cases were treated with GM plus MPSS (observation group). The two groups were then comparatively analyzed from the following perspectives: Efficacy, neurological function (sensory and motor function scores), occurrence of adverse events, recovery (time to sphincter function recovery, limb muscle strength recovery above grade 2, and ambulation), and inflammatory factors [interleukin-6 (IL-6); C-reactive protein (CRP); tumor necrosis factor-α (TNF-α)].

Research results

The treatment efficacy and sensory and motor function scores of the observation group were significantly higher than those of the control group, while the total incidence of adverse events such as rash, gastrointestinal discomfort, dyslipidemia and osteoporosis, as well as recovery indexes such as the time to sphincter function recovery, limb muscle strength recovery above grade 2, and ambulation was significantly lower. In addition, IL-6, CRP, and TNF-α levels reduced markedly in the observation group after treatment, significantly lower than the baseline and those of the control group.

Research conclusions

GM combined with MPSS shows significant advantages in enhancing efficacy and nerve function in patients with AM, accelerating recovery, inhibiting serum inflammation, and improving safety.

Research perspectives

Our findings may provide new insights and clinical references for the management and treatment of patients with AM.

FOOTNOTES

Co-first authors: Yu-Fei Sun and Li-Li Liu.

Author contributions: Sun YF and Liu LL contributed equally to this work and are co-first authors. Sun YF and Liu LL designed the research and wrote the first manuscript; Sun YF, Liu LL, Jiang SS, Zhang XJ, Liu FJ, and Zhang WM contributed to conceiving the research and analyzing data; Sun YF, Liu LL, and Zhang WM conducted the analysis and provided guidance for the research; and all authors reviewed and approved the final manuscript.

Institutional review board statement: This study was approved by the Ethic Committee of Basic Medical College of Qingdao University (Approval No. QDWMkj-2020-012).

Informed consent statement: Patients were not required to give informed consent to the study because the analysis used anonymous clinical data that were obtained after each patient agreed to treatment by written consent.

Conflict-of-interest statement: All the authors report no relevant conflicts of interest for this article.

Data sharing statement: All data and materials are available from the corresponding author.

Open-Access: This article is an open-access article that was selected by an in-house editor and fully peer-reviewed by external reviewers. It is distributed in accordance with the Creative Commons Attribution NonCommercial (CC BY-NC 4.0) license, which permits others to distribute, remix, adapt, build upon this work non-commercially, and license their derivative works on different terms, provided the original work is properly cited and the use is non-commercial. See: https://creativecommons.org/Licenses/by-nc/4.0/

Country/Territory of origin: China

ORCID number: Wan-Ming Zhang 0000-0001-8053-4886.

S-Editor: Wang JJ
L-Editor: A
P-Editor: Zhang YL

REFERENCES

1 **Vegezzi E**, Ravaglia S, Buongarzone G, Bini P, Diamanti L, Gastaldi M, Prunetti P, Rognone E, Marchioni E. Acute myelitis and ChAdOx1 nCoV-19 vaccine: Casual or causal association? *J Neuroimmunol* 2021; **359**: 577686 [PMID: 34392078 DOI: 10.1016/j.jneuroim.2021.577686]
2 **Prete S**, McShannic JD, Fertel BS, Simon EL. Acute transverse myelitis progressing to permanent quadriplegia following COVID-19 infection. *Am J Emerg Med* 2022; **56**: 391.e1-391.e3 [PMID: 35248410 DOI: 10.1016/j.ajem.2022.02.038]
3 **Águila-Gordo D**, Manuel Flores-Barragán J, Ferragut-Lloret F, Portela-Gutierrez J, LaRosa-Salas B, Porras-Leal L, Carlos Villa Guzmán J. Acute myelitis and SARS-CoV-2 infection. A new etiology of myelitis? *J Clin Neurosci* 2020; **80**: 280-281 [PMID: 33099361 DOI: 10.1016/j.jocn.2020.07.074]
4 **Hwang M**, Flanagan A, Graf A, Kruger KM, Scullion N, Tayne S, Altiok H. Gait Characteristics in Youth With Transverse Myelitis. *Top Spinal Cord Inj Rehabil* 2021; **27**: 38-48 [PMID: 34456545 DOI: 10.46292/sci20-00048]
5 **Abbatemarco JR**, Galli JR, Sweeney ML, Carlson NG, Samara VC, Davis H, Rodenbeck S, Wong KH, Paz Soldan MM, Greenlee JE, Rose JW, Delic A, Clardy SL. Modern Look at Transverse Myelitis and Inflammatory Myelopathy: Epidemiology of the National Veterans Health Administration Population. *Neurol Neuroimmunol Neuroinflamm* 2021; **8** [PMID: 34465615 DOI: 10.1212/NXI.0000000000001071]
6 **Gupta A**, Kumar SN, Taly AB. Neurological and functional recovery in acute transverse myelitis patients with inpatient rehabilitation and magnetic resonance imaging correlates. *Spinal Cord* 2016; **54**: 804-808 [PMID: 26927295 DOI: 10.1038/sc.2016.23]
7 **Schnaar RL**. The Biology of Gangliosides. *Adv Carbohydr Chem Biochem* 2019; **76**: 113-148 [PMID: 30851743 DOI: 10.1016/bs.accb.2018.09.002]
8 **Ohmi Y**, Ohkawa Y, Tajima O, Sugiura Y, Furukawa K. Ganglioside deficiency causes inflammation and neurodegeneration *via* the activation of complement system in the spinal cord. *J Neuroinflammation* 2014; **11**: 61 [PMID: 24673754 DOI: 10.1186/1742-2094-11-61]
9 **Ji J**, Yan X, Li Z, Lai Z, Liu J. Therapeutic effects of intrathecal versus intravenous monosialoganglioside against bupivacaine-induced spinal neurotoxicity in rats. *Biomed Pharmacother* 2015; **69**: 311-316 [PMID: 25661376 DOI: 10.1016/j.biopha.2014.12.020]
10 **Kamalov MI**, Đặng T, Petrova NV, Laikov AV, Luong D, Akhmadishina RA, Lukashkin AN, Abdullin TI. Self-assembled nanoformulation of methylprednisolone succinate with carboxylated block copolymer for local glucocorticoid therapy. *Colloids Surf B Biointerfaces* 2018; **164**: 78-88 [PMID: 29413623 DOI: 10.1016/j.colsurfb.2018.01.014]
11 **Fehlings MG**, Tetreault LA, Wilson JR, Kwon BK, Burns AS, Martin AR, Hawryluk G, Harrop JS. A Clinical Practice Guideline for the Management of Acute Spinal Cord Injury: Introduction, Rationale, and Scope. *Global Spine J* 2017; **7**: 84S-94S [PMID: 29164036 DOI: 10.1177/2192568217703387]
12 **Absoud M**, Greenberg BM, Lim M, Lotze T, Thomas T, Deiva K. Pediatric transverse myelitis. *Neurology* 2016; **87**: S46-S52 [PMID: 27572861 DOI: 10.1212/WNL.0000000000002820]
13 **Kirshblum S**, Snider B, Rupp R, Read MS; International Standards Committee of ASIA and ISCoS. Updates of the International Standards for Neurologic Classification of Spinal Cord Injury: 2015 and 2019. *Phys Med Rehabil Clin N Am* 2020; **31**: 319-330 [PMID: 32624097 DOI: 10.1016/j.pmr.2020.03.005]
14 **Konstantinou GN**. Enzyme-Linked Immunosorbent Assay (ELISA). *Methods Mol Biol* 2017; **1592**: 79-94 [PMID: 28315213 DOI: 10.1007/978-1-4939-6925-8_7]
15 **Rodríguez Y**, Rojas M, Pacheco Y, Acosta-Ampudia Y, Ramírez-Santana C, Monsalve DM, Gershwin ME, Anaya JM. Guillain-Barré syndrome, transverse myelitis and infectious diseases. *Cell Mol Immunol* 2018; **15**: 547-562 [PMID: 29375121 DOI: 10.1038/cmi.2017.142]
16 **Fukuoka M**, Kuki I, Kawawaki H, Kim K, Hattori Y, Tsuji H, Horino A, Nukui M, Okazaki S. A pediatric patient of hemorrhagic acute transverse myelitis. *Brain Dev* 2017; **39**: 252-255 [PMID: 27686688 DOI: 10.1016/j.braindev.2016.09.007]
17 **Merchan-Del Hierro X**, Halalau A. Cytomegalovirus-related transverse myelitis in an immunocompetent host: a subacute onset of an immune-mediated disease? *BMJ Case Rep* 2017; **2017** [PMID: 28801328 DOI: 10.1136/bcr-2017-220563]
18 **New PW**, Astrakhantseva I. Rehabilitation outcomes following infections causing spinal cord myelopathy. *Spinal Cord* 2014; **52**: 444-448

[PMID: 24663003 DOI: 10.1038/sc.2014.29]

19 **Tandon R**, Kumar A. Long-Segment Myelitis, Meningoencephalitis, and Axonal Polyneuropathy in a Case of Scrub Typhus. *Ann Indian Acad Neurol* 2019; **22**: 237-240 [PMID: 31007446 DOI: 10.4103/aian.AIAN_66_18]

20 **Wang J**, Zhang Q, Lu Y, Dong Y, Dhandapani KM, Brann DW, Yu RK. Ganglioside GD3 is up-regulated in microglia and regulates phagocytosis following global cerebral ischemia. *J Neurochem* 2021; **158**: 737-752 [PMID: 34133773 DOI: 10.1111/jnc.15455]

21 **Chio JCT**, Xu KJ, Popovich P, David S, Fehlings MG. Neuroimmunological therapies for treating spinal cord injury: Evidence and future perspectives. *Exp Neurol* 2021; **341**: 113704 [PMID: 33745920 DOI: 10.1016/j.expneurol.2021.113704]

22 **Shen J**, Gao F, Zhao L, Hao Q, Yang YL. MicroRNA-34c promotes neuronal recovery in rats with spinal cord injury through the C-X-C motif ligand 14/Janus kinase 2/signal transducer and activator of transcription-3 axis. *Chin Med J (Engl)* 2020; **133**: 2177-2185 [PMID: 32826607 DOI: 10.1097/CM9.0000000000001022]

23 **Zeng Y**, Xiong M, Yu H, He N, Wang Z, Liu Z, Han H, Chen S. [Clinical effect of methylprednisolone sodium succinate and mouse nerve growth factor for injection in treating acute spinal cord injury and cauda equina injury]. *Zhongguo Xiu Fu Chong Jian Wai Ke Za Zhi* 2010; **24**: 1208-1211 [PMID: 21049601]

24 **Zhai HW**, Gong ZK, Sun J, Chen W, Zhang M, Zhou JJ, Zheng B. Ganglioside with nerve growth factor for the recovery of extremity function following spinal cord injury and somatosensory evoked potential. *Eur Rev Med Pharmacol Sci* 2015; **19**: 2282-2286 [PMID: 26166655]

25 **Hu H**, Wang H, Liu W. Effect of ganglioside combined with Chip Jiaji electro-acupuncture on Nogo-NgR signal pathway in SCI rats. *Saudi J Biol Sci* 2021; **28**: 4132-4136 [PMID: 34354392 DOI: 10.1016/j.sjbs.2021.02.031]

26 **Schmidt SC**, Hamann S, Langrehr JM, Höflich C, Mittler J, Jacob D, Neuhaus P. Preoperative high-dose steroid administration attenuates the surgical stress response following liver resection: results of a prospective randomized study. *J Hepatobiliary Pancreat Surg* 2007; **14**: 484-492 [PMID: 17909718 DOI: 10.1007/s00534-006-1200-7]

World Journal of Clinical Cases

Submit a Manuscript: https://www.f6publishing.com

World J Clin Cases 2023 November 26; 11(33): 7980-7986

DOI: 10.12998/wjcc.v11.i33.7980

ISSN 2307-8960 (online)

ORIGINAL ARTICLE

Retrospective Study

Treatment of postpartum depression with integrated traditional Chinese and Western medicine nursing and electrical stimulation

Wen-Hui Zhai, Mei-Jiao Wang, Yi-Jing Zhao, Shuang-Ling Hu, Jin-Man Zhou

Specialty type: Medicine, research and experimental

Provenance and peer review: Unsolicited article; Externally peer reviewed.

Peer-review model: Single blind

Peer-review report's scientific quality classification

Grade A (Excellent): 0
Grade B (Very good): 0
Grade C (Good): C
Grade D (Fair): 0
Grade E (Poor): 0

P-Reviewer: Cotie LM, Canada

Received: September 14, 2023
Peer-review started: September 14, 2023
First decision: September 28, 2023
Revised: October 9, 2023
Accepted: November 10, 2023
Article in press: November 10, 2023
Published online: November 26, 2023

Wen-Hui Zhai, Mei-Jiao Wang, Yi-Jing Zhao, Shuang-Ling Hu, Psychiatric Intensive Care Unit 2, Wudong Hospital, Wuhan 430084, Hubei Province, China

Jin-Man Zhou, Department of Nursing, Wuchang Hospital Affiliated to Wuhan University of Science and Technology, Wuhan 430063, Hubei Province, China

Corresponding author: Jin-Man Zhou, MD, Doctor, Department of Nursing, Wuchang Hospital Affiliated to Wuhan University of Science and Technology, No. 116 Yangyuan Street, Wuchang District, Wuhan 430063, Hubei Province, China. zhoujinman2023@163.com

Abstract

BACKGROUND

Postpartum depression (PPD) is a common psychological disease among puerperal women, and postpartum pelvic floor dysfunction is a common disease among pregnant women. The occurrence of postpartum pelvic floor dysfunction will increase the incidence of PPD.

AIM

To explore the therapeutic effect of integrated traditional Chinese and Western medicine nursing combined with electrical stimulation of pelvic floor muscles and the rectus abdominis on PPD.

METHODS

From April 2020 to January 2022, 100 parturients with a rectus abdominis muscle separation distance > 2.0 cm who underwent reexamination 6 wk after delivery at our hospital were selected as the research subjects. According to the random number table method, the patients were divided into either an observation group (n = 50) or a control group (n = 50). There was no significant difference in the general data between the two groups (P > 0.05). Both groups were treated by electrical stimulation. The observation group was additionally treated by integrated traditional Chinese and Western medicine nursing. A self-designed Depression Knowledge Questionnaire was used to evaluate the awareness of knowledge on depression in all patients 3 wk after intervention. The Hamilton Depression Scale (HAMD) was used to evaluate the depression before intervention and 1 wk and 3 wk after intervention, and the Morisky Medication Adherence Scale (MMAS-8) was used to evaluate the medication compliance. SPSS19.0 was used for statistical analyses.

RESULTS
The rate of awareness of knowledge on depression in the observation group was significantly higher than that of the control group ($P < 0.05$). The scores of MMAS-8 were comparable between the two groups before intervention ($P > 0.05$), but were significantly higher in the observation group than in the control group at 1 wk and 3 wk after intervention ($P < 0.05$). The HAMD scores were comparable between the two groups before intervention ($P > 0.05$), but were significantly lower in the observation group than in the control group at 1 wk and 3 wk after intervention ($P < 0.05$).

CONCLUSION
Integrated traditional Chinese and Western medicine nursing combined with electrical stimulation of pelvic floor muscles and the rectus abdominis is effective in the treatment of postpartum depression and worthy of clinical promotion.

Key Words: Integrated traditional Chinese and Western medicine nursing; Pelvic floor muscles; Rectus abdominis; Electrical stimulation; Postpartum depression

©The Author(s) 2023. Published by Baishideng Publishing Group Inc. All rights reserved.

Core Tip: As a common disease among pregnant women, postpartum pelvic floor dysfunction can seriously increase the incidence of postpartum depression (PPD). The purpose of this study was to explore the therapeutic effect of integrated traditional Chinese and Western medicine nursing combined with electrical stimulation of pelvic floor muscles and the rectus abdominis on PPD. After randomly selecting parturients with pelvic floor dysfunction, they were given electric stimulation therapy, either alone or in combination with integrated traditional Chinese and Western medicine nursing. The results showed that the combination of traditional Chinese and Western medicine nursing and electrical stimulation of pelvic floor muscles and the rectus abdominis was effective in the treatment of PPD.

Citation: Zhai WH, Wang MJ, Zhao YJ, Hu SL, Zhou JM. Treatment of postpartum depression with integrated traditional Chinese and Western medicine nursing and electrical stimulation. *World J Clin Cases* 2023; 11(33): 7980-7986
URL: https://www.wjgnet.com/2307-8960/full/v11/i33/7980.htm
DOI: https://dx.doi.org/10.12998/wjcc.v11.i33.7980

INTRODUCTION

Postpartum depression (PPD) refers to maternal depression during the puerperium. The prevalence of PPD in Western developed countries is 7%-40%, and it is 3.5%-63.3% in Asian countries[1]. The reported prevalence of PPD in China ranges from 1.1%-52.1%, with an average of 14.7%[2]. The strongest correlation factors include not only previous history of mental illness and positive family history, but also individual psychological factors and obstetric factors[3]. Postpartum pelvic floor dysfunction is a common disease in pregnant women[4]. Pregnancy and childbirth can lead to different degrees of damage to the structure and function of the pelvic floor[5]. If postpartum pelvic floor injury is not recovered in time and effectively, different degrees of pelvic floor dysfunction diseases may occur, such as pelvic organ prolapse, stress urinary incontinence, chronic pelvic pain, sexual dysfunction, and abnormal defecation, affecting the patient's physical and mental health and quality of life and thus aggravating PPD[6]. The three main current treatments for PPD are medication, psychotherapy, and physical therapy. Evidence-based medical evidence has shown that the effect of comprehensive treatment is better than that of any single treatment[7-9]. Electrical stimulation of pelvic floor muscles and the rectus abdominis can achieve the contraction and tension of pelvic floor muscles and the rectus abdominis, provide structural support for the lower abdomen, bladder, and urethra, and enhance the strength of the urethral sphincter, thereby greatly reducing the occurrence of rectus abdominis muscle dehiscence, pelvic organ prolapse, urinary incontinence, and other dysfunction diseases[10]. This study aimed to explore the therapeutic effect of integrated traditional Chinese and Western medicine nursing combined with electrical stimulation of pelvic floor muscles and the rectus abdominis in the treatment of PPD[11].

MATERIALS AND METHODS

Research subjects

From April 2020 to January 2022, 100 parturients with a rectus abdominis separation distance > 2.0 cm at our hospital were selected as the research subjects. The inclusion criteria were as follows: A distance between rectus abdominis muscles > 2 cm and receiving outpatient examination at our hospital 6 wk after delivery. Informed consent was provided by the patients and their families in accordance with the Declaration of Helsinki of the World Medical Association. Their

age ranged from 20 to 40 years. The exclusion criteria were: Previous history of abdominal surgery (except cesarean section); congenital abdominal wall dysplasia; patients with abdominal rash, infection, and other diseases; contraindications for electrical stimulation therapy; withdrawal of consent or loss to follow-up. Using the random number table method, the patients were divided into either an observation group (n = 50) or a control group (n = 50). The age of patients in the observation group was 21-42 years, with an average of 31.83 ± 2.68 years. The mean gestational age was 39.54 ± 1.03 wk (range, 36-42 wk). The mean number of pregnancies was 1.54 ± 0.27 (range, 0-3). Regarding the mode of delivery, vaginal delivery was used in 16 cases and cesarean section in 36 cases. The average age of patients in the control group was 31.22 ± 2.45 years (range, 21-40 years). Gestational age ranged from 36 to 41 wk, with an average of 39.19 ± 1.35 wk. The mean number of pregnancies ranged from 0 to 3 (mean, 1.46 ± 0.23). Vaginal delivery was used in 13 cases and caesarean section in 38 cases. There was no significant difference in the general data between the two groups (P > 0.05).

Research methods

Both groups were treated by electrical stimulation: Phenix USB 4 neuromuscular therapy instrument (French Sugiyaman) was used to connect the electrode lines A1+, A1-, A2+, A2-, B1+, B1-, B2+, and B2- channels, and the electrode sheets were glued to the rectus abdominis, transverse abdominis, and external abdominal oblique and internal abdominal oblique muscles on both sides. The power supply of the therapeutic instrument was switched on, and the interval distance program (U8) was used to set the frequency and pulse width parameters as 30 Hz/200 s, 75 Hz/400 s, 4 Hz/300 s, and 3 Hz/150 s, and the treatment time as 8 s, 7 s, 11 s, and 6 s, respectively. According to the standard of muscle tingling and contraction without pain, the current was set at 30 min/time, once a day, and the treatment was continued for 15 d.

The observation group was additionally treated by integrated traditional Chinese and Western medicine nursing consisting of: (1) Traditional Chinese medicine emotional nursing. The seven emotions are people's emotional reactions to objective things. In the emotional state, the human body's tolerance is not high, which leads to the disorder of the body and the imbalance of Yin and Yang of the Zang Fu organs and causes diseases. As a result, there will be bad psychological concerns such as anxiety, depression, and fear. Therefore, nursing staff can conduct modern modulation. Specifically, nursing staff can keep close relations with patients, keep patience to listen to their inner emotion expression, speech implement induction, modern guide pathogenesis and abnormal emotional reflection. Nursing staff can also inform patients to guard against arrogance and impatience, actively comply with medical and nursing instructions, and relieve physical and mental discomfort; (2) Strengthening the health education of patients and improving their self-care ability. This occurred mainly in the form of explanation, demonstration, and publicity materials, so that patients and their families can obtain the related knowledge of postpartum care, gradually get rid of the dependence of patients, and improve their self-care ability; (3) Diet care. Postoperative diet conditioning was mainly adopted. The initial diet should be from less to more, from thin to thick, and from simple to complex. Light foods with low residue and no stimulation and appropriate amount of vegetables and fruits should be given so that the stool is soft but not loose. During the recovery period, the diet nursing followed the principle of syndrome differentiation and feeding. Patients with Yin deficiency were given light nourishing food such as lily and tremella; those with Qi deficiency were given jujube, pigeons, and other Qi nourishing food; those with blood deficiency to give pig liver, longan meat, and other blood supplementing food. If the stool was loose, apple juice was given to neutralize the spleen and stomach and stop diarrhea; and (4) Pelvic floor muscle relaxation may only manifest as vaginal laxity, lower abdominal distention, frequent urination, and urgency at the beginning, but it will slowly evolve into urinary incontinence, uterine prolapse, *etc*. Sphincter contraction was conducted in a sitting position by consciously contracting the urethra, vagina, and rectal sphincter, and then relaxing. This was repeated 50 to 100 times, 2 to 3 times a day. During urination, patients were asked to consciously contract the perineum, stop urination, and then relax the perineal muscles and continue to urinate. This was repeated 2-3 times a day until the urine was emptied.

Investigation and analysis of depression

A self-designed Depression Knowledge Questionnaire was used to evaluate the awareness on knowledge of disease in all patients 3 wk after intervention. The Hamilton Depression Scale (HAMD) was used to evaluate the depression before intervention and 1 wk and 3 wk after intervention, and the Morisky Medication Adherence Scale (MMAS-8) was used to evaluate the medication compliance. The degree of awareness of disease knowledge, medication compliance, and depression before intervention and 1 wk and 3 wk after intervention were statistically analyzed. The Depression Knowledge Questionnaire has a 5-point scale (1-5 points), including disease knowledge, drug usage and dosage and precautions, psychological adjustment, outpatient review, self-emotion adjustment, recurrence prevention, *etc*., with a total of 100 points; the higher the score, the better the knowledge. The Cronbach's reliability coefficient is 0.888, and the validity coefficient is 0.840. A score < 60 was classified as unawareness, 60-80 was classified as basic awareness, > 80 was classified as awareness, and the awareness rate was calculated as (number of patients with awareness + number of patients with basic awareness)/total number of cases × 100%. The MMAS-8 questionnaire has a 1-point scale (0-1 points), with a total of eight items, and the total score is 8 points. The higher the score, the better the compliance. The Cronbach's α reliability coefficient is 0.892, and the validity coefficient is 0.848. The HAMD scale has a 4-point scale (0-4 points), with 17 items, and the total score is 68 points. The higher the score, the more serious the depression. The Cronbach's α reliability coefficient is 0.896, and the validity coefficient is 0.851.

Statistical analysis

Statistical analyses were performed using SPSS 19.0. Measurement data are expressed as the mean ± standard deviation and were compared using the t-test, while count data are expressed as n (%) and were compared using the χ^2 test. All data were considered statistically significant at P < 0.05.

Table 1 Comparison of awareness of depression knowledge between the two groups (*n*)

Group	*n*	Awareness	Basic awareness	Unawareness	Compliance rate (%)
Control	50	10	31	9	82.00
Observation	50	15	34	1	98.00
χ^2					7.111
P value					0.015

Table 2 Comparison of Morisky Medication Compliance Questionnaire scores between the two groups

Group	*n*	Before intervention	1 wk after intervention	3 wk after intervention
Control	50	4.75 ± 0.58	5.32 ± 0.65	6.35 ± 0.85
Observation	50	4.81 ± 0.60	6.15 ± 0.76	7.43 ± 0.92
t value		0.508	5.869	6.097
P value		0.522	< 0.001	< 0.001

Table 3 Comparison of Hamilton Depression Scale scores between the two groups

Group	*n*	Before intervention	1 wk after intervention	3 wk after intervention
Control	50	38.72 ± 5.52	35.21 ± 4.72	28.25 ± 3.94
Observation	50	39.08 ± 5.48	31.17 ± 4.29	23.52 ± 3.57
t value		0.327	4.479	6.291
P value		0.711	< 0.001	< 0.001

RESULTS

Comparison of awareness of depression knowledge between the two groups

The ***awareness*** rate of depression knowledge in the observation group was significantly higher than that of the control group ($P < 0.05$; Table 1).

Comparison of MMAS-8 scores between the two groups

The MMAS-8 scores in the control group and the observation group before intervention were comparable ($P > 0.05$), but they were significantly higher in the observation group than in the control group at 1 wk and 3 wk after intervention ($P < 0.05$; Table 2).

Comparison of HAMD scores between the two groups

The HAMD scores of the control group and the observation group before intervention were comparable ($P > 0.05$), but they were significantly lower in the observation group than in the control group at 1 wk and 3 wk after intervention ($P < 0.05$; Table 3).

DISCUSSION

Depression, also known as depressive disorder, is characterized by significant and persistent low mood, with high incidence, high recurrence, high disability, high suicide rate, and other characteristics. Depression can range from melancholy to grief, accompanied by anxiety, hallucinations, delusions, and other psychotic symptoms. At present, the main treatment for depression is drug therapy, which can effectively control the patient's condition, and the degree of awareness of disease knowledge plays an important role in drug therapy. The rectus abdominis is located on both sides of the median line of the anterior abdominal wall[11-13]. It is a band shaped multi-abdominal muscle with a narrow upper and wide lower structure[14]. As a core abdominal muscle group, the rectus abdominis can not only control the spine and pelvis movement, but also maintain negative pressure to assist breathing and body movement. Rectus abdominis separation may lead to increased intra-abdominal pressure, low back pain, abnormal posture, pelvic anteversion, and so on[15]. With the opening of the second and third child policy in China, multiple pregnancies, macrocephaly, and cesarean section are considered to be the important influencing factors of rectus abdominis muscle separation[16-17].

In China, the current mainstream psychological intervention is a trinity intervention model (bio-psychology-social model), the greatest feature of which is to decompose the causes of all psychological diseases and find out the primary causes of psychological diseases by tracing to its source[18,19]. Although theoretically it is generally applicable, for individuals, it is often necessary to formulate corresponding intervention plans according to the experiences and living conditions of different individuals in advance, so as to make specific analysis of specific problems. At the same time, the corresponding auxiliary means usually do not have a high threshold in the application process, so it has a strong advantage in the field of specific analysis of mental illness[20,21].

Emotional disorder mainly refers to the phenomenon of uncontrolled emotional self-regulation caused by the comprehensive action of internal and external factors. The causes of this disorder are complex, including endocrine disorders, emotional vulnerability to small environment and climate, the past pressure that has not been reasonably released, too paranoid attitude towards some things, *etc.* The process of childbirth described above can be seen either as a previous stressor or as a unique experience, which can be considered as a psychogenic risk factor for maternal mood disorders[22-23]. However, there are some shortcomings in this study. The HAMD and MMAS-8 data were measured only at 1 and 3 wk after the intervention[24]. Although there was marked improvement in depression, long-term measures of antidepressant and medication adherence remain unclear.

Therefore, future studies should increase the follow-up time and systematically measure the therapeutic effects of integrated traditional Chinese and Western medicine nursing combined with electrical stimulation of pelvic floor muscles and the rectus abdominis.

CONCLUSION

In conclusion, integrated traditional Chinese and Western medicine nursing combined with electrical stimulation of pelvic floor muscles and the rectus abdominis has good therapeutic effects in the treatment of PPD, which is worthy of clinical promotion.

ARTICLE HIGHLIGHTS

Research background

Puerperal women are prone to postpartum pelvic floor dysfunction and psychological depression, and postpartum pelvic floor dysfunction often aggravates psychological depression.

Research motivation

Integrated traditional Chinese and Western medicine nursing and electrical stimulation of pelvic floor muscles and the rectus abdominis can relieve mental depression and postpartum pelvic floor dysfunction, respectively, which may relieve the psychological depression of parturient women.

Research objectives

The purpose of this study was to explore the clinical therapeutic effects of integrated traditional Chinese and Western medicine nursing combined with electrical stimulation of pelvic floor muscles and the rectus abdominis.

Research methods

Through a randomized controlled trial, puerperal women were treated by electrical stimulation of pelvic floor muscles and the rectus abdominis, alone or in combination with integrated traditional Chinese and Western medicine nursing, and their psychological status was assessed.

Research results

The awareness rate of depression knowledge in the observation group was significantly higher than that of the control group. After 1 wk and 3 wk of intervention, the Morisky Medication Compliance Questionnaire score in the observation group was significantly higher than that of the control group, and the Hamilton Depression Scale score was significantly lower than that of the control group.

Research conclusions

Integrated traditional Chinese and Western medicine nursing combined with electrical stimulation of pelvic floor muscles and the rectus abdominis has a significant effect on postpartum depression.

Research perspectives

Integrated traditional Chinese and Western medicine nursing combined with electrical stimulation of pelvic floor muscles and the rectus abdominis can relieve postpartum pelvic floor dysfunction and maternal depression, which has extensive clinical significance.

ACKNOWLEDGEMENTS

We would like to express my gratitude to all those who helped us during the writing of this paper. We acknowledge the help of my colleagues for their suggestions in academic studies.

FOOTNOTES

Co-first authors: Wen-Hui Zhai and Mei-Jiao Wang.

Author contributions: Zhai WH and Wang MJ conceived, designed, and refined the study protocol; Zhao YJ and Zhou JM were involved in data collection; Zhai WH, Wang MJ, Zhou JMz, and Hu SL analyzed the data; Zhai WH and Wang MJ drafted the manuscript; all authors were involved in the critical review of the results and read and approved the final manuscript. Zhai WH and Wang MJ as co-first authors contributed equally to this work. The reasons for designating Zhai WH and Wang MJ as co-first authors are threefold. First, the research was performed as a collaborative effort, and the designation of co-first authorship accurately reflects the distribution of responsibilities and burdens associated with the time and effort required to complete the study and the resultant paper. This also ensures effective communication and management of post-submission matters, ultimately enhancing the paper's quality and reliability. Second, the overall research team encompassed authors with a variety of expertise and skills from different fields, and the designation of co-first authors best reflects this diversity. This also promotes the most comprehensive and in-depth examination of the research topic, ultimately enriching readers' understanding by offering various expert perspectives. Third, Zhai WH and Wang MJ contributed efforts of equal substance throughout the research process. The choice of these researchers as co-first authors acknowledges and respects this equal contribution, while recognizing the spirit of teamwork and collaboration of this study. In summary, we believe that designating Wen-Hui Zhai and Mei-Jiao Wang as co-first authors is fitting for our manuscript as it accurately reflects our team's collaborative spirit, equal contributions, and diversity.

Supported by 2017 Wuhan Medical Research Project, No. WZ17Z11; 2021 Wuhan Medical Research Project, No. WX21Z65.

Institutional review board statement: This study was approved by the Wuchang Hospital Affiliated to Wuhan University of Science and Technology.

Informed consent statement: All the patients voluntarily participated in the study and signed informed consent forms.

Conflict-of-interest statement: The authors declare no conflict of interest for this paper.

Data sharing statement: Data generated from this investigation are available upon reasonable quest from the corresponding author.

Open-Access: This article is an open-access article that was selected by an in-house editor and fully peer-reviewed by external reviewers. It is distributed in accordance with the Creative Commons Attribution NonCommercial (CC BY-NC 4.0) license, which permits others to distribute, remix, adapt, build upon this work non-commercially, and license their derivative works on different terms, provided the original work is properly cited and the use is non-commercial. See: https://creativecommons.org/Licenses/by-nc/4.0/

Country/Territory of origin: China

ORCID number: Jin-Man Zhou 0009-0009-9992-7116.

S-Editor: Lin C
L-Editor: Wang TQ
P-Editor: Xu ZH

REFERENCES

1 **Rogers SL**, Hughes BA, Tomlinson JW, Blissett J. Cortisol metabolism, postnatal depression and weight changes in the first 12 month postpartum. *Clin Endocrinol (Oxf)* 2016; **85**: 881-890 [PMID: 27374760 DOI: 10.1111/cen.13150]
2 **Zhang AH**, Li CL. A study on the impact of refined nursing combined with health care on postpartum depression based on the concept of humanization. *Lingchuang Yixue Gongcheng* 2022; **29**: 1273-1274
3 **Zhou L**, Wu ZT, Wang GH, Xiao L, Wang HL. Research progress on the construction of postpartum depression model and the effect of mother-infant separation on postpartum depression. *Wuhan Daxue Xuebao (Yixueban)* 2023; **44**: 1023-1026 [DOI: 10.14188/J.1671-8852.2021.0731]
4 **Wu P**. Current status of drug therapy for postpartum depression. *Tianjin Yaoxue***34**: 69-73
5 **Nishibayashi M**, Okagaki R. Ultrasonographic evaluation of pelvic floor structure at antepartum and postpartum periods using three-dimensional transperineal ultrasound. *J Med Ultrason (2001)* 2021; **48**: 345-351 [PMID: 33963946 DOI: 10.1007/s10396-021-01100-7]
6 **Khorasani F**, Ghaderi F, Bastani P, Sarbakhsh P, Berghmans B. The Effects of home-based stabilization exercises focusing on the pelvic floor on postnatal stress urinary incontinence and low back pain: a randomized controlled trial. *Int Urogynecol J* 2020; **31**: 2301-2307 [PMID: 32274521 DOI: 10.1007/s00192-020-04284-7]
7 **Kroska EB**, Stowe ZN. Postpartum Depression: Identification and Treatment in the Clinic Setting. *Obstet Gynecol Clin North Am* 2020; **47**: 409-419 [PMID: 32762926 DOI: 10.1016/j.ogc.2020.05.001]
8 **Li W**, Yin P, Lao L, Xu S. Effectiveness of Acupuncture Used for the Management of Postpartum Depression: A Systematic Review and

Meta-Analysis. *Biomed Res Int* 2019; **2019**: 6597503 [PMID: 31016194 DOI: 10.1155/2019/6597503]
9 **Frieder A**, Fersh M, Hainline R, Deligiannidis KM. Pharmacotherapy of Postpartum Depression: Current Approaches and Novel Drug Development. *CNS Drugs* 2019; **33**: 265-282 [PMID: 30790145 DOI: 10.1007/s40263-019-00605-7]
10 **Liu X**, Wang Q, Chen Y, Luo J, Wan Y. Factors Associated With Stress Urinary Incontinence and Diastasis of Rectus Abdominis in Women at 6-8 Weeks Postpartum. *Urogynecology (Phila)* 2023; **29**: 844-850 [PMID: 37093577 DOI: 10.1097/SPV.0000000000001353]
11 **Liang P**, Liang M, Shi S, Liu Y, Xiong R. Rehabilitation programme including EMG-biofeedback- assisted pelvic floor muscle training for rectus diastasis after childbirth: a randomised controlled trial. *Physiotherapy* 2022; **117**: 16-21 [PMID: 36219918 DOI: 10.1016/j.physio.2022.05.001]
12 **Brummelte S**, Galea LA. Postpartum depression: Etiology, treatment and consequences for maternal care. *Horm Behav* 2016; **77**: 153-166 [PMID: 26319224 DOI: 10.1016/j.yhbeh.2015.08.008]
13 **Dennis CL**, Dowswell T. Psychosocial and psychological interventions for preventing postpartum depression. *Cochrane Database Syst Rev* 2013; CD001134 [PMID: 23450532 DOI: 10.1002/14651858.CD001134.pub3]
14 **Mughal S**, Azhar Y, Siddiqui W. Postpartum Depression. In: StatPearls [Internet]. Treasure Island (FL): StatPearls Publishing, 2023
15 **Tani F**, Castagna V. Maternal social support, quality of birth experience, and post-partum depression in primiparous women. *J Matern Fetal Neonatal Med* 2017; **30**: 689-692 [PMID: 27123699 DOI: 10.1080/14767058.2016.1182980]
16 **Dennis CL**, Creedy D. Psychosocial and psychological interventions for preventing postpartum depression. *Cochrane Database Syst Rev* 2004; CD001134 [PMID: 15495008 DOI: 10.1002/14651858.CD001134.pub2]
17 **Ma YM**, Zhang LH, Wang F, Li J, Wei YY, Qin C. Research advances in the care of postpartum depression [J]. *Zhongguo Yiyao Kexue* 2022; **12**: 54-56+70
18 **Li C**, Yu T, Wang XQ. Knowledge graph evolution of domestic postpartum depression research based on CiteSpace bibliometrics. *Bengbu Yixueyuan Xuebao* 2022; **47**: 236-241 [DOI: 10.13898/j.cnki.issn.1000-2200.2022.02.025]
19 **Ye S**, Xie WS, Fang L, Hu Y, Hu ZY. Research progress of non-drug therapy for postpartum depression. *Xinyixue***53**: 1-4
20 **Lin PZ**, Xue JM, Yang B, Li M, Cao FL. Effectiveness of self-help psychological interventions for treating and preventing postpartum depression: a meta-analysis. *Arch Womens Ment Health* 2018; **21**: 491-503 [PMID: 29616334 DOI: 10.1007/s00737-018-0835-0]
21 **Anokye R**, Acheampong E, Budu-Ainooson A, Obeng EI, Akwasi AG. Prevalence of postpartum depression and interventions utilized for its management. *Ann Gen Psychiatry* 2018; **17**: 18 [PMID: 29760762 DOI: 10.1186/s12991-018-0188-0]
22 **Jiang L**, Wang ZZ, Qiu LR, Wan GB, Lin Y, Wei Z. Psychological intervention for postpartum depression. *J Huazhong Univ Sci Technolog Med Sci* 2014; **34**: 437-442 [PMID: 24939313 DOI: 10.1007/s11596-014-1297-x]
23 **Loughnan SA**, Joubert AE, Grierson A, Andrews G, Newby JM. Internet-delivered psychological interventions for clinical anxiety and depression in perinatal women: a systematic review and meta-analysis. *Arch Womens Ment Health* 2019; **22**: 737-750 [PMID: 31101993 DOI: 10.1007/s00737-019-00961-9]
24 **Terrone G**, Bianciardi E, Fontana A, Pinci C, Castellani G, Sferra I, Forastiere A, Merlo M, Marinucci E, Rinaldi F, Falanga M, Pucci D, Siracusano A, Niolu C. Psychological Characteristics of Women with Perinatal Depression Who Require Psychiatric Support during Pregnancy or Postpartum: A Cross-Sectional Study. *Int J Environ Res Public Health* 2023; **20** [PMID: 37107790 DOI: 10.3390/ijerph20085508]

World Journal of Clinical Cases

Submit a Manuscript: https://www.f6publishing.com

World J Clin Cases 2023 November 26; 11(33): 7987-7993

DOI: 10.12998/wjcc.v11.i33.7987

ISSN 2307-8960 (online)

ORIGINAL ARTICLE

Retrospective Study

Prolonged impacts of COVID-19-associated cystitis: A study on long-term consequences

Sophie Wittenberg, Jack Vercnocke, Michael Chancellor, Sorabh Dhar, Aron Liaw, Steven Lucas, Nivedita Dhar

Specialty type: Urology and nephrology

Provenance and peer review: Invited article; Externally peer reviewed.

Peer-review model: Single blind

Peer-review report's scientific quality classification
Grade A (Excellent): 0
Grade B (Very good): 0
Grade C (Good): C, C
Grade D (Fair): 0
Grade E (Poor): 0

P-Reviewer: Ait Addi R, Morocco; Dai DL, China

Received: August 28, 2023
Peer-review started: August 28, 2023
First decision: November 1, 2023
Revised: November 6, 2023
Accepted: November 17, 2023
Article in press: November 17, 2023
Published online: November 26, 2023

Sophie Wittenberg, Jack Vercnocke, Aron Liaw, Steven Lucas, Department of Urology, Wayne State University School of Medicine, Detroit, MI 48201, United States

Michael Chancellor, Department of Urology, Beaumont Hospital, Royal Oak, MI 48067, United States

Sorabh Dhar, Infectious Disease, Wayne State University School of Medicine, Detroit, MI 48201, United States

Sorabh Dhar, Infectious Disease, John D. Dingell VA Medical Center, Detroit, MI 48201, United States

Sorabh Dhar, Infectious Disease, Detroit Medical Center, Detroit, MI 48201, United States

Aron Liaw, Steven Lucas, Nivedita Dhar, Department of Urology, John D. Dingell VA Medical Center, Detroit, MI 48201, United States

Nivedita Dhar, Department of Urology, Detroit Medical Center, Detroit, MI 48201, United States

Corresponding author: Nivedita Dhar, MD, Doctor, Department of Urology, John D. Dingell VA Medical Center, 4646 John R Street, Detroit, MI 48201, United States. ec0362@wayne.edu

Abstract

BACKGROUND

The Coronavirus Disease 2019 (COVID-19) caused by the severe acute respiratory syndrome coronavirus 2 virus is an international health concern with substantial morbidity and mortality. COVID-associated cystitis (CAC), presents as new onset or exacerbated urinary symptoms, resembling overactive bladder (OAB) symptoms.

AIM

To examines the long-term outcomes of patients with CAC in the context of Long COVID.

METHODS

A cohort of 350 patients admitted to Detroit Hospitals with COVID-19 between May and December 2020, displaying CAC symptoms following discharge, was

prospectively followed. Initial urologic evaluations occurred at 10-14 wk and were repeated at 21-28 mo post-discharge. Symptoms were managed conservatively, employing behavioral modifications and standard OAB medications. Participants completed surveys assessing urinary symptoms and quality of life (QoL) at both time points. The primary outcome was the Urology Care Foundation Overactive Bladder Assessment Tool.

RESULTS

87% of the final cohort (n = 310) reported symptom improvement at 21-28 mo post-discharge. Patients with new onset CAC symptoms showed a median decrease of 9-10 points in OAB and QoL scores, while those with existing symptoms experienced a decrease of 6 points. Overall, 95.4% of patients with new onset symptoms reported symptom improvement at follow-up, contrasting with 60.7% among those with existing symptoms.

CONCLUSION

This study presents the first long-term follow-up of adult patients with CAC, revealing a promising prognosis with conservative management measures in the context of Long COVID. These findings provide reassurance to patients regarding symptom resolution and underscore the need for further research into this evolving aspect of COVID-19's impact on urological health.

Key Words: COVID associated cystitis; COVID-19; Long COVID; Overactive bladder

©The Author(s) 2023. Published by Baishideng Publishing Group Inc. All rights reserved.

Core Tip: Coronavirus disease (COVID)-associated cystitis (CAC), presents as new onset or exacerbated urinary symptoms that may resemble overactive bladder symptoms. To our knowledge, this study is the first long-term follow-up of adult patients with CAC. Our data reveals a promising prognosis with conservative management measures in the context of Long COVID. These findings provide reassurance to patients regarding symptom resolution and underscore the need for further research into this evolving aspect of COVID-19's impact on urological health.

Citation: Wittenberg S, Vercnocke J, Chancellor M, Dhar S, Liaw A, Lucas S, Dhar N. Prolonged impacts of COVID-19-associated cystitis: A study on long-term consequences. *World J Clin Cases* 2023; 11(33): 7987-7993
URL: https://www.wjgnet.com/2307-8960/full/v11/i33/7987.htm
DOI: https://dx.doi.org/10.12998/wjcc.v11.i33.7987

INTRODUCTION

Coronavirus Disease 2019 (COVID-19) is an infection caused by the severe acute respiratory syndrome coronavirus 2 (SARS-CoV-2) virus which was originally identified in late 2019. There have been over 100 million reported cases and over 1 million deaths from COVID-19 in the United States since January 2020. It is clinically defined by a constellation of symptoms including fever, upper respiratory symptoms, and fatigue, among many others. While most of the symptoms associated with acute COVID-19 infection are upper respiratory in nature, numerous organ systems have been recognized to be associated with COVID-19 infection. Urologic manifestations of COVID-19 have been limited, with the coronavirus family in general causing renal and testicular dysfunction, and having only a low likelihood of being detected in the urine [1,2]. Early studies noted increases in urinary frequency, urgency, and nocturia post COVID-19 infection and termed this condition COVID-associated cystitis (CAC)[3].

The COVID-19 recovery time ranges from up to 7 days for mild illness to > 6 wk for severe cases[4]. However, approximately 80% of recovered patients will have one or more long-lasting symptoms[5]. CAC, a condition associated with new onset urinary symptoms or exacerbations of existing urinary symptoms is believed to be a manifestation of Long COVID [6]. Most commonly, patients experience new onset or exacerbation of existing symptoms consistent with overactive bladder (OAB). Clinical presentation can include urgency, frequency, nocturia, dysuria and/or urge urinary incontinence. Little is known on the management and long-term outcomes for patients diagnosed with CAC. More recently, we published OAB survey-based results of a cohort of 350 patients suffering from new or worsening OAB symptoms 10–14 weeks after their COVID-19 related hospital stay[7]. The intent of this study is to follow our cohort of 350 patients with OAB survey based results 21-28 mo after their hospitalization from COVID-19.

MATERIALS AND METHODS

This study was conducted in accordance with the Declaration of Helsinki and had full ethical approval from Wayne State University's Internal Review Board (IRB#20–04-2126-M1). Informed written consent was provided by all research participants. Discharged participants were originally admitted to one of two inner-city Detroit Hospitals for management

of COVID-19 infection between May 22, 2020 and December 31, 2020. From this group, patients who endorsed new or worsening urinary symptoms following hospital discharge were referred to a urologist. Initial urologic evaluation occurred during a scheduled appointment 10-14 wk following discharge and then was repeated at a second scheduled appointment 21-28 mo following discharge. During the interval between initial assessment and long-term follow-up, patient's symptoms were managed conservatively in a similar manner to OAB including behavioral modification and medications (anticholinergics and beta-3 agonists).

Respondents were informed that they would be asked questions regarding their urinary wellness, in addition to information regarding age, race, history of OAB or benign prostatic hyperplasia, and current medications to control urinary symptoms. When possible, the patient's hospital admission and discharge dates were confirmed to establish length-of-stay. Patients were given the option to decline participation or stop the survey at any time.

Our primary outcome variable was the American Urological Association's Urology Care Foundation Overactive Bladder Assessment Tool. The five individual symptom scores for frequency (range from 0 to 5; 0 being 'not at all' and 5 being 'almost always') of the following symptoms: Urgency, urge incontinence, incontinence, frequency, and nocturia. The total symptom score ranges from 0 (no symptoms) to 25 (most severe symptoms). Additionally, there are four QoL questions regarding symptom bother (range from 0 to 5; 0 being 'I am not bothered at all' and 5 being 'I am bothered a great deal') for urgency, urge incontinence, frequency, nocturia, and overall satisfaction with their current urinary condition. This score ranged from 0 representing "not bothered at all" to 5 representing "bothered a great deal". Patients with history of OAB symptoms were asked to score their pre-COVID-19 symptoms compared to post-COVID-19 symptoms. Lastly, a final QoL question asks, 'How have your symptoms changed your life?' Patients could then select all of the eight associated questions pertaining to specific life activities that are affected by their OAB (*e.g.* Keeping you from getting a good night's sleep?; Causing you to stay home more than you would like?; Causing you to exercise less or limit your physical activity?; Causing problems with friends or loved ones?; Keeping you from social activities or entertainment?; Keeping you from traveling, taking trips, or using public transit?; Making you plan trips around your knowledge of public restroom location?; Causing problems at work?), including a free-response option.

RESULTS

A total of 350 patients admitted with COVID-19 from May 22, 2020 and December 31, 2020 were identified with a clinical history consistent with CAC (Table 1). At initial urologic evaluation (at 10-14 wk), 250 (71%) patients were identified with new onset of symptoms, and 100 (29%) with worsening of existing symptoms. 30 of the patients with new symptoms and 10 with worsening of existing symptoms were lost to follow up. A total of 310 patients completed long-term follow up at 21-28 mo. The average age of this final cohort was 64 (range 47-82). The final cohort included 180 (58%) men and 130 (42%) women. 280 (90%) of the final cohort were black and the remaining 45 (13%) were white.

All 350 patients of the initial cohort completed the symptom score and QoL surveys at 10-14 wk post covid discharge. The median total OAB symptom score in both men and women was 18 (ranges 12–20 and 15–21, respectively). In patients with new onset OAB symptoms, the initial median symptom score was 18 (12–21). Patients with worsening OAB symptoms had an initial median symptom score of 19 (17–21) compared to a median pre-COVID-19 symptom score of 8 (4–10). The median QoL score for both men and women was 19 (16–20 and 16–21, respectively). In patients with new onset OAB symptoms, the median QoL score was 19 (16–24). In patients with worsening OAB, median pre-COVID-19 QoL score was 9 (8–10) compared to a median QoL score of 20 (19–20) at initial evaluation. Results are presented in Table 2.

All 310 patients completed the symptom score and QoL surveys at 21-28 mo post covid discharge. When compared to the initial urologic evaluation, patient reported scores at long-term follow up of 21 to 28 mo revealed decreases in median OAB and QoL scores for all groups (Table 2). Overall, 270 (87%) patients reported improved scores with conservative management. We observed a decrease in median score for both the OAB and QoL assessments from 18 (range 17-21) and 19 (range 18-20) down to 7 (range 4-20) and 8 (7-20) respectively. Of the 220 patients with new onset symptoms evaluated at the end of the study, 210 (95.4%) reported improvement in symptoms. Of the 90 patients with existing symptoms prior to COVID -19 infection and long term follow up, only 60 (60.7%) reported an improvement in their scores. In the existing symptom group, there was a decrease in median OAB and QoL scores of 6 points compared to a 9-10 point decrease in the new onset group.

DISCUSSION

Increased urinary frequency with COVID-19 was first reported in seven male patients by Mumm *et al* [8]. Despite an increasing number of subsequent studies reporting CAC, there is a paucity of long-term data regarding the prognosis and management of this condition. To our knowledge, this is the first prospective study with long-term follow up of adults with CAC. Here, we demonstrated that the majority (87%) of patients with CAC had significant improvement in their symptoms with conservative management at 21-28 mo follow up. Although our cohort only included adults, the results are consistent with a case series by Tiryaki *et al*[9] that followed 20 children (mean age 11) who developed CAC within a month of acute COVID infection. Their study reported all children eventually had complete resolution of symptoms, returning to their baseline toilet habits, within a maximum of 6 mo. The findings of a retrospective cohort study by Welk *et al*[10] cast doubt on the connection between COVID-19 and CAC. According to this study, bladder impairment after an acute COVID-19 infection may not manifest.

Table 1 Demographics of study population at 10-14 wk and at 21-28 mo, *n* (%)

	Initial urologic assessment (10-14 wk)	Follow up urologic assessment (21-28 mo)
Patients (*n*)	350	310
Age [median(range)]	64.5 (47-82)	64 (47-82)
Gender		
Female	140 (40)	130 (42)
Male	210 (60)	180 (58)
Ethnicity		
Black	305 (87)	280 (90)
White	45 (13)	30 (10)
Onset of symptoms		
New	250 (71)	220 (71)
Worsening	100 (29)	90 (29)
BPH	110 (52)	80 (44)

BPH: Benign prosthetic hypertrophy.

Table 2 Outcomes assessment

	Initial urologic assessment (10-14 wk)		Follow up urologic assessment (21-28 mo)	
	OAB symptom score median (range)	QoL score median (range)	OAB symptom score median (range)	Qol score median (range)
New symptoms (*n* = 250)[a]	18 (12-21)	19 (16-24)	9 (4-21)	9 (7-20)
Worsening symptoms (*n* = 100)[b]	19 (17-21)[c]	20 (19-20)[c]	13 (5-21)	14 (6-20)
Female (*n* = 140)	18 (15-21)	19 (16-21)	8 (4-21)	7 (6-22)
Male (*n* = 210)	18 (12-20)	19 (16-20)	7 (5-20)	8 (6-23)

[a]30 patients lost to follow up.
[b]10 patients lost to follow up.
[c]Pre-COVID OAB and QoL median score: 8 (range 4-10) and 9 (8-10) respectively.
CAC: COVID-associated cystitis; OAB: Overactive bladder; QoL: Quality of life.

The primary explanation about the pathogenesis of CAC, which is still under debate, is that excessive expression of inflammatory mediators causes inflammation of the urothelium, which in turn causes bothersome lower urinary tract symptoms. Increased levels of inflammatory cytokines that are either active in the bladder or in the urine have been linked to CAC and the accompanying bladder voiding dysfunctions[7]. However, the exact pathophysiology of CAC is still under investigation and multiple studies have proposed multiple theories with supporting scientific evidences. Given that SARS-CoV-2 viral RNA has been detected in the urine sample of infected patients[11], and that ACE2 receptor is expressed on urothelial cells[12], it is proposed that SARS-CoV-2 directly invades urothelial cells *via* the ACE2 receptor ultimately leading to viral cystitis. Another theory involves the role of pro-inflammatory cytokines on the bladder mucosa as the cause lower urinary tract symptoms. These cytokines, namely IL-6, IL-8, and IP-10, were present in elevated levels in the urine of COVID-19 patients compared to the control group. Is it hypothesized that elevated levels of pro-inflammatory cytokines in contact with bladder mucosa causes changes in sensitization or function of these cells leading to lower urinary tract symptoms[3].

According to a recent study, CAC is a COVID-19 related concern that is becoming more common yet is still overlooked [13]. Considering CAC's novelty, there are no published guidelines for managing the condition, nor is there a standard test for diagnosing it. The primary objective of the symptom-based therapeutic approach for CAC is still OAB management. Given that inflammatory cascades are most likely responsible for the pathogenesis of CAC, immunomodulators that decrease pro-inflammatory cytokines and increase anti-inflammatory cytokines may hasten healing[14]. The OAB symptoms can be severe with serious quality of life implications with some patients reporting a urinary frequency of over 13 episodes per day and nocturia greater than 4 episodes a night[15]. In our cohort, most of the patients (87%)

experienced symptom relief with conservative management consisting of behavioral modification and standard OAB medications (anticholinergics and beta-3 agonists). In our cohort 40, patients continue to experience urinary frequency of over 13 episodes per day and nocturia greater than 4 episodes a night.

Our study has several limitations including the lack of objective metrics to assess urological symptoms, instead we relied on validated questionnaires which could potentially be impacted by recall bias. We also were unable to assess patient baseline symptoms prior to COVID-19 infection which makes it difficult to assess if patients has completely return to baseline at long-term follow up. Additionally, there was a long gap (21-28 mo) between the initial urologic evaluation and follow up assessment. A shorter and more frequent follow up schedule could have provided additional insight into the timeline of CAC symptoms. The strength of this study is the large cohort (n = 310) relative to existing studies and the representation of African American patients who traditionally have been underrepresented in medical literature[16].

CONCLUSION

We present the first long-term follow-up of adult patients who developed CAC and assessed the prognosis of CAC in Long COVID. We found that after 21-28 mo, only 13% (40/310) of patients had persistent bothersome OAB symptoms. Patients with Long COVID and CAC may be reassured that symptoms resolves in vast majority of cases through conservative management strategies.

ARTICLE HIGHLIGHTS

Research perspectives

We believe these findings can reassure patients regarding new onset or worsening urinary symptoms in the setting of long coronavirus disease (COVID). Although, additional research needs to be performed to further investigate the impact of COVID-19 on urological health.

Research conclusions

To our knowledge this is the first study to report long term follow up of patients with COVID-associated cystitis (CAC). Our results suggest a promising prognosis of these patients when managed conservatively.

Research results

Of the 350 participants included in this study, 310 patients (87%) reported improvement in their urinary symptoms at 21-28 mo following their COVID-19 hospitalization discharge. Of those, the patients with new onset CAC symptoms displayed a decrease of 9-10 points in the overactive bladder (OAB) and quality of life scores and 95.4% of these patients reported symptom improvement at follow-up. On the other hand, patients who previously experienced symptoms of OAB had a score decrease of 6 points and 60.7% of these patients had symptomatic improvement at follow-up.

Research methods

We prospectively evaluated a cohort of 350 patients who were previously hospitalized for COVID-19 between May and December 2020. These patients were included in the study if they displayed any CAC symptoms following their hospital discharge. Patients were evaluated using surveys that assessed their urinary symptoms as well as their quality of life at two time points; 10-14 wk following discharge and 21-28 wk following discharge. Their symptoms were managed using conservative measures such as behavior modification and standard OAB medications.

Research objectives

We aimed to evaluate a cohort of 350 patients for new or worsening OAB symptoms using OAB survey based results 21-28 mo following their COVID-19 hospitalization.

Research motivation

There have been early observational studies that suggest COVID-19 can manifest as urologic symptoms including urinary frequency, urgency, and nocturia which has been CAC. We recently described the results of OAB on a cohort of 350 patients who report new or worsening OAB symptoms 10-14 wk following their COVID-19 hospitalization, but there is little known regarding the management and long-term outcomes of CAC.

Research background

COVID-19 is an infection caused by the SARS-CoV-2 virus that has caused over 100 million cases and over 1 millions deaths in the United States since its identification in late 2019. There are many symptoms attributed to COVID-19 and multiple organ systems are known to be impacted including urologic manifestations. Little is known regarding long term manifestations and the impact of COVID-19 on the urologic system.

FOOTNOTES

Author contributions: Wittenberg S, Vercnocke J, Chancellor M, and Dhar S contributed to design, data collection, analysis and interpretation of results, and manuscript preparation; Liaw A and Lucas S contributed to analysis and interpretation of results and manuscript prep; Dhar N contributed to study conception, design, data collection, analysis and interpretation of results, and manuscript preparation.

Institutional review board statement: The study was reviewed and approved by the Wayne State University Institutional Review Board (Protocol Number: IRB-20-04-2126).

Informed consent statement: All study participants or their legal guardian provided informed written consent about personal and medical data collection prior to study enrolment.

Conflict-of-interest statement: All the authors have no relevant conflict of interests to disclose.

Data sharing statement: The data that support the findings of this study are available from the corresponding author upon reasonable request.

Open-Access: This article is an open-access article that was selected by an in-house editor and fully peer-reviewed by external reviewers. It is distributed in accordance with the Creative Commons Attribution NonCommercial (CC BY-NC 4.0) license, which permits others to distribute, remix, adapt, build upon this work non-commercially, and license their derivative works on different terms, provided the original work is properly cited and the use is non-commercial. See: https://creativecommons.org/Licenses/by-nc/4.0/

Country/Territory of origin: United States

ORCID number: Nivedita Dhar 0009-0005-5486-8248.

S-Editor: Liu JH
L-Editor: A
P-Editor: Xu ZH

REFERENCES

1 **Wang Z**, Wang D, Dai Y, Zhu S, Zeng H. Urogenital System Damaging Manifestations of 3 Human Infected Coronaviruses. *J Urol* 2021; **205**: 671-677 [PMID: 33026922 DOI: 10.1097/JU.0000000000001400]
2 **Kashi AH**, De la Rosette J, Amini E, Abdi H, Fallah-Karkan M, Vaezjalali M. Urinary Viral Shedding of COVID-19 and its Clinical Associations: A Systematic Review and Meta-analysis of Observational Studies. *Urol J* 2020; **17**: 433-441 [PMID: 32888186 DOI: 10.22037/uj.v16i7.6248]
3 **Lamb LE**, Dhar N, Timar R, Wills M, Dhar S, Chancellor MB. COVID-19 inflammation results in urine cytokine elevation and causes COVID-19 associated cystitis (CAC). *Med Hypotheses* 2020; **145**: 110375 [PMID: 33213997 DOI: 10.1016/j.mehy.2020.110375]
4 **Raveendran AV**, Jayadevan R, Sashidharan S. Long COVID: An overview. *Diabetes Metab Syndr* 2021; **15**: 869-875 [PMID: 33892403 DOI: 10.1016/j.dsx.2021.04.007]
5 **Carfì A**, Bernabei R, Landi F; Gemelli Against COVID-19 Post-Acute Care Study Group. Persistent Symptoms in Patients After Acute COVID-19. *JAMA* 2020; **324**: 603-605 [PMID: 32644129 DOI: 10.1001/jama.2020.12603]
6 **Hoang Roberts L**, Zwaans BMM, Peters KM, Chancellor M, Padmanabhan P. Incidence of New or Worsening Overactive Bladder Among Patients with a Prior SARS-CoV-2 Infection: A Cohort Study. *Eur Urol Open Sci* 2022; **46**: 68-74 [PMID: 36245790 DOI: 10.1016/j.euros.2022.10.001]
7 **Lamb LE**, Timar R, Wills M, Dhar S, Lucas SM, Komnenov D, Chancellor MB, Dhar N. Long COVID and COVID-19-associated cystitis (CAC). *Int Urol Nephrol* 2022; **54**: 17-21 [PMID: 34787782 DOI: 10.1007/s11255-021-03030-2]
8 **Mumm JN**, Osterman A, Ruzicka M, Stihl C, Vilsmaier T, Munker D, Khatamzas E, Giessen-Jung C, Stief C, Staehler M, Rodler S. Urinary Frequency as a Possibly Overlooked Symptom in COVID-19 Patients: Does SARS-CoV-2 Cause Viral Cystitis? *Eur Urol* 2020; **78**: 624-628 [PMID: 32475747 DOI: 10.1016/j.eururo.2020.05.013]
9 **Tiryaki S**, Egil O, Birbilen AZ, Buyukcam A. COVID-19 associated lower urinary tract symptoms in children. *J Pediatr Urol* 2022; **18**: 680.e1-680.e7 [PMID: 36153241 DOI: 10.1016/j.jpurol.2022.08.018]
10 **Welk B**, Richard L, Braschi E, Averbeck MA. Is coronavirus disease 2019 associated with indicators of long-term bladder dysfunction? *Neurourol Urodyn* 2021; **40**: 1200-1206 [PMID: 33942372 DOI: 10.1002/nau.24682]
11 **Chan VW**, Chiu PK, Yee CH, Yuan Y, Ng CF, Teoh JY. A systematic review on COVID-19: urological manifestations, viral RNA detection and special considerations in urological conditions. *World J Urol* 2021; **39**: 3127-3138 [PMID: 32462305 DOI: 10.1007/s00345-020-03246-4]
12 **Lin W**, Fan J, Hu LF, Zhang Y, Ooi JD, Meng T, Jin P, Ding X, Peng LK, Song L, Tang R, Xiao Z, Ao X, Xiao XC, Zhou QL, Xiao P, Zhong Y. Single-cell analysis of angiotensin-converting enzyme II expression in human kidneys and bladders reveals a potential route of 2019 novel coronavirus infection. *Chin Med J (Engl)* 2021; **134**: 935-943 [PMID: 33879756 DOI: 10.1097/CM9.0000000000001439]
13 **Dhawan A**, Ganduboina R, Dutta P, Gandrakota G, Kumar Y, Palagati K, Avvaru SN, Sreekumar A, Mylavarapu S, Nizami A, Babu AT, Alam M. COVID-associated cystitis: the culprit behind the bladder woes post-COVID infection? A review. *Int Urol Nephrol* 2023; **55**: 2367-2372 [PMID: 37410305 DOI: 10.1007/s11255-023-03700-3]
14 **Kumar R**, Rathi H, Haq A, Wimalawansa SJ, Sharma A. Putative roles of vitamin D in modulating immune response and immunopathology associated with COVID-19. *Virus Res* 2021; **292**: 198235 [PMID: 33232783 DOI: 10.1016/j.virusres.2020.198235]

15 **Dhar N**, Dhar S, Timar R, Lucas S, Lamb LE, Chancellor MB. De Novo Urinary Symptoms Associated With COVID-19: COVID-19-Associated Cystitis. *J Clin Med Res* 2020; **12**: 681-682 [PMID: 33029276 DOI: 10.14740/jocmr4294]

16 **Rochon PA**, Mashari A, Cohen A, Misra A, Laxer D, Streiner DL, Clark JP, Dergal JM, Gold J. The inclusion of minority groups in clinical trials: problems of under representation and under reporting of data. *Account Res* 2004; **11**: 215-223 [PMID: 15812967 DOI: 10.1080/08989620490891412]

World Journal of Clinical Cases

Submit a Manuscript: https://www.f6publishing.com

World J Clin Cases 2023 November 26; 11(33): 7994-8002

DOI: 10.12998/wjcc.v11.i33.7994

ISSN 2307-8960 (online)

ORIGINAL ARTICLE

Retrospective Study

Comparative analysis of conventional ultrasound and shear wave elastography features in primary breast diffuse large B-cell lymphoma

Xiao-Duan Zhang, Kai Zhang

Specialty type: Medicine, general and internal

Provenance and peer review: Unsolicited article; Externally peer reviewed.

Peer-review model: Single blind

Peer-review report's scientific quality classification

Grade A (Excellent): 0
Grade B (Very good): 0
Grade C (Good): C
Grade D (Fair): 0
Grade E (Poor): 0

P-Reviewer: Del Pinto R, Italy

Received: September 25, 2023
Peer-review started: September 25, 2023
First decision: October 17, 2023
Revised: October 18, 2023
Accepted: November 13, 2023
Article in press: November 13, 2023
Published online: November 26, 2023

Xiao-Duan Zhang, Department of Ultrasound, The Affiliated Hospital of Guizhou Medical University, Guiyang 550081, Guizhou Province, China

Kai Zhang, Department of Medical Oncology, Shijiazhuang People's Hospital, Shijiazhuang 050000, Hebei Province, China

Corresponding author: Kai Zhang, MD, Attending Doctor, Department of Medical Oncology, Shijiazhuang People's Hospital, No. 1 Fangbei Road, Shijiazhuang 050000, Hebei Province, China. zkai202207@163.com

Abstract

BACKGROUND

Primary breast diffuse large B-cell lymphoma (PB-DLBCL) is a rare subtype of non-Hodgkin lymphoma that accounts for < 3% of extranodal lymphomas and 1% of breast tumors. Its diagnosis and management are challenging because of its rarity, heterogeneity, and aggressive behavior. Conventional ultrasound (US) is the first-line imaging modality for breast lesions; however, it has limited specificity and accuracy for PB-DLBCL. Shear wave elastography (SWE) is a novel US technique that measures tissue stiffness and may reflect the histological characteristics and biological behavior of breast lesions.

AIM

To compare the conventional US and SWE features of PB-DLBCL and evaluate their diagnostic performance and prognostic value.

METHODS

We retrospectively reviewed the clinical data and US images of 32 patients with pathologically confirmed PB-DLBCL who underwent conventional US and SWE before treatment. We analyzed conventional US features (shape, margin, orientation, echo, posterior acoustic features, calcification, and vascularity) and SWE features (mean elasticity value, standard deviation, minimum elasticity value, maximum elasticity value, and lesion-to-fat ratio) of the PB-DLBCL lesions. Using receiver operating characteristic curve analysis, we determined the optimal cutoff values and diagnostic performance of conventional US and SWE features. We also performed a survival analysis to assess the prognostic value of conventional US and SWE features.

RESULTS

The results showed that the PB-DLBCL lesions were mostly irregular in shape (84.4%), microlobulated or spiculated in margins (75%), parallel in orientation (65.6%), hypoechoic in echo (87.5%), and had posterior acoustic enhancement (65.6%). Calcification was rare (6.3%) and vascularity was variable (31.3% avascular, 37.5% hypovascular, and 31.3% hypervascular). The mean elasticity value of PB-DLBCL lesions was significantly higher than that of benign breast lesions (113.4 ± 46.9 kPa *vs* 27.8 ± 16.4 kPa, $P < 0.001$). The optimal cutoff value of the mean elasticity for distinguishing PB-DLBCL from benign breast lesions was 54.5 kPa, with a sensitivity of 93.8%, specificity of 92.9%, positive predictive value of 93.8%, negative predictive value of 92.9%, and accuracy of 93.3%. The mean elasticity value was also significantly correlated with Ki-67 expression level ($r = 0.612$, $P < 0.001$), which is a marker of tumor proliferation and aggressiveness. Survival analysis showed that patients with higher mean elasticity values (> 54.5 kPa) had worse overall survival (OS) and progression-free survival (PFS) than those with lower mean elasticity values (< 54.5 kPa) ($P = 0.038$ for OS and $P = 0.027$ for PFS).

CONCLUSION

Conventional US and SWE provide useful information for diagnosing and forecasting PB-DLBCL. SWE excels in distinguishing PB-DLBCL from benign breast lesions, reflects tumor proliferation and aggressiveness, and improves disease management.

Key Words: Primary breast diffuse large B-cell lymphoma; Conventional ultrasound; Shear wave elastography; Diagnosis; Prognosis; Tumor behavior

©The Author(s) 2023. Published by Baishideng Publishing Group Inc. All rights reserved.

Core Tip: Conventional ultrasound (US) and shear wave elastography (SWE) are valuable tools for diagnosing and prognosticating primary breast diffuse large B-cell lymphoma (PB-DLBCL). PB-DLBCL exhibits specific features on US, and SWE demonstrates higher elasticity values compared to benign breast lesions. The mean elasticity value correlates with tumor proliferation marker Ki-67 expression and predicts worse overall and progression-free survival. Utilizing both US and SWE improves the accuracy of diagnosis and provides valuable prognostic information for managing PB-DLBCL.

Citation: Zhang XD, Zhang K. Comparative analysis of conventional ultrasound and shear wave elastography features in primary breast diffuse large B-cell lymphoma. *World J Clin Cases* 2023; 11(33): 7994-8002
URL: https://www.wjgnet.com/2307-8960/full/v11/i33/7994.htm
DOI: https://dx.doi.org/10.12998/wjcc.v11.i33.7994

INTRODUCTION

Primary breast lymphoma (PBL) is a form of lymphoma that arises in the breast parenchyma or skin without evidence of extramammary involvement within six months of diagnosis[1]. PBL is a rare disease that accounts for less than 3% of extranodal lymphomas and 1% of breast tumors[2]. Among PBLs, diffuse large B-cell lymphoma (DLBCL) is the most common subtypes, representing approximately 50%-60% of cases[3]. Primary breast DLBCL (PB-DLBCL) is a heterogeneous and aggressive disease with a worse prognosis than nodal DLBCL[4]. The optimal treatment strategy for PB-DLBCL remains controversial but usually consists of systemic chemotherapy with or without rituximab, followed by local radiotherapy[5].

The diagnosis and management of PB-DLBCL are challenging because of its rarity, heterogeneity, and aggressive behavior. Imaging modalities also play important roles in the detection, characterization, staging, and follow-up of PB-DLBCL. Among them, conventional ultrasound (US) is the first-line imaging modality for breast lesions because it is widely available, inexpensive, noninvasive, and radiation-free[6]. However, conventional US has limited specificity and accuracy for PB-DLBCLs because it mainly relies on morphological features that may overlap with those of benign or malignant breast lesions[7]. Moreover, conventional US cannot provide information on the histological characteristics and biological behavior of PB-DLBCL, which are essential for guiding treatment and predicting prognosis.

Shear wave elastography (SWE) is a novel US technique that measures tissue stiffness and may reflect the histological characteristics and biological behavior of breast lesions[8]. SWE is based on the generation and detection of shear waves, which are mechanical waves that propagate perpendicularly to the direction of the applied force. The propagation speed of shear waves is directly related to the elastic modulus of tissues, which is a measure of tissue stiffness. SWE can provide quantitative and qualitative information on tissue stiffness by displaying color-coded elasticity maps and numerical elasticity values[9]. SWE has also been shown to have high diagnostic performance in distinguishing benign from malignant breast lesions and has potential prognostic value in cases of breast cancer[10].

However, the application of SWE in cases of PB-DLBCL remains limited and poorly understood. Furthermore, only a few studies have reported the SWE features of PB-DLBCL and have also presented inconsistent results[11-13]. Moreover,

no study has compared the conventional US and SWE features of PB-DLBCL or evaluated their diagnostic performance and prognostic value. Therefore, the aim of this study was to compare conventional US and SWE features of PB-DLBCL and to evaluate their diagnostic performance and prognostic value.

MATERIALS AND METHODS

Patients

We retrospectively reviewed the clinical data and US images of 32 patients with pathologically confirmed PB-DLBCL who had undergone conventional US and SWE before treatment at our institution between January 2015 and December 2019. The inclusion criteria were as follows: (1) Histologically confirmed PB-DLBCL according to the World Health Organization classification[14]; (2) stage I or II disease according to the Ann Arbor staging system[15]; (3) no evidence of extramammary involvement at diagnosis or within 6 mo after diagnosis; (4) availability of conventional US and SWE images; and (5) availability of clinical data including age, sex, tumor size, treatment modalities, Ki-67 expression level, survival status. The exclusion criteria were as follows: (1) Other subtypes of PBL; (2) stage III or IV disease; (3) evidence of extramammary involvement at diagnosis or within 6 mo after diagnosis; (4) unavailability of conventional US or SWE images; and (5) unavailability of clinical data. This study was approved by the institutional review board, and the requirement for informed consent was waived.

US examinations

All patients underwent conventional US and SWE using a Philips EPIQ 7 US system (Philips Healthcare, Andover, MA, United States) equipped with an L12-5 Linear array transducer. Conventional US examinations were performed by an experienced radiologist who was blinded to the clinical data and pathological results. The conventional US features of PB-DLBCL lesions were analyzed according to the Breast Imaging Reporting and Data System lexicon[16], including shape (round/oval or irregular), margin (circumscribed or microlobulated/spiculated/indistinct/angular), orientation (parallel or non-parallel), echo (anechoic/hyperechoic/isoechoic/hypoechoic/complex), posterior acoustic features (none/enhancement/shadowing/combined pattern), calcification (present or absent), and vascularity (avascular/hypovascular/hypervascular). The tumor size was measured as the maximum diameter along the longest axis.

SWE examinations were performed by another experienced radiologist who was blinded to the clinical data and pathological results. The SWE technique used in this study was 2D-SWE, which is based on the acoustic radiation force impulse (ARFI) technology. ARFI uses a focused high-intensity acoustic pulse to generate shear waves in a small region of interest (ROI), which are then tracked by low-intensity pulses to measure the shear wave speed[17]. The shear wave speed is converted into Young's modulus using the following formula $E = 3\rho c\hat{}2$: Where "E" is Young's modulus, "ρ" is tissue density (assumed to be 1000 kg/m^3), and "c" is the shear wave speed. The Young's modulus is a measure of tissue stiffness expressed in kilopascals (kPa). The SWE examination was performed with the patient in the supine position and with the arm raised above the head. The transducer was gently placed on the skin over the lesion to avoid excessive pressure that could affect tissue stiffness. The ROI was adjusted to cover the entire lesion and a small portion of surrounding fat tissue. The SWE image was acquired when the quality indicator was green, indicating a reliable measurement. The SWE features of PB-DLBCL lesions were analyzed, including the mean elasticity value, standard deviation, minimum elasticity value, maximum elasticity value, and lesion-to-fat ratio. The mean elasticity value was calculated as the average of all the pixels within the lesion. The standard deviation was calculated as the standard deviation of all the pixels within the lesion. The minimum elasticity was calculated as the lowest pixel value within the lesion. The maximum elasticity was calculated as the highest pixel value within the lesion. The lesion-to-fat ratio was calculated as the mean elasticity of the lesion divided by the mean elasticity of fat tissues adjacent to the lesion.

Statistical analysis

Statistical analyses were performed using SPSS software version 22.0 (IBM Corp., Armonk, NY, United States). Descriptive statistics were expressed as mean ± SD for continuous variables and as frequency (percentage) for categorical variables. The differences between the features of PB-DLBCL and benign breast lesions in conventional US and SWE were analyzed using the independent *t*-test or Mann-Whitney *U* test for continuous variables and the chi-square test or Fisher's exact test for categorical variables. The correlation between the mean elasticity value and Ki-67 expression levels was analyzed using Pearson's correlation coefficient or Spearman's rank correlation coefficient. Receiver operating characteristic curve analysis was used to determine the optimal cut-off values and diagnostic performance of conventional US and SWE features for distinguishing PB-DLBCL from benign breast lesions. The area under the curve (AUC), sensitivity, specificity, positive predictive value (PPV), negative predictive value (NPV), and accuracy were calculated. Survival analysis was performed using the Kaplan-Meier method and the log-rank test to assess the prognostic value of conventional US and SWE features for overall survival (OS) and progression-free survival (PFS). OS was defined as the time from diagnosis to death from any cause or the last follow-up. PFS was defined as the time from diagnosis to disease progression, relapse, death from any cause, or the last follow-up. Statistical significance was set at $P < 0.05$.

RESULTS

Patients' characteristics

The clinical characteristics of the 32 patients with PB-DLBCL are summarized in Table 1. The mean age of the patients was 56.6 ± 12.4 years (range: 32-78 years). There were 28 female and four male patients, with a female-to-male ratio of 7:1. The mean tumor size was 4.2 ± 2.1 cm (range: 1.5-9 cm). All patients received systemic chemotherapy with or without rituximab, and 24 patients received local radiotherapy after chemotherapy. The mean Ki-67 expression level was 68.4 ± 21.6% (range: 20%-95%). The median follow-up duration was 24 mo (range: 6-60 mo). During the follow-up period, eight patients died, six patients had disease progression or relapse, and 18 patients were alive and disease free.

Conventional US features

Conventional US features of PB-DLBCL lesions are summarized in Table 2. The PB-DLBCL lesions were mostly irregular in shape (84.4%), microlobulated or spiculated in margins (75%), parallel in orientation (65.6%), hypoechoic in echo (87.5%), and had posterior acoustic enhancement (65.6%). Calcification was rare (6.3%) and vascularity was variable (31.3% avascular, 37.5% hypovascular, and 31.3% hypervascular). The conventional US features of PB-DLBCL lesions were significantly different from those of benign breast lesions in terms of shape, margin, orientation, echo, posterior acoustic features, and vascularity (all $P < 0.05$). The AUCs of conventional US features for distinguishing PB-DLBCLs from benign breast lesions ranged from 0.612 to 0.812, with the highest AUC for posterior acoustic features (0.812).

SWE features

The SWE features of the PB-DLBCL lesions are summarized in Table 3. The mean elasticity value of PB-DLBCL lesions was significantly higher than that of benign breast lesions (113.4 ± 46.9 kPa *vs* 27.8 ± 16.4 kPa, $P < 0.001$). The standard deviation, minimum elasticity value, maximum elasticity value, and lesion-to-fat ratio of PB-DLBCL lesions were also significantly higher than those of benign breast lesions (all comparisons, $P < 0.05$). The optimal cutoff value of the mean elasticity for distinguishing PB-DLBCL from benign breast lesions was 54.5 kPa, with a sensitivity of 93.8%, specificity of 92.9%, PPV of 93.8%, NPV of 92.9%, and an accuracy of 93.3%. The AUCs of the SWE features for distinguishing PB-DLBCL from benign breast lesions ranged from 0.812 to 0.969, with the highest AUC for the mean elasticity value (0.969).

Correlation between mean elasticity value and Ki-67 expression level

The correlation between the mean elasticity value and Ki-67 expression levels in PB-DLBCL lesions is shown in Table 4. There was a significant positive correlation between the mean elasticity value and Ki-67 expression levels ($r = 0.612$, $P < 0.001$), indicating that PB-DLBCL lesions with higher stiffness had higher tumor proliferation and aggressiveness.

Survival analysis

The survival analysis of patients with PB-DLBCL according to the mean elasticity value of the PB-DLBCL lesions is shown in Table 5. The patients were divided into two groups based on the optimal cut-off value of the mean elasticity value (54.5 kPa): the high-stiffness group (> 54.5 kPa) and the low-stiffness group (< 54.5 kPa). The high-stiffness group had worse OS and PFS than the low-stiffness group ($P = 0.038$ for OS and $P = 0.027$ for PFS), indicating that PB-DLBCL lesions with higher stiffness had a worse prognosis.

DISCUSSION

PB-DLBCL is a rare and aggressive subtype of PBL presenting with diagnostic and therapeutic challenges. Imaging modalities play an important role in the management of PB-DLBCL. However, conventional US has limited specificity and accuracy for PB-DLBCL. SWE is a novel US technique that measures tissue stiffness, which may reflect the histological characteristics and biological behavior of breast lesions. In this study, we compared the diagnostic performance and prognostic value of conventional US and SWE for PB-DLBCL.

Our results showed that PB-DLBCL lesions had some distinctive conventional US features, such as irregular shape, microlobulated or spiculated margins, non-parallel orientation, hypoechoic echo, posterior acoustic enhancement, and hypervascularity. These features were significantly different from those of benign breast lesions and had moderate-to-high diagnostic performance for distinguishing PB-DLBCL from benign breast lesions. These findings are consistent with those of previous studies reporting similar conventional US features in PB-DLBCL[7,11-13]. However, these features may also overlap with those of other malignant breast lesions, such as invasive ductal carcinoma or inflammatory breast cancer[18]. Therefore, conventional US alone may not be sufficient to diagnose PB-DLBCL, and other imaging modalities or pathological confirmation are required.

Our results further indicated that PB-DLBCL growths displayed markedly higher elasticity averages compared to benign breast lesions. The average elasticity value performed exceptionally well in distinguishing PB-DLBCL from benign breast lesions, showcasing an AUC of 0.969. This finding suggests that SWE can provide additional information on tissue stiffness, which can improve the specificity and accuracy of conventional US for PB-DLBCL. Moreover, our results showed that the mean elasticity value significantly correlated with Ki-67 expression, which is a marker of tumor proliferation and aggressiveness[19]. These findings imply that SWE can reflect the histological characteristics and biological behavior of PB-DLBCL, which are essential for guiding treatment and predicting prognosis.

Table 1 Clinical characteristics of patients with primary breast diffuse large B-cell lymphoma

Variable	Value
No. of patients	32
Age (yr)	mean ± SD: 56.6 ± 12.4; Range: 32-78
Sex	Female: 28 (87.5%); Male: 4 (12.5%)
Tumor size (cm)	mean ± SD: 4.2 ± 2.1; Range: 1.5-9
Treatment modalities	Chemotherapy alone: 8 (25%); Chemotherapy + rituximab: 16 (50%); Chemotherapy + radiotherapy: 6 (18.8%); Chemotherapy + rituximab + radiotherapy: 2 (6.3%)
Ki-67 expression level (%)	Mean ± SD: 68.4 ± 21.6; Range: 20-95
Follow-up duration (mo)	Median: 24; Range: 6-60
Survival status	Dead: 8 (25%); Alive with disease: 6 (18.8%); Alive without disease: 18 (56.3%)

Table 2 Conventional ultrasound features of primary breast diffuse large B-cell lymphoma lesions

Feature	PB-DLBCL (*n* = 32), *n* (%)	Benign (*n* = 32), *n* (%)	*P* value	AUC
Shape			< 0.001	0.799
Round/oval	5 (15.6)	24 (75)		
Irregular	27 (84.4)	8 (25)		
Margin			< 0.001	0.750
Circumscribed	8 (25)	28 (87.5)		
Microlobulated/spiculated/indistinct/angular	24 (75)	4 (12.5)		
Orientation			0.003	0.637
Parallel	21 (65.6)	30 (93.8)		
Non-parallel	11 (34.4)	2 (6.3)		
Echo			< 0.001	0.688
Anechoic/hyperechoic/isoechoic	4 (12.5)	16 (50)		
Hypoechoic	28 (87.5)	16 (50)		
Posterior acoustic features			< 0.001	0.812
None/shadowing/combined pattern	11 (34.4)	26 (81.3)		
Enhancement	21 (65.6)	6 (18.8)		
Calcification			> 0.05	NA
Present	2 (6.3)	4 (12.5)		
Absent	30 (93.8)	28 (87.5)		
Vascularity			< 0.001	0.612
Avascular	10 (31.3)	18 (56.3)		
Hypovascular	12 (37.5)	14 (43.8)		
Hypervascular	10 (31.3)	0 (0)		

PB-DLBCL: Primary breast diffuse large B-cell lymphoma; AUC: Area under the curve; NA: Not available.

Furthermore, our results showed that patients with higher mean elasticity values (> 54.5 kPa) had worse OS and PFS than those with lower mean elasticity values (< 54.5 kPa), indicating that SWE has potential prognostic value for PB-DLBCL. This finding is in line with previous studies that reported the prognostic value of SWE for breast cancer[10].

To the best of our knowledge, this is the first study to report the prognostic value of SWE in PB-DLBCL. A possible explanation for this finding is that a higher stiffness may reflect higher tumor cellularity, lower tumor necrosis, higher

Table 3 Shear wave elastography features of primary breast diffuse large B-cell lymphoma lesions

Feature	PB-DLBCL (*n* = 32)	Benign (*n* = 32)	*P* value	AUC
	mean ± SD/range	mean ± SD/range		
Mean elasticity value (kPa)	113.4 ± 46.9/(42-212)	27.8 ± 16.4/(9-68)	< 0.001	0.969
Standard deviation (kPa)	29.6 ± 14/(11-64)	11 ± 6/(4-28)	< 0.001	0.875
Minimum elasticity value (kPa)	51 ± 21/(19-97)	13 ± 7/(5-34)	< 0.001	0.906
Maximum elasticity value (kPa)	175 ± 67/(82-321)	46 ± 23/(18-98)	< 0.001	0.938
Ratio of lesion to fat	7.1 ± 3.2/(2.6-14.5)	1.8 ± 0.9/(0.7-4.2)	< 0.001	0.812

PB-DLBCL: Primary breast diffuse large B-cell lymphoma; AUC: Area under the curve.

Table 4 Mean elasticity value and Ki-67 expression level of primary breast diffuse large B-cell lymphoma lesions

Ki-67 expression level (%)	Mean elasticity value (kPa)
20	42
25	46
30	51
35	55
40	59
45	64
50	68
55	73
60	78
65	83
70	88
75	93
80	98
85	103
90	108
95	113

tumor invasiveness, higher tumor angiogenesis, and higher tumor resistance to chemotherapy or radiotherapy[20]. Therefore, SWE may be a valuable adjunct to conventional US to improve the management of PB-DLBCL.

This study has certain limitations that should be acknowledged. First, this was a retrospective study with a small sample size and a single-center design, which may limit the generalizability and validity of the results. Second, one type of SWE technique (2D-SWE) was used. It may perform differently from other SWE techniques (such as point SWE or 3D-SWE)[21]. Third, the conventional US and SWE features of PB-DLBCL were compared with those of benign breast lesions but not with those of other malignant breast lesions. This may have resulted in different diagnostic and prognostic implications. Fourth, only the conventional US and SWE features of PB-DLBCL before treatment were analyzed. No analysis was carried out after treatment. This may have influenced the different changes and correlations with the treatment response and outcome identified. Fifth, only the mean elasticity value was used as the main SWE feature for analysis. Other SWE features (such as standard deviation, minimum elasticity value, maximum elasticity value, or ratio of lesion to fat), with different possible diagnostic and prognostic values, were not considered. Sixth, only the Ki-67 expression level was used as the main histological and biological marker for correlation analysis. Other markers (such as BCL-2, BCL-6, MUM-1, CD10, or MYC)[4], which may have different associations with conventional US and SWE features of PB-DLBCL, were not obtained.

Table 5 Overall survival and progression-free survival of primary breast diffuse large B-cell lymphoma patients according to the mean elasticity value of primary breast diffuse large B-cell lymphoma lesions

Time (mo)	High-stiffness group OS (%)	High-stiffness group PFS (%)	Low-stiffness group OS (%)	Low-stiffness group PFS (%)
0	100	100	100	100
6	87.5	75	93.8	87.5
12	75	62.5	87.5	81.3
18	62.5	50	81.3	75
24	50	37.5	75	68.8
30	37.5	25	68.8	62.5
36	25	12.5	62.5	56.3
42	12.5	0	56.3	50
48	0	NA	50	43.8
54	NA	NA	43.8	NA
60	NA	NA	NA	NA

OS: Overall survival; PFS: Progression-free survival; NA: Not available.

CONCLUSION

In conclusion, conventional US and SWE provide useful information for the diagnosis and prognosis of PB-DLBCL. SWE has high diagnostic performance for distinguishing PB-DLBCL from benign breast lesions and can also reflect tumor proliferation and aggressiveness. SWE may be a valuable adjunct to conventional US to improve the management of PB-DLBCL.

ARTICLE HIGHLIGHTS

Research background

Primary breast diffuse large B-cell lymphoma (PB-DLBCL) is a rare invasive breast tumor. The accuracy of traditional ultrasound (US) imaging for PB-DLBCL is limited. By comparing traditional US and shear wave elastography (SWE), it is expected to achieve more accurate diagnosis, predict patient survival and disease progression, and improve decision-making and treatment strategies. SWE has also enhanced the understanding of the biological characteristics of PB-DLBCL, laying the foundation for future research. This study is of great significance in improving the diagnosis and treatment of PB-DLBCL.

Research motivation

It aims to understand its characteristics, diagnosis, and management. The study evaluates the limitations of conventional breast US and explores the potential of SWE in improving diagnosis and prognosis. Success in this research could lead to more accurate diagnoses, personalized treatment plans, and advancements in PB-DLBCL care.

Research objectives

Research compares conventional US and SWE features in PB-DLBCL. It aims to establish diagnostic criteria, explore the correlation between SWE and tumor aggressiveness (Ki-67 expression), and assess prognostic value for overall survival and progression-free survival. The goal is to enhance PB-DLBCL diagnosis and management, with SWE showing promise for disease differentiation and prognosis evaluation.

Research methods

This retrospective study compared conventional US and SWE in PB-DLBCL. The study included 32 patients with PB-DLBCL and analyzed US and SWE features. Findings showed distinct characteristics in PB-DLBCL lesions and identified a cutoff value of 54.5 kPa for SWE mean elasticity. Conventional US and SWE were valuable for diagnosing and forecasting PB-DLBCL, with SWE showing promise in differentiating PB-DLBCL from benign lesions and correlating with tumor aggressiveness. These findings highlight SWE's potential as an adjunct diagnostic tool in challenging breast lymphoma cases.

Research results

Research on PB-DLBCL revealed distinct US and SWE characteristics. PB-DLBCL exhibited specific US traits, while SWE had significantly higher mean elasticity values distinguishing it from benign lesions. SWE demonstrated high diagnostic performance, correlated with tumor aggressiveness, and predicted survival outcomes. This research highlights SWE's efficacy in PB-DLBCL diagnosis and prognosis, providing valuable insights for managing this challenging lymphoma subtype.

Research conclusions

This study highlights the diagnostic and prognostic significance of imaging techniques in PB-DLBCL. Conventional US has limitations in accuracy, while SWE effectively distinguishes PB-DLBCL from benign lesions. SWE's diagnostic performance correlates with tumor aggressiveness (Ki-67 expression), reflecting its potential for assessing proliferation. Higher SWE mean elasticity values are associated with poorer survival outcomes, indicating its promising role in disease management. These insights offer valuable guidance for managing this rare and challenging lymphoma subtype.

Research perspectives

This study suggests promising research perspectives for PB-DLBCL. These include advanced imaging, validation studies, treatment strategy impact, long-term monitoring, clinical guidelines, patient outcomes, and cost-benefit analyses. These directions can enhance PB-DLBCL understanding, improve diagnosis and management, and lead to personalized treatment approaches, benefiting patients with this challenging condition.

FOOTNOTES

Author contributions: Zhang XD proposed the concept of this study, contributed to data collection, and drafted the first draft; Zhang K contributed to the formal analysis, guides research, methodlogy, and visualization of this study; Zhang XD and Zheng K participated in the research, validated this study, jointly reviewed and edited the manuscript.

Institutional review board statement: This study was reviewed and approved by the Ethics Committee of the Affiliated Hospital of Guizhou Medical University.

Informed consent statement: Patients were not required to give informed consent to the study because the analysis used anonymous clinical data that were obtained after each patient agreed to treatment by written consent.

Conflict-of-interest statement: The authors of this manuscript having no conflicts of interest to disclose.

Data sharing statement: No additional data are available.

Open-Access: This article is an open-access article that was selected by an in-house editor and fully peer-reviewed by external reviewers. It is distributed in accordance with the Creative Commons Attribution NonCommercial (CC BY-NC 4.0) license, which permits others to distribute, remix, adapt, build upon this work non-commercially, and license their derivative works on different terms, provided the original work is properly cited and the use is non-commercial. See: https://creativecommons.org/Licenses/by-nc/4.0/

Country/Territory of origin: China

ORCID number: Xiao-Duan Zhang 0009-0001-3467-2767; Kai Zhang 0009-0004-2964-339X.

S-Editor: Yan JP
L-Editor: A
P-Editor: Zhao S

REFERENCES

1 **James ER**, Miranda RN, Turner SD. Primary Lymphomas of the Breast: A Review. *JPRAS Open* 2022; **32**: 127-143 [PMID: 35402679 DOI: 10.1016/j.jpra.2022.01.004]
2 **Sakhri S**, Aloui M, Bouhani M, Bouaziz H, Kamoun S, Slimene M, Ben Dhieb T. Primary breast lymphoma: a case series and review of the literature. *J Med Case Rep* 2023; **17**: 290 [PMID: 37370180 DOI: 10.1186/s13256-023-03998-8]
3 **Avilés A**, Delgado S, Nambo MJ, Neri N, Murillo E, Cleto S. Primary breast lymphoma: results of a controlled clinical trial. *Oncology* 2005; **69**: 256-260 [PMID: 16166814 DOI: 10.1159/000088333]
4 **Feng R**, Huang W, Chen L, Min J, Shu W, Yu Y, Wang X, Cao X, Liu B. Clinicopathological characteristics, local treatment, and prognostic factors in IE/IIE primary breast lymphoma: a retrospective study of 67 patients. *World J Surg Oncol* 2023; **21**: 127 [PMID: 37032326 DOI: 10.1186/s12957-023-03007-8]
5 Correction. *Cancer Sci* 2019; **110**: 1503 [PMID: 30945406 DOI: 10.1111/cas.13927]
6 **Berg WA**, Blume JD, Cormack JB, Mendelson EB, Lehrer D, Böhm-Vélez M, Pisano ED, Jong RA, Evans WP, Morton MJ, Mahoney MC, Larsen LH, Barr RG, Farria DM, Marques HS, Boparai K; ACRIN 6666 Investigators. Combined screening with ultrasound and

mammography vs mammography alone in women at elevated risk of breast cancer. *JAMA* 2008; **299**: 2151-2163 [PMID: 18477782 DOI: 10.1001/jama.299.18.2151]

7 **Alvarez S**, Añorbe E, Alcorta P, López F, Alonso I, Cortés J. Role of sonography in the diagnosis of axillary lymph node metastases in breast cancer: a systematic review. *AJR Am J Roentgenol* 2006; **186**: 1342-1348 [PMID: 16632729 DOI: 10.2214/AJR.05.0936]

8 **Treece GM**, Gee AH, Prager RW, Cash CJ, Berman LH. High-definition freehand 3-D ultrasound. *Ultrasound Med Biol* 2003; **29**: 529-546 [PMID: 12749923 DOI: 10.1016/s0301-5629(02)00735-4]

9 **Shiina T**, Nightingale KR, Palmeri ML, Hall TJ, Bamber JC, Barr RG, Castera L, Choi BI, Chou YH, Cosgrove D, Dietrich CF, Ding H, Amy D, Farrokh A, Ferraioli G, Filice C, Friedrich-Rust M, Nakashima K, Schafer F, Sporea I, Suzuki S, Wilson S, Kudo M. WFUMB guidelines and recommendations for clinical use of ultrasound elastography: Part 1: basic principles and terminology. *Ultrasound Med Biol* 2015; **41**: 1126-1147 [PMID: 25805059 DOI: 10.1016/j.ultrasmedbio.2015.03.009]

10 **Berg WA**, Cosgrove DO, Doré CJ, Schäfer FK, Svensson WE, Hooley RJ, Ohlinger R, Mendelson EB, Balu-Maestro C, Locatelli M, Tourasse C, Cavanaugh BC, Juhan V, Stavros AT, Tardivon A, Gay J, Henry JP, Cohen-Bacrie C; BE1 Investigators. Shear-wave elastography improves the specificity of breast US: the BE1 multinational study of 939 masses. *Radiology* 2012; **262**: 435-449 [PMID: 22282182 DOI: 10.1148/radiol.11110640]

11 **Voria P**, Eby PR, Allison K. Primary breast lymphoma. *Radiol Case Rep* 2010; **5**: 351 [PMID: 27307845 DOI: 10.2484/rcr.v5i1.351]

12 **Huang EH**, Lin SF, Yin HL, Hsu JS. Primary breast lymphoma. *Kaohsiung J Med Sci* 2013; **29**: 464-465 [PMID: 23906238 DOI: 10.1016/j.kjms.2012.12.008]

13 **Foo MY**, Lee WP, Seah CMJ, Kam C, Tan SM. Primary breast lymphoma: A single-centre experience. *Cancer Rep (Hoboken)* 2019; **2**: e1140 [PMID: 32721093 DOI: 10.1002/cnr2.1140]

14 **Swerdlow SH**, Campo E, Pileri SA, Harris NL, Stein H, Siebert R, Advani R, Ghielmini M, Salles GA, Zelenetz AD, Jaffe ES. The 2016 revision of the World Health Organization classification of lymphoid neoplasms. *Blood* 2016; **127**: 2375-2390 [PMID: 26980727 DOI: 10.1182/blood-2016-01-643569]

15 **Harris NL**, Jaffe ES, Stein H, Banks PM, Chan JK, Cleary ML, Delsol G, De Wolf-Peeters C, Falini B, Gatter KC. A revised European-American classification of lymphoid neoplasms: a proposal from the International Lymphoma Study Group. *Blood* 1994; **84**: 1361-1392 [PMID: 8068936]

16 **American College of Radiology**. Breast Imaging Reporting and Data System (BI-RADS®). Reston, VA: American College of Radiology, 2013. [cited Sep 20, 2023]. Available from: https://www.acr.org/Clinical-Resources/Reporting-and-Data-Systems/Bi-Rads

17 **Hofstetter LW**, Parker DL. Corrections to "The Role of Viscosity in the Impulse Diffraction Field of Elastic Waves Induced by the Acoustic Radiation Force" and "Supersonic Shear Imaging: A New Technique for Soft Tissue Elasticity Mapping". *IEEE Trans Ultrason Ferroelectr Freq Control* 2020; **67**: 1492-1494 [PMID: 32070952 DOI: 10.1109/TUFFC.2020.2973565]

18 **Huang R**, Jiang L, Xu Y, Gong Y, Ran H, Wang Z, Sun Y. Comparative Diagnostic Accuracy of Contrast-Enhanced Ultrasound and Shear Wave Elastography in Differentiating Benign and Malignant Lesions: A Network Meta-Analysis. *Front Oncol* 2019; **9**: 102 [PMID: 30891425 DOI: 10.3389/fonc.2019.00102]

19 **Wiesner FG**, Magener A, Fasching PA, Wesse J, Bani MR, Rauh C, Jud S, Schrauder M, Loehberg CR, Beckmann MW, Hartmann A, Lux MP. Ki-67 as a prognostic molecular marker in routine clinical use in breast cancer patients. *Breast* 2009; **18**: 135-141 [PMID: 19342238 DOI: 10.1016/j.breast.2009.02.009]

20 **Taljanovic MS**, Gimber LH, Becker GW, Latt LD, Klauser AS, Melville DM, Gao L, Witte RS. Shear-Wave Elastography: Basic Physics and Musculoskeletal Applications. *Radiographics* 2017; **37**: 855-870 [PMID: 28493799 DOI: 10.1148/rg.2017160116]

21 **Mercier L**, Langø T, Lindseth F, Collins DL. A review of calibration techniques for freehand 3-D ultrasound systems. *Ultrasound Med Biol* 2005; **31**: 449-471 [PMID: 15831324 DOI: 10.1016/j.ultrasmedbio.2004.11.015]

World Journal of Clinical Cases

Submit a Manuscript: https://www.f6publishing.com

World J Clin Cases 2023 November 26; 11(33): 8003-8012

DOI: 10.12998/wjcc.v11.i33.8003

ISSN 2307-8960 (online)

ORIGINAL ARTICLE

Retrospective Study

Artificial dermis combined with skin grafting for the treatment of hand skin and soft tissue defects and exposure of bone and tendon

Wei Wang, Dong-Sheng Chen, Zhao-Di Guo, Dan Yu, Qin Cao, Xiao-Wei Zhu

Specialty type: Surgery

Provenance and peer review: Unsolicited article; Externally peer reviewed.

Peer-review model: Single blind

Peer-review report's scientific quality classification

Grade A (Excellent): 0
Grade B (Very good): 0
Grade C (Good): C
Grade D (Fair): 0
Grade E (Poor): 0

P-Reviewer: Grabiec AM, Poland

Received: September 25, 2023
Peer-review started: September 25, 2023
First decision: October 17, 2023
Revised: October 25, 2023
Accepted: October 30, 2023
Article in press: October 30, 2023
Published online: November 26, 2023

Wei Wang, Dong-Sheng Chen, Dan Yu, Xiao-Wei Zhu, Department of Operating Room, The First People Hospital of Jiangxia District, Wuhan 430200, Hubei Province, China

Zhao-Di Guo, Qin Cao, Department of Hand Surgery, The First People Hospital of Jiangxia District, Wuhan 430200, Hubei Province, China

Corresponding author: Xiao-Wei Zhu, MD, Chief Physician, Department of Operating Room, The First People Hospital of Jiangxia District, No. 1 Cultural Avenue, Jiangxia District, Wuhan 430200, Hubei Province, China. xiaoweizhu0818@163.com

Abstract

BACKGROUND

The recovery time of hand wounds is long, which can easily result in chronic and refractory wounds, making the wounds unable to be properly repaired. The treatment cycle is long, the cost is high, and it is prone to recurrence and disability. Double layer artificial dermis combined with autologous skin transplantation has been used to repair hypertrophic scars, deep burn wounds, exposed bone and tendon wounds, and post tumor wounds.

AIM

To investigate the therapeutic efficacy of autologous skin graft transplantation in conjunction with double-layer artificial dermis in treating finger skin wounds that are chronically refractory and soft tissue defects that expose bone and tendon.

METHODS

Sixty-eight chronic refractory patients with finger skin and soft tissue defects accompanied by bone and tendon exposure who were admitted from July 2021 to June 2022 were included in this study. The observation group was treated with double layer artificial dermis combined with autologous skin graft transplantation (n = 49), while the control group was treated with pedicle skin flap transplantation (n = 17). The treatment status of the two groups of patients was compared, including the time between surgeries and hospital stay. The survival rate of skin grafts/flaps and postoperative wound infections were evaluated using the Vancouver Scar Scale (VSS) for scar scoring at 6 mo after surgery, as well as the sensory injury grading method and two-point resolution test to assess the recovery of skin sensation at 6 mo. The satisfaction of the two groups of patients was also compared.

RESULTS

Wound healing time in the observation group was significantly longer than that in the control group ($P < 0.05$, 27.92 ± 3.25 d *vs* 19.68 ± 6.91 d); there was no significant difference in the survival rate of skin grafts/flaps between the two patient groups ($P > 0.05$, 95.1 ± 5.0 *vs* 96.3 ± 5.6). The interval between two surgeries (20.0 ± 4.3 d) and hospital stay (21.0 ± 10.1 d) in the observation group were both significantly shorter than those in the control group (27.5 ± 9.3 d) and (28.4 ± 17.7 d), respectively ($P < 0.05$). In comparison to postoperative infection (23.5%) and subcutaneous hematoma (11.8%) in the control group, these were considerably lower at (10.2%) and (6.1%) in the observation group. When comparing the two patient groups at six months post-surgery, the excellent and good rate of sensory recovery (91.8%) was significantly higher in the observation group than in the control group (76.5%) ($P < 0.05$). There was also no statistically significant difference in two point resolution ($P > 0.05$). The VSS score in the observation group (2.91 ± 1.36) was significantly lower than that in the control group (5.96 ± 1.51), and group satisfaction was significantly higher ($P < 0.05$, 90.1 ± 6.3 *vs* 76.3 ± 5.2).

CONCLUSION

The combination of artificial dermis and autologous skin grafting for the treatment of hand tendon exposure wounds has a satisfactory therapeutic effect. It is a safe, effective, and easy to operate treatment method, which is worthy of clinical promotion.

Key Words: Bilayer artificial dermis; Autologous skin graft; Tendon exposure; Bone exposure

©The Author(s) 2023. Published by Baishideng Publishing Group Inc. All rights reserved.

Core Tip: In this study, the observation group and the control group were treated with Lando double-layer artificial dermis and pedicled skin flap transplantation to repair hand wounds, respectively. There was no significant difference in the survival rate between the two groups of skin grafts/flaps after surgery. However, compared to the control group, the observation group had shorter surgical intervals and hospital stays, and the appearance of the fingers after surgery was better. The observation group also had better skin contracture and scar formation than the control group, resulting in higher satisfaction in the observation group.

Citation: Wang W, Chen DS, Guo ZD, Yu D, Cao Q, Zhu XW. Artificial dermis combined with skin grafting for the treatment of hand skin and soft tissue defects and exposure of bone and tendon. *World J Clin Cases* 2023; 11(33): 8003-8012
URL: https://www.wjgnet.com/2307-8960/full/v11/i33/8003.htm
DOI: https://dx.doi.org/10.12998/wjcc.v11.i33.8003

INTRODUCTION

As the primary organs used for labor and work, the hands and arms account for the majority of work-related injuries[1,2]. Hand injuries can have a major impact on a person's social work and everyday activities, causing patients to experience both physical and financial hardship[3,4]. The patient can be greatly impacted by pressure injuries to the hand, and due to the lengthy healing period, chronic and refractory wounds are easily formed, resulting in the wound being inadequately treated. The inability to recover quickly makes it challenging to return to a regular functional state. Patients may continue to have severe problems with the inflammatory response[5-7]. Pressure damage wounds can be chronic and resistant if they are not treated promptly, which will have a major negative impact on the wound's ability to heal[8,9].

The inability of skin and subcutaneous soft tissue to undergo a normal, orderly, and timely repair under the influence of internal and external factors, exhibit a pathological inflammatory response: wound non-healing is the complex formation mechanism of chronic refractory wounds[10,11]. The quality of life is significantly impacted by its intricate pathophysiology, which is frequently incurable, and secondary infections can occur[12]. In addition, the etiology is complicated, the course of therapy is protracted, expensive, and it is likely to reoccur and cause disability. In the medical field, treating refractory wounds is not easy[13]. Tissue engineering advancements have made it possible to treat refractory wounds with a novel approach that combines autologous skin graft with double layer artificial dermis, offering a fresh approach to treating minor finger skin abnormalities. Hypertrophic scars, severe burn wounds, exposed bone and tendon wounds, and postoperative tumor wounds have all been repaired using this approach[14]. This technique can reduce harm to the skin donor area, speed up the healing process, improve the appearance of the healed wound surface, and encourage functional recovery of the hands and feet. It can also lower the chance of scarring and recurrence.

In this study, a prospective analysis of 68 patients with refractory hand wounds admitted to the First People's Hospital of Jiangxia District, Wuhan City from July 2021 to June 2022 was conducted. Double layer artificial dermis combined with autologous skin graft was applied to treat these refractory wounds, which achieved satisfactory results, as described below.

MATERIALS AND METHODS

Clinical data

Sixty-eight patients with chronic and refractory hand wounds who were admitted to our hospital from July 2021 to June 2022 were included in this study. The general information and wound status of these patients are shown in Table 1.

Inclusion and exclusion criteria

Inclusion criteria: (1) Comply with the diagnostic criteria for hand bone and joint injuries in the "Diagnostic Standards for Orthopedic Diseases", with finger skin and soft tissue defects accompanied by tendon or bone exposure, and comply with skin flap transplantation; (2) Receive treatment 12 h after injury; and (3) No severe organ and tissue diseases such as heart, brain, blood vessels, liver, kidney, lung, *etc.*

Exclusion criteria: (1) Individuals with infections in other parts such as the urinary system, respiratory system, *etc.*; (2) People with diabetes, heart disease, and arterial occlusive disease of lower limbs; and (3) Individuals with severe mental, neurological, immune, and hematological disorders.

Methods

After admission, the patients underwent thorough debridement to remove necrotic and degenerative skin, soft tissue, periosteum, and other tissues attached to the wound surface, tendons, and phalanges. The necrotic tendons were removed where appropriate and the periosteum and aponeurosis were preserved as much as possible. After sufficient hemostasis, the wound surface was repeatedly rinsed with hydrogen peroxide and physiological saline.

The observation group was treated with double-layer artificial dermis combined with autologous skin graft. Artificial dermis implantation: A suitable model of double-layer artificial dermis (Lando, Shenzhen Qikang Medical Equipment Co., Ltd.) was selected based on the size and shape of the wound, the artificial dermis was cut to size, soaked in sterile 0.9% physiological saline, the saline was replaced after 5 min, and this procedure was repeated 3 times. A thick needle was used to puncture the artificial dermis for drainage purposes. The upper and lower layers of the artificial dermis were distinguished, collagen was tightly fitted on the wound surface avoiding wrinkles and gaps, and the edges were sown and fixed. The inner layer was covered with sterile Vaseline gauze, and the outer layer was wrapped with sterile gauze. After 3-5 d, the Vaseline gauze and sterile gauze were replaced, and the wound surface covered by the artificial dermis. If fluid accumulated under the artificial dermis, it was squeezed and discharged appropriately. After treatment, Vaseline gauze and sterile gauze use was continued for wrapping. The dressing was replaced every 2-3 d and the condition of the artificial dermis autologous skin grafting was observed: After 2-3 wk, when the color of the artificial dermis changed to reddish yellow or orange, the outer layer of the artificial dermis was removed. Based on the size of the patient's wound, an autologous medium thickness skin graft approximately 0.4 mm thick was obtained from normal skin (forearm). A thick needle was used to appropriately puncture the autologous skin, it was covered with vascularized artificial dermis, and then sutured and fixed. The inner layer was padded with sterile Vaseline gauze, and the outer layer was padded with sterile gauze for wrapping. The skin supply area was covered with sterile Vaseline gauze, and sterile gauze was used for pressure wrapping. The dressing was changed 7-10 d after surgery, survival of the skin graft was determined, and the dressing was then changed every 2-3 d. According to the survival status of the skin graft, the dressing and sutures were removed 12 to 14 d after surgery.

The control group was treated with pedicle flap transplantation using an abdominal pedicle flap. The skin flap was designed based on the size of the finger wound and the flap extended 20% beyond the area of the finger skin defect. Layered intermittent suturing repair of the flap donor area was performed. The affected finger was placed in the appropriate position of the abdominal skin flap, the skin flap was intermittently sutured and the skin margin of the finger wound the flap has a broken pedicle. Four weeks after surgery, the pedicle of the abdominal pedicle skin flap was performed.

Observation indicators

The following treatment outcomes in the two groups of patients were compared: (1) The interval between two surgeries and hospitalization time; (2) Wound healing through complete closure and epithelialization of the wound edge; and (3) The survival rate of skin grafts by assessing the proportion of active skin fragments on the wound surface.

The following postoperative wound infections between the two groups of patients were compared: (1) The amount of exudate using the Falange score of 4, with 1 being the minimum value; 2: Moderate; and 3: Out of control; and (2) Assessment of subcutaneous hematoma.

The postoperative wound recovery in the two groups of patients was compared as follows: (1) Skin sensation recovery after 6 mo using the sensory injury grading method and two-point resolution test. With regard to the sensory injury grading method S5: Completely normal sensation; S4: Some pain and tactile sensation with two-point discrimination; S3: Some pain and tactile sensation; S2: Pain and local touch; S1: Deep pain; S0: No sensation. S0 and S1 were considered poor, S2 and S3 were considered good, and S4 and S5 were considered excellent. The excellent rate and good rate were calculated; The two-point discrimination test, with higher scores and smaller distances indicated better finger recovery; and (2) After 6 mo, the Vancouver Scar Scale (VSS) was used to evaluate scar status in the receptor area, which included four aspects: color, vascular distribution, thickness, and softness, with a score of 0 to 15 points; The higher the score, the greater the scarring, and vice versa.

Satisfaction in the two groups of patients was compared using a questionnaire at the end of the sixth month of follow-up, with the score ranging from 0 to 100. The higher the score, the higher the patient satisfaction.

Table 1 General information on the study patients

Variable	Observation group	Control group
Sex (male/female)	42/7	14/3
Age, yr (mean ± SD)	45.18 ± 14.04	45.94 ± 13.06
BMI	26.72 ± 6.35	27.08 ± 5.07
Wound area, cm^2 (mean ± SD)	3.6 ± 0.47	3.7 ± 0.43
Exposed area, cm^2 (mean ± SD)	3.0 ± 0.32	3.1 ± 0.35
Leakage type (Tendon/bone)	5/45	1/17

BMI: Body mass index.

Statistical analysis

Data analysis was conducted using SPSS 26.0 statistical software. The chi square test was used to compare differences in categorical variables, such as postoperative wound infection and subcutaneous hematoma. For continuous variables, a normality test was first performed. For variables with a normal distribution, such as exudate volume and VSS, independent sample testing was used to compare differences and the values are reported as mean ± SD (standard deviation). $P < 0.05$ indicates a statistically significant difference.

Ethical considerations

All adult subjects provided written informed consent, and all clinical studies followed the principles of the Helsinki Declaration. Prior to analysis, all patient data were anonymous. The patients agreed in writing to the use of accompanying photographs in research, reports, and publications. The implementation of clinical monitoring was to monitor whether informed consent was obtained from all selected patients, whether the treatment process had been carried out correctly, and whether the recorded data were sufficient and accurate.

RESULTS

All 68 cases of chronic and refractory wounds of the hand healed. After wound healing all patients were discharged and followed up once a month for 6 mo.

Postoperative wound condition of the patients

Table 2 and Figure 1 show that the interval between two surgeries (20.0 ± 4.3 d) and hospitalization time (21.0 ± 10.1 d) in the observation group (artificial dermis combined with autologous skin graft transplantation) were significantly shorter than those in the control group (skin flap transplantation) (27.5 ± 9.3 d) and hospitalization time (28.4 ± 17.7 d), ($P < 0.05$), but the wound healing time in the observation group was significantly longer than that in the control group ($P < 0.05$, 27.92 ± 3.25 d *vs* 19.68 ± 6.91 d); There was no significant difference in the survival rate of skin grafts/flaps between the two groups of patients ($P > 0.05$, 95.1 ± 5.0 *vs* 96.3 ± 5.6). The rates of postoperative infection (10.2%) and subcutaneous hematoma (6.1%) in the observation group were significantly lower than those in the control group (23.5%) and (11.8%), respectively. At 6 mo after surgery, the excellent and good rate of sensory recovery in the observation group (91.8%) was significantly higher than that in the control group (76.5%) ($P < 0.05$), and there was no statistically significant difference in two-point resolution between the two groups of patients ($P > 0.05$); The VSS score in the observation group (2.91 ± 1.36) was significantly lower than that of the control group (5.96 ± 1.51), and satisfaction in the observation group was significantly higher than that in the control group ($P < 0.05$, 90.1 ± 6.3 *vs* 76.3 ± 5.2).

Typical cases

Figures 2 and 3 show representative cases of the natural progress of skin grafts after surgery in the two groups.

DISCUSSION

Exposed wounds of hand and foot tendons are extremely common in the clinical work of hand and foot surgeons and burn plastic surgeons. Due to the extremely important role of hands and feet in the daily life of patients, priority should be given to the function and aesthetic appearance of the affected limb when deciding on the repair method for such wounds[15]. Free flap transplantation is currently the most widely used treatment method for full-thickness skin defects [16]. However, as people's pursuit of beauty continues to improve, restoration of the appearance of hand and foot wounds after injury is increasingly valued, and the main factor affecting the appearance is excessive scar hyperplasia. Studies have shown[17-19] that the main cause of scar formation is contraction of the wound surface. Inhibiting the

Table 2 Postoperative wound conditions, *n* (%)

Variable	Observation group	Control group
Interval between two surgeries (d)	20.0 ± 4.3	27.5 ± 9.3
Hospital stay (d)	21.0 ± 10.1	28.4 ± 17.7
Wound healing time (d)	27.92 ± 3.25	19.68 ± 6.91
Skin graft/flap survival rate	95.1 ± 5.0	96.3 ± 5.6
Postoperative infection	5 (10.2)	4 (23.5)
Subcutaneous hematoma	3 (6.1)	2 (11.8)
Recovery of skin sensation		
Optimal	25 (51.0)	5 (29.4)
Good	20 (40.8)	8 (47.1)
Poor	4 (8.2)	4 (23.5)
Two point resolution		
≥ 7 mm	18 (36.7)	10 (58.5)
4-6 mm	31 (63.3)	7 (41.2)
VSS score	2.91 ± 1.36	5.96 ± 1.51
Satisfaction	90.1 ± 6.3	76.3 ± 5.2

VSS: Vancouver Scar Scale.

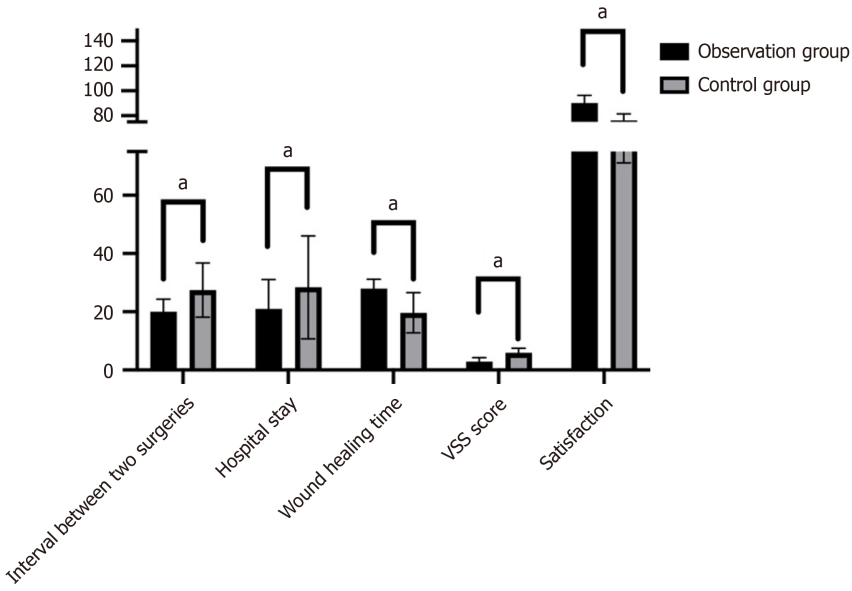

DOI: 10.12998/wjcc.v11.i33.8003 **Copyright** ©The Author(s) 2023.

Figure 1 Significant differences in the time between surgeries, hospital stay, wound healing time, Vancouver Scar Scale score, and satisfaction between the artificial dermis combined with skin flap transplantation group and the skin flap transplantation group ($P < 0.05$).

contraction of the wound surface helps to promote scar free regeneration, while artificial dermis, as a wound contraction inhibitor, can eliminate contraction and achieve scar minimization when used to treat soft tissue defects. Currently, artificial dermis has been widely used in the repair of burns, severe injuries, and non-healing wounds, and has achieved satisfactory results[20-22]. However, there are few reports on the application of artificial dermis combined with autologous skin patches in exposed wounds of hand and foot tendons.

Double layer artificial dermis is a substitute for dermis, with characteristics such as biomimetic and biodegradable properties[23]. The domestically produced double-layer artificial dermis Lando is composed of a medical silicone film on

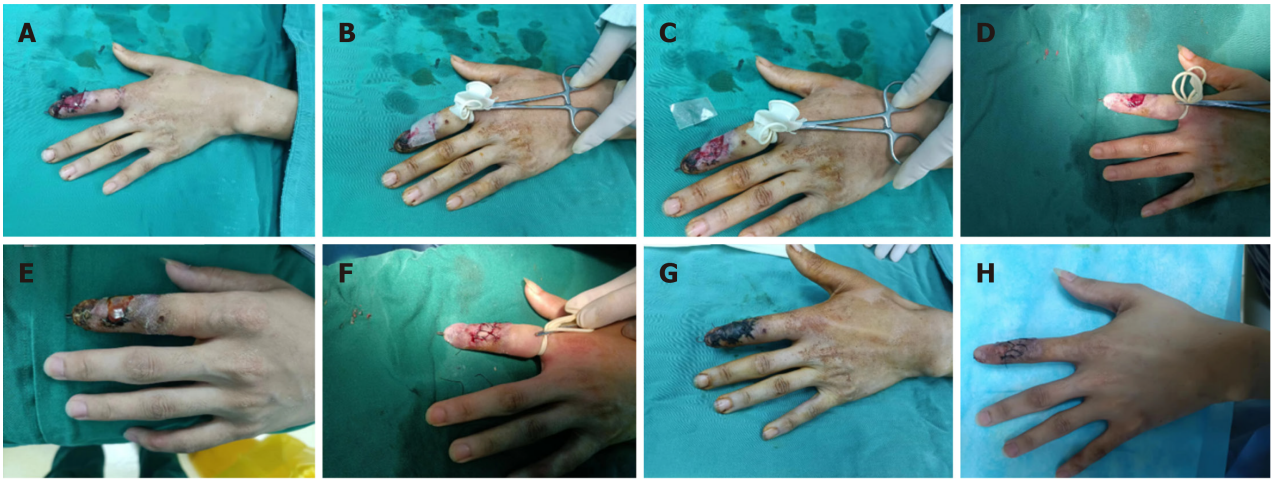

DOI: 10.12998/wjcc.v11.i33.8003 **Copyright** ©The Author(s) 2023.

Figure 2 Typical case in the observation group: A 53-year-old male patient with skin avulsion and necrosis of the left index finger. A: Physical examination showed a defect in the radial skin and soft tissue of the distal segment of the left index finger, with exposed bones and tendons. No fracture was found on preoperative X-ray examination; B: Left index finger debridement under local anesthesia and double layer artificial dermis (Lando) transplantation; C and D: Two weeks after surgery, the double layer artificial dermis was removed, and the exposed wound of the left index finger tendon bone was fresh and completely covered with granulation tissue; E: Under local anesthesia, left middle finger wound debridement and free forearm thick skin graft transplantation were performed, followed by postoperative pressure bandage; F and G: One week after removal of the compression pack, the skin graft on the affected finger wound survived well and the wound healed completely; H: After surgery, the skin grafting wound on the left index finger was smooth, with slight pigmentation and mild scar formation. The function of the injured finger recovered well. During follow-up, the patient was satisfied with the appearance and functional recovery of the wound, and the final Vancouver Scar Scale score was 2.0.

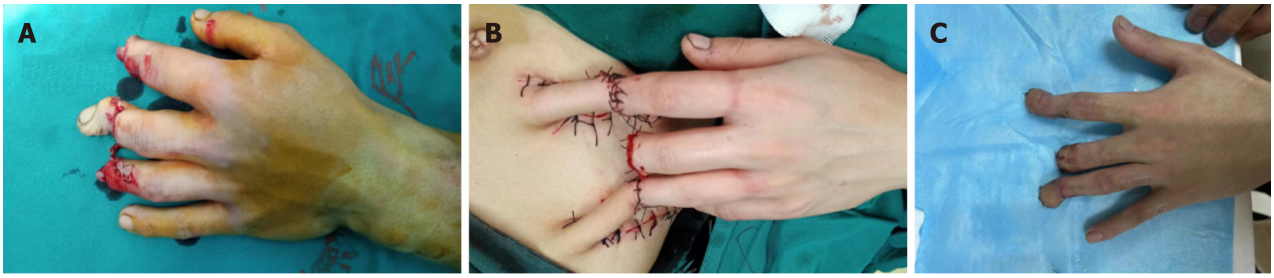

DOI: 10.12998/wjcc.v11.i33.8003 **Copyright** ©The Author(s) 2023.

Figure 3 Typical case in the control group. A: A 32-year-old male patient with degloving injury of the distal segment of the left index, middle, and ring fingers. Physical examination showed skin and soft tissue defects of the distal segment of the left index, middle, and ring fingers, with exposed bones and tendons. No fractures were found on preoperative X-ray examination; B: Left index and ring finger abdominal pedicle flap under local anesthesia; C: The appearance of the postoperative flap was relatively bulky, and its function was acceptable, but the feeling was not good. During follow-up, the patient was generally satisfied with the appearance and functional recovery of the wound, and the final Vancouver Scar Scale score was 6.0.

the surface layer and a bovine Achilles tendon collagen and polysaccharide removed from the end peptide on the lower layer. The semi-transparent medical silicone film on its surface has biomimetic functions, which can play a role in breathability, controlling moisture, and blocking bacteria. It has suitable flexibility, can fit the wound surface and has mechanical strength, ensuring the sealing of the wound and reducing the risk of infection. The lower dermis has a degradable function, and its sponge-like scaffold layer guides the inward migration, proliferation, and gradual maturation of vascular endothelial cells and capillaries to form new blood vessels and dermal regeneration, reducing scar formation, contracture, and restoring skin elasticity[24]. Artificial dermis is commonly used to repair burn wounds and has gradually been used in recent years to repair exposed wounds of bones and tendons[25].

Artificial dermis is divided into a silicone membrane on the surface and a collagen sponge on the bottom. The collagen sponge provides a scaffold for the orderly growth of fibroblasts and the formation of capillaries on the wound surface, constructing dermoid tissue with a rich blood supply, covering exposed tendons and bone tissue, thereby providing a good transplant bed for autologous skin graft transplantation and promoting skin graft survival. Therefore, patient satisfaction and the incidence of limb deformities in the observation group in the present study were better than those in the control group. In addition, due to the similar composition and structure of artificial dermis to natural human skin, it can guide the growth of cells and blood vessels, thereby achieving orderly regeneration and permanent reconstruction of dermal tissue[19]. When the artificial dermis is fully vascularized, the silicone membrane is removed and a very thin layer of autologous skin is transplanted onto the newly formed granulation tissue, achieving effects similar to medium or even full thickness skin transplantation. Therefore, in this study, patients with exposed hand and foot tendons were treated

with artificial dermis combined with autologous skin grafting. Due to the traditional free skin flap transplantation, the donor site healing time, wound surface, and scar growth in the donor site were repaired.

In this study, Lando double-layer artificial dermis and pedicled skin flap transplantation were used to repair wounds in the observation group and the control group, respectively. There was no significant difference in the survival rate of the skin graft/flap between the two groups after surgery. However, the observation group had shorter surgical intervals and hospital stays compared to the control group, and the postoperative appearance of the fingers was better. Skin contracture and scar formation after repair surgery are also important factors in evaluating the effectiveness of repair. We assessed the VSS score of the patient's wound surface during a follow-up period of 6 mo after surgery, and the results showed that the VSS score in the observation group was significantly lower than that in the control group. This indicated that Lando double-layer artificial dermis combined with autologous skin grafting is an effective method for repairing finger skin and soft tissue defects with bone and tendon exposure. In addition, the results of this study showed that with the prolongation of time after surgery, both groups of patients gradually recovered finger sensation, and the observation group had a significantly higher sensory recovery score at 6 mo after surgery than the control group, indicating that the use of Lando double-layer artificial dermis for wound repair was more effective than pedicle skin flap transplantation. This may be because newly generated fibroblasts and capillaries in the adjacent tissues after implantation of artificial dermis are immersed in the pores of the collagen sponge layer, and degrade to form a dermal-like granulation tissue matrix. On this basis, thin skin grafting was carried out, effectively reducing epidermal contracture and scar hyperplasia, and improving finger sensation recovery and flexibility. The proportion of patients in the observation group who had a 2-point resolution of 4-6 mm was higher than that in the control group at 6 mo after surgery, despite the fact that there was no significant difference in two-point resolution between the two groups. This finding may be related to the bias resulting from the small number of cases.

The results of this study show that compared with traditional skin flap repair methods, the application of artificial dermis in wound repair has the following advantages: (1) It can significantly inhibit scar growth and reduce skin contracture; (2) It can directly cover exposed tendons, reduce tendon adhesion, and create an excellent transplantation bed for blade thick skin grafting; (3) Increase the thickness and quality of soft tissue to achieve thinner autologous epidermal transplantation, minimizing trauma to the donor site; (4) After wound healing, the appearance is close to normal, effectively avoiding secondary scar repair; and (5) The surgical time is short, the surgery is simple and easy to perform, and the risk is low.

The results of this study indicate that thorough debridement of the wound surface is crucial before using double-layer artificial dermis, which is an important foundation for smooth vascularization of the artificial dermis[26,27]. In addition, we found that newly formed dermal tissue slowly grows inward from the outer edge of the wound, gradually covering the exposed bones and tendons until they are completely covered. Therefore, when double-layer artificial dermis is used to cover the wound, it should cover the fresh tissue at the edge of the wound to ensure successful vascularization of the artificial dermis and lay a solid foundation for later skin grafting. Infection and hematoma on the wound surface are the most common causes of failure in artificial dermis transplantation; thus, thorough debridement, hemostasis, and postoperative pressure bandages are all important for postoperative efficacy[28]. We chose to change the dressing for the first time 3-5 d after surgery, observe the condition of the wound, and if hematoma or infection was present, they were removed in a timely manner. The remaining artificial dermis can still be successfully vascularized, and measures such as a gauze dressing soaked with physiological saline containing antibiotics such as gentamicin or combined with negative pressure drainage can be applied. During the treatment process, the treatment strategy can be adjusted in a timely manner according to the patient's actual situation[29].

However, as reported in some studies[30,31], there are also some problems with the combination of artificial dermis and autologous skin graft repair: (1) This technology inevitably involves secondary surgery; in our study, patients in the observation group had longer wound healing time than those in the control group, and some patients in the observation group were dissatisfied with the long treatment cycle; (2) Although artificial dermis is relatively expensive, due to the obvious scars, transfer flap surgery often requires secondary scar repair treatment; thus, the overall cost increase is not significant. Therefore, in order to compare the hospital stay, cost, and surgical frequency of artificial dermis combined with autologous skin flap repair with traditional skin flap repair, a cost-benefit analysis is still needed; (3) The anti-infection ability of artificial dermis is poor, and the combination of artificial dermis and autologous blade thickness skin grafting requires strict aseptic procedures; and (4) The formation of hematoma is a common complication of artificial dermis and can easily lead to interruption of healing and loss of artificial dermis. Therefore, the combination of artificial dermis and autologous skin graft requires careful hemostasis and appropriate fixation.

The limitation of our research is that firstly, this graduate student center is small; therefore, our sample size was limited and larger studies are needed to determine the clinical efficacy of treatment with artificial dermis combined with skin grafting. Secondly, this study did not take into account factors that may affect wound recovery, such as the patient's job type, and whether they smoke or drink alcohol.

CONCLUSION

In summary, it is preliminarily believed that the combination of artificial dermis and autologous skin graft has a satisfactory therapeutic effect on hand tendon exposure wounds. It provides a safe, effective, and easy to operate treatment method, which is worthy of clinical promotion.

ARTICLE HIGHLIGHTS

Research background

When paired with autologous skin transplantation, double layer artificial dermis can promote functional recovery of hands and feet, limit damage to the skin donor area, improve the appearance of the healed wound surface, speed up the healing process, and lower the chance of scar formation and recurrence.

Research motivation

Treatment of chronic and refractory skin and soft tissue defects of the fingers with exposed bones and tendons.

Research objectives

To explore the clinical effect of double layer artificial dermis combined with autologous skin graft in repairing chronic refractory skin and soft tissue defects of the fingers with exposed bone and tendon.

Research methods

Sixty-eight chronic refractory patients with finger skin and soft tissue defects accompanied by bone and tendon exposure admitted to our hospital were selected and divided into the observation group (double layer artificial dermis combined with autologous skin grafting) and the control group (pedicle skin flap transplantation). The treatment status of the two groups of patients was compared, as well as the survival rate, scar formation, recovery, and patient satisfaction with skin grafts/flaps at 6 mo after surgery.

Research results

Recovery, postoperative infection, treatment, and patient satisfaction were better in the observation group than in the control group. Skin sensation recovery and skin graft/flap survival rate did not significantly differ between the control and observation groups.

Research conclusions

The combination of artificial dermis and autologous skin graft has a satisfactory therapeutic effect on hand tendon exposure wounds.

Research perspectives

The combination of artificial dermis and autologous skin grafting can be an effective method for treating hand tendon exposed wounds.

ACKNOWLEDGEMENTS

I would like to express my gratitude to all those helped me during the writing of this thesis. I acknowledge the help of my colleagues, they have offered me suggestions in academic studies.

FOOTNOTES

Co-first authors: Wei Wang and Dong-Sheng Chen.

Author contributions: Wang W and Chen DS designed the research; Wang W, Chen DS, Guo ZD, Cao Q, and Yu D performed the research; Zhu XW contributed new reagents/analytic tools; Zhu XW, Guo ZD, Cao Q, and Yu D analyzed the data; Wang W and Chen DS wrote the paper; All authors were involved in the critical review of the results and have contributed to, read, and approved the final manuscript. Wang W and Chen DS contributed equally to this work as co-first authors. The reasons for designating Wang W and Chen DS as co-first authors are threefold. First, the research was performed as a collaborative effort, and the designation of co-corresponding authorship accurately reflects the distribution of responsibilities and burdens associated with the time and effort required to complete the study and the resultant paper. This also ensures effective communication and management of post-submission matters, ultimately enhancing the paper's quality and reliability; Second, the overall research team encompassed authors with a variety of expertise and skills from different fields, and the designation of co-first authors best reflects this diversity. This also promotes the most comprehensive and in-depth examination of the research topic, ultimately enriching readers' understanding by offering various expert perspectives; Third, Wang W and Chen DS contributed efforts of equal substance throughout the research process. The choice of these researchers as co-first authors acknowledges and respects this equal contribution, while recognizing the spirit of teamwork and collaboration of this study. In summary, we believe that designating Wang W and Chen DS as co-first authors is fitting for our manuscript as it accurately reflects our team's collaborative spirit, equal contributions, and diversity.

Supported by Clinical Study of Artificial Dermis Combined with Skin Flap Replacement Flap in Limb Wound Repair, No. WX21C27.

Institutional review board statement: This study protocol was approved by The First People's Hospital of Jiangxia District, and all the families have voluntarily participated in the study and have signed informed consent forms.

Informed consent statement: All study participants or their legal guardian provided informed written consent prior to study enrolment.

Conflict-of-interest statement: All authors declare no conflicts of interest related to this study.

Data sharing statement: Data generated from this investigation are available upon reasonable quest from the corresponding author.

Open-Access: This article is an open-access article that was selected by an in-house editor and fully peer-reviewed by external reviewers. It is distributed in accordance with the Creative Commons Attribution NonCommercial (CC BY-NC 4.0) license, which permits others to distribute, remix, adapt, build upon this work non-commercially, and license their derivative works on different terms, provided the original work is properly cited and the use is non-commercial. See: https://creativecommons.org/Licenses/by-nc/4.0/

Country/Territory of origin: China

ORCID number: Xiao-Wei Zhu 0009-0000-4954-4736.

S-Editor: Liu JH
L-Editor: Webster JR
P-Editor: Xu ZH

REFERENCES

1 **Sozbilen MC**, Dastan AE, Gunay H, Kucuk L. One-year prospective analysis of hand and forearm injuries in children. *J Pediatr Orthop B* 2021; **30**: 364-370 [PMID: 32932418 DOI: 10.1097/BPB.0000000000000802]
2 **Luria S**, Talmud D, Volk I, Liebergall M, Calderon-Margalit R. The epidemiology of wrist and hand injury in two hospitals in Jerusalem: substantial differences between population subgroups. *Isr J Health Policy Res* 2019; **8**: 7 [PMID: 30626435 DOI: 10.1186/s13584-018-0278-0]
3 **Zhang J**, Ren J, Liu Y, Huang D, Lu L. Resveratrol regulates the recovery of rat sciatic nerve crush injury by promoting the autophagy of Schwann cells. *Life Sci* 2020; **256**: 117959 [PMID: 32531375 DOI: 10.1016/j.lfs.2020.117959]
4 **Lee JK**, Hwang D, Han SH, Lee Y. Complete Occlusion of Radial and Ulnar Arteries Following Hand Crush Injury with Multiple Carpometacarpal Joint Fracture-Dislocations. *J Hand Surg Asian Pac Vol* 2022; **27**: 376-380 [PMID: 35443882 DOI: 10.1142/S2424835522720122]
5 **Güntürk ÖB**, Kaplan İ, Yıldırım T, Gürbüz Y, Ademoğlu Y, Ada S. Reconstruction of mutilating hand injuries by microsurgical free tissue transfers from the foot. *Injury* 2021; **52**: 3646-3652 [PMID: 33838878 DOI: 10.1016/j.injury.2021.03.044]
6 **Shrestha S**, Tamrakar S, Banskota AK. Outline of Hand and Wrist Injuries Presenting to an Emergency of a Tertiary Care Centre in Nepal. *J Nepal Health Res Counc* 2019; **17**: 340-344 [PMID: 31735929 DOI: 10.33314/jnhrc.v17i3.1806]
7 **Kerschhagl M**, Larcher L, Mattiassich G, Prantl L. Replantation of a circumferentially degloved thumb in an occupational crush injury - A case report and review of the literature. *Clin Hemorheol Microcirc* 2019; **71**: 403-414 [PMID: 31006678 DOI: 10.3233/CH-199004]
8 **Messana F**, Faccio D, Rizzato S, Marchica P, Bassetto F, Vindigni V, Tiengo C. Combining traditional and microsurgical reconstruction after a complex hand trauma with multiple tissue defects. A case report. *Ann Ital Chir* 2021; **10** [PMID: 34569471]
9 **Zhou H**, Yu T. Effect of Comprehensive Rehabilitation Training Program in Orthopedic Nursing of Patients with Residual Limb Injury Caused by Crush. *J Healthc Eng* 2022; **2022**: 6769572 [PMID: 35126938 DOI: 10.1155/2022/6769572]
10 **Wilkinson HN**, Hardman MJ. Wound healing: cellular mechanisms and pathological outcomes. *Open Biol* 2020; **10**: 200223 [PMID: 32993416 DOI: 10.1098/rsob.200223]
11 **Cheng B**, Jiang Y, Fu X, Hao D, Liu H, Liu Y, Huang Z, Tan Q, Wang L, Hu D, Yang Y, Han C, Cheng Z, Ran X, Li Y. Epidemiological characteristics and clinical analyses of chronic cutaneous wounds of inpatients in China: Prevention and control. *Wound Repair Regen* 2020; **28**: 623-630 [PMID: 32585756 DOI: 10.1111/wrr.12825]
12 **Raziyeva K**, Kim Y, Zharkinbekov Z, Kassymbek K, Jimi S, Saparov A. Immunology of Acute and Chronic Wound Healing. *Biomolecules* 2021; **11** [PMID: 34066746 DOI: 10.3390/biom11050700]
13 **Falanga V**, Saap LJ, Ozonoff A. Wound bed score and its correlation with healing of chronic wounds. *Dermatol Ther* 2006; **19**: 383-390 [PMID: 17199681 DOI: 10.1111/j.1529-8019.2006.00096.x]
14 **Boyce ST**, Lalley AL. Tissue engineering of skin and regenerative medicine for wound care. *Burns Trauma* 2018; **6**: 4 [PMID: 30009192 DOI: 10.1186/s41038-017-0103-y]
15 **Lv Z**, Yu L, Wang Q, Jia R, Ding W, Shen Y. The use of dermal regeneration template for treatment of complex wound with bone/tendon exposed at the forearm and hand, a prospective cohort study. *Medicine (Baltimore)* 2019; **98**: e17726 [PMID: 31689814 DOI: 10.1097/MD.0000000000017726]
16 **Wang Y**, Xu R, Luo G, Lei Q, Shu Q, Yao Z, Li H, Zhou J, Tan J, Yang S, Zhan R, He W, Wu J. Biomimetic fibroblast-loaded artificial dermis with "sandwich" structure and designed gradient pore sizes promotes wound healing by favoring granulation tissue formation and wound re-epithelialization. *Acta Biomater* 2016; **30**: 246-257 [PMID: 26602823 DOI: 10.1016/j.actbio.2015.11.035]
17 **Rippa AL**, Kalabusheva EP, Vorotelyak EA. Regeneration of Dermis: Scarring and Cells Involved. *Cells* 2019; **8** [PMID: 31216669 DOI: 10.3390/cells8060607]
18 **Yannas IV**, Tzeranis DS, So PTC. Regeneration of injured skin and peripheral nerves requires control of wound contraction, not scar formation. *Wound Repair Regen* 2017; **25**: 177-191 [PMID: 28370669 DOI: 10.1111/wrr.12516]
19 **Yannas IV**, Tzeranis DS, So PTC. Regeneration mechanism for skin and peripheral nerves clarified at the organ and molecular scales. *Curr Opin Biomed Eng* 2018; **6**: 1-7 [PMID: 29392187 DOI: 10.1016/j.cobme.2017.12.002]
20 **Verbelen J**, Hoeksema H, Pirayesh A, Van Landuyt K, Monstrey S. Exposed tibial bone after burns: Flap reconstruction versus dermal substitute. *Burns* 2016; **42**: e31-e37 [PMID: 26376411 DOI: 10.1016/j.burns.2015.08.013]
21 **Chen X**, Chen H, Zhang G. Management of wounds with exposed bone structures using an artificial dermis and skin grafting technique. *Clin*

Plast Surg 2012; **39**: 69-75 [PMID: 22099850 DOI: 10.1016/j.cps.2011.09.011]

22 **Seavey JG**, Masters ZA, Balazs GC, Tintle SM, Sabino J, Fleming ME, Valerio IL. Use of a bioartificial dermal regeneration template for skin restoration in combat casualty injuries. *Regen Med* 2016; **11**: 81-90 [PMID: 26681342 DOI: 10.2217/rme.15.83]

23 **Qiu X**, Wang J, Wang G, Wen H. Vascularization of Lando(®) dermal scaffold in an acute full-thickness skin-defect porcine model. *J Plast Surg Hand Surg* 2018; **52**: 204-209 [PMID: 29320909 DOI: 10.1080/2000656X.2017.1421547]

24 **Wang W**, Zhang L, Sun L, She ZD, Tan RW, Niu XF. Biocompatibility and Immunotoxicology of the Preclinical Implantation of a Collagen-based Artificial Dermal Regeneration Matrix. *Biomed Environ Sci* 2018; **31**: 829-842 [PMID: 30558703 DOI: 10.3967/bes2018.110]

25 **Karami A**, Tebyanian H, Sayyad Soufdoost R, Motavallian E, Barkhordari A, Nourani MR. Extraction and Characterization of Collagen with Cost-Effective Method from Human Placenta for Biomedical Applications. *World J Plast Surg* 2019; **8**: 352-358 [PMID: 31620338 DOI: 10.29252/wjps.8.3.352]

26 **Widjaja W**, Tan J, Maitz PKM. Efficacy of dermal substitute on deep dermal to full thickness burn injury: a systematic review. *ANZ J Surg* 2017; **87**: 446-452 [PMID: 28304144 DOI: 10.1111/ans.13920]

27 **Nilforoushzadeh MA**, Sisakht MM, Amirkhani MA, Seifalian AM, Banafshe HR, Verdi J, Nouradini M. Engineered skin graft with stromal vascular fraction cells encapsulated in fibrin-collagen hydrogel: A clinical study for diabetic wound healing. *J Tissue Eng Regen Med* 2020; **14**: 424-440 [PMID: 31826321 DOI: 10.1002/term.3003]

28 **Hicks KE**, Huynh MN, Jeschke M, Malic C. Dermal regenerative matrix use in burn patients: A systematic review. *J Plast Reconstr Aesthet Surg* 2019; **72**: 1741-1751 [PMID: 31492583 DOI: 10.1016/j.bjps.2019.07.021]

29 **Ribeiro LM**, Guerra AS. [Hidradenitis Suppurativa: Combined Treatment with Dermal Template, Skin Graft and Negative Pressure Wound Therapy, a Case Study]. *Acta Med Port* 2018; **31**: 59-62 [PMID: 29573770 DOI: 10.20344/amp.8656]

30 **Yeong EK**, Yu YC, Chan ZH, Roan TL. Is artificial dermis an effective tool in the treatment of tendon-exposed wounds? *J Burn Care Res* 2013; **34**: 161-167 [PMID: 23292584 DOI: 10.1097/BCR.0b013e3182685f0a]

31 **Yeong EK**, Chen SH, Tang YB. The treatment of bone exposure in burns by using artificial dermis. *Ann Plast Surg* 2012; **69**: 607-610 [PMID: 23154329 DOI: 10.1097/SAP.0b013e318273f845]

World Journal of Clinical Cases

Submit a Manuscript: https://www.f6publishing.com

World J Clin Cases 2023 November 26; 11(33): 8013-8021

DOI: 10.12998/wjcc.v11.i33.8013

ISSN 2307-8960 (online)

ORIGINAL ARTICLE

Observational Study

Subcutaneous fat thickness and abdominal depth are risk factors for surgical site infection after gastric cancer surgery

Kuan-Yong Yu, Rong-Kang Kuang, Ping-Ping Wu, Guang-Hui Qiang

Specialty type: Gastroenterology and hepatology

Provenance and peer review: Unsolicited article; Externally peer reviewed.

Peer-review model: Single blind

Peer-review report's scientific quality classification

Grade A (Excellent): 0
Grade B (Very good): B
Grade C (Good): 0
Grade D (Fair): 0
Grade E (Poor): 0

P-Reviewer: Aydin S, Turkey

Received: August 14, 2023
Peer-review started: August 14, 2023
First decision: October 9, 2023
Revised: October 19, 2023
Accepted: November 2, 2023
Article in press: November 2, 2023
Published online: November 26, 2023

Kuan-Yong Yu, Rong-Kang Kuang, Guang-Hui Qiang, Department of Gastrointestinal Surgery, Nanjing Jiangbei Hospital, Nanjing 210044, Jiangsu Province, China

Ping-Ping Wu, Department of Endocrinology, Nanjing Jiangbei Hospital, Nanjing 210044, Jiangsu Province, China

Corresponding author: Guang-Hui Qiang, MD, Doctor, Surgeon, Department of Gastrointestinal Surgery, Nanjing Jiangbei Hospital, No. 552 Geguan Road, Jiangbei New District, Nanjing 210044, Jiangsu Province, China. guanghqiang@126.com

Abstract

BACKGROUND

Surgical site infection (SSI) is one of the most common complications after gastric cancer (GC) surgery. The occurrence of SSI can lead to a prolonged postoperative hospital stay and increased medical expenses, and it can also affect postoperative rehabilitation and the quality of life of patients. Subcutaneous fat thickness (SFT) and abdominal depth (AD) can be used as predictors of SSI in patients undergoing radical resection of GC.

AIM

To explore the potential relationship between SFT or AD and SSI in patients undergoing elective radical resection of GC.

METHODS

Demographic, clinical, and pre- and intraoperative information of 355 patients who had undergone elective radical resection of GC were retrospectively collected from hospital electronic medical records. Univariate analysis was performed to screen out the significant parameters, which were subsequently analyzed using binary logistic regression and receiver-operating characteristic curve analysis.

RESULTS

The prevalence of SSI was 11.27% (40/355). Multivariate analyses revealed that SFT [odds ratio (OR) = 1.150; 95% confidence interval (95%CI): 1.090–1.214; $P < 0.001$], AD (OR = 1.024; 95%CI: 1.009–1.040; $P = 0.002$), laparoscopic-assisted surgery (OR = 0.286; 95%CI: 0.030–0.797; $P = 0.017$), and operation time (OR = 1.008; 95%CI: 1.001–1.015; $P = 0.030$) were independently associated with the incidence of SSI after elective radical resection of GC. In addition, the product of SFT and AD was a better potential predictor of SSI in these patients than either

SFT or AD alone.

CONCLUSION
SFT and AD are independent risk factors and can be used as predictors of SSI in patients undergoing radical resection of GC.

Key Words: Subcutaneous fat thickness; Abdomen depth; Surgical site infection; Gastric cancer; Radical resection; Risk factors

©The Author(s) 2023. Published by Baishideng Publishing Group Inc. All rights reserved.

Core Tip: Surgical site infection (SSI) is one of the most common complications after gastric cancer (GC) surgery. We identified subcutaneous fat thickness (SFT) and abdominal depth (AD) as independent risk factors that can be used as predictors of SSI in patients undergoing radical resection of GC. Our findings may assist clinicians in evaluating the risk of SSI in patients with higher SFT and AD values.

Citation: Yu KY, Kuang RK, Wu PP, Qiang GH. Subcutaneous fat thickness and abdominal depth are risk factors for surgical site infection after gastric cancer surgery. *World J Clin Cases* 2023; 11(33): 8013-8021
URL: https://www.wjgnet.com/2307-8960/full/v11/i33/8013.htm
DOI: https://dx.doi.org/10.12998/wjcc.v11.i33.8013

INTRODUCTION

Gastric cancer (GC) is the fifth most common type of cancer worldwide and the third most fatal cancer[1]. Surgical resection accompanied by systemic adjuvant chemotherapy is still the best treatment for potentially treatable GC[2].

Surgical site infection (SSI) is the most common among all healthcare-associated infections[3]. SSI frequently occurs after gastric surgery, with an incidence ranging from 3.9% to 18.7%[4-7]. In addition to increasing hospital costs, SSI clearly prolongs hospital stay and results in long-term disability[8]. Prolonged operative duration[9], higher body mass index (BMI)[10], total gastrectomy, open surgery, and intraoperative blood transfusion[11] have been proven to be predictors of the development of SSI after elective gastrectomy.

As abdominal anatomical characteristics, subcutaneous fat thickness (SFT) and abdominal depth (AD) vary dramatically among individuals. Recently, SFT has been reported to be an independent risk factor for the development of SSI in intestinal resection [odds ratio (OR) = 2.519; 95% confidence interval (95%CI): 1.350–4.698; P = 0.004][12] and open appendectomy (OR = 3.52; 95%CI: 1.75–7.08; P < 0.001)[13]. Teppa *et al*[14] showed that when the SFT increases by more than 2.5 cm, the risk of SSI increases in abdominal surgeries. In Zhang *et al*'s study of patients undergoing radical resection of colorectal cancer, the complication group had a greater AD (9.24 ± 2.91 *vs* 7.77 ± 2.08, P < 0.001) compared to the non-complication group, and they thus concluded that a greater AD is associated with an increased risk of short-term postoperative complications for these patients[15]. Another study revealed a correlation between AD and heightened SSI risk following elective radical resection for colon cancer[16].

However, there are few studies on SFT, AD, and SSI after GC surgery. Therefore, we conducted a retrospective study to explore the relationship between SFT or AD and the incidence of SSI after elective radical resection of GC.

MATERIALS AND METHODS

Patients

Patients who had undergone GC surgery at our hospital between January 2015 and April 2023 were screened for eligibility. The exclusion criteria encompassed: (1) Emergent radical resection of GC; (2) reoperation for the recurrence of GC; (3) the presence of concomitant abdominal infectious diseases before the operation; and (4) incomplete clinical data (Figure 1). The eligible patients were those who underwent gastrectomy for GC and were histopathologically diagnosed with GC. The study cohort comprised 355 patients who had undergone elective radical resection of GC. Of these, 40 patients developed an SSI.

The patients' data, including demographic information, clinical data, preoperative laboratory results, surgical information, and pathological diagnosis, were collected from the electronic medical record system of the hospital. Computed tomography (CT) was performed to measure SFT and AD. SFT and AD were both measured at the level of the umbilicus in supine CT images (Figure 2). SFT was defined as the maximum sagittal distance between the parietal and visceral sides of the subcutaneous fat. AD was defined as the sagittal distance between the bottom of the umbilicus and the top of the vertebra. These parameters were measured by three independent operators, and the mean value was further analyzed.

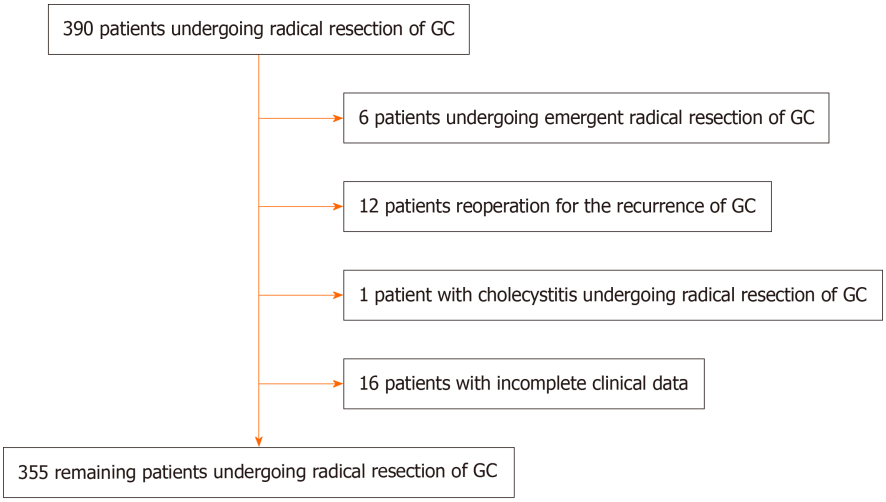

DOI: 10.12998/wjcc.v11.i33.8013 **Copyright** ©The Author(s) 2023.

Figure 1 Flowchart of patient exclusion. GC: Gastric cancer.

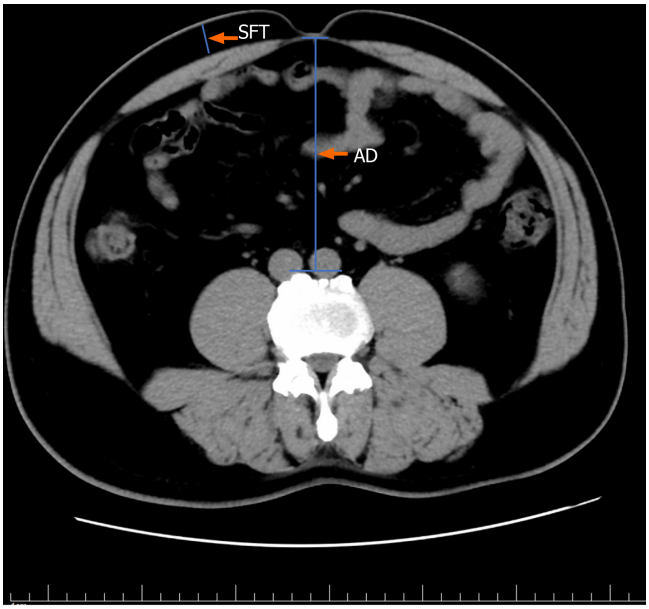

DOI: 10.12998/wjcc.v11.i33.8013 **Copyright** ©The Author(s) 2023.

Figure 2 Illustration of measurement of subcutaneous fat thickness and abdominal depth. SFT: Subcutaneous fat thickness; AD: Abdominal depth.

We assessed whether there was an infection at the surgical site in line with the World Health Organization criteria[17]. SSIs were classified into three groups, namely, superficial, deep, and organ/space infections. Briefly, an SSI occurred at the surgical site within 30 d of surgery, and was characterized by at least one of the following conditions: Purulent drainage from the surgical site, organisms isolated from an aseptically obtained culture of fluid or tissue from the surgical site, and/or incisional inflammation, including pain or tenderness, redness, and localized swelling. Based on the outcome, we divided all eligible patients into either an SSI or a non-SSI group.

A second-generation cephalosporin was administered intravenously as a prophylactic antibiotic in all of the patients within 30 min before the surgery, and an additional dose was administered every 3 h during the surgery. Quinolones or penicillin were administered to the patients allergic to cephalosporins. The duration of prophylactic antibiotic administration was generally 3–5 d after the surgery. This study was approved by the Medical Ethics Committee of the Nanjing Jiangbei Hospital. The need for informed consent was waived because of the retrospective nature of the study.

Statistical analysis

Continuous data were evaluated for normality using the Shapiro–Wilk test. Normally distributed data were analyzed using an unpaired *t*-test and are represented as the mean and standard deviation (mean ± SD). Non-normally distributed data were analyzed using the Mann–Whitney *U* test and are represented as the median and interquartile range. Categorical data were analyzed using Fisher's exact probability test and are expressed as frequencies and percentages. Univariate and multivariate logistic regression analyses were used to identify the risk factors for SSI. Multivariate logistic

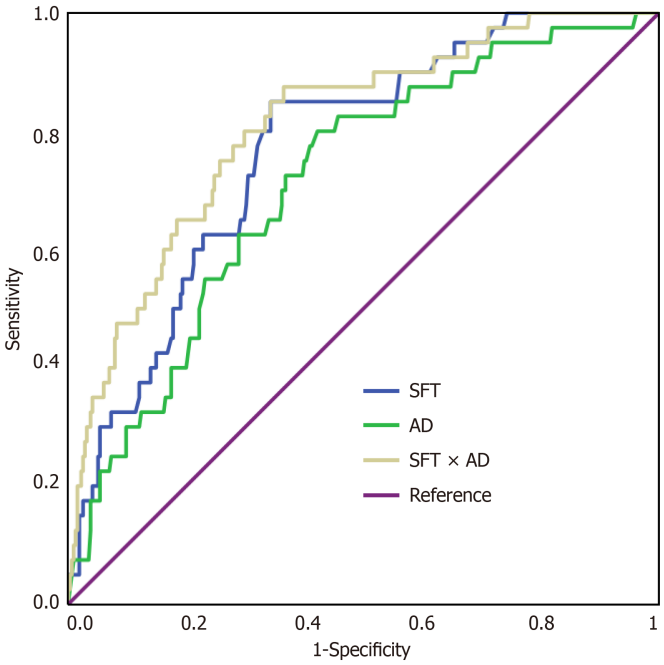

DOI: 10.12998/wjcc.v11.i33.8013 **Copyright** ©The Author(s) 2023.

Figure 3 Receiver-operating characteristic curve analysis of risk factors for surgical site infection. SFT: Subcutaneous fat thickness; AD: Abdominal depth; SFT × AD: The product of SFT and AD.

regression analysis was performed only on variables with $P < 0.05$ in the univariate analysis. Receiver-operating characteristic (ROC) curve analysis was performed to evaluate the predictive ability and optimal cutoff value of all biomarkers. All statistical analyses were performed using SPSS software (version 24.0; SPSS Inc., Chicago, IL, United States). All tests were two-tailed. Statistical significance was set at $P < 0.05$.

RESULTS

We analyzed 355 patients who had undergone elective radical resection of GC. Their mean age was 65.6 years (range, 29–91 years), and 71.9% of the patients were male. The characteristics of the patients with and without SSI are compared in Table 1. While no statistically significant difference in age, gender, smoking, alcohol use, diabetes, hypertension, type of resection, blood loss, history of laparotomy, albumin, prealbumin, or tumor-node-metastasis stage was observed between the SSI and non-SSI groups, there were statistically significant differences in BMI ($P < 0.001$), SFT ($P < 0.001$), AD ($P < 0.001$), laparoscopic-assisted surgery ($P = 0.042$), and operation time ($P = 0.013$).

To study the relationship between the individual risk factors and the incidence of SSI, we performed multivariate analysis on the factors with $P < 0.05$ in the univariate analysis. As shown in Table 2, the univariate analysis revealed that the incidence of SSI was significantly associated with BMI ($P < 0.001$), SFT ($P < 0.001$), AD ($P < 0.001$), the product of SFT and AD (SFT × AD) ($P < 0.001$), laparoscopic-assisted surgery ($P = 0.048$), and operation time (P = 0.010). The multivariate analysis revealed that SFT (OR = 1.150; 95%CI: 1.090–1.214; $P < 0.001$), AD (OR = 1.024; 95%CI: 1.009–1.040; $P = 0.002$), laparoscopic-assisted surgery (OR = 0.322; 95%CI: 0.119–0.870; $P = 0.025$), and operation time (OR = 1.008; 95%CI: 1.001–1.015; $P = 0.026$) were independently associated with the incidence of SSI.

ROC analysis was performed to determine the predictive value of SFT, AD, and SFT × AD value for SSI in patients who underwent elective radical resection of GC (Table 3 and Figure 3). The optimum cutoff values for SFT, AD, and SFT × AD were 16.55, 67.85, and 11.11, respectively. The area under the ROC (AUC) values of SFT and AD were 0.770 (95%CI: 0.700–0.839) and 0.715 (95%CI: 0.635–0.795), respectively. The use of SFT × AD (AUC = 0.810; 95%CI: 0.740–0.879) demonstrated higher diagnostic value than the use of either SFT or AD alone.

DISCUSSION

By comparing 315 non-SSI and 40 SSI patients who had received elective radical resection of GC, we found that the two groups significantly differed in BMI, SFT, AD, laparoscopic-assisted surgery, and operation time; these variables may be risk factors for SSI. In addition, SFT, AD, laparoscopic-assisted surgery, and operation time were independently associated with SSI as evidenced by the logistic regression analysis. Further diagnostic power analysis identified that SFT × AD was a better potential predictor of SSI in these patients than either SFT or AD alone. These findings may assist clinicians in evaluating the risk of SSI in patients with a higher SFT × AD value.

Table 1 Characteristics of the study group, *n* (%)

Variable	Surgical site infection		*P* value
	Absent (*n* = 315)	Present (*n* = 40)	
Age (yr)	65.3 ± 9. 6	66.4 ± 9.8	0.529
Male	227 (72.10)	28 (70.00)	0.785
BMI (kg/m^2)	22.68 ± 3.22	25.12 ± 2.78	< 0.001[a]
SFT (mm)	14.20 (10.00–18.40)	20.45 (17.00–26.63)	< 0.001[a]
AD (mm)	64.90 (50.60–78.20)	82.50 (68.43–97.00)	< 0.001[a]
Smoking	87 (27.60)	15 (37.50)	0.193
Alcohol use	66 (21.00)	11 (27.50)	0.344
Diabetes	40 (12.70)	9 (22.50)	0.090
Laparoscopic-assisted surgery	96 (30.5)	6 (15.00)	0.042[a]
Hypertension	95 (30.2)	12 (30.0)	0.984
Type of resection			0.371
Total gastrectomy	206 (65.40)	29 (34.60)	
Partial gastrectomy	109 (35.98)	11 (27.50)	
Operation time (min)	210.00 (180.00–240.00)	240.00 (209.25–270.00)	0.013[a]
Blood loss (mL)	150.00 (100.00–200.00)	150.00 (112.00–200.00)	0.099
History of laparotomy	47 (14.90)	7 (17.50)	0.669
Albumin (g/dL)	39.37 ± 4.99	40.29 ± 3.55	0.258
Prealbumin (g/dL)	188.25 ± 59.06	194.92 ± 63.09	0.509
TNM stage			0.304
I	96 (29.2)	10 (25.0)	
II	92 (30.5)	17 (42.5)	
III	127 (40.3)	13 (32.5)	

[a]$P < 0.05$.

BMI: Body mass index; SFT: Subcutaneous fat thickness; AD: Abdominal depth; TNM: Tumor-node-metastasis.

SSI remains a significant cause of morbidity after gastric surgery. SSI prolongs the length of hospital stay and increases the risk of incisional hernias. Although various measures to prevent the occurrence of SSI have recently been reported, the incidence of infection has not dropped below a negligible level. In this study, we explored the relationship between abdominal anatomical characteristics, including SFT, AD, and SFT × AD, and the rate of SSI following gastric surgery.

Thicker subcutaneous fat can increase the tension of the suture at the incision site, thereby reducing the blood supply to the incision site, which increases the risk of incision liquefaction and delayed healing. As previously reported, SFT is an independent risk factor for SSI in a variety of surgical procedures, including surgery for Crohn's disease[12], acute appendicitis surgery[13], elective colorectal surgery[18], and posterior cervical fusion surgery[19]. However, Liu *et al*[16] found that although the SFT was higher in patients with SSI after colorectal surgery than in non-SSI patients, it was not an independent risk factor for SSI. In our study, SFT was positively associated with the rate of SSI after elective radical resection of GC.

A previous study reported that the sagittal abdominal diameter was closely associated with general and visceral obesity[20]. Sur *et al* revealed that visceral obesity was related to SSI in patients undergoing surgery for colon cancer[21]. For patients with a deeper abdomen, surgical exposure is usually more difficult and the operation time is longer, which increases the risk of postoperative SSI. In the study by Liu *et al*[16], involving 55 SSI-afflicted patients juxtaposed against 55 propensity-score-matched counterparts without SSI, both groups having experienced elective radical resection for colon cancer, elevated AD value emerged as a potential risk factor for SSI. This observation is consistent with the conclusion drawn in the current research.

Increased BMI as a biomarker to measure obesity has been reported to be an incremental and independent risk factor for SSI in patients undergoing colorectal surgery[22]. The same was confirmed in patients undergoing gastric surgery [23]. Our univariate model data revealed that the patients in the SSI group exhibited high BMI values compared with those in the non-SSI group, but the significance was lost in the multivariate model, so BMI could not be used as a biomarker for SSI prediction.

Table 2 Risk factors for surgical site infection in univariate and multivariate analysis

Variable	Univariate analysis	*P* value	Multivariate analysis	*P* value
	OR (95%CI)		OR (95%CI)	
Age (yr)	1.011 (0.977–1.047)	0.528		
Male	0.905 (0.440–1.858)	0.785		
BMI (kg/m^2)	1.259 (1.133–1.398)	< 0.001	-	-
SFT (mm)	1.137 (1.186–1.192)	< 0.001	1.150 (1.090–1.214)	< 0.001[a]
AD (mm)	1.031 (1.017–1.046)	< 0.001	1.024 (1.009–1.040)	0.002[a]
Smoking	1.572 (0.792–3.123)	0.196		
Alcohol use	1.431 (0.679–3.015)	0.346		
Diabetes	1.996 (0.885–4.500)	0.096		
Laparoscopic-assisted surgery	0.403 (0.164–0.991)	0.048	0.286 (0.03–0.797)	0.017[a]
Hypertension	0.992 (0.484–2.034)	0.984		
Type of resection				
Total gastrectomy	1.395 (0.671–2.900)	0.373		
Operation time (min)	1.008 (1.002–1.015)	0.010	1.008 (1.001–1.015)	0.030[a]
Blood loss (mL)	1.000 (0.999–1.002)	0.659		
History of laparotomy	1.210 (0.505–2.894)	0.669		
Albumin (g/dL)	1.041 (0.971–1.116)	0.258		
Prealbumin (g/dL)	1.002 (0.996–1.001)	0.508		
TNM stage				
I	–	–		
II	1.629 (0.709–3.743)	0.250		
III	0.942 (0.396–2.241)	0.892		

[a]$P < 0.05$.

BMI: Body mass index; SFT: Subcutaneous fat thickness; AD: Abdominal depth.

Table 3 Diagnostic value of subcutaneous fat thickness, abdominal depth, and the product of subcutaneous fat thickness and abdominal depth for surgical site infection

	Cutoff value	Sensitivity	Specificity	+LR	−LR	AUC
SFT	16.55	0.850	0.657	2.479	0.228	0.770 (0.700–0.839)
AD	67.85	0.800	0.578	1.895	0.346	0.715 (0.635–0.795)
SFT × AD	11.11	0.875	0.635	2.397	0.197	0.810 (0.740–0.879)

+LR: Positive likelihood ratio; −LR: Negative likelihood ratio; SFT: Subcutaneous fat thickness; AD: Abdominal depth; SFT × AD: The product of SFT and AD.

A meta-analysis has shown that prolonged operative duration bears an increased risk of SSI after various surgical procedures, such as colorectal surgery, urological surgery, plastic and maxillofacial surgery, obstetrics and gynecology surgery, and orthopedic surgery[24]. According to Michael *et al*, increased operative duration is associated with an increased risk of SSI after unicompartmental knee arthroplasty, and the authors believe that the operative duration is a surgeon-dependent and potentially modifiable risk factor, which may indicate the complexity and difficulty of the operation[25]. In the present study, the longer operation time was an independent risk factor for the rate of SSI after GC surgery.

To the best of our knowledge, this study is the first to investigate the relationship between SFT or AD and SSI after elective radical resection of GC. Our findings reveal the relationship between these two abdominal anatomical indicators and the development of SSI in patients undergoing elective radical gastrectomy, which can help clinicians in the early

identification and treatment of postoperative SSI.

The present study has several limitations. First, this was a single-center retrospective study with some inevitable recall and selection biases, which may limit its generalizability. Second, this study did not assess other known potential predictors related to SSI, such as intraoperative hypothermia, anemia, and inadequate oxygenation. Third, the present study did not investigate the mechanism by which abdominal anatomical features affect the risk of SSI. Therefore, a multicenter prospective study is warranted to confirm the accuracy of the results and to provide strategies to prevent SSI in patients with GC.

CONCLUSION

Our results suggest that preoperative SFT, AD, and operation time are independent risk factors for SSI after GC surgery, while laparoscopic-assisted surgery is a protective factor. The multiplied value of SFT and AD can be used as a predictor of SSI in patients after elective radical resection of GC.

ARTICLE HIGHLIGHTS

Research background

Surgical site infection (SSI) is one of the most common complications after gastric cancer (GC) surgery. The occurrence of SSI has an adverse impact on the prognosis of patients. There are very few studies that focus on the effect of subcutaneous fat thickness (SFT) and abdominal depth (AD) on postoperative SSI.

Research motivation

In this study, the authors sought to identify ways to assist clinicians in the early identification and treatment of postoperative SSI after GC surgery.

Research objectives

To explore the potential relationship between SFT or AD and SSI in patients after elective radical resection of GC.

Research methods

Demographic, clinical, and pre- and intraoperative information of 355 patients who had undergone elective radical resection of GC were retrospectively collected from hospital electronic medical records. Univariate and multivariate logistic regression analyses were used to screen for the risk factors contributing to SSI incidence. Furthermore, the receiver-operating characteristic (ROC) curve method was employed to evaluate the predictive power and best cutoff value for the biomarkers under consideration.

Research results

The prevalence of SSI was 11.27% (40/355). Multivariate analyses revealed that SFT, AD, laparoscopic-assisted surgery, and operation time were independently associated with the incidence of SSI after elective radical resection of GC. The area under the ROC curve values of SFT, AD, and the product of SFT and AD (SFT × AD) were 0.770 [95% confidence interval (95%CI): 0.700–0.839], 0.715 (95%CI: 0.635–0.795), and 0.810 (95%CI: 0.740–0.879), respectively.

Research conclusions

Our results suggest that preoperative SFT, AD, and operation time are independent risk factors for SSI after GC surgery, while laparoscopic-assisted surgery is a protective factor. In addition, SFT × AD is a better potential predictor of SSI in these patients than either SFT or AD alone.

Research perspectives

In the future, we will increase the sample size used to construct the model and conduct a multicenter study.

FOOTNOTES

Author contributions: Qiang GH and Yu KY designed the study; Kuang RK drafted the work; Wu PP and Yu KY collected the data; Yu KY and Kuang RK analyzed and interpreted the data; Yu KY and Wu PP wrote the manuscript; Qiang GH and Kuang RK revised the manuscript; all authors read and confirmed the final revision of the manuscript.

Supported by The Nanjing Health Science and Technology Development Fund Project, No. YKK18241.

Institutional review board statement: The study was reviewed and approved by the Ethics Committee of the Nanjing Jiangbei Hospital.

Informed consent statement: The need for informed consent was waived because of the retrospective nature of the study.

Conflict-of-interest statement: There are no conflicts of interest to report.

Data sharing statement: No additional data are available.

STROBE statement: The authors have read the STROBE Statement—checklist of items, and the manuscript was prepared and revised according to the STROBE Statement—checklist of items.

Open-Access: This article is an open-access article that was selected by an in-house editor and fully peer-reviewed by external reviewers. It is distributed in accordance with the Creative Commons Attribution NonCommercial (CC BY-NC 4.0) license, which permits others to distribute, remix, adapt, build upon this work non-commercially, and license their derivative works on different terms, provided the original work is properly cited and the use is non-commercial. See: https://creativecommons.org/Licenses/by-nc/4.0/

Country/Territory of origin: China

ORCID number: Kuan-Yong Yu 0000-0003-0441-9282; Rong-Kang Kuang 0000-0002-2178-6693; Ping-Ping Wu 0009-0003-9457-7598; Guang-Hui Qiang 0000-0002-6360-3883.

S-Editor: Liu JH
L-Editor: Wang TQ
P-Editor: Xu ZH

REFERENCES

1 **Bray F**, Ferlay J, Soerjomataram I, Siegel RL, Torre LA, Jemal A. Global cancer statistics 2018: GLOBOCAN estimates of incidence and mortality worldwide for 36 cancers in 185 countries. *CA Cancer J Clin* 2018; **68**: 394-424 [PMID: 30207593 DOI: 10.3322/caac.21492]

2 **Japanese Gastric Cancer Association**. Japanese gastric cancer treatment guidelines 2018 (5th edition). *Gastric Cancer* 2021; **24**: 1-21 [PMID: 32060757 DOI: 10.1007/s10120-020-01042-y]

3 **Ban KA**, Minei JP, Laronga C, Harbrecht BG, Jensen EH, Fry DE, Itani KM, Dellinger EP, Ko CY, Duane TM. American College of Surgeons and Surgical Infection Society: Surgical Site Infection Guidelines, 2016 Update. *J Am Coll Surg* 2017; **224**: 59-74 [PMID: 27915053 DOI: 10.1016/j.jamcollsurg.2016.10.029]

4 **Qiao YQ**, Zheng L, Jia B, Wang WH, Zheng XH, Fan LL, Xie YB, Tian YT. Risk factors for surgical-site infections after radical gastrectomy for gastric cancer: a study in China. *Chin Med J (Engl)* 2020; **133**: 1540-1545 [PMID: 32568869 DOI: 10.1097/CM9.0000000000000860]

5 **Hirao M**, Tsujinaka T, Imamura H, Kurokawa Y, Inoue K, Kimura Y, Shimokawa T, Furukawa H; Osaka Gastrointestinal Cancer Chemotherapy Study Group (OGSG). Overweight is a risk factor for surgical site infection following distal gastrectomy for gastric cancer. *Gastric Cancer* 2013; **16**: 239-244 [PMID: 22782464 DOI: 10.1007/s10120-012-0174-1]

6 **Morikane K**, Honda H, Suzuki S. Factors Associated With Surgical Site Infection Following Gastric Surgery in Japan. *Infect Control Hosp Epidemiol* 2016; **37**: 1167-1172 [PMID: 27430979 DOI: 10.1017/ice.2016.155]

7 **Olmez T**, Gulmez S, Karakose E, Ofluoglu CB, Senger AS, Bozkurt H, Duman M, Polat E. Relation between Sarcopenia and Surgical Site Infection in Patients Undergoing Gastric Cancer Surgery. *Surg Infect (Larchmt)* 2021; **22**: 551-555 [PMID: 33180010 DOI: 10.1089/sur.2020.211]

8 **Allegranzi B**, Zayed B, Bischoff P, Kubilay NZ, de Jonge S, de Vries F, Gomes SM, Gans S, Wallert ED, Wu X, Abbas M, Boermeester MA, Dellinger EP, Egger M, Gastmeier P, Guirao X, Ren J, Pittet D, Solomkin JS; WHO Guidelines Development Group. New WHO recommendations on intraoperative and postoperative measures for surgical site infection prevention: an evidence-based global perspective. *Lancet Infect Dis* 2016; **16**: e288-e303 [PMID: 27816414 DOI: 10.1016/S1473-3099(16)30402-9]

9 **Jeong SJ**, Ann HW, Kim JK, Choi H, Kim CO, Han SH, Choi JY, Peck KR, Kang CI, Yeom JS, Choi YH, Lim SK, Song YG, Choi HJ, Yoon HJ, Kim HY, Kim YK, Kim MJ, Park YS, Kim JM. Incidence and risk factors for surgical site infection after gastric surgery: a multicenter prospective cohort study. *Infect Chemother* 2013; **45**: 422-430 [PMID: 24475356 DOI: 10.3947/ic.2013.45.4.422]

10 **Ruiz-Tovar J**, Oller I, Llavero C, Arroyo A, Muñoz JL, Calero A, Diez M, Zubiaga L, Calpena R. Pre-operative and early post-operative factors associated with surgical site infection after laparoscopic sleeve gastrectomy. *Surg Infect (Larchmt)* 2013; **14**: 369-373 [PMID: 23718274 DOI: 10.1089/sur.2012.114]

11 **Kosuga T**, Ichikawa D, Komatsu S, Kubota T, Okamoto K, Konishi H, Shiozaki A, Fujiwara H, Otsuji E. Clinical and surgical factors associated with organ/space surgical site infection after laparoscopic gastrectomy for gastric cancer. *Surg Endosc* 2017; **31**: 1667-1674 [PMID: 27506433 DOI: 10.1007/s00464-016-5156-7]

12 **Cai X**, Shen W, Guo Z, Li Y, Cao L, Gong J, Zhu W. Thickness of Subcutaneous Fat Is a Predictive Factor of Incisional Surgical Site Infection in Crohn's Disease Surgery: A Retrospective Study. *Gastroenterol Res Pract* 2018; **2018**: 1546075 [PMID: 30140279 DOI: 10.1155/2018/1546075]

13 **Thapa B**, Sutanto E, Bhandari R. Thickness of subcutaneous fat is a risk factor for incisional surgical site infection in acute appendicitis surgery: a prospective study. *BMC Surg* 2021; **21**: 6 [PMID: 33397364 DOI: 10.1186/s12893-020-01029-7]

14 **Teppa R**, Sude NS, Karanam VPK, Mallipudi BVP. Relevance of Subcutaneous Fat Thickness as a Risk Factor for Surgical Site Infections in Abdominal Surgeries. *Cureus* 2022; **14**: e20946 [PMID: 35004090 DOI: 10.7759/cureus.20946]

15 **Zhang X**, Yang Z, Meng C, Gao J, Liu Y, Shi B, Sun L, Wu G, Yao H, Zhang Z. Abdomen anatomic characteristics on CT scans as predictive markers for short-term complications following radical resection of colorectal cancer. *Front Surg* 2022; **9**: 899179 [PMID: 35923439 DOI: 10.3389/fsurg.2022.899179]

16 **Liu S**, Wang M, Lu X, Feng M, Wang F, Zheng L, Guan W. Abdomen Depth and Rectus Abdominis Thickness Predict Surgical Site Infection in Patients Receiving Elective Radical Resections of Colon Cancer. *Front Oncol* 2019; **9**: 637 [PMID: 31380276 DOI: 10.3389/fonc.2019.00637]

17 **Allegranzi B**, Bischoff P, de Jonge S, Kubilay NZ, Zayed B, Gomes SM, Abbas M, Atema JJ, Gans S, van Rijen M, Boermeester MA, Egger M, Kluytmans J, Pittet D, Solomkin JS; WHO Guidelines Development Group. New WHO recommendations on preoperative measures for surgical site infection prevention: an evidence-based global perspective. *Lancet Infect Dis* 2016; **16**: e276-e287 [PMID: 27816413 DOI: 10.1016/S1473-3099(16)30398-X]

18 **Fujii T**, Tsutsumi S, Matsumoto A, Fukasawa T, Tabe Y, Yajima R, Asao T, Kuwano H. Thickness of subcutaneous fat as a strong risk factor for wound infections in elective colorectal surgery: impact of prediction using preoperative CT. *Dig Surg* 2010; **27**: 331-335 [PMID: 20689296 DOI: 10.1159/000297521]

19 **Donnally CJ**, Henstenburg JM, Pezzulo JD, Farronato D, Patel PD, Sherman M, Canseco JA, Kepler CK, Vaccaro AR. Increased Surgical Site Subcutaneous Fat Thickness Is Associated with Infection after Posterior Cervical Fusion. *Surg Infect (Larchmt)* 2022; **23**: 364-371 [PMID: 35262398 DOI: 10.1089/sur.2021.271]

20 **Saad MAN**, Jorge AJL, de Ávila DX, Martins WA, Dos Santos MMS, Tedeschi LT, Cavalcanti IL, Rosa MLG, Filho RADC. Sagittal abdominal diameter as a marker of visceral obesity in older primary care patients. *J Geriatr Cardiol* 2020; **17**: 279-283 [PMID: 32547611 DOI: 10.11909/j.issn.1671-5411.2020.05.007]

21 **Sur MD**, Namm JP, Hemmerich JA, Buschmann MM, Roggin KK, Dale W. Radiographic Sarcopenia and Self-reported Exhaustion Independently Predict NSQIP Serious Complications After Pancreaticoduodenectomy in Older Adults. *Ann Surg Oncol* 2015; **22**: 3897-3904 [PMID: 26242367 DOI: 10.1245/s10434-015-4763-1]

22 **Wahl TS**, Patel FC, Goss LE, Chu DI, Grams J, Morris MS. The Obese Colorectal Surgery Patient: Surgical Site Infection and Outcomes. *Dis Colon Rectum* 2018; **61**: 938-945 [PMID: 29994958 DOI: 10.1097/DCR.0000000000001085]

23 **Kambara Y**, Yuasa N, Takeuchi E, Miyake H, Nagai H, Yoshioka Y, Okuno M, Miyata K. Overweight or Obesity is an Unfavorable Long-Term Prognostic Factor for Patients who Underwent Gastrectomy for Stage II/III Gastric Cancer. *World J Surg* 2019; **43**: 1766-1776 [PMID: 30820737 DOI: 10.1007/s00268-019-04969-1]

24 **Cheng H**, Clymer JW, Po-Han Chen B, Sadeghirad B, Ferko NC, Cameron CG, Hinoul P. Prolonged operative duration is associated with complications: a systematic review and meta-analysis. *J Surg Res* 2018; **229**: 134-144 [PMID: 29936980 DOI: 10.1016/j.jss.2018.03.022]

25 **Held MB**, Boddapati V, Sarpong NO, Cooper HJ, Shah RP, Geller JA. Operative Duration and Short-Term Postoperative Complications after Unicompartmental Knee Arthroplasty. *J Arthroplasty* 2021; **36**: 905-909 [PMID: 33012597 DOI: 10.1016/j.arth.2020.09.007]

World Journal of Clinical Cases

Submit a Manuscript: https://www.f6publishing.com

World J Clin Cases 2023 November 26; 11(33): 8022-8029

DOI: 10.12998/wjcc.v11.i33.8022

ISSN 2307-8960 (online)

CASE REPORT

Pathological diagnosis and immunohistochemical analysis of minute pulmonary meningothelial-like nodules: A case report

Xin Ruan, Liu-Sheng Wu, Zheng-Yang Fan, Qi Liu, Jun Yan, Xiao-Qiang Li

Specialty type: Pathology

Provenance and peer review: Unsolicited article; Externally peer reviewed.

Peer-review model: Single blind

Peer-review report's scientific quality classification

Grade A (Excellent): 0
Grade B (Very good): B
Grade C (Good): 0
Grade D (Fair): 0
Grade E (Poor): 0

P-Reviewer: Alkhatib AJ, Jordan

Received: July 9, 2023
Peer-review started: July 9, 2023
First decision: August 30, 2023
Revised: October 10, 2023
Accepted: October 30, 2023
Article in press: October 30, 2023
Published online: November 26, 2023

Xin Ruan, Qi Liu, Xiao-Qiang Li, Department of Thoracic Surgery, Peking University Shenzhen Hospital, Shenzhen 518036, Guangdong Province, China

Xin Ruan, School of Medicine, Shantou University, Shantou 515041, Guangdong Province, China

Liu-Sheng Wu, Jun Yan, School of Medicine, Tsinghua University, Beijing 100084, China

Zheng-Yang Fan, Department of Graduate School, Xinjiang Medical University, Urumchi 830011, Xinjiang Uygur Autonomous Region, China

Corresponding author: Jun Yan, Doctor, Chief Doctor, School of Medicine, Tsinghua University, No. 30 Shuangqing Road, Haidian District, Beijing 100084, China.
yanjun1619@tsinghua.edu.cn

Abstract

BACKGROUND

Minute Pulmonary Meningothelial-like Nodules (MPMNs) are rare benign pulmonary nodules, which are more common in elderly women and have a higher detection rate in lung tissues of patients with lung malignant diseases. Its origin is not yet clear. At present, there are few reports on the diagnostic methods such as imaging and pathological manifestations of MPMNs. This article reports a 70-year-old female patient with pulmonary adenocarcinoma combined with MPMNs and reviews of the relevant literature.

CASE SUMMARY

A 70-year-old women was admitted to our institution with feeling sour in her back and occasional cough for more than 2 mo. Computerized electronic scanning scan and 3D reconstruction images in our institution showed there were multiple ground-glass nodules in both of her two lungs. The biggest one was in the apicoposterior segment of left upper lobe, about 2.5 mm × 9 mm in size. We performed thoracoscopic resection of the left upper lung apicoposterior segment of the patient, and the final pathological report was minimally invasive adenocarcinoma. Re-examination of high resolution computed tomography 21 mo after surgery showed multiple ground-glass nodules in both lungs, and a new ground-glass nodule was found in the superior segment of the right lower lobe. We took pathological biopsy of the right upper lung and right lower lung nodules for the patient under thoracoscopy. The histomorphology of the right lower lobe nodule showed multiple lesions in the lung tissue, and the small foci in the alveolar

septum were distributed in mild form of the aggregation of short spindle cells. The immunohistochemistry showed that the lesion was epithelial membrane antigen (EMA) (+), somatostatin receptor 2a (SSTR2a) (+), S-100 (-), chromogranin A (-), Syn (-), cytokeratin (-) and HMB-45 (-). The final diagnosis was minimally invasive adenocarcinoma, accompanied by MPMNs. We recommend that patients continue to receive treatment after surgery and to do regular follow-up observations.

CONCLUSION
The imaging manifestations of MPMNs are atypical, histomorphology and immunohistochemistry can assist in its diagnosis. This article reviews the relevant literature of MPMNs immunohistochemistry and shows that MPMNs are positive for EMA, SSTR2a, and progesterone receptor.

Key Words: Lung; Pathology; Immunohistochemistry; Multiple pulmonary nodules; Minute pulmonary meningothelial-like nodules; Case report

©The Author(s) 2023. Published by Baishideng Publishing Group Inc. All rights reserved.

Core Tip: Minute Pulmonary Meningothelial-like Nodules (MPMNs) are rare benign pulmonary nodules, which have a higher detection rate in lung tissues of patients with lung malignant diseases. The diagnosis of MPMN is difficult and often results in unnecessary or inappropriate treatment. Therefore, it is particularly important to correctly identify and diagnose the disease. This article reports a 70-year-old female patient with pulmonary adenocarcinoma combined with MPMNs and reviews of the relevant literature in order to better identify and diagnose MPMN.

Citation: Ruan X, Wu LS, Fan ZY, Liu Q, Yan J, Li XQ. Pathological diagnosis and immunohistochemical analysis of minute pulmonary meningothelial-like nodules: A case report. *World J Clin Cases* 2023; 11(33): 8022-8029
URL: https://www.wjgnet.com/2307-8960/full/v11/i33/8022.htm
DOI: https://dx.doi.org/10.12998/wjcc.v11.i33.8022

INTRODUCTION

Minute pulmonary meningothelial-like nodules (MPMNs) are rare benign pulmonary nodule, which is often found accidentally in pathological specimens after surgical resection or autopsy due to other lung diseases[1,2]. Studies have shown that MPMNs are common in women, especially elderly women[3]. MPMNs are often manifested as single or multiple small lung lesions, which can be distributed anywhere in the lungs, and are often found in combination with other lung diseases[4,5]. Unlike benign lung diseases, MPMNs are more likely to be detected in lung malignant tumors, and the detection rate in pulmonary adenocarcinoma is higher than other lung diseases[6]. Because the lesions of MPMNs are very small and have no characteristic imaging features, it is difficult to diagnose, or because the imaging appearance is very similar to the misdiagnosis of malignant nodules, unnecessary or inappropriate treatment may be caused[7,8]. Therefore, it is particularly important to correctly identify and diagnose this disease. In this article, we reported a case of lung microinvasive adenocarcinoma with MPMNs, and reviewed the clinical manifestations, imaging features, pathological diagnosis and immunohistochemistry of MPMNs to help better identify and diagnose MPMNs.

CASE PRESENTATION

Chief complaints
Experiencing consistent back pain and an intermittent cough for over two months.

History of present illness
A 70-year-old female patient was admitted to our institution with feeling sour in her back and occasional cough for more than 2 mo. No other special clinical symptoms and signs were complained. Before admission, a computed tomography (CT) scan of her chest revealed multiple pulmonary nodules in both left and right upper lungs. No special treatment was given.

History of past illness
A history of hypertension, regular oral antihypertensive medication treatment, and well-controlled blood pressure.

Personal and family history
Nothing special.

Physical examination

Nothing special.

Imaging examinations

CT scanning scan and 3D reconstruction images showed that there were a ground-glass nodule with rough edges (about 2.5 mm × 9 mm in size) in the apicoposterior segment of left upper lobe, a ground-glass nodule with clear edges (about 6 mm × 4 mm in size) in the lateral basal segment of left lower lobe and ground-glass density shadows were seen in the apex of right lungs, with blurred edges, and the range was approximately 9 mm × 6 mm (Figure 1).

We performed thoracoscopic resection of the left upper lung apicoposterior segment of the patient. During the operation, the rapid freezing pathology suggested that the carcinoma in situ was accompanied by multifocal microinfiltration. Thus, we performed preventive dissection of the mediastinum and hilar lymph nodes for pathological examination. Postoperative pathological report was Minimally Invasive Adenocarcinoma, no metastatic in each group of lymph nodes.

Re-examination of chest CT scan and high resolution computed tomography (HRCT) 21 mo after surgery showed: postoperative changes in the left upper lung, a pure ground-glass nodule in the apical segment of the right upper lobe (about 13.2 mm × 5.6 mm in size), a mixed ground glass in the superior segment of the right lower lobe Nodules (about 4.3 mm × 2.9 mm in size), a pure ground-glass nodule in the lateral basal segment of the left lower lobe (about 7.2 mm × 5.3 mm in size) (Figure 2), and there are other ground-glass nodules about 2-4 mm in diameter in the lower lobe of both lungs. We took pathological biopsy of the right upper lung and right lower lung lesions for the patient under thoracoscopy.

Laboratory examinations

The histological findings of the right upper lobe nodule showed that cancer cells grew in a monolayer, with large nuclei, rich cytoplasm, mitotic figures were not easy to see, focal septal widening, interstitial fiber and fibroblast proliferation, dense proliferation or clustered proliferation of tumor cells, nucleoli was visible.

The immunohistochemistry experimental protocol for this project comprises the following key steps: Sample fixation, dehydration, paraffin embedding, sectioning, antibody staining, and result analysis. Firstly, tissue samples are subjected to fixation, followed by dehydration and paraffin embedding to prepare paraffin sections. Subsequently, specific antibodies such as CK7, thyroid transcription factor-1 (TTF-1), and EMA are used for staining, followed by microscopic observation and image recording. Finally, result analysis and pathological diagnosis are conducted based on the staining outcomes. Immunohistochemistry experiments are a crucial step in the study, utilized to identify immune markers, thereby supporting accurate disease diagnosis and classification.

The pathological manifestation of the right lower lobe nodule was no obvious nodule was visible to the naked eye. Histomorphology showed multiple lesions in the lung tissue, with diameter of 0.5-1.8 mm, and the small foci in the alveolar septum were distributed in mild form of the aggregation of short spindle cells (Figure 3). And the Immunohistochemistry showed that the lesion was positive for Epithelial membrane antigen (EMA) and somatostatin receptor 2a (Figure 4), and negative for S-100, Chromogranin A (CgA), Synaptophysin (Syn), Cytokeratin (CK) and HMB-45.

FINAL DIAGNOSIS

The pathological diagnosis was Micro-invasive Adenocarcinoma with Minute Pulmonary Meningothelial-like Nodules.

TREATMENT

We recommend that patients continue to receive treatment after surgery and to do regular follow-up observations.

OUTCOME AND FOLLOW-UP

The patient recovered after operation, and no recurrence was found after 3 mo.

DISCUSSION

MPMNs, fist describe by Korn *et al*[9] in 1960, who considered they might be kinds of endocrine tumor called *Minute Pulmonary Chemodectoma* based on its cytologic characteristics, arrangement of cells and special relationship to vessels, have been considered to be benign lung lesions. Therefore, Gaffey *et al*[10] renamed it as "Minute Pulmonary Meningothelial-like Nodules". Many subsequent studies have shown that it lacked the immunohistochemical and ultrastructural characteristics of endocrine cells, and did not contain endocrine particles[11,12]. MPMNs patients often have no special symptoms or mild symptoms, or show corresponding clinical symptoms due to other lung diseases[13]. If MPMNs are diffuse in the patient's lungs and involve a large amount of lung tissue, it is called *Diffuse Pulmonary Meningotheliomatosis*,

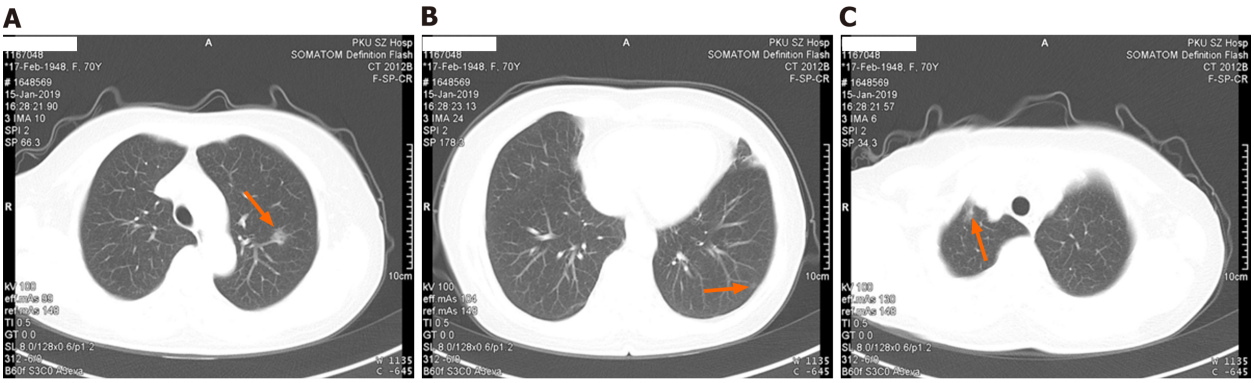

DOI: 10.12998/wjcc.v11.i33.8022 **Copyright** ©The Author(s) 2023.

Figure 1 Computed tomography examination before surgery. A: A ground-glass nodule with rough edges (about 2.5 mm × 9 mm in size) in the apicoposterior segment of left upper lobe; B: A ground-glass nodule with clear edges (about 6 mm × 4 mm in size) in the lateral basal segment of left lower lobe; C: Ground-glass density shadows were seen in the apex of right lungs, with blurred edges, and the range was approximately 9 mm × 6 mm.

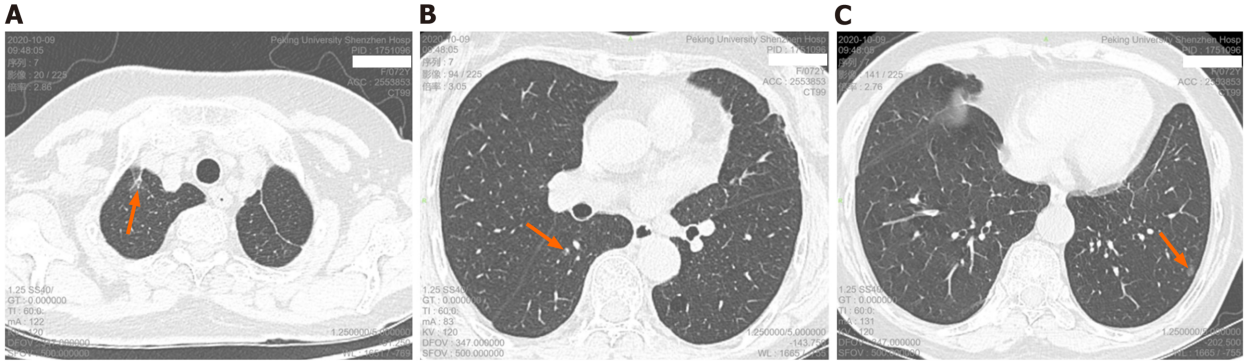

DOI: 10.12998/wjcc.v11.i33.8022 **Copyright** ©The Author(s) 2023.

Figure 2 High-resolution computed tomography 21 mo after surgery. A: A pure ground-glass nodule in the apical segment of the right upper lobe (about 13.2 mm × 5.6 mm in size); B: A mixed ground glass in the superior segment of the right lower lobe Nodules (about 4.3 mm × 2.9 mm in size); C: A pure ground-glass nodule in the lateral basal segment of the left lower lobe (about 7.2 mm × 5.3 mm in size).

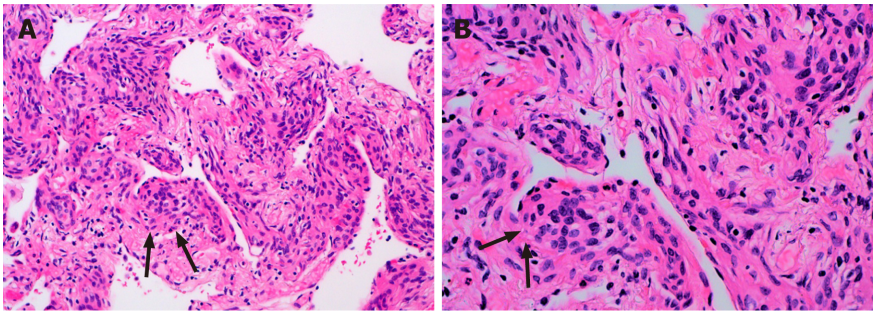

DOI: 10.12998/wjcc.v11.i33.8022 **Copyright** ©The Author(s) 2023.

Figure 3 Histomorphological manifestation of right lower lobe nodule was the small foci in the alveolar septum were distributed in mild form of the aggregation of short spindle cells. A: Original magnification 200×; B: Original magnification 400×.

patients will have more serious respiratory symptoms, such as cough, chest tightness, dyspnea or restrictive lung disease [14]. The CT characteristics of MPMNs are very similar to lung malignant lesions. In most cases, they appear as single or multiple small nodules in the lung, usually less than 10mm in diameter. Kuroki *et al*[15] compared the microscopic examination of MPMNs and believed that HRCT The observed ground glass attenuation may be related to the expansion of the alveolar wall caused by the spread of the lesion along the alveolar wall. The imaging features are ground glass or solid nodules, some lesions may be cystic or hollow, but usually not accompanied by calcification or necrosis[16-18]. HRCT is also used for lung imaging because it can describe the small areas of ground glass attenuation. MPMNs often show ground glass attenuation on HRCT. Due to its lack of characteristic imaging findings, clinical diagnosis is difficult and may lead to inappropriate treatment cause by misdiagnosis. Therefore, fine-needle aspiration or bronchoscopy or

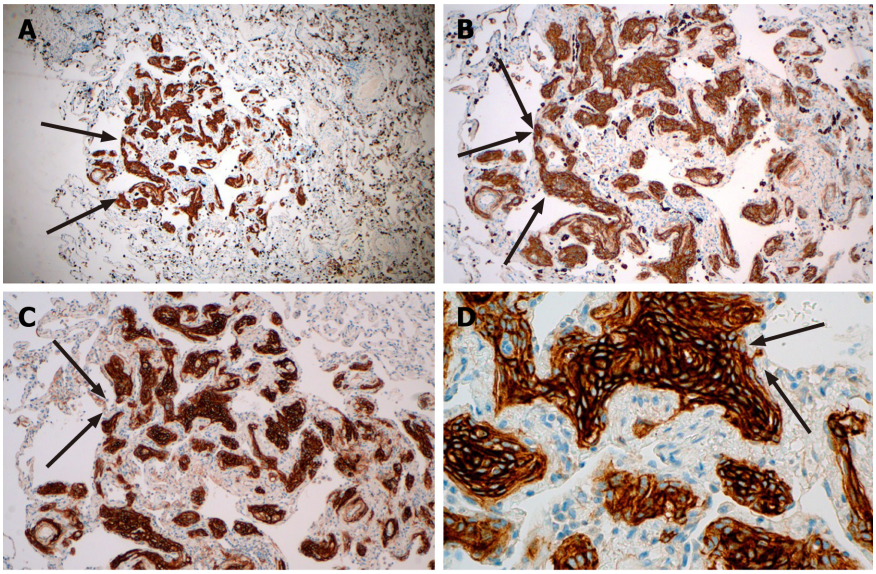

DOI: 10.12998/wjcc.v11.i33.8022 **Copyright** ©The Author(s) 2023.

Figure 4 The Immunohistochemistry showed that the lesion was positive for epithelial membrane antigen and somatostatin receptor 2a. A: The lesion was positive for epithelial membrane antigen, original magnification 200×; B: The lesion was positive for epithelial membrane antigen, original magnification 400×; C: The lesion was positive for somatostatin receptor 2a, original magnification 200×; D: The lesion was positive for somatostatin receptor 2a, original magnification 400×.

thoracoscopic biopsy under appropriate conditions can detect and identify the disease early, help identify malignant pulmonary nodules, and avoid unnecessary treatments. However, because the nodules are generally small, it is difficult to perform a needle biopsy in terms of operation and technology. Pathological biopsy is the gold standard for diagnosis. On gross specimens, MPMNs are often too small to be observed with the naked eye, or the lesions appear as yellow or gray-white solid masses with interstitial nodular hyperplasia[19]. It can be seen under the microscope that MPMNs lesions are mostly located in the alveolar septum, which is composed of oval or fusiform epithelioid cell nests gathered into small foci and arranged in a whirlpool around the central venule. The alveolar septum is often widened due to the presence of the lesion, and there are certain degree of fibrosis.

The immunohistochemistry markers selected for this project include CK7, TTF-1, and EMA, which play crucial roles in pathological diagnosis. CK7 is a cytokeratin commonly expressed in epithelial cells, particularly in tissues like the lung, stomach, and biliary tract, making it highly useful for determining the epithelial origin of tumor cells. TTF-1 is a nuclear transcription factor, highly expressed in normal lung tissue, and frequently found in lung adenocarcinomas, aiding in distinguishing lung cancer from other malignancies. EMA is a membrane-bound antigen specific to epithelial cells, providing valuable assistance in confirming epithelial lesions. The selection of these immunohistochemistry markers is based on their specific expression in lung and epithelial cells, aiding in the identification and classification of MPMNs. Immunohistochemistry experiments rely on the specificity of these markers, assisting in determining pathological types, guiding treatment strategy selection, and providing critical insights into disease progression and prognosis. Therefore, immunohistochemistry plays an indispensable role in MPMN pathological diagnosis, enhancing diagnostic accuracy and precision in clinical management.

The diagnosis of MPMNs needs to be confirmed by immunohistochemistry. Table 1 shows the literature review of MPMNs immunohistochemistry[20]. We can see that almost all MPMNs immunohistochemically showed positive responses to Vimentin, EMA, SSTR-2a, and CD56, and more than half of MPMNs were positive to PR; while negative for S-100, CK, Actin, HMB- 45. Syn and Cga. For NSE, the study[21] found that almost all MPMNs were weakly positive for NSE, but they believed that this behavior was non-specific because normal alveolar epithelium was also weakly positive for the antigen. The source of MPMNs is still unclear. They may come from reactive rather than neoplastic origin. At present, most studies believe that there are similarities between pulmonary meningeal epithelioid nodules and meningiomas in their histological, ultrastructural and immunohistochemical characteristics[22]. According to the research of Higuchi *et al*[23], both MPMNs and meningioma of the central nervous system may be related to the ectopic or deletion of neurofibromatosis type-2 gene, indicating that they may have a common genetic changes. However, a genotypic comparison between MPMNs and meningiomas showed that MPMNs lacked the molecular changes associated with loss of heterozygosity on chromosome 22 in meningioma cells. Imaging examination of the heads of most patients with MPMNs did not find signs of meningioma in some studies, indicating that it is not a metastasis of meningioma. At present, most studies believe that it is very similar to meningeal epithelial cells or meningioma cells. Multiple studies have shown that almost all MPMNs are positive for Vimentin and EMA phenotypes, which are very similar to meningeal epithelial cells or meningioma cells. Almost all MPMNs were positive for progesterone receptors and they believed that this once again proved the similarity between MPMNs and meningeal epithelial cells or meningioma cells, because progesterone receptors are in normal meningeal epithelial cells and the expression in meningiomas has been well confirmed, and it is believed that there might be lung meningeal epithelioid cells in normal lung tissues, while proges-

Table 1 Literature review of the immunohistochemistry of minute pulmonary meningothelial-like nodules

Ref.	Number of nodules/lesions evaluated	Immunophenotype											
		EMA	VIM	PR	CD56	SSTR2a	CK	Syn	Actin	S100	HMB-45	NSE	CgA
Bernabeu *et al*[13], 2013	1	1/0[a]	1/0	1/0	1/0	–	0/1	0/1	0/1	–	0/1	–	0/1
Lee *et al*[18], 2013	1	1/0	1/0	1/0	1/0	–	0/1	–	–	–	–	–	–
Tao *et al*[4], 2019	39	29/10	–	11/28	–	39/0	0/39	0/39	–	0/39	–	–	0/39
Niho *et al*[6], 1999	29	22/0[b]	29/0	9/9	–	–	0/29	2/27	–	10/11	0/28	25/4	1/28
Pelosi *et al*[21], 2002	9	9/0	9/0	9/0	–	–	0/6	0/6	0/6	0/6	0/6	–	–
Peng *et al*[8], 2019	8	7/0	8/0	6/0	–	–	0/2	–	–	–	–	–	–
Agozzino *et al*[19], 2006	1	1/0	1/0	0/1	–	–	0/1	0/1	0/1	0/1	–	0/1	0/1
Kfour *et al*[20], 2012	2	2/0	2/0	2/0	–	–	–	–	–	–	–	–	–
Torikata *et al*[5], 1990	24	0/18	24/0	–	–	–	0/17	–	0/21	0/16	–	0/17	–
Gaffey *et al*[10], 1988	14	12/2	10/2	–	–	–	0/14	–	0/7	0/14	–	0/14	–
Harada *et al*[7], 2019	1	1/0	1/0	1/0	1/0	NR	NR	NR	NR	NR	NR	NR	NR
Total	129	85/30	86/2	40/38	3/0	39/0	0/110	2/74	0/36	10/87	0/35	25/36	1/68

[a]Number of lesions with positive immunocytochemical staining/negative immunocytochemical staining.

[b]Not all nodules/lesions are evaluated for specific immunophenotypes.

EMA: Epithelial membrane antigen; VIM: Vimentin; PR: Progesterone receptor; SSTR2a: Somatostatin receptor 2a; CK: Cytokeratin; Syn: Synaptophysin; NSE: Neuron-specific enolase; CgA: Chromogranin A; NR: Not reported; –: Not evaluated.

terone probably played an important role in controlling their growth. In addition, the retrospective analysis of the immunophenotypes of MPMNs including SSTR-2a, and found that all MPMNs lesions expressed constant expression of SSTR-2a, which once again proved MPMNs immunohistochemical characteristics similar to meningeal epithelial cells.

In terms of treatment, MPMNs are benign lesions and can be treated conservatively, with long-term follow-up without further intervention. The study of Lin *et al*[24] found that patients with MPMNs surgically removed can get a good prognosis, but they believe that compared with the trauma of surgery, long-term follow-up observation may benefit more. However, MPMNs often appear along with other lung diseases. Therefore, it is particularly important to detect and identify their accompanying diseases in time and carry out corresponding clinical interventions. In general, the clinical manifestations of MPMNs are not typical. Image characteristics show single or multiple ground-glass nodules in the lungs with a diameter of no more than 10mm. Pathological biopsy is the gold standard for diagnosis. Immunohistochemically shows positive for Vimentin, EMA, SSTR-2a, CD56, PR, but negative for S-100, CK, Actin, HMB-45, Syn, and Cga. Its source is currently unclear, but most studies currently believe that it is similar to meningeal epithelial cells or meningioma cells. MPMNs are benign lesions and can be treated conservatively, but they often appear along with other lung diseases. Therefore, timely detection and identification of MPMNs and their accompanying diseases, and corres-

ponding clinical interventions are also particularly important.

CONCLUSION

Through a comprehensive pathological diagnosis and immunohistochemical analysis of one case of MPMNs, we delved into the characteristics of this rare condition. The results demonstrated a certain diversity in immunohistochemical markers for MPMNs, with CK7, TTF-1, and EMA playing crucial roles in pathological diagnosis. Literature review further supported our findings. In conclusion, the diagnosis and differential diagnosis of MPMNs remain challenging and require the integration of various clinical and immunohistochemical information to ensure accurate diagnosis and selection of treatment strategies. This study provides valuable insights and references for the clinical management of MPMNs.

FOOTNOTES

Co-first authors: Liu-Sheng Wu, Zheng-Yang Fan, and Qi Liu.

Co-corresponding authors: Jun Yan and Xiao-Qiang Li.

Author contributions: Ruan X and Wu LS analyzed the data and wrote the paper; Li XQ designed the research; Yan J guided the research; Liu Q and Fan ZY collected and downloaded the data of our research; All the authors revised it critically for important intellectual content, gave final approval of the version to be published and agreed to be accountable for all aspects of the work; At the beginning, the paper was designed and written by Ruan X and Wu LS as co-first authors; Later, in the first revision, Fan ZY provided the imaging image support and analysis, and Liu Q provided the experimental analysis of HE staining and immunohistochemistry in pathology; Therefore, they all have equally important contributions.

Supported by the National Natural Science Foundation of China, No. 81972829.

Informed consent statement: Informed written consent was obtained from the patient for publication of this report and any accompanying images.

Conflict-of-interest statement: All the authors declare no conflicts of interest.

CARE Checklist (2016) statement: The authors have read the CARE Checklist (2016), and the manuscript was prepared and revised according to the CARE Checklist (2016).

Open-Access: This article is an open-access article that was selected by an in-house editor and fully peer-reviewed by external reviewers. It is distributed in accordance with the Creative Commons Attribution NonCommercial (CC BY-NC 4.0) license, which permits others to distribute, remix, adapt, build upon this work non-commercially, and license their derivative works on different terms, provided the original work is properly cited and the use is non-commercial. See: https://creativecommons.org/Licenses/by-nc/4.0/

Country/Territory of origin: China

ORCID number: Liu-Sheng Wu 0000-0001-9580-2257; Jun Yan 0000-0003-9580-2258; Xiao-Qiang Li 0000-0002-9692-1458.

S-Editor: Liu JH
L-Editor: A
P-Editor: Zhang YL

REFERENCES

1 **Asakawa A**, Horio H, Hishima T, Yamamichi T, Okui M, Harada M. Clinicopathologic features of minute pulmonary meningothelial-like nodules. *Asian Cardiovasc Thorac Ann* 2017; **25**: 509-512 [PMID: 28871800 DOI: 10.1177/0218492317731390]

2 **Mizutani E**, Tsuta K, Maeshima AM, Asamura H, Matsuno Y. Minute pulmonary meningothelial-like nodules: clinicopathologic analysis of 121 patients. *Hum Pathol* 2009; **40**: 678-682 [PMID: 19144385 DOI: 10.1016/j.humpath.2008.08.018]

3 **Arafah MA**, Raddaoui E, Alsheikh A, Hajjar WM, Alyousef F. Mimicry of sugar tumor and minute pulmonary meningothelial-like nodule to metastatic lung deposits in a patient with rectal adenocarcinoma. *Ann Saudi Med* 2013; **33**: 400-403 [PMID: 24060722 DOI: 10.5144/0256-4947.2013.400]

4 **Tao L**, Chen Y, Huang Q, Yong J, Yan S, Huang Y. Constant expression of somatostatin receptor 2a in minute pulmonary meningothelial-like nodules. *J Clin Pathol* 2019; **72**: 525-528 [PMID: 31208995 DOI: 10.1136/jclinpath-2019-205913]

5 **Torikata C**, Mukai M. So-called minute chemodectoma of the lung. An electron microscopic and immunohistochemical study. *Virchows Arch A Pathol Anat Histopathol* 1990; **417**: 113-118 [PMID: 2164277 DOI: 10.1007/bf02190528]

6 **Niho S**, Yokose T, Nishiwaki Y, Mukai K. Immunohistochemical and clonal analysis of minute pulmonary meningothelial-like nodules. *Hum Pathol* 1999; **30**: 425-429 [PMID: 10208464 DOI: 10.1016/s0046-8177(99)90118-1]

7 **Harada M**, Aono Y, Yasui H, Uto T, Sato J, Imokawa S, Suzuki S, Tanioka F, Suda T. Minute Pulmonary Meningothelial-like Nodules Showing Multiple Ring-shaped Opacities. *Intern Med* 2019; **58**: 3149-3152 [PMID: 31327818 DOI: 10.2169/internalmedicine.2108-18]

8 **Peng XX**, Yan LX, Liu C, Wang SY, Li WF, Gao X, Wei XW, Zhou Q. Benign disease prone to be misdiagnosed as malignant pulmonary nodules: Minute meningothelioid nodules. *Thorac Cancer* 2019; **10**: 1182-1187 [PMID: 30964241 DOI: 10.1111/1759-7714.13061]

9 **KORN D**, BENSCH K, LIEBOW AA, CASTLEMAN B. Multiple minute pulmonary tumors resembling chemodectomas. *Am J Pathol* 1960; **37**: 641-672 [PMID: 13753180]

10 **Gaffey MJ**, Mills SE, Askin FB. Minute pulmonary meningothelial-like nodules. A clinicopathologic study of so-called minute pulmonary chemodectoma. *Am J Surg Pathol* 1988; **12**: 167-175 [PMID: 2830799 DOI: 10.1097/00000478-198803000-00001]

11 **Kuhn C 3rd**, Askin FB. The fine structure of so-called minute pulmonary chemodectomas. *Hum Pathol* 1975; **6**: 681-691 [PMID: 171214 DOI: 10.1016/s0046-8177(75)80077-3]

12 **Churg AM**, Warnock ML. So-called "minute pulmonary chemodectoma": a tumor not related to paragangliomas. *Cancer* 1976; **37**: 1759-1769 [PMID: 177176 DOI: 10.1002/1097-0142(197604)37:4<1759::aid-cncr2820370422>3.0.co;2-3]

13 **Bernabeu Mora R**, Sánchez Nieto JM, Hu C, Alcaraz Mateos E, Giménez Bascuñana A, Rodríguez Rodríguez M. Diffuse pulmonary meningotheliomatosis diagnosed by transbronchial lung biopsy. *Respiration* 2013; **86**: 145-148 [PMID: 23796886 DOI: 10.1159/000350430]

14 **Alkurashi AK**, Almodallal Y, Albitar HAH, Cheville JC, Iyer VN. Diffuse Pulmonary Meningotheliomatosis: A Rare Lung Disease Presenting with Diffuse Ground-Glass Opacities and Cavitation. *Am J Case Rep* 2020; **21**: e926172 [PMID: 33166273 DOI: 10.12659/AJCR.926172]

15 **Kuroki M**, Nakata H, Masuda T, Hashiguchi N, Tamura S, Nabeshima K, Matsuzaki Y, Onitsuka T. Minute pulmonary meningothelial-like nodules: high-resolution computed tomography and pathologic correlations. *J Thorac Imaging* 2002; **17**: 227-229 [PMID: 12082375 DOI: 10.1097/00005382-200207000-00008]

16 **Sellami D**, Gotway MB, Hanks DK, Webb WR. Minute pulmonary meningothelial-like nodules: thin-section CT appearance. *J Comput Assist Tomogr* 2001; **25**: 311-313 [PMID: 11242234 DOI: 10.1097/00004728-200103000-00028]

17 **Kraushaar G**, Ajlan AM, English JC, Müller NL. Minute pulmonary meningothelial-like nodules: a case of incidentally detected diffuse cystic micronodules on thin-section computed tomography. *J Comput Assist Tomogr* 2010; **34**: 780-782 [PMID: 20861786 DOI: 10.1097/RCT.0b013e3181e47c28]

18 **Lee SK**, Kim GJ, Kim YJ, Leem AY, Hwang ED, Kim SK, Chang J, Kang YA, Kim SY. Minute pulmonary meningothelial-like nodules simulating hematogenous lung metastasis: a case report. *Tuberc Respir Dis (Seoul)* 2013; **75**: 67-70 [PMID: 24023559 DOI: 10.4046/trd.2013.75.2.67]

19 **Agozzino M**, Inzani F, Cavallero A, Arbustini E, Meloni F, Oggionni T, Dore R, D'Armini A, Viganò M. Minute pulmonary meningothelial-like nodules in the transbronchial biopsy of a lung transplant recipient. *J Heart Lung Transplant* 2006; **25**: 148-150 [PMID: 16399548 DOI: 10.1016/j.healun.2005.07.016]

20 **Kfoury H**, Arafah MA, Arafah MM, Alnassar S, Hajjar W. Mimicry of Minute Pulmonary Meningothelial-like Nodules to Metastatic Deposits in a Patient with Infiltrating Lobular Carcinoma: A Case Report and Review of the Literature. *Korean J Pathol* 2012; **46**: 87-91 [PMID: 23109985 DOI: 10.4132/KoreanJPathol.2012.46.1.87]

21 **Pelosi G**, Maffini F, Decarli N, Viale G. Progesterone receptor immunoreactivity in minute meningothelioid nodules of the lung. *Virchows Arch* 2002; **440**: 543-546 [PMID: 12021930 DOI: 10.1007/s00428-001-0580-y]

22 **Ionescu DN**, Sasatomi E, Aldeeb D, Omalu BI, Finkelstein SD, Swalsky PA, Yousem SA. Pulmonary meningothelial-like nodules: a genotypic comparison with meningiomas. *Am J Surg Pathol* 2004; **28**: 207-214 [PMID: 15043310 DOI: 10.1097/00000478-200402000-00008]

23 **Higuchi M**, Watanabe M, Inoue T, Yamaura T, Suzuki T, Saito M, Niitsuma K, Endo K, Oshibe I, Soeta N, Saito T, Hojo H, Munakata M, Suzuki H. Brief report on similar mutational changes in neurofibromatosis type 2 gene in minute pulmonary meningothelial-like nodule and meningioma of the central nervous system. *Oncotarget* 2018; **9**: 36012-36016 [PMID: 30542514 DOI: 10.18632/oncotarget.26325]

24 **Lin D**, Yu Y, Wang H, Fang Y, Yin J, Shen Y, Tan L. Radiological manifestations, histological features and surgical outcomes of pulmonary meningothelial proliferation: a case series and rethinking. *Transl Lung Cancer Res* 2020; **9**: 1159-1168 [PMID: 32953494 DOI: 10.21037/tlcr-19-699]

World Journal of Clinical Cases

Submit a Manuscript: https://www.f6publishing.com

World J Clin Cases 2023 November 26; 11(33): 8030-8037

DOI: 10.12998/wjcc.v11.i33.8030

ISSN 2307-8960 (online)

CASE REPORT

Giant complex hepatic cyst causing pseudocystitis: A case report

Song Li, Jie Tang, De-Sheng Ni, A-Dong Xia, Guo-Liang Chen

Specialty type: Medicine, research and experimental

Provenance and peer review: Unsolicited article; Externally peer reviewed.

Peer-review model: Single blind

Peer-review report's scientific quality classification

Grade A (Excellent): 0
Grade B (Very good): 0
Grade C (Good): C
Grade D (Fair): 0
Grade E (Poor): 0

P-Reviewer: Kodama T, Japan

Received: September 14, 2023
Peer-review started: September 14, 2023
First decision: September 28, 2023
Revised: October 9, 2023
Accepted: November 13, 2023
Article in press: November 13, 2023
Published online: November 26, 2023

Song Li, De-Sheng Ni, A-Dong Xia, Guo-Liang Chen, Department of Hepatobilary Pancreatic Gastrointestinal Surgery, Jinhua People's Hospital, Jinhua 321000, Zhejiang Province, China

Jie Tang, Department of General Surgery, The Second Affiliated Hospital of Bengbu Medical College, Bengbu 233000, Anhui Province, China

Jie Tang, Anhui Key Laboratory of Tissue Transplantation, Bengbu Medical College, Bengbu 233000, Anhui Province, China

Corresponding author: De-Sheng Ni, MD, Chief Physician, Department of Hepatobilary Pancreatic Gastrointestinal Surgery, Jinhua People's Hospital, No. 267 Danxi East Road, Jindong District, Jinhua 321000, Zhejiang Province, China. 13868987870@163.com

Abstract

BACKGROUND

Hepatic cysts are common benign liver tumors that are typically asymptomatic. However, larger cysts, particularly giant liver cysts, can potentially induce symptoms. If the diameter of the cyst exceeds 10 cm, it can exert pressure on adjacent organs, leading to manifestations of corresponding symptoms. Here, we report the case of a complex giant hepatic cyst that caused pseudocystitis.

CASE SUMMARY

A 16-year-old girl was admitted to our hospital with frequent and urgent urination. Ultrasonography revealed no obvious uterine adnexal abnormalities but showed a hypoechoic, cystic mass (173 mm × 84 mm × 138 mm) with clear boundaries, and an unclear blood flow signal in the abdominal cavity (extending from the lower edge of the left lobe of liver to the upper edge of the bladder). Abdominal contrast-enhanced computed tomography revealed a giant cystic mass in the abdominal and pelvic cavities, possibly originating from the liver, and a small amount of free fluid in the pelvic cavity, which subsequent magnetic resonance imaging confirmed. The imaging characteristics were consistent with a benign lesion. The patient underwent laparoscopic resection of the giant liver cyst with partial liver resection. Post-surgery her symptoms urinary symptoms were relieved completely and she was discharged on the sixth postoperative day.

CONCLUSION

Our patient presented with symptoms suggestive of pseudocystitis, stressing the need for considering possibilities of other etiologies and differential diagnoses.

Key Words: Giant hepatic cyst; Pseudocystitis; Symptoms; Case report

©The Author(s) 2023. Published by Baishideng Publishing Group Inc. All rights reserved.

Core Tip: Giant hepatic cysts can cause symptoms upon reaching a significant size. We present a case of a complex giant liver cyst causing pseudocystitis in a 16-year-old girl with frequent and urgent urination. Imaging revealed a large cystic lesion in the liver. Laparoscopic resection with partial liver resection was performed, resulting in the resolution of the urinary symptoms. Therefore, clinicians should consider the possibility of giant liver cysts in patients presenting with similar symptoms.

Citation: Li S, Tang J, Ni DS, Xia AD, Chen GL. Giant complex hepatic cyst causing pseudocystitis: A case report. *World J Clin Cases* 2023; 11(33): 8030-8037
URL: https://www.wjgnet.com/2307-8960/full/v11/i33/8030.htm
DOI: https://dx.doi.org/10.12998/wjcc.v11.i33.8030

INTRODUCTION

Liver cysts are common asymptomatic benign tumors with an incidence of 4.5%–7.0%[1,2] and a female preponderance (1.5:1)[3,4]. Liver cysts are mostly diagnosed in adults aged around 40 years and are usually detected incidentally during imaging using computed tomography and/or ultrasonography[5-7]. Frequent and urgent micturition in women, especially married women, is mostly caused by urinary tract and gynecological pathologies. Liver cysts do not cause symptoms related to other abdominal organs unless they expand in size, and cause compression on adjacent structures and symptoms subsequent to that[8,9]. Pseudocystitis resulting from a liver cyst is rare. Here, we report a case of pseudocystitis caused by a giant liver cyst.

CASE PRESENTATION

Chief complaints

Frequent and urgent urination and discovery of an abdominal mass.

History of present illness

A 16-year-old girl was admitted to our hospital with frequent and urgent urination. She had no nausea, vomiting, abdominal pain, or feeling of bloating. Gynecological examination using ultrasonography revealed no obvious uterine adnexal abnormalities. A hypoechoic cystic mass measuring approximately 173 mm × 84 mm × 138 mm with clear boundaries and an unclear blood flow signal was observed in the abdominal cavity, extending from the lower edge of the left liver lobe to the upper edge of the bladder.

History of past illness

The patient was in good health condition with no history of acute or chronic infectious diseases, no history of drug or food allergies, no history of surgery or trauma, and no history of blood transfusion. She was fully vaccinated per societal schedules.

Personal and family history

The patient had a history of pancreatitis in the previous year, no history of hypertension or diabetes, and no family history of liver or renal cysts. Her family members had no similar medical history. Furthermore, she denied any history of familial hereditary diseases.

Physical examination

Physical examination revealed the following: Temperature, 36.8°C; heart rate, 108 beats/min; respiratory rate, 18 beats/min; and blood pressure, 114/82 mmHg. There was no yellowing of the skin or sclera, or swelling of superficial lymph nodes throughout the body. The neck was soft, and the chest was symmetrical, with no obvious abnormalities heard during cardiac and pulmonary auscultation. Her abdomen was flat. A mass measuring approximately 12 cm × 10 cm was palpated in the lower abdomen. The mass was soft in texture, with smooth surface, rounded edges, and clear boundaries, had a range of motion, and could be pushed forward without tenderness. It did not extend to the liver or spleen under the ribs, and Murphy's sign was negative. There was no pain on percussion in the renal area and no bilateral lower limb edema. Her examination was negative for shifting dullness, and bowel sounds were normal.

Laboratory examinations

Laboratory examination revealed the following: White blood cell count, 3.93 × 10^9/L; neutrophil percentage, 36.00%;

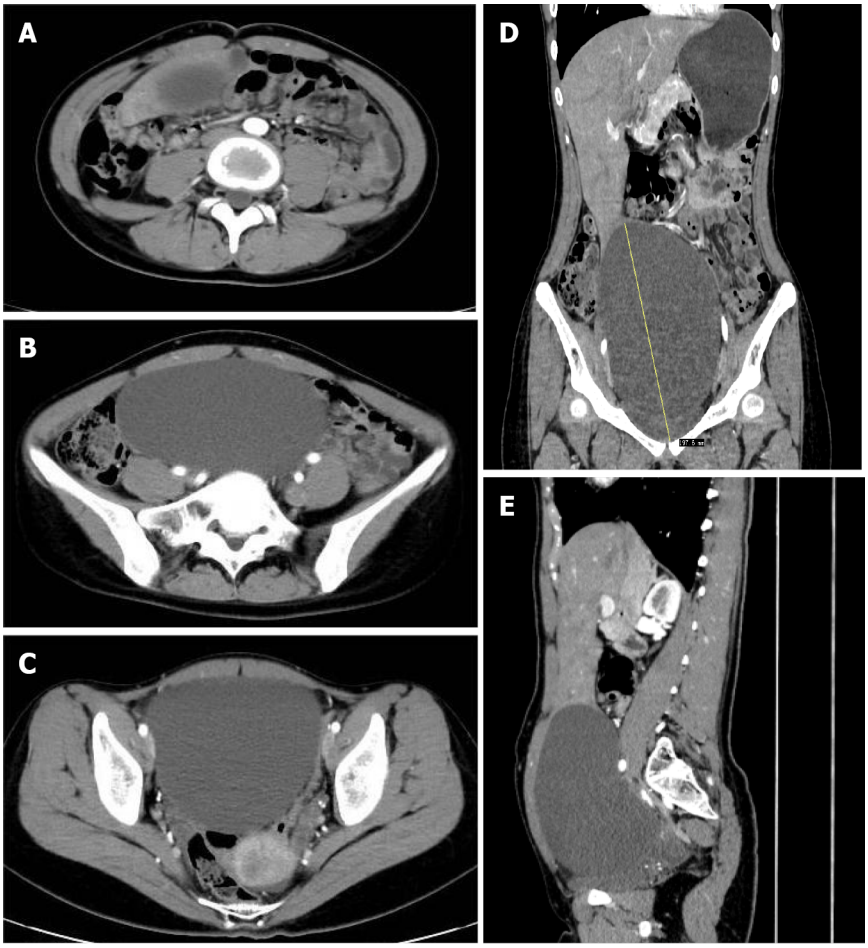

DOI: 10.12998/wjcc.v11.i33.8030 **Copyright** ©The Author(s) 2023.

Figure 1 Abdominal contrast-enhanced computed tomography images. Images show a huge cystic mass in the abdominal and pelvic cavities, possibly arising from the liver. A small amount of free fluid is present in the pelvic cavity. A: Middle abdomen; B: Lower abdomen; C: Pelvic cavity; D: Coronal plane of the abdomen; E: Sagittal plane of the abdomen.

neutrophil count, 1.421 × 10^9/L; hemoglobin concentration, 109.00 g/L; serum C-reactive protein level, 0.23 mg/L; β-human chorionic gonadotropin level, 0.23 mIU/mL; serum albumin level, 38.6 g/L; total bilirubin level, 21.0 μmol/L; and serum alanine aminotransferase level, 12.4 U/L. After 2 d of bladder fluid cultivation, no bacterial or fungal growth was observed. The remaining findings are shown in Tables 1-5.

Imaging examinations

Abdominal contrast-enhanced computed tomography revealed a giant cystic mass in the abdominal and pelvic cavities, possibly originating from the liver. Furthermore, a small amount of free fluid was observed in the pelvic cavity (Figure 1). Magnetic resonance imaging revealed a large cystic mass in the abdominal and pelvic cavities, with features suggesting a benign lesion (Figure 2).

FINAL DIAGNOSIS

Bile duct derived complex liver cyst.

TREATMENT

The patient underwent laparoscopic resection of the giant liver cyst along with partial liver resection. Her presenting symptoms of frequent or urgent urination were completely relieved post-surgery and she was discharged on the sixth postoperative day.

Table 1 Patient laboratory data at the time of admission

Parameter	Patient's value	Reference value
White blood cell count (10^9/L)	3.93	3.50–9.50
C-reactive protein (mg/L)	0.23	0–6
Neutrophils (%)	36.00	40–75
Lymphocytes (%)	55.70	20–50
Monocytes (%)	5.20	3–10
Hemoglobin (g/L)	109.00	115.0–150.0
Platelet count (10^9/L)	172	125–350
Activated thromboplastin time (s)	13.50	9.4-12.5
Activated partial thromboplastin time (s)	11.0	11–14
Albumin (g/L)	38.6	40.0–55.0
Total protein (g/L)	62.8	65.0–85.0
Total bilirubin (μmol/L)	21.0	0.0–21.0
Aspartate aminotransferase (U/L)	15.1	13.0–35.0
Alanine aminotransferase (U/L)	12.4	7.0–40.0
Blood creatinine (μmol/L)	54.5	41.0–81.0

Table 2 Tumor indicators at the time of admission

Parameter	Patient's value	Reference value
Carcinoembryonic antigen (ng/mL)	1.36	0–5.0
Alpha-fetoprotein (ng/mL)	1.71	< 9.0[1]
CA-199 (U/mL)	3.40	0–25
β-human chorionic gonadotropin (mIU/mL)	0.24	0–35
CA-125 (U/mL)	15.17	0–5
CA-15-3 (U/mL)	3.10	0–14
CA-50 (U/mL)	3.91	< 25
CA-72-4 (U/mL)	4.02	0–10
CA-24-2 (U/mL)	4.27	< 25
Squamous cell carcinoma-associated antigen (ng/mL)	0.78	0–1.5
Cytokeratin 19 fragment (ng/mL)	1.59	< 3.3
Neuron specific enolase (ng/mL)	9.93	0–20

[1]Alpha-fetoprotein (ng/ml) < 9.0 in males and non-pregnant females.

OUTCOME AND FOLLOW-UP

The patient recovered well, with no symptoms of frequent or urgent urination, and no specific discomfort was observed during follow-up at 0.5, 1, and 3 mo after discharge.

DISCUSSION

Liver cysts are a benign disease with genetic characteristics[10,11]. Simple liver cysts are typical cystic thin-walled masses that originate from bile duct cells that form abnormally during embryonic development[5]. In most cases, cysts occur only in the liver and patients generally have no obvious clinical symptoms. However, in some patients, the expansion of liver cysts can cause abdominal symptoms, mainly due to a series of corresponding clinical symptoms caused by compression

Table 3 Cystic fluid - routine testing findings

Parameter	Patient's value	Reference value
Color	Yellow	
Solidification	No solidification	
Pellucidity	Slightly turbid	
Proportion	1.010	Leakage fluid < 1.015 Exudate > 1.018
Rivalta test	+	Leakage fluid: - Exudate: +
White blood cell count (10^9/L)	0.04	Leakage fluid < 0.1 Exudate > 0.5
Red blood cell count (10^9/L)	0.40	0
Other	Cholesterol crystals detected	

Table 4 Biochemical indicators of cystic fluid

Parameter	Patient's value
TG (mmol/L)	0.12
GLU (mmol/L)	0.37
CH (mmol/L)	0.67
AMY (U/L)	55
ADA (U/L)	25.6
LDH (U/L)	58.6
ACE (U/L)	6.1
Total protein (g/L)	66.4
Albumin (g/L)	42.4

TG: Triacylglycerol; GLU: Glutamate; CH: Cholesterol; AMY: Amylase; ADA: Adenosine deaminase; LDH: Serum lactic dehydrogenase; ACE: Angiotensin-converting enzyme.

Table 5 Cystic fluid alpha-fetoprotein and carcinoembryonic antigen

Parameter	Patient's value	Reference value
Carcinoembryonic antigen (ng/mL)	0.43	0–5.0
Alpha-fetoprotein (ng/mL)	0.72	< 9.0[1]

[1]Alpha-fetoprotein (ng/ml) < 9.0 in males and non-pregnant females.

of the surrounding tissues or organs caused by oversized liver cysts[12]. Asymptomatic simple liver cysts usually do not require treatment. The treatments for liver cysts with obvious clinical symptoms include percutaneous puncture, aspiration, sclerotherapy, and surgery[5].

Herein, we report a case of pseudocystitis caused by a giant complex liver cyst that was pathologically suggestive of a bile duct derived liver cyst and was different from a conventional liver cyst (Figure 3). There are no reports in the literature of complex liver cysts causing symptoms of pseudocystitis. Liver cysts are typically asymptomatic. An increase in cyst size, particularly in giant liver cysts, can initiate symptoms. If the diameter of the cyst exceeds 10 cm, it can expand and cause pressure effect on adjacent organs and corresponding symptoms may appear[8], including abdominal pain, nausea, vomiting, obstructive jaundice, superior vena cava thrombosis, acute pulmonary embolism, and acute pancreatitis[6,13-15]. Giant liver cysts should be differentiated from Caroli disease[16], giant mesenchymal hamartomas of the liver[17], teratomas[18], and other diseases[19-21]. Our patient had previously experienced symptoms of pancreatitis. Therefore, we assumed that the pain was caused by a liver cyst. At the time of presentation, the liver cyst caused symptoms in distant organs that disappeared postoperatively. Thus, it was confirmed that the giant liver cyst caused the

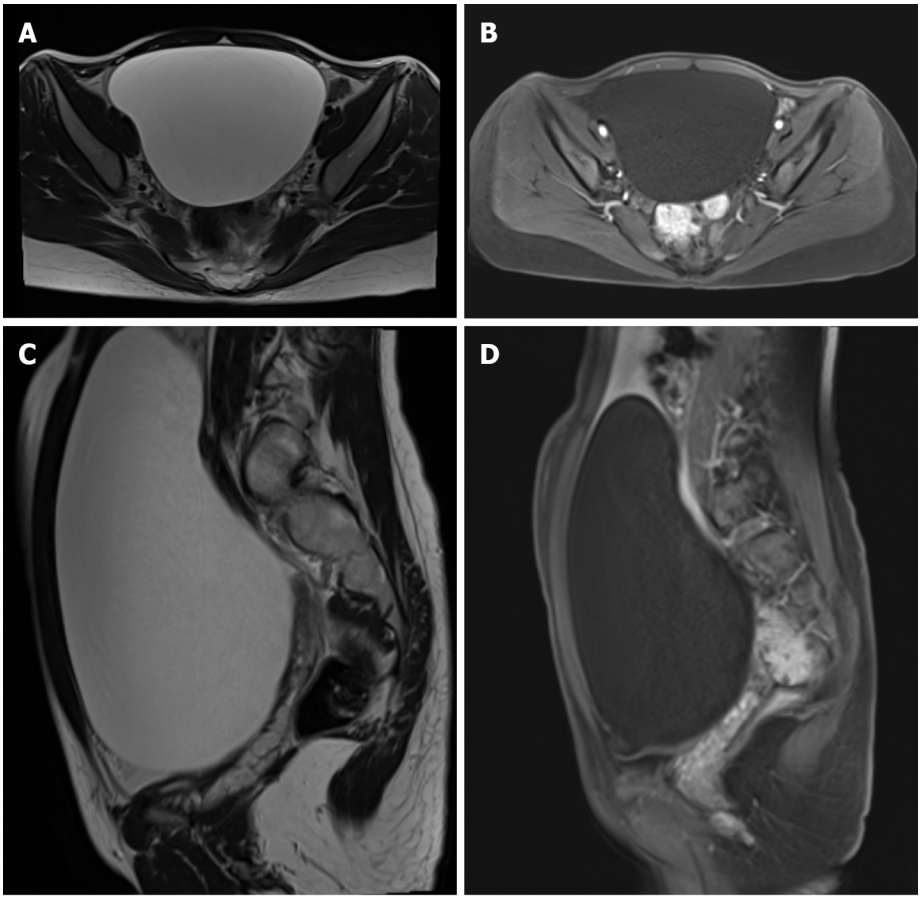

DOI: 10.12998/wjcc.v11.i33.8030 **Copyright** ©The Author(s) 2023.

Figure 2 Magnetic resonance imaging. Images show a large cystic mass in the abdominal and pelvic cavities that was considered a benign lesion. A small amount of free fluid is present in the pelvic cavity. A: Pelvic cavity; B: Enhanced pelvic cavity; C: Sagittal plane of the abdomen; D: Enhanced sagittal plane of the abdomen.

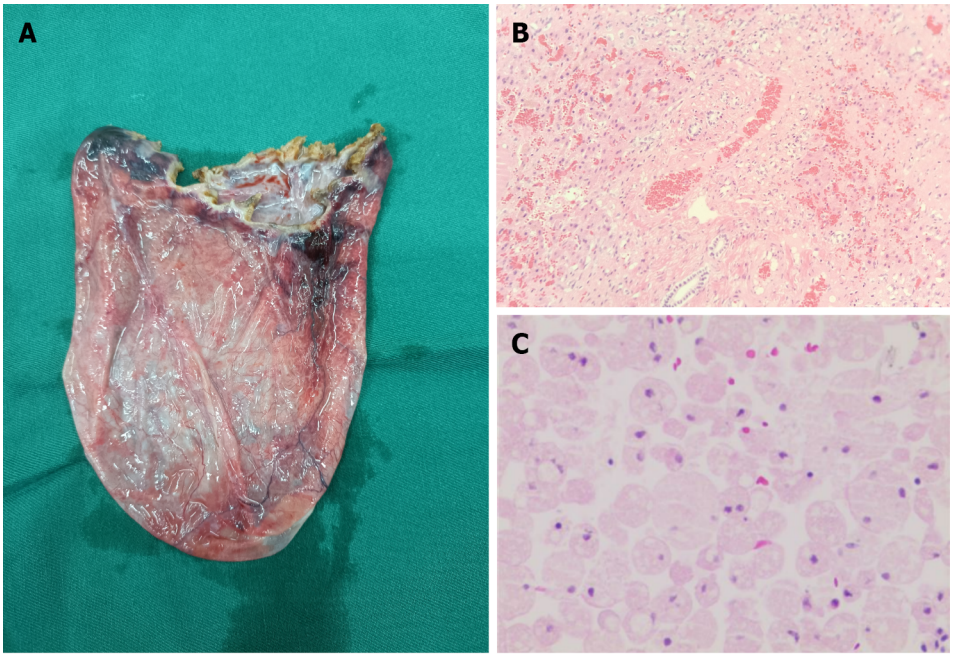

DOI: 10.12998/wjcc.v11.i33.8030 **Copyright** ©The Author(s) 2023.

Figure 3 Postoperative specimen and pathological diagnosis. A: Postoperative specimen; B: Bile duct derived cyst liver tissue showing bleeding and a compression injury (liver tissue); C: A few red blood cells and histiocytes (ascites cell mass).

pain. These cysts usually require surgical intervention. In our patient, the giant cyst was located at the edge of the liver; thus, the liver was stretched and deformed under the influence of gravity. During the surgical process, we obtained biopsy samples of adjacent tissues to determine the possibility of further deterioration of liver architecture, and to rule out possible recurrence, which the liver cysts are prone to.

CONCLUSION

Our case report highlights that the diagnosis and treatment of complex giant liver cysts that cause pseudocystitis should be comprehensive and multidimensional. The differential diagnosis of such abdominal masses should be considered before treatment. The patient was a young, unmarried girl, and a detailed plan was specified to minimize major trauma and achieve the best treatment outcomes. These patients require close follow-up because liver cysts are prone to recurrence.

FOOTNOTES

Co-first authors: Song Li and Jie Tang.

Author contributions: Li S, Tang J, Ni DS, and Xia AD conceived, designed, and refined the study protocol; Li S, Tang J, Xia AD, and Chen GL were involved in data collection; Li S, Tang J, and Chen GL analyzed the data; Li S, Tang J, and Ni DS drafted the manuscript; all authors were involved in the critical review of the results and have contributed to, read, and approved the final manuscript. Li S and Tang J contributed equally to this work as co-first authors. The reasons for designating Li S and Tang J as co-first authors are threefold. First, the research was performed as a collaborative effort, and the designation of co-first authors accurately reflects the distribution of responsibilities and burdens associated with the time and effort required to complete the study and the resultant paper. This also ensures effective communication and management of post-submission matters, ultimately enhancing the paper's quality and reliability. Second, the overall research team encompassed authors with a variety of expertise and skills from different fields, and the designation of co-first authors best reflects this diversity. This also promotes the most comprehensive and in-depth examination of the research topic, ultimately enriching readers' understanding by offering various expert perspectives. Third, Li S and Tang J contributed efforts of equal substance throughout the research process. The choice of these researchers as co-first authors acknowledges and respects this equal contribution, while recognizing the spirit of teamwork and collaboration of this study. In summary, we believe that designating Li S and Tang J as co-first authors is fitting for our manuscript as it accurately reflects our team's collaborative spirit, equal contributions, and diversity.

Informed consent statement: Informed consent was obtained from the patient before the publication of this case report.

Conflict-of-interest statement: The authors declare no competing financial interest for this article.

CARE Checklist (2016) statement: The authors have read the CARE Checklist (2016), and the manuscript was prepared and revised according to the CARE Checklist (2016).

Open-Access: This article is an open-access article that was selected by an in-house editor and fully peer-reviewed by external reviewers. It is distributed in accordance with the Creative Commons Attribution NonCommercial (CC BY-NC 4.0) license, which permits others to distribute, remix, adapt, build upon this work non-commercially, and license their derivative works on different terms, provided the original work is properly cited and the use is non-commercial. See: https://creativecommons.org/Licenses/by-nc/4.0/

Country/Territory of origin: China

ORCID number: Song Li 0009-0004-6327-8525; De-Sheng Ni 0009-0008-4168-7335; A-Dong Xia 0009-0006-1412-0064; Guo-Liang Chen 0009-0002-1750-3256.

S-Editor: Lin C
L-Editor: Wang TQ
P-Editor: Lin C

REFERENCES

1 **Regev A**, Reddy KR, Berho M, Sleeman D, Levi JU, Livingstone AS, Levi D, Ali U, Molina EG, Schiff ER. Large cystic lesions of the liver in adults: a 15-year experience in a tertiary center. *J Am Coll Surg* 2001; **193**: 36-45 [PMID: 11442252 DOI: 10.1016/s1072-7515(01)00865-1]
2 **Gomez A**, Wisneski AD, Luu HY, Hirose K, Roberts JP, Hirose R, Freise CE, Nakakura EK, Corvera CU. Contemporary Management of Hepatic Cyst Disease: Techniques and Outcomes at a Tertiary Hepatobiliary Center. *J Gastrointest Surg* 2021; **25**: 77-84 [PMID: 33083858 DOI: 10.1007/s11605-020-04821-1]
3 **Xu WP**, Wang XH, Wu SP, Shi PM, Yuan ZL, Guo YB, Zeng X, Xie WF. The prevalence and associated factors of simple hepatic cysts in Shanghai: a population-based cross-sectional study. *Chin Med J (Engl)* 2021; **134**: 1248-1250 [PMID: 33410628 DOI: 10.1097/CM9.0000000000001361]
4 **Cowles RA**, Mulholland MW. Solitary hepatic cysts. *J Am Coll Surg* 2000; **191**: 311-321 [PMID: 10989905 DOI:

10.1016/s1072-7515(00)00345-8]

5 **Shimizu T**, Yoshioka M, Kaneya Y, Kanda T, Aoki Y, Kondo R, Takata H, Ueda J, Kawano Y, Hirakata A, Matsushita A, Taniai N, Mamada Y, Yoshida H. Management of Simple Hepatic Cyst. *J Nippon Med Sch* 2022; **89**: 2-8 [PMID: 34526451 DOI: 10.1272/jnms.JNMS.2022_89-115]

6 **Miyamoto M**, Oka M, Izumiya T, Nagaoka T, Ishihara Y, Ueda K, Enomoto S, Yanaoka K, Arii K, Tamai H, Shimizu Y, Ichinose M. Nonparasitic solitary giant hepatic cyst causing obstructive jaundice was successfully treated with monoethanolamine oleate. *Intern Med* 2006; **45**: 621-625 [PMID: 16755093 DOI: 10.2169/internalmedicine.45.1408]

7 **Tsuruya K**, Nishizaki Y, Tatemichi M, Mishima Y, Shimma Y, Arase Y, Hirose S, Shiraishi K, Kagawa T. The prevalence and natural history of hepatic cysts examined by ultrasound: a health checkup population retrospective cohort study. *Sci Rep* 2022; **12**: 12797 [PMID: 35896780 DOI: 10.1038/s41598-022-16875-z]

8 **Fantola G**, Barth X, Monneuse O. Education and imaging. Hepatobiliary and pancreatic: Pancreatitis associated with a large hepatic cyst. *J Gastroenterol Hepatol* 2010; **25**: 1333 [PMID: 20594268 DOI: 10.1111/j.1440-1746.2010.06394.x]

9 **Panchal M**, Alansari A, Wallack M, Visco F, Williams S, Sy AM. Hepatic Cyst Compressing The Right Atrial and Ventricular Inflow Tract: An Uncommon Cardiac Complication. *Ann Hepatol* 2018; **17**: 165-168 [PMID: 29311401 DOI: 10.5604/01.3001.0010.7549]

10 **Choi BY**, Nguyen MH. The diagnosis and management of benign hepatic tumors. *J Clin Gastroenterol* 2005; **39**: 401-412 [PMID: 15815209 DOI: 10.1097/01.mcg.0000159226.63037.a2]

11 **Lantinga MA**. Evaluation of hepatic cystic lesions. *World J Gastroenterol* 2013; **19**: 3543-3554 [DOI: 10.3748/wjg.v19.i23.3543]

12 **Temmerman F**, Missiaen L, Bammens B, Laleman W, Cassiman D, Verslype C, van Pelt J, Nevens F. Systematic review: the pathophysiology and management of polycystic liver disease. *Aliment Pharmacol Ther* 2011; **34**: 702-713 [PMID: 21790682 DOI: 10.1111/j.1365-2036.2011.04783.x]

13 **Wijnands TF**, Görtjes AP, Gevers TJ, Jenniskens SF, Kool LJ, Potthoff A, Ronot M, Drenth JP. Efficacy and Safety of Aspiration Sclerotherapy of Simple Hepatic Cysts: A Systematic Review. *AJR Am J Roentgenol* 2017; **208**: 201-207 [PMID: 27824501 DOI: 10.2214/AJR.16.16130]

14 **Wijnands TF**, Neijenhuis MK, Kievit W, Nevens F, Hogan MC, Torres VE, Gevers TJ, Drenth JP. Evaluating health-related quality of life in patients with polycystic liver disease and determining the impact of symptoms and liver volume. *Liver Int* 2014; **34**: 1578-1583 [PMID: 24313956 DOI: 10.1111/liv.12430]

15 **Torzilli G**, Santambrogio R, Vellini S, Palmisano A, Donadon M, Cornalba G, Montorsi M. Inferior vena cava thrombosis: an unusual complication of a large simple non-parasitic liver cyst requiring an integrated approach. *Hepatogastroenterology* 2003; **50**: 2188-2191 [PMID: 14696494]

16 **Almohtadi A**, Ahmed F, Mohammed F, Sanhan M, Ghabisha A, Al-Moliki L. Caroli's disease incidentally discovered in a 16-years-old female: a case report. *Pan Afr Med J* 2022; **41**: 204 [PMID: 35685111 DOI: 10.11604/pamj.2022.41.204.34088]

17 **Bezabih YS**, Tessema WA, Getu ME. Giant biliary mucinous cystadenoma mimicking mesenchymal hamartoma of the liver in a child: A case report. *Int J Surg Case Rep* 2021; **88**: 106523 [PMID: 34688072 DOI: 10.1016/j.ijscr.2021.106523]

18 **Lešková J**, Kříž JT, Štichhauer R. Bilateral Mature Ovarian Teratoma with Torsion in a Premenarchal Girl. *Acta Medica (Hradec Kralove)* 2022; **65**: 33-36 [PMID: 35793507 DOI: 10.14712/18059694.2022.14]

19 **Matsuo H**, Katayama K, Hayasaki A, Iizawa Y, Endo M, Murata T, Mizuno S, Dohi K. Biliary peritonitis due to liver cyst rupture in autosomal dominant polycystic kidney disease. *BMC Gastroenterol* 2021; **21**: 267 [PMID: 34167461 DOI: 10.1186/s12876-021-01845-y]

20 **Cnossen WR**, Drenth JP. Polycystic liver disease: an overview of pathogenesis, clinical manifestations and management. *Orphanet J Rare Dis* 2014; **9**: 69 [PMID: 24886261 DOI: 10.1186/1750-1172-9-69]

21 **Gevers TJ**, Drenth JP. Diagnosis and management of polycystic liver disease. *Nat Rev Gastroenterol Hepatol* 2013; **10**: 101-108 [PMID: 23296249 DOI: 10.1038/nrgastro.2012.254]

World Journal of Clinical Cases

Submit a Manuscript: https://www.f6publishing.com

World J Clin Cases 2023 November 26; 11(33): 8038-8043

DOI: 10.12998/wjcc.v11.i33.8038

ISSN 2307-8960 (online)

CASE REPORT

Carotid-subclavian bypass and endovascular aortic repair of Kommerell's diverticulum with aberrant left subclavian artery: A case report

Wajeehullahi Akilu, Yi Feng, Xiao-Xue Zhang, Shi-Liang Li, Xian-Tao Ma, Min Hu, Cai Cheng

Specialty type: Cardiac and cardiovascular systems

Provenance and peer review: Unsolicited article; Externally peer reviewed.

Peer-review model: Single blind

Peer-review report's scientific quality classification

Grade A (Excellent): 0
Grade B (Very good): 0
Grade C (Good): C
Grade D (Fair): 0
Grade E (Poor): 0

P-Reviewer: Barik R, India

Received: August 10, 2023
Peer-review started: August 10, 2023
First decision: August 30, 2023
Revised: September 14, 2023
Accepted: November 10, 2023
Article in press: November 10, 2023
Published online: November 26, 2023

Wajeehullahi Akilu, Yi Feng, Xiao-Xue Zhang, Shi-Liang Li, Xian-Tao Ma, Min Hu, Cai Cheng, Division of Cardiothoracic Surgery and Vascular Surgery, Tongji Hospital, Tongji Medical College, Huazhong University of Science and Technology, Wuhan 430030, Hubei Province, China

Corresponding author: Wajeehullahi Akilu, Master's Student, Division of Cardiothoracic Surgery and Vascular Surgery, Tongji Hospital, Tongji Medical College, Huazhong University of Science and Technology, No. 1095 Jiefang Avenue, Wuhan 430030, Hubei Province, China. 2838164393@qq.com

Abstract

BACKGROUND

Kommerell's diverticulum (KD) with aberrant left subclavian artery is a rare congenital deformity and also has very little research literature about it (35% of case study). There are three types of aortic arch diverticulum. Even literature concerning the treatment options are limited.

CASE SUMMARY

We present a case report of a 50-year-old male with KD in the right aortic arch with aberrant left subclavian artery. We conducted a total endovascular repair procedure, which is innovative and will spread more light in the medical world. Our patient has no past medical history and is a non-smoker and non-alcoholic. Patient presented with shortness of breath, chest pain and dizziness for six months. Blood tests were done and computerized tomography (CT) angiogram of the chest confirmed the diagnosis, illustrating showed a 3.9 cm KD. On Day 1, the CT angiogram showed mild dilatation of the thoracic aorta, adjacent esophagus, trachea was compressed and displaced. Surgery was planned as the treatment modality. Carotid-Subclavian artery bypass and endovascular aortic repair was conducted. We used prolene 5-0 C1 sutures to precisely anastomose a 6-mm Dacron graft to the left subclavian artery. Haemostasis was secured and wounds were closed. Protamine was administered and patient was shifted to intensive care unit. Post-operative, patient responded favorably and was discharged. Regular follow-up is done.

CONCLUSION

The procedure we performed is novel. This will help the cardio-thoracic surgeons

a better insight about the full procedures we conducted, thereby bringing more light and better treatment options in managing KD with aberrant subclavian artery.

Key Words: Kommerell's diverticulum; Left common carotid artery; Aberrant left subclavian artery; Carotid-subclavian bypass; Medtronic stent catheter endovascular repair; Case report

©The Author(s) 2023. Published by Baishideng Publishing Group Inc. All rights reserved.

Core Tip: Kommerell's diverticulum with aberrant left subclavian artery is an infrequent congenital deformity. Research, and literature about its treatment options is minimal. We present a case report of a 50-year-old male with no comorbidities, with Kommerell's diverticulum in the right aortic arch with aberrant left subclavian artery. The patient presented with shortness of breath, chest pain and dizziness for six months. Blood tests and a computerized tomography angiogram confirmed the diagnosis. Carotid-subclavian artery bypass and endovascular aortic repair, using a Dacron graft was conducted, which is an innovative procedure, shedding more light on it. Post-operatively, the patient responded favorably.

Citation: Akilu W, Feng Y, Zhang XX, Li SL, Ma XT, Hu M, Cheng C. Carotid-subclavian bypass and endovascular aortic repair of Kommerell's diverticulum with aberrant left subclavian artery: A case report. *World J Clin Cases* 2023; 11(33): 8038-8043
URL: https://www.wjgnet.com/2307-8960/full/v11/i33/8038.htm
DOI: https://dx.doi.org/10.12998/wjcc.v11.i33.8038

INTRODUCTION

Originally described in 1936, by a German radiologist, named Kommerell[1], Kommerell's diverticulum (KD) is also known as "lusoria diverticulum", "lusoria root" or "remnant diverticulum"[1]. This was seen in a patient with left sided aortic arch, where a pulsatile mass seen to the posterior of the oesophagus, leading to the compression of that part of gut, detected in barium swallow[1]. It is defined as the aneurysmal dilatation of the descending aorta at the origin of an aberrant subclavian artery (ASCA), that can be located in both right and left sided aortic arches[2]. KD is due to persistence remnant of the fourth primitive dorsal arch, which failed to retrogress[3].

As per the classification of Salomonowitz *et al*[4], there are three types of aortic arch diverticulum namely: (1) Diverticulum in left aortic arch with right ASCA; (2) diverticulum in right aortic arch with left ASCA; and (3) aortic diverticulum without ASCA (at the aortic-ductal junction).We present a case study of patient detected with KD with left ASCA.

CASE PRESENTATION

Chief complaints

A 50-year-old Chinese man was admitted to our hospital, presented with difficulty in breathing, sudden onset chest pain and dizziness on and off for 6 mo.

History of present illness

There was no dysphagia, syncopal attacks, abdominal pain, palpitations or other symptoms.

History of past illness

His past medical history, past surgical history.

Personal and family history

Personal history: Smoking-drinking habits are not significant.

Family history: Family history and drug allergy were not major.

Physical examination

The vital signs were: Blood pressure was 120/70 mmHg, temperature was 36.5 °C, pulse was 73 bpm, regular (bilateral radial, brachial sides were normal), no pallor, no cyanosis, no clubbing, no pedal oedema, no peripheral vascular signs. The systemic examinations were normal.

Laboratory examinations

The blood investigations such as the hematological and biochemical investigations were within normal limits.

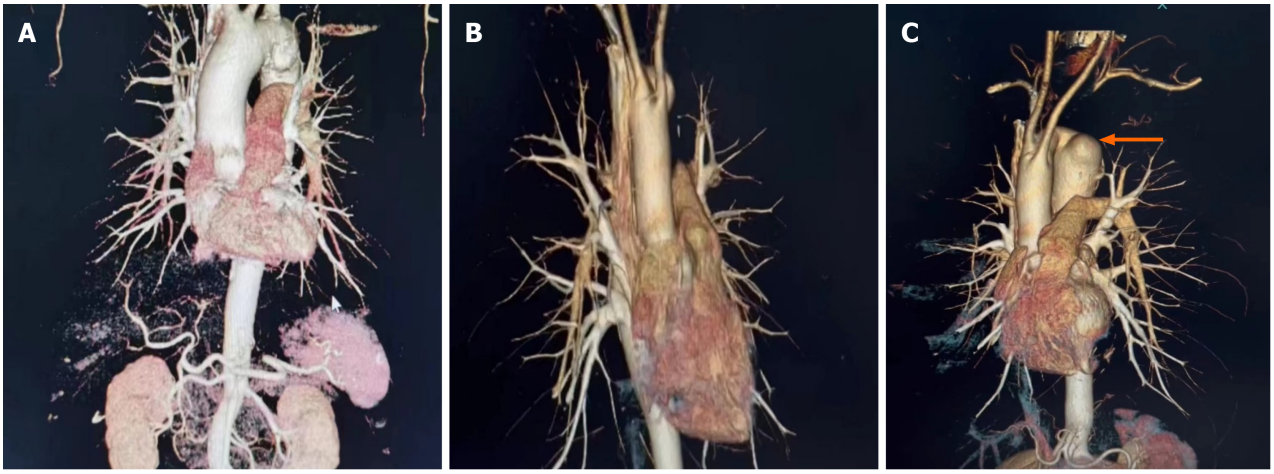

DOI: 10.12998/wjcc.v11.i33.8038 **Copyright** ©The Author(s) 2023.

Figure 1 Computed tomographic aortography images. A: The normal shape of the aorta of this patient; B: The shape of the patient's aorta; C: White arrow showing Kommerell's diverticulum in the arch of aorta, left subclavian, left cervical spine.

Imaging examinations

A computed tomography aortography (CTA) was performed on him as diagnostic assessment and findings as shown below (Figure 1).

At the local provincial hospital, on day 1 admission, CTA of the brain and neck region identified aortic arch KD with esophageal compression, left subclavian artery was stenosed (Figure 2) and left subclavian artery steal syndrome was seen. The patient was referred to our Cardiothoracic Surgery Department. On day 5, Another CTA was performed and showed mild dilatation of the thoracic aorta, adjacent esophagus and trachea was compressed and displaced (Figure 1B; Video 1). The right upper lobe tip was streaked, and were mostly inflammatory lesions, several small round low-density foci in the liver.

The treatment options were then discussed with the patient including that of a surgical treatment along with all the risks and benefits involved. The patient agreed for surgical intervention.

FINAL DIAGNOSIS

On day 5, Another CTA was performed and showed mild dilatation of the thoracic aorta, adjacent esophagus and trachea was compressed and displaced (Figure 1B; Video 1). The right upper lobe tip was streaked, and were mostly inflammatory lesions, several small round low-density foci in the liver.

TREATMENT

The treatment options were then discussed with the patient including that of a surgical treatment along with all the risks and benefits involved. The patient agreed for surgical intervention.

Surgical open repair

Pre-operative CT angiography film of the chest showed a 3.9 cm KD (Figure 1C; Video 1). After placing the patient in supine position, general anaesthesia was administered successfully. The anterior aspect of the chest wall and groin area were routinely disinfected. We began a transverse supraclavicular 5 cm incision (Figure 3A). We separated the platysma muscle and proceeded to the two heads of the sternocleidomastoid muscle.

Firstly, a dissection was done to reach the internal jugular vein. We applied deep wound spreaders to help expose the vessels (Figure 3A). Medial to this vein, we cautiously isolated the vagus nerve, which lies between the internal jugular vein and the left common carotid artery (LCCA) and we opened the carotid sheath. This allowed the chance to do anastomosis proximally on the LCCA at the left lateral side (Figure 3B).

The next procedure was exposing the left subclavian artery (LSA), 1 cm deeper in the neck and its lateral away from the LCC. There was subcutaneous fatty tissue with lymph nodes that obstructs LSA dissection, hence these lymph nodes were resected. We also exposed and looped the left internal thoracic artery using a vessel loop.

We then finally revealed the deep LSA in the neck (Figure 3A) and the associations between the LCCA and LSA were obviously seen. A prescribed heparin dose was administered. We clamped the LSA and incised to make round-shape incision. We used prolene 5-0 C1 sutures to meticulously anastomosed 6-mm Dacron graft (Polymaille C, Perous Medical, France) to the LSA round-shape incised artery and haemostasis was checked afterwards. We made a good size length of our Dacron graft and it was able to stretch from the left subclavian artery to the lateral side of LCCA.

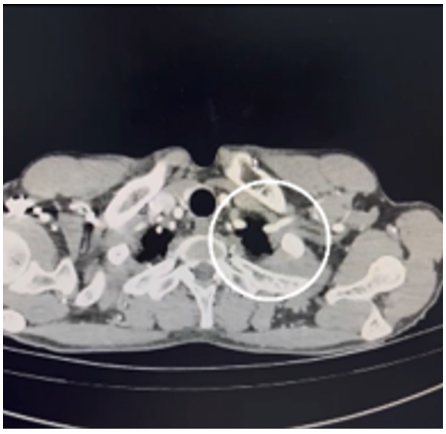

DOI: 10.12998/wjcc.v11.i33.8038 **Copyright** ©The Author(s) 2023.

Figure 2 Computed tomography scan image showing: The location of left subclavian artery stenosis encircled.

We clamped the LCCA while at the same time monitoring the transcranial Doppler signals. We ensured that there was enough cerebral perfusion pressure by letting the mean blood pressure stable at 90 mmHg. We made a tinny incision on the LCCA at the lateral side and a mild punch to create a round-hole. We then started our anastomosis using 5-0 C1 sutures on a 6-mm Dacron graft (Polymaille C, Perous Medical, France) end to end approach with LCCA. A clamp was used clamping the distal LCCA and then was flushed. Afterwards, we unclamped the LSA and the previously clamped LCCA to de-air them. Also, haemostasis was checked from the vessels after unclamping the vessels.

Total endovascular repair

Preoperative CT angiography revealed morphology of right femoral artery, the LCCA, the right common carotid artery, right subclavian artery, the proximal end of the left subclavian artery was stenosed, and the descending aorta was obviously bulged (33 mm × 25 mm). In accordance to what we have in the patient's history and CT results, this guided us in our interventional approach for this procedure. The groin femoral region was opened (Figure 3D) and 34200 mm Medtronic Stent graft (Medtronic Inc. United States) (Figure 3C) was placed through the femoral artery, positioned by the right subclavian artery angiographic catheter, and deployed at the proximal end of the right subclavian artery and the areas of the left subclavian artery were covered successfully. There was no leakage of contrast agent after re-angiography. We closed all incisions by way of suturing and systemic Protamine was administered to the Patient, then transferred to the intensive care unit.

OUTCOME AND FOLLOW-UP

The post-operative care was done meticulously, including the daily nursing care. Patient was discharged on Tablet Plavix 75 mg once a day and later shifted to enteric coated Aspirin tablet 100 mg orally once a day and its side-effects (such as bleeding gums, bleeding from any orifices, gastrointestinal bleeding, black stools) have been explained to the patient and to attend hospital immediately once any of it happens.

We suggest the patient for regular monitoring of blood pressure, heart rate, blood routine examination including renal function, liver function tests, cardiac enzymes, electrocardiogram and cardiac echography and to have regular follow-up after 1, 3, 6, 12-mo. The patient's recovery was normal without any symptoms and he continued to be uneventful one-year post-surgery.

DISCUSSION

KD in brief, is a rare abnormal congenital condition that occurs in either right or left sided aortic arch and seen to be associated with an ASCA[2]. KD are aneurysmal dilated changes in the aortic walls and have the tendency of dissection [5]. In 1936, initially described in a patient with left sided aortic arch, German radiologist Kommerell saw on barium swallow: a pulsatile mass compressing the esophagus posteriorly[1]. The incidence of KD with a right-sided aortic arch; seen in radiological studies is 0.05-0.1%[6,7].

KD symptoms of oesophageal or tracheal origins, are indicative factors for a surgical treatment. A KD with a size greater than 30 mm in diameter should be considered for operation[5]. It is known that KD has tendency of activating aortic aneurysm, or dissection or even rupture. Open repair and revascularization of the left arm was the surgical approach of preference. Using the techniques of minimally invasive and endovascular techniques for surgical repairs, have recently helped to reduce anguish, pain when compared to open sternotomy[8-10].

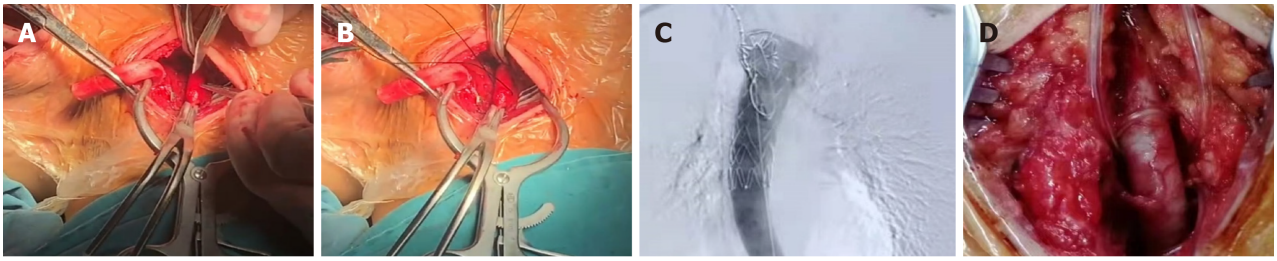

DOI: 10.12998/wjcc.v11.i33.8038 **Copyright** ©The Author(s) 2023.

Figure 3 Surgical incision images and image after endovascular aortic repair. A: Transverse supraclavicular 5 cm incision exposing the surgical site; B: Clamping and anastomosis of the left subclavian artery to the left common carotid artery; C: Angiography picture showing the insertion of the deployed aortic stent replacement (Medtronic Inc., United States); D: Area of the groin: femoral artery opening.

CONCLUSION

We demonstrated rare combined case study of endovascular and open surgical treatment involving KD with aberrant left subclavian artery. Being a rare disease, little literature was found about the surgical treatment. The procedure we conducted is innovative and will bring more understanding and better treatment options in managing KD with ASCA. Again, our technique was able to give a full comprehensive insight on how the stent replacement and left sided revascularization can be performed in an orderly way. Thus, bringing scientific progress in the field.

ACKNOWLEDGEMENTS

We would like to thank the patient for giving the consent in writing the paper.

FOOTNOTES

Author contributions: All authors contributed equally in writing the paper; all authors have read and approved the manuscript.

Informed consent statement: Informed written consent was taken from the patient.

Conflict-of-interest statement: There was no conflict of interest declared by the authors.

CARE Checklist (2016) statement: The authors have read the CARE Checklist (2016), and the manuscript was prepared and revised according to the CARE Checklist (2016).

Open-Access: This article is an open-access article that was selected by an in-house editor and fully peer-reviewed by external reviewers. It is distributed in accordance with the Creative Commons Attribution NonCommercial (CC BY-NC 4.0) license, which permits others to distribute, remix, adapt, build upon this work non-commercially, and license their derivative works on different terms, provided the original work is properly cited and the use is non-commercial. See: https://creativecommons.org/Licenses/by-nc/4.0/

Country/Territory of origin: China

ORCID number: Wajeehullahi Akilu 0009-0006-4851-7000.

S-Editor: Yan JP
L-Editor: A
P-Editor: Xu ZH

REFERENCES

1 **Kommerell B**. Verlagerung des oesophagus durch eine abnorm veranfende arteria subclavia dextra (arteria lusoria). *Fortschr Geb Roentgenstr* 1936; **54**: 590-595
2 **Bhatt TC**, Muralidharan CG, Singh G, Jain NK. Kommerell's diverticulum: A rare aortic arch anomaly. *Med J Armed Forces India* 2016; **72**: S80-S83 [PMID: 28050078 DOI: 10.1016/j.mjafi.2016.09.003]
3 **EDWARDS JE**. Anomalies of the derivatives of the aortic arch system. *Med Clin North Am* 1948; **32**: 925-949 [PMID: 18877614 DOI: 10.1016/s0025-7125(16)35662-0]
4 **Salomonowitz E**, Edwards JE, Hunter DW, Castaneda-Zuniga WR, Lund G, Cragg AH, Amplatz K. The three types of aortic diverticula. *AJR Am J Roentgenol* 1984; **142**: 673-679 [PMID: 6422713 DOI: 10.2214/ajr.142.4.673]

5 **Cinà CS**, Althani H, Pasenau J, Abouzahr L. Kommerell's diverticulum and right-sided aortic arch: a cohort study and review of the literature. *J Vasc Surg* 2004; **39**: 131-139 [PMID: 14718830 DOI: 10.1016/j.jvs.2003.07.021]

6 **Tsukube T**, Ataka K, Sakata M, Wakita N, Okita Y. Surgical treatment of an aneurysm in the right aortic arch with aberrant left subclavian artery. *Ann Thorac Surg* 2001; **71**: 1710-1711 [PMID: 11383841 DOI: 10.1016/s0003-4975(00)02698-9]

7 **Svensson LG**, Crawford ES. Cardiovascular and vascular disease of the aorta. Philadelphia: W.B. Saunders Company, 1997

8 **Idrees J**, Keshavamurthy S, Subramanian S, Clair DG, Svensson LG, Roselli EE. Hybrid repair of Kommerell diverticulum. *J Thorac Cardiovasc Surg* 2014; **147**: 973-976 [PMID: 23535153 DOI: 10.1016/j.jtcvs.2013.02.063]

9 **Hayakawa M**, Nagano T, Nishijima I, Shinzato K, Ikemura R, Miyagi K, Iha K, Senaha S, Shimoji M, Akasaki M. Successful Endovascular Repair of a Kommerell's Diverticulum and a Right-Sided Aortic Arch. *Heart Surg Forum* 2020; **23**: E860-E862 [PMID: 33234198 DOI: 10.1532/hsf.3267]

10 **Ghincea CV**, Ikeno Y, Weyant MJ, Mitchell JD, Aftab M, Reece TB. Right Thoracoscopic Aberrant Right Subclavian Artery Division and Subclavian-Carotid Transposition. *Ann Thorac Surg* 2020; **110**: e431-e433 [PMID: 32407854 DOI: 10.1016/j.athoracsur.2020.03.106]

World Journal of Clinical Cases

Submit a Manuscript: https://www.f6publishing.com

World J Clin Cases 2023 November 26; 11(33): 8044-8049

DOI: 10.12998/wjcc.v11.i33.8044

ISSN 2307-8960 (online)

CASE REPORT

Granular cell tumor of the breast: A case report and review of literature

Jun Yan

Specialty type: Medicine, research and experimental

Provenance and peer review: Unsolicited article; Externally peer reviewed.

Peer-review model: Single blind

Peer-review report's scientific quality classification

Grade A (Excellent): 0
Grade B (Very good): B, B
Grade C (Good): C
Grade D (Fair): 0
Grade E (Poor): 0

P-Reviewer: Mahmoud MZ, Saudi Arabia; Xu JD, China

Received: August 21, 2023
Peer-review started: August 21, 2023
First decision: August 30, 2023
Revised: September 26, 2023
Accepted: November 13, 2023
Article in press: November 13, 2023
Published online: November 26, 2023

Jun Yan, Department of Breast Surgery, The University of Hong Kong - Shenzhen Hospital, Shenzhen 518000, Guangdong Province, China

Corresponding author: Jun Yan, MD, Doctor, Surgeon, Department of Breast Surgery, The University of Hong Kong - Shenzhen Hospital, No. 1 Haiyuan 1st Road, Futian District, Shenzhen 518000, Guangdong Province, China. yanj@hku-szh.org

Abstract

BACKGROUND

Granular cell tumor (GCT) of the breast (GCTB) is a rare neoplasm that can exhibit malignant characteristics both clinically and radiologically. This tumor can also coexist and colocalize with breast carcinoma.

CASE SUMMARY

We present a patient with this uncommon tumor and discuss the diagnostic and therapeutic approaches in order to further the knowledge of GCTB and prevent misdiagnosis and overtreatment. The characteristics of the tumor, methods of diagnosis, therapy and postoperative pathological outcomes were analyzed, and relevant literatures of GCTs were reviewed. The patient underwent surgery after core needle biopsy, and the excised neoplasm was sent for pathological examination. Histological analysis revealed nests of cells with abundant pink granular cytoplasm, confirming the diagnosis of GCTB.

CONCLUSION

As manifestations of GCT and malignancy can mimic each other, a careful histological examination is essential before major surgery. Treatment consisting of complete excision with close clinical follow-up is recommended.

Key Words: Granular cell tumor; Breast; Neoplasm; Tumor; Literature review; Case report

©The Author(s) 2023. Published by Baishideng Publishing Group Inc. All rights reserved.

Core Tip: Granular cell tumor of the breast is a rare neoplasm that can exhibit malignant characteristics both clinically and radiologically. This tumor can also coexist and colocalize with breast carcinoma. This could result in the potential misdiagnosis of breast carcinoma and overtreatment of patients. We report a patient with this tumor and discuss the methods of diagnosis and treatment. As manifestations of the disease and malignancy can mimic each other, a careful histological examination is essential before major surgery. Complete excision with close clinical follow-up is recommended.

Citation: Yan J. Granular cell tumor of the breast: A case report and review of literature. *World J Clin Cases* 2023; 11(33): 8044-8049
URL: https://www.wjgnet.com/2307-8960/full/v11/i33/8044.htm
DOI: https://dx.doi.org/10.12998/wjcc.v11.i33.8044

INTRODUCTION

Granular cell tumors (GCTs) were first described by Abrikossoff in 1926[1]. These tumors can occur in any part of the body, but are commonly observed in the skin, oral cavity, digestive tract, and subcutaneous tissue. The overall incidence of GCTs in surgical specimens is 0.03%[2]. Breast involvement has been reported in 15% of cases[3]. One to two percent of these lesions can be malignant, with a poor prognosis and few curative options besides surgery[4]. GCT of the breast (GCTB) can mimic breast carcinoma both clinically and radiologically, making it difficult to distinguish from breast malignancies. In order to improve the understanding of GCTB and prevent misdiagnosis and overtreatment, we report a patient with GCTB, who was admitted to our hospital. A brief review of the literature was conducted to further our understanding of this unique disease.

CASE PRESENTATION

Chief complaints

A 57-year-old woman presented in December 2021 with a lump in her left breast, which had been palpable for approximately 4 mo.

History of present illness

The tumor had not significantly increased in size since its discovery.

History of past illness

The patient had previously undergone bilateral breast augmentation surgery.

Personal and family history

The patient had no family history of breast cancer.

Physical examination

Physical examination revealed a spherical, firm, mobile, painless lump measuring approximately 1 cm in diameter and was 5 cm from the nipple in the upper outer quadrant of the left breast. No lymphadenopathy, skin retraction, discharge, thickness or dimpling was observed.

Laboratory examinations

No evident abnormalities were detected.

Imaging examinations

A standard mammogram showed a 13 mm × 12 mm dense poorly circumscribed tumor in the inner upper quadrant of the left breast. No suspicious calcification or enlarged lymph nodes were found. There were no previous mammograms available for comparison. Ultrasonography demonstrated a hypoechoic nodule, measuring approximately 9.8 mm × 10.6 mm × 9.1 mm at the 10-11 o'clock position close to the margin of left breast gland. The nodule was irregular, with a high depth to width ratio, indistinct, no envelope, the internal echo was non-uniform, a mild posterior shadow was seen without significant peripheral vascularization. No evidence of distant metastasis was found. Magnetic resonance imaging (MRI) revealed a heterogeneous enhanced round mass with a spiculated microlobulated indistinct margin, measuring 9 mm × 8 mm × 9 mm in the left breast at the 10 o'clock position, with a slightly higher signal intensity than adjacent glandular tissue in T1 and T2-weighted sequences. Following contrast administration, heterogeneous enhancement was observed with a slow initial increase in signal intensity followed by a plateau. There were no indications of implant rupture (Figure 1).

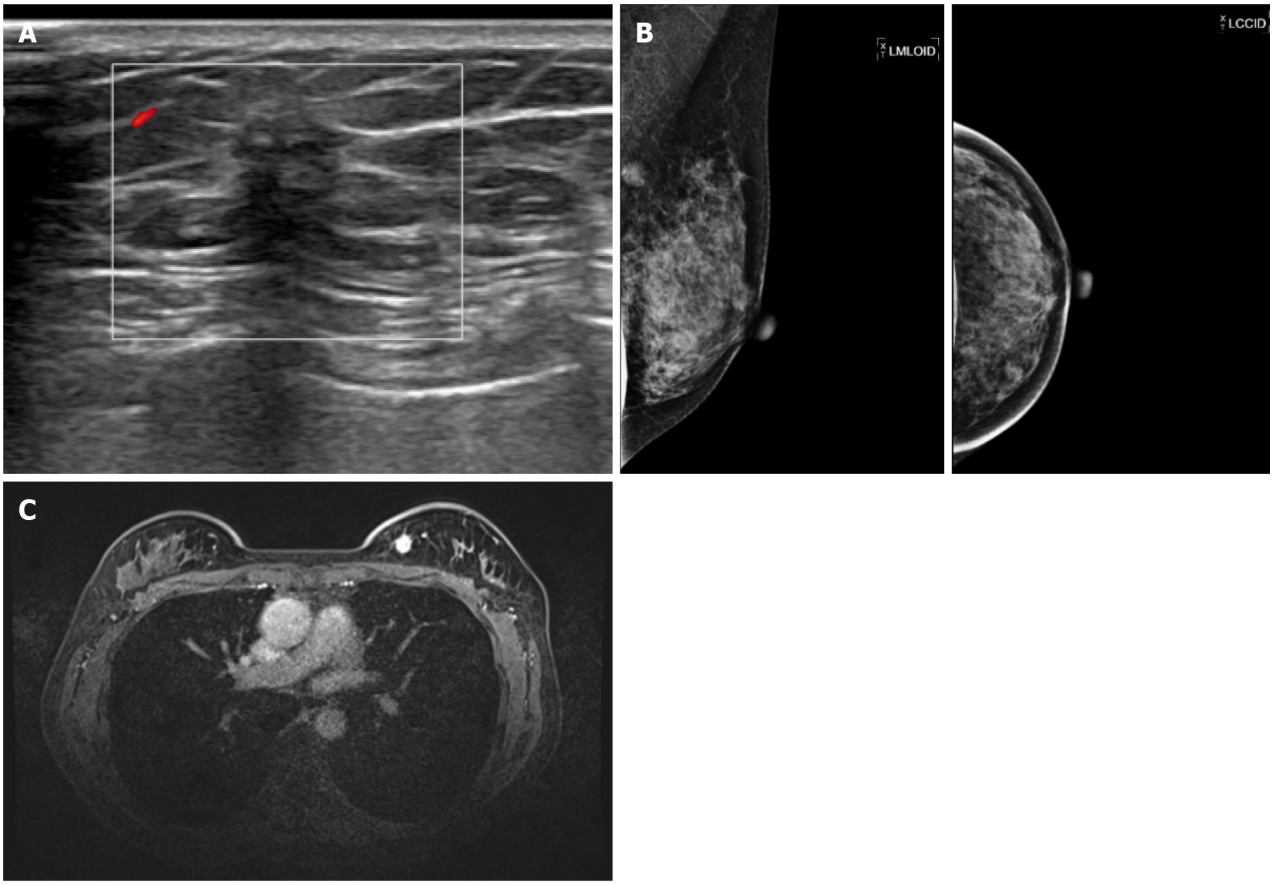

DOI: 10.12998/wjcc.v11.i33.8044 **Copyright** ©The Author(s) 2023.

Figure 1 Imaging photos. A: Sonography demonstrated a hypoechoic nodule, measuring about 9.8 mm × 10.6 mm × 9.1 mm at the 10-11 o'clock position close to the margin of left breast gland; B: Mammogram showed a 13 mm × 12 mm dense poor-circumscribed mass in inner upper quadrant of the left breast; C: Magnetic resonance imaging revealed a heterogeneous enhancing round-shaped mass with an spiculated microlobulated indistinct margin, measured 9 mm × 8 mm × 9 mm, located at 10 o'clock position of left breast.

FINAL DIAGNOSIS

Given the suspicion of breast malignancy, core needle biopsy was performed. Histologic assessment indicated a GCTB.

TREATMENT

The patient underwent wide local excision of the tumor.

OUTCOME AND FOLLOW-UP

The tumor was identified as a GCT on the basis of its histological characteristics. Six months after surgery, the patient is still doing well.

DISCUSSION

GCTs were first described by Abrikossoff in 1926[1]. These tumors can occur in any part of the body. The overall incidence of GCTs in surgical specimens is 0.03%[2]. Breast involvement is observed in 15% of cases[3]. GCTs can occur in all age groups and genders; however, in general, GCTs are almost twice as common in women as in men, predominantly affecting patients in their fourth to sixth decades[2-4]. With a poor prognosis and few curative options besides surgery, one to two percent of these lesions may be cancerous[5]. GCTB mainly occurs in females similar to breast malignancies, but has also been reported in the male population, accounting for 6.6% of all GCTB cases[6]. GCTB frequently resembles malignant neoplasms both clinically and radiologically, making it challenging to distinguish from breast cancers.

Previously, most cases of GCTB were symptomatic; however, with improved breast screening, more asymptomatic cases are being detected. Though some patients have experienced discomfort, pruritis, skin retraction, thickness or dimpling, and reactive lymphadenopathy at presentation, the majority of these tumors are painless, smooth, slow-growing solitary nodules. They can also be multicentric, and even coexist and colocalize with breast carcinoma[1,7]. Therefore, GCTB is difficult to distinguish from carcinoma clinically.

Radiological findings of GCT can be nonspecific in the breast, and are often indistinguishable from those of breast malignancies. They can be small, round, well-circumscribed masses, but also present as indistinct, stellate, sometimes combined with hypodense rims, spiculated with or without calcifications, and skin thickening, associated with the pectoralis on mammography[8].

These tumors on ultrasound are frequently heterogeneous, solid, and poorly defined masses with a posterior shadow and a high depth to width ratio, which often denotes malignancy. Similar to mammography, GCTB on ultrasound has a wide range of properties[9]. The appearance of GCTB on MRI is variable. Benign characteristics such as gradual augmentation, high end intensity, and equal or low signal on T1 and T2 weighted sequences may be present. In addition, malignant features such as fast enhancement, rim enhancement, washout phenomenon, irregular and indistinct lesions may also be observed[10,11]. MRI may be useful in delineating the extent of disease, the presence of aggressive features and contralateral screening; however, no specific features of GCTB have been outlined and GCTB can closely resemble primary breast malignancies[12,13].

To date, only one study has investigated the positron emission tomography/computed tomography features of GCTB. In this case, no evidence of focally enhanced tracer accumulation was revealed. The lesion displayed an average standardized uptake value of 1.8 indicating a benign lesion. Pathological investigation identified this tumor as GCT which infiltrated the subcutaneous and muscular tissue with no mitotic activity. Given the high sensitivity and specificity of positron emission tomography/computed tomography for malignant masses, further study and health economics evaluation are required[12]. Although GCTB are mostly benign, a conclusive pathological diagnosis is essential before surgery to avoid unnecessary radical treatment. Ultrasound guided percutaneous core biopsy of the tumor is well established as the diagnostic procedure for suspicious lesions. While fine needle aspiration cytology smear interpretation has diagnostic challenges including delicate cell membrane and cytoplasm, and insufficient material for immunohistochemical procedures, core biopsy is able to provide specimens that retain their native intracellular architecture to facilitate specific histological diagnosis[14,15]. Pre-operative histological confirmation with core biopsy may contribute to avoiding mastectomy and axillary dissection[16].

Despite the fact that GCTs are often benign, 1%-2% of these lesions can be malignant[5]. Fanburg-Smith *et al*[17] outlined six features including necrosis, increased mitotic count (greater than 2 per 10 high power fields), spindle tumor cells, nuclear pleomorphism, prominent nucleoli, vesicular nuclei, and a high nuclear to cytoplasmic ratio in 1998. If three of these six features are present this is indicative of malignancy, and is atypical if only two features are seen.

It was previously widely accepted that GCTs were derived from Schwann cells of the peripheral nervous system due to the presence S-100 protein[18]. Additionally, GCTs also stained positive for CD68, neuron-specific enolase, vimentin, CD57, CD56, SOX-10 and inhibin[1,19,20]. However, a subset of S100-negative "non-neural" GCTs has been identified[21-25]. The histogenesis of GCT is still debatable at this time.

Complete excision with negative margins and close clinical follow-up is the gold standard treatment strategy for GCTB. Axillary lymph node evaluation, including sentinel lymph node biopsy and lymph node dissection, is only indicated for malignant GCTB[6]. Since the approval of pazopanib for advanced soft tissue sarcomas and metastatic soft tissue sarcomas in the phase III trial, several patients with malignant GCTs have demonstrated a response following treatment with this drug. Establishing the mechanism of action responsible for the disease response *via* limited instances is challenging due to the overexpression of multiple genes by the tumor and various targets of medicines. Clinical trials and appropriate cell lines or mouse models are essential to ascertain the exact mode of action responsible for the tumor response[26-30]. Given the absence of randomized clinical trials on this particular lesion, it is currently believed that there is a limited role for adjuvant therapy, and there is no current standard chemotherapy regimen and radiation therapy for this specific tumor[1].

The prognosis of benign GCT is excellent. However, patients with malignant GCT have a poor prognosis. Malignant GCT has an overall cause-specific survival rate of 74.3% after 5 years and 65.2% after 10 years, respectively. Patients with tumors larger than 5 cm had a worse chance of survival (90.0% *vs* 51.3%, respectively; $P = 0.02$) than patients with tumors smaller than 5 cm. The prognosis was much worse for those who had regional or distant metastases at the time of diagnosis[31].

In this report, we describe a rare breast neoplasm that was radiologically indicative of a malignant tumor but was later determined to be a benign GCTB following extensive local excision. Complete imaging analysis and biopsies could be of significant assistance in making the diagnosis and avoiding invasive procedures. Following a review of the literature, clinical trials and gene research are still required for a deeper knowledge of this rare condition.

CONCLUSION

GCTB is a rare disease and can often resemble breast cancer. In the present case, the patient had imaging characteristics of a malignant tumor; however, histologic analysis revealed that the lesion was benign. A thorough imaging evaluation and core needle biopsy are necessary prior to major surgery. Complete excision with negative margins and close clinical follow-up is currently the gold standard treatment strategy for GCTB. Clinical trials and objective molecular data before treatment initiation are needed for deeper knowledge of malignant GCT and the development of effective treatment.

FOOTNOTES

Author contributions: Yan J performed this research, reviewed the articles and wrote the manuscript.

Informed consent statement: The patient provided informed written consent prior to study enrollment.

Conflict-of-interest statement: The author reported no relevant conflicts of interest for this article.

CARE Checklist (2016) statement: The authors have read the CARE Checklist (2016), and the manuscript was prepared and revised according to the CARE Checklist (2016).

Open-Access: This article is an open-access article that was selected by an in-house editor and fully peer-reviewed by external reviewers. It is distributed in accordance with the Creative Commons Attribution NonCommercial (CC BY-NC 4.0) license, which permits others to distribute, remix, adapt, build upon this work non-commercially, and license their derivative works on different terms, provided the original work is properly cited and the use is non-commercial. See: https://creativecommons.org/Licenses/by-nc/4.0/

Country/Territory of origin: China

ORCID number: Jun Yan 0009-0009-4392-5832.

S-Editor: Wang JJ
L-Editor: A
P-Editor: Zhao S

REFERENCES

1 **Neelon D**, Lannan F, Childs J. Granular Cell Tumor. 2023 Jul 3. In: StatPearls [Internet]. Treasure Island (FL): StatPearls Publishing; 2023 Jan- [PMID: 33085297]
2 **Lack EE**, Worsham GF, Callihan MD, Crawford BE, Klappenbach S, Rowden G, Chun B. Granular cell tumor: a clinicopathologic study of 110 patients. *J Surg Oncol* 1980; **13**: 301-316 [PMID: 6246310 DOI: 10.1002/jso.2930130405]
3 **Becelli R**, Perugini M, Gasparini G, Cassoni A, Fabiani F. Abrikossoff's tumor. *J Craniofac Surg* 2001; **12**: 78-81 [PMID: 11314193 DOI: 10.1097/00001665-200101000-00013]
4 **Mirza FN**, Tuggle CT, Zogg CK, Mirza HN, Narayan D. Epidemiology of malignant cutaneous granular cell tumors: A US population-based cohort analysis using the Surveillance, Epidemiology, and End Results (SEER) database. *J Am Acad Dermatol* 2018; **78**: 490-497.e1 [PMID: 28989104 DOI: 10.1016/j.jaad.2017.09.062]
5 **Rose B**, Tamvakopoulos GS, Yeung E, Pollock R, Skinner J, Briggs T, Cannon S. Granular cell tumours: a rare entity in the musculoskeletal system. *Sarcoma* 2009; **2009**: 765927 [PMID: 20169099 DOI: 10.1155/2009/765927]
6 **Brown AC**, Audisio RA, Regitnig P. Granular cell tumour of the breast. *Surg Oncol* 2011; **20**: 97-105 [PMID: 20074934 DOI: 10.1016/j.suronc.2009.12.001]
7 **Al-Ahmadie H**, Hasselgren PO, Yassin R, Mutema G. Colocalized granular cell tumor and infiltrating ductal carcinoma of the breast. *Arch Pathol Lab Med* 2002; **126**: 731-733 [PMID: 12033967 DOI: 10.5858/2002-126-0731-CGCTAI]
8 **Leo C**, Briest S, Pilch H, Schütz A, Horn LC, Leinung S. Granular cell tumor of the breast mimicking breast cancer. *Eur J Obstet Gynecol Reprod Biol* 2006; **127**: 268-270 [PMID: 16849031 DOI: 10.1016/j.ejogrb.2006.01.026]
9 **Irshad A**, Pope TL, Ackerman SJ, Panzegrau B. Characterization of sonographic and mammographic features of granular cell tumors of the breast and estimation of their incidence. *J Ultrasound Med* 2008; **27**: 467-475 [PMID: 18314525 DOI: 10.7863/jum.2008.27.3.467]
10 **Iglesias A**, Arias M, Santiago P, Rodríguez M, Mañas J, Saborido C. Benign breast lesions that simulate malignancy: magnetic resonance imaging with radiologic-pathologic correlation. *Curr Probl Diagn Radiol* 2007; **36**: 66-82 [PMID: 17331838 DOI: 10.1067/j.cpradiol.2006.12.001]
11 **Scaranelo AM**, Bukhanov K, Crystal P, Mulligan AM, O'Malley FP. Granular cell tumour of the breast: MRI findings and review of the literature. *Br J Radiol* 2007; **80**: 970-974 [PMID: 17940129 DOI: 10.1259/bjr/95130566]
12 **Hoess C**, Freitag K, Kolben M, Allgayer B, Laemmer-Skarke I, Nathrath WB, Avril N, Roemer W, Schwaiger M, Graeff H. FDG PET evaluation of granular cell tumor of the breast. *J Nucl Med* 1998; **39**: 1398-1401 [PMID: 9708516]
13 **Patel A**, Lefemine V, Yousuf SM, Abou-Samra W. Granular cell tumour of the pectoral muscle mimicking breast cancer. *Cases J* 2008; **1**: 142 [PMID: 18775077 DOI: 10.1186/1757-1626-1-142]
14 **Pieterse AS**, Mahar A, Orell S. Granular cell tumour: a pitfall in FNA cytology of breast lesions. *Pathology* 2004; **36**: 58-62 [PMID: 14757558 DOI: 10.1080/00313020310001646640]
15 **Miller JA**, Karcnik TJ, Karimi S. Granular cell tumor of the breast: definitive diagnosis by sonographically guided percutaneous biopsy. *J Clin Ultrasound* 2000; **28**: 89-93 [PMID: 10641006 DOI: 10.1002/(sici)1097-0096(200002)28:2<89::aid-jcu6>3.0.co;2-n]
16 **Ohnishi H**, Nishihara K, Tamae K, Mitsuyama S, Abe R, Toyoshima S, Abe E. Granular cell tumors of the breast: a report of two cases. *Surg Today* 1996; **26**: 929-932 [PMID: 8931228 DOI: 10.1007/BF00311799]
17 **Fanburg-Smith JC**, Meis-Kindblom JM, Fante R, Kindblom LG. Malignant granular cell tumor of soft tissue: diagnostic criteria and clinicopathologic correlation. *Am J Surg Pathol* 1998; **22**: 779-794 [PMID: 9669341 DOI: 10.1097/00000478-199807000-00001]
18 **Kurtin PJ**, Bonin DM. Immunohistochemical demonstration of the lysosome-associated glycoprotein CD68 (KP-1) in granular cell tumors and schwannomas. *Hum Pathol* 1994; **25**: 1172-1178 [PMID: 7959661 DOI: 10.1016/0046-8177(94)90033-7]
19 **Maiorano E**, Favia G, Napoli A, Resta L, Ricco R, Viale G, Altini M. Cellular heterogeneity of granular cell tumours: a clue to their nature? *J Oral Pathol Med* 2000; **29**: 284-290 [PMID: 10890560 DOI: 10.1034/j.1600-0714.2000.290608.x]

20 **An S**, Jang J, Min K, Kim MS, Park H, Park YS, Kim J, Lee JH, Song HJ, Kim KJ, Yu E, Hong SM. Granular cell tumor of the gastrointestinal tract: histologic and immunohistochemical analysis of 98 cases. *Hum Pathol* 2015; **46**: 813-819 [PMID: 25882927 DOI: 10.1016/j.humpath.2015.02.005]

21 **Lazar AJ**, Fletcher CD. Primitive nonneural granular cell tumors of skin: clinicopathologic analysis of 13 cases. *Am J Surg Pathol* 2005; **29**: 927-934 [PMID: 15958858 DOI: 10.1097/01.pas.0000157294.55796.d3]

22 **Shen Z**, Yao L, Jiang H, Li M, Tang Y. Clinicopathological and immunohistochemical analysis of maxillofacial granular cell tumor. *Hua Xi Kou Qiang Yi Xue Za Zhi* 2023; **41**: 414-420 [PMID: 37474473 DOI: 10.7518/hxkq.2023.2023035]

23 **El Ochi MR**, Essaoudi A, Allaoui M, Abrid JE, Touri S, Moussaoui N, El Ktaibi A, Damiri A, Chahdi H, Oukabli M. Dermal nonneural granular cell tumor: a case report. *J Surg Case Rep* 2022; **2022**: rjac317 [PMID: 35794991 DOI: 10.1093/jscr/rjac317]

24 **Solomon LW**, Velez I. S-100 Negative Granular Cell Tumor of the Oral Cavity. *Head Neck Pathol* 2016; **10**: 367-373 [PMID: 26643916 DOI: 10.1007/s12105-015-0673-6]

25 **Kim BG**, Song JY, Zo S, Im Y, Choi S, Han J, Jeong BH, Kim H. S-100-Negative malignant pulmonary granular cell tumor: A case report. *Respir Med Case Rep* 2020; **29**: 101002 [PMID: 32015959 DOI: 10.1016/j.rmcr.2020.101002]

26 **van der Graaf WT**, Blay JY, Chawla SP, Kim DW, Bui-Nguyen B, Casali PG, Schöffski P, Aglietta M, Staddon AP, Beppu Y, Le Cesne A, Gelderblom H, Judson IR, Araki N, Ouali M, Marreaud S, Hodge R, Dewji MR, Coens C, Demetri GD, Fletcher CD, Dei Tos AP, Hohenberger P; EORTC Soft Tissue and Bone Sarcoma Group; PALETTE study group. Pazopanib for metastatic soft-tissue sarcoma (PALETTE): a randomised, double-blind, placebo-controlled phase 3 trial. *Lancet* 2012; **379**: 1879-1886 [PMID: 22595799 DOI: 10.1016/S0140-6736(12)60651-5]

27 **Morita S**, Hiramatsu M, Sugishita M, Gyawali B, Shibata T, Shimokata T, Urakawa H, Mitsuma A, Moritani S, Kubota T, Ichihara S, Ando Y. Pazopanib monotherapy in a patient with a malignant granular cell tumor originating from the right orbit: A case report. *Oncol Lett* 2015; **10**: 972-974 [PMID: 26622607 DOI: 10.3892/ol.2015.3263]

28 **Katiyar V**, Vohra I, Uprety A, Yin W, Gupta S. Recurrent Unresectable Malignant Granular Cell Tumor With Response to Pazopanib. *Cureus* 2020; **12**: e8287 [PMID: 32601562 DOI: 10.7759/cureus.8287]

29 **Conley AP**, Koplin S, Caracciollo JT, Reed DR, Webber NP, Attia S. Dramatic response to pazopanib in a patient with metastatic malignant granular cell tumor. *J Clin Oncol* 2014; **32**: e107-e110 [PMID: 24550417 DOI: 10.1200/JCO.2012.47.1078]

30 **Wei L**, Liu S, Conroy J, Wang J, Papanicolau-Sengos A, Glenn ST, Murakami M, Liu L, Hu Q, Miles KM, Nowak DE, Liu B, Qin M, Bshara W, Omilian AR, Head K, Bianchi M, Burgher B, Darlak C, Kane J, Merzianu M, Cheney R, Fabiano A, Salerno K, Talati C, Khushalani NI, Trump DL, Johnson CS, Morrison CD. Whole-genome sequencing of a malignant granular cell tumor with metabolic response to pazopanib. *Cold Spring Harb Mol Case Stud* 2015; **1**: a000380 [PMID: 27148567 DOI: 10.1101/mcs.a000380]

31 **Moten AS**, Zhao H, Wu H, Farma JM. Malignant granular cell tumor: Clinical features and long-term survival. *J Surg Oncol* 2018; **118**: 891-897 [PMID: 30196562 DOI: 10.1002/jso.25227]

World Journal of Clinical Cases

Submit a Manuscript: https://www.f6publishing.com

World J Clin Cases 2023 November 26; 11(33): 8050-8057

DOI: 10.12998/wjcc.v11.i33.8050

ISSN 2307-8960 (online)

CASE REPORT

Fibula allograft transplantation combined with locking plate for treatment of recurrent monostotic fibular fibrous dysplasia: A case report

Lun-Li Xie, Xiao Yuan, Hong-Xia Zhu, Lei Fu, Dan Pu

Specialty type: Medicine, research and experimental

Provenance and peer review: Unsolicited article; Externally peer reviewed.

Peer-review model: Single blind

Peer-review report's scientific quality classification

Grade A (Excellent): 0
Grade B (Very good): B
Grade C (Good): 0
Grade D (Fair): 0
Grade E (Poor): 0

P-Reviewer: Hoveidaei AH, Iran

Received: August 25, 2023
Peer-review started: August 25, 2023
First decision: October 10, 2023
Revised: October 11, 2023
Accepted: November 14, 2023
Article in press: November 14, 2023
Published online: November 26, 2023

Lun-Li Xie, Xiao Yuan, Lei Fu, Department of Joint and Hand Orthopedics, Hunan University of Medicine General Hospital, Huaihua 418000, Hunan Province, China

Hong-Xia Zhu, Department of Traumatic Orthopedics, Hunan University of Medicine General Hospital, Huaihua 418000, Hunan Province, China

Dan Pu, Department of Orthopedics, Hunan University of Medicine General Hospital, Huaihua 418000, Hunan Province, China

Corresponding author: Lun-Li Xie, MD, Attending Doctor, Doctor, Department of Joint and Hand Orthopedics, Hunan University of Medicine General Hospital, No. 144 Jinxi South Road, Huaihua 418000, Hunan Province, China. xielunli@163.com

Abstract

BACKGROUND

Fibrous dysplasia is a congenital disorder in which normal bone is replaced by fibro-osseous tissue or irregular trabeculae of woven bone intermixed with mature collagenous tissue. A single or multiple bones are affected. This rare bone disorder has three clinical patterns including monostotic, polyostotic, and that associated with McCune–Albright syndrome. Most studies report primary fibrous dysplasia. However, a few cases of recurrent monostotic fibular fibrous dysplasia have been reported. Here, we report a therapeutic strategy for recurrent fibular fibrous dysplasia.

CASE SUMMARY

A 4-year-old boy was admitted for persistent pain in the left lower limb and abnormal gait over the previous 9 mo. He had no history of present or past illness. Preoperative imaging data showed erosion-like changes with bone expansion of the left middle and lower fibular segment. Tumor tissue in the fibular bone marrow cavity was removed by curettage, and rapid intraoperative pathological examination suggested fibular fibrous dysplasia. An allograft was implanted into the fibular medullary cavity. However, he was readmitted with clinical symptoms including persistent pain, abnormal gait, and local swelling at the age of 6 years. He was diagnosed with recurrent fibular fibrous dysplasia based on the second medical examination. He underwent fibular bone tumor radical resection and longus fibular allograft transplantation combined with fibular bone locking plate

and screws. Good host bone to allogenic bone graft fusion was observed by the physician on postoperative regular follow-up.

CONCLUSION
Radical resection of fibrous dysplasia and longus fibula allograft combined with internal fixation for reconstruction are suitable for the treatment of recurrent monostotic fibular fibrous dysplasia.

Key Words: Recurrent fibrous dysplasia; Longus fibula allograft; Bone fusion; Case report

©The Author(s) 2023. Published by Baishideng Publishing Group Inc. All rights reserved.

Core Tip: The incidence of recurrent monostotic fibular fibrous dysplasia is low. For recurrent fibrous dysplasia, radical resection combined with allograft bone for biodynamic reconstruction is a suitable therapy. We report a case of recurrent fibrous dysplasia in the left fibular bone treated by longus fibula allograft transplantation combined with fibula bone locking plate and screws.

Citation: Xie LL, Yuan X, Zhu HX, Fu L, Pu D. Fibula allograft transplantation combined with locking plate for treatment of recurrent monostotic fibular fibrous dysplasia: A case report. *World J Clin Cases* 2023; 11(33): 8050-8057
URL: https://www.wjgnet.com/2307-8960/full/v11/i33/8050.htm
DOI: https://dx.doi.org/10.12998/wjcc.v11.i33.8050

INTRODUCTION

As a benign fibrous-osseous lesion, fibrous dysplasia was first reported by Lichtenstein and Jaffe[1] in 1947. Usually, fibrous dysplasia is characterized by bone developmental failure due to abnormal bone proliferation, including fibro-osseous tissue, irregular trabeculae of woven bone, and mature collagenous tissue. Some symptoms such as pain, deformity, claudication, and pathological fractures are caused by insufficient mineralization with substantial loss of mechanical strength[2]. One or several bones can be affected by fibrous dysplasia. *GNAS* gene mutations have been shown to participate in the pathogenesis of fibrous dysplasia and have been confirmed to have diagnostic significance[3]. Some authors have reported recurrent monostotic fibrous dysplasia in the mandible, and suggested that conservative surgery may not be suitable for the treatment of this lesion[4]. A few cases of recurrent monostotic fibular fibrous dysplasia have been reported. Here, we present a case of recurrent monostotic fibular fibrous dysplasia, which was studied by imaging, and the pathological results. Radical surgery and longus fibula allograft combined with fibula bone locking plate and screws were performed to improve the patient's contour and function.

CASE PRESENTATION

Chief complaints
A 4-year-old boy was admitted because of persistent lower limb pain and claudication in the left lower limb over the past 9 mo.

History of present illness
The patient had mild persistent lower limb pain and claudication without any inducement. Claudication worsened in one day. The child had no fever, urinary frequency or urgency, numbness, fatigue, or lameness. For further assessment and treatment, he was admitted to our joint hand surgery department.

History of past illness
The child had no history past illness.

Personal and family history
The child had no history of family illness, and his medical history was unremarkable.

Physical examination
Pressing pain and local swelling were present in the left shank. The results of sensation and strengthening test, and tendon reflex test were normal in both lower limbs. No pathological signs were observed upon physical examination.

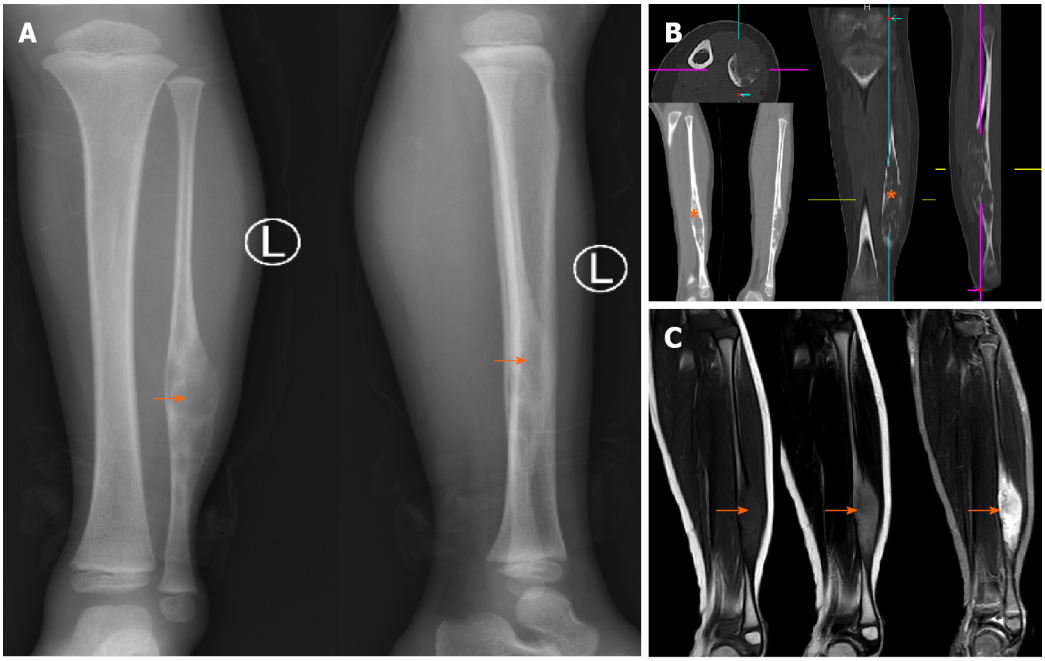

DOI: 10.12998/wjcc.v11.i33.8050 **Copyright** ©The Author(s) 2023.

Figure 1 Preoperative radiographic images of fibular fibrous dysplasia. A: Preoperative anteroposterior and lateral X-ray showed ground-glass appearance and partial radiolucent lesions with clear borders around soft tissue (arrows); B: Preoperative computed tomography showed erosion-like changes and cystic appearance without extraosseous soft tissue mass destruction (asterisks); C: Preoperative magnetic resonance imaging (MRI). T1-weighted, T2-weighted, and fat-suppressed MRI of the left fibular bone showed low to intermediate signals on T1 and T2-weighted images and high signals on fat-suppressed image (arrows).

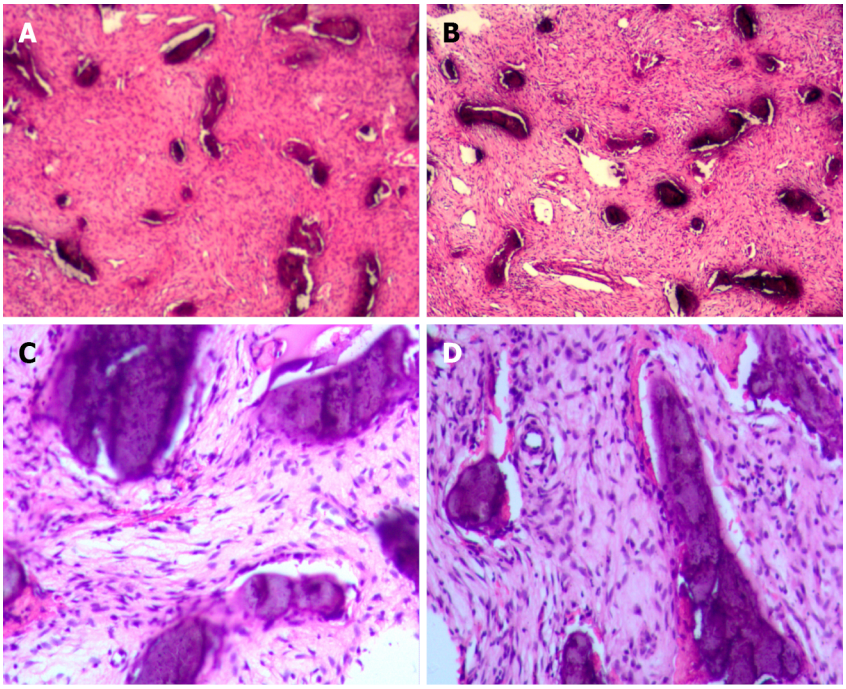

DOI: 10.12998/wjcc.v11.i33.8050 **Copyright** ©The Author(s) 2023.

Figure 2 First results of intraoperative and postoperative pathological examination. A and B: Hematoxylin and eosin staining (magnification 40 ×). Intraoperative rapid pathological examination showed typical appearance of fibrous dysplasia. The lesion contained some irregular immature bone trabeculae scattered within fibrous tissue; C and D: Postoperative regular pathological examination showed the same appearance of irregular trabecular bone and hyperplastic fibrous tissue with woven bone formation.

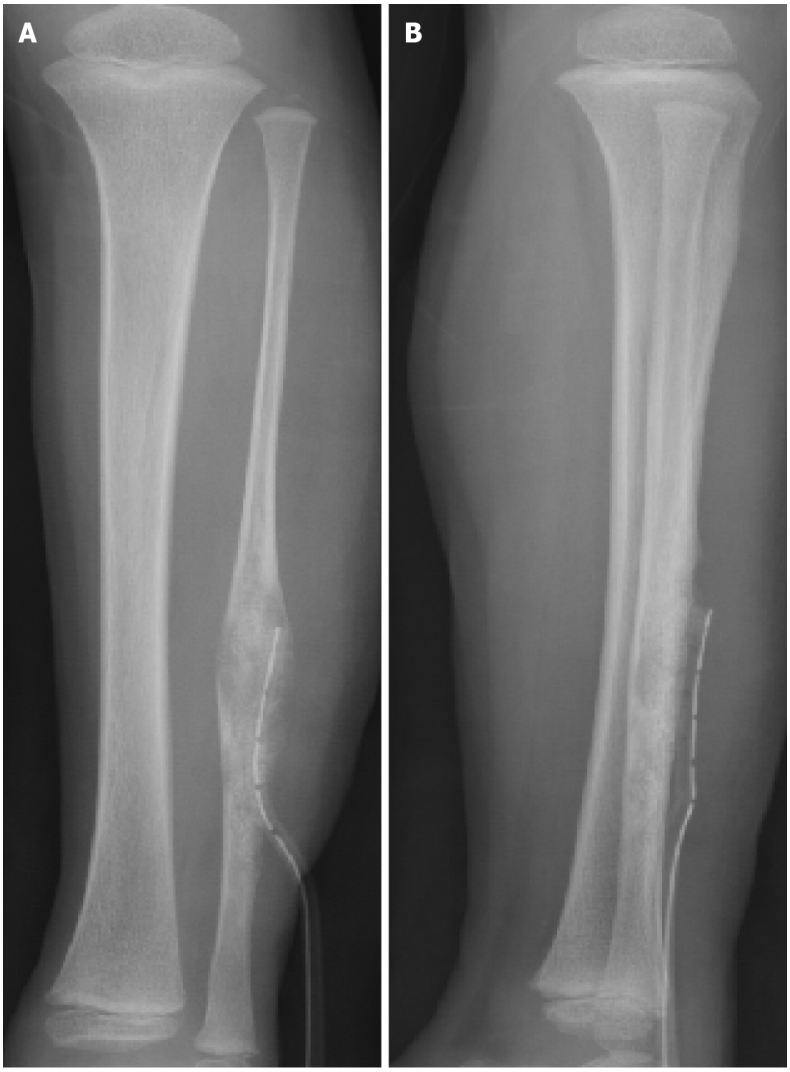

DOI: 10.12998/wjcc.v11.i33.8050 **Copyright** ©The Author(s) 2023.

Figure 3 First postoperative X-ray images of fibular fibrous dysplasia. A and B: Postoperative anteroposterior and lateral X-ray showed a radiographically apparent allogeneic bone refilling of ground-glass and partial radiolucent sites in X-ray images compared to preoperative X-ray images as showed in Figure 1A.

Laboratory examinations

Laboratory examinations were normal.

Imaging examinations

Preoperative imaging examinations, including X-ray photography, computed tomography, and magnetic resonance imaging, showed erosion-like changes with bone expansion of the left middle and lower fibular segment (Figure 1). No invasion of circumferential soft tissue or pathological fracture of the lesion site was observed. Initial pathological examination revealed fibular fibrous dysplasia (Figure 2). Postoperative photography showed that an allograft bone was implanted into the fibular medullary cavity (Figure 3). Recurrent fibular fibrous dysplasia was observed at the age of 6 years (Figure 4).

FINAL DIAGNOSIS

The second postoperative pathological examination also revealed recurrent fibular fiber dysplasia (Figure 5). The patient was diagnosed with recurrent fibular fibrous dysplasia based on the medical history, physical examination, laboratory and pathological results, and imaging findings.

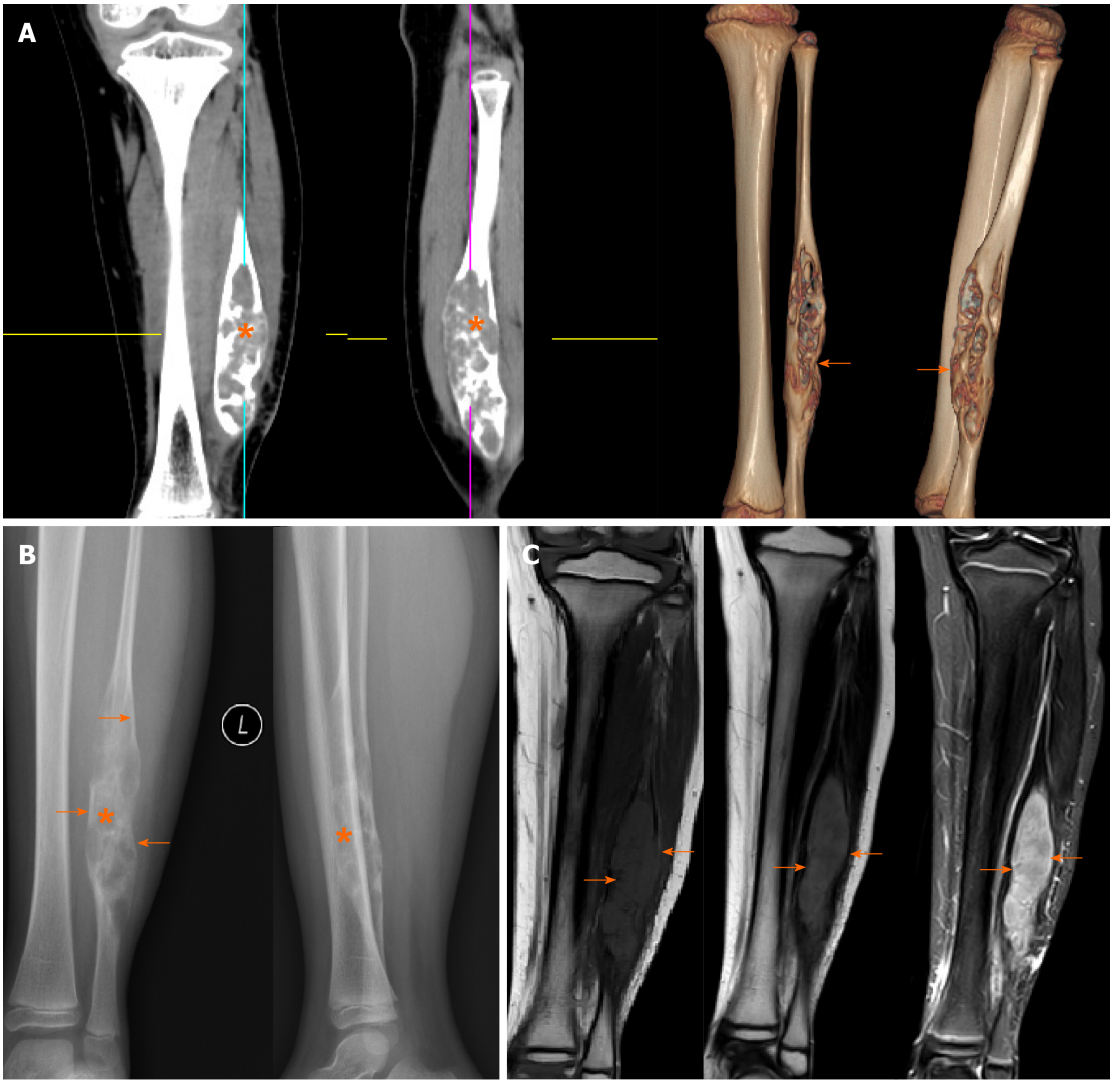

DOI: 10.12998/wjcc.v11.i33.8050 **Copyright** ©The Author(s) 2023.

Figure 4 Preoperative radiographic images of recurrent fibular fibrous dysplasia. A: Preoperative computed tomography showed expanded lesions with a shell (asterisks), and small perforations with erosion-like changes (arrows); B: Preoperative anteroposterior and lateral X-ray also showed ground-glass appearance (asterisks) and sclerotic borders and expanded lesions with well-circumscribed margins (arrows); C: Preoperative magnetic resonance imaging (MRI). T1-weighted, T2-weighted, and fat-suppressed MRI of the left fibular bone showed low to intermediate signals on T1 and T2-weighted images and high signals on fat-suppressed image, and well-circumscribed margins without extraosseous soft tissue mass destruction were observed (arrows).

TREATMENT

Treatment strategies were based on multidisciplinary expert consultation and professional discussion of the case data, including clinical symptoms and signs, and imaging and pathological findings. After communication with his guardian, the patient underwent fibular bone tumor resection and longus fibular allograft combined with fibula bone locking plate for treatment of recurrent fibular fibrous dysplasia. A left straight lateral incision was made to expose the site of the fibular bone tumor. All fibular bone tumor tissue was completely excised. Radical resection of the lesion from outside the periosteum to the normal bone and soft tissue was performed. The surgeon soaked the incision with sterilized water for 10 min. A longus fibular allograft bone combined with fibula bone locking plate and screws was used for reconstruction of the left fibula under the guidance of C-arm X-ray (Figure 6). The patient was encouraged to complete postoperative functional exercises in bed. Postoperative routine pathological examination revealed fibular fibrous dysplasia (Figure 5). After 3 mo, he was gradually mobilized and achieved complete weight bearing without crutches after X-ray examination and senior physician assessment. According to postoperative imaging and senior physician assessment, strong autogenous fibular bone fused to allogenic fibular bone was observed, and the internal fixation was removed after 1 year (Figure 6).

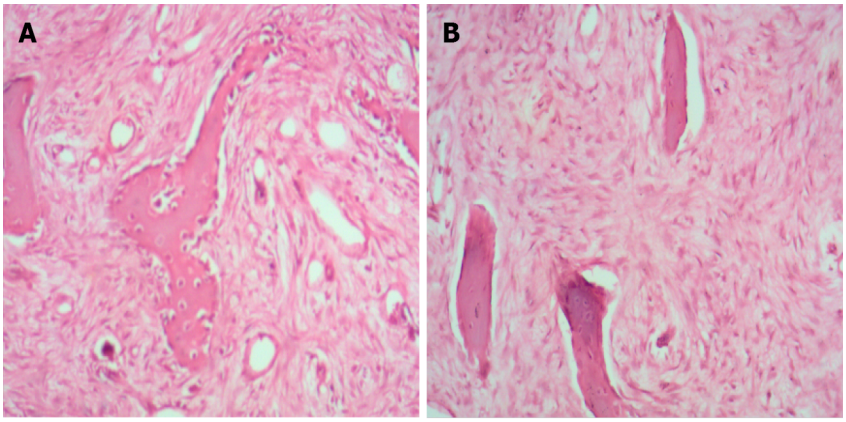

DOI: 10.12998/wjcc.v11.i33.8050 **Copyright** ©The Author(s) 2023.

Figure 5 Postoperative pathological examination of recurrent fibular fibrous dysplasia. A and B: Hematoxylin and eosin staining (magnification 40 ×). Areas of fibrous dysplasia and curvilinear trabeculae of metaplastic woven bone in hypocellular fibroblastic stroma were observed.

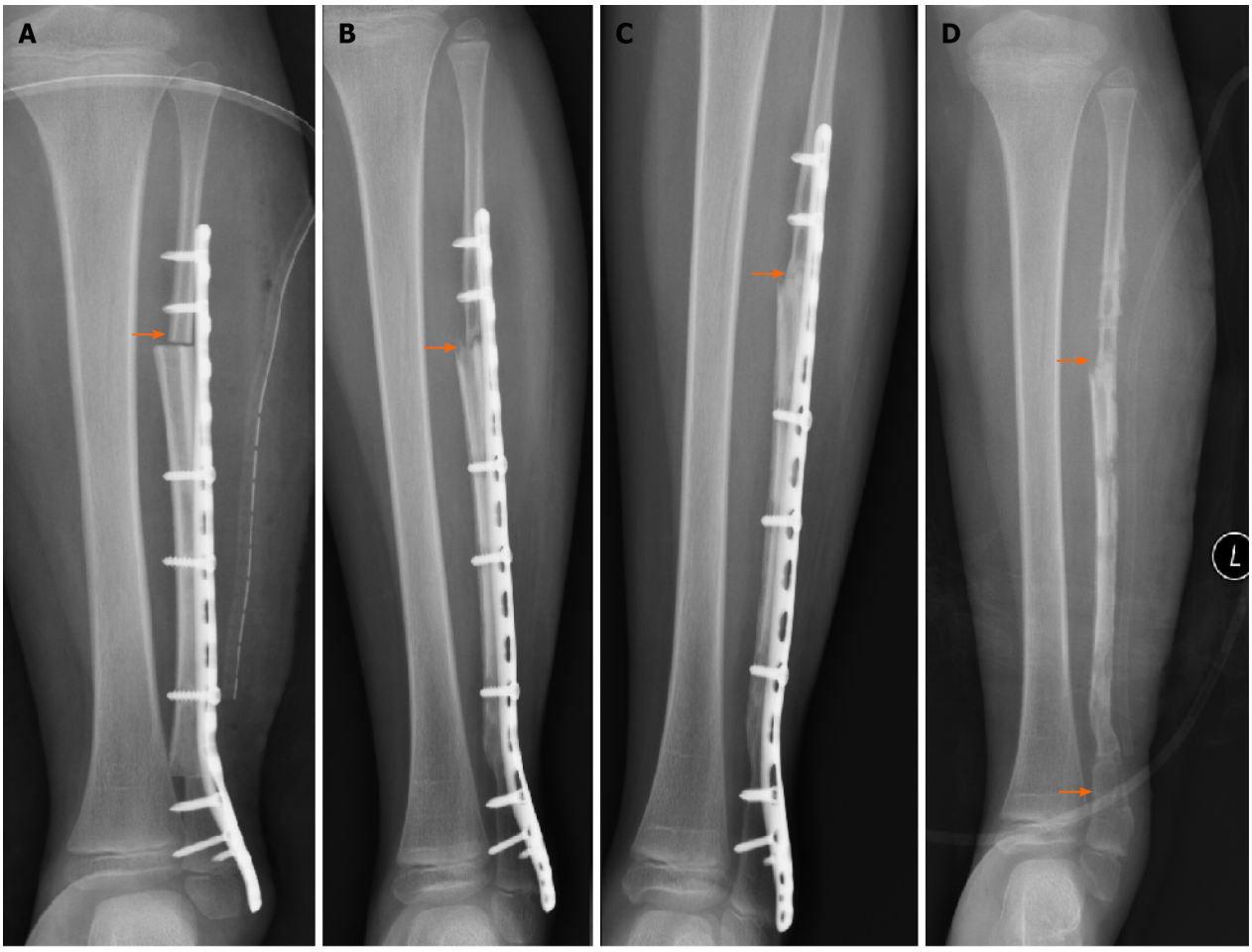

DOI: 10.12998/wjcc.v11.i33.8050 **Copyright** ©The Author(s) 2023.

Figure 6 Postoperative radiographic images of recurrent fibular fibrous dysplasia. A: Preoperative anteroposterior showed that longus fibula allograft transplantation combined with fibular bone locking plate and screws was performed for reconstruction. Clear boundaries are shown by X-ray at the proximal fibular lesion (arrow); B: Bony callus of autogenous fibular bone and allogenic fibular bone were found by X-ray of the proximal fibular lesion at 6 mo postoperatively (arrow); C: Fusion of strong autogenous fibular bone with allogenic fibular bone was found by X-ray after 1 year postoperatively (arrow); D: Fibular locking plate and screws were removed surgically after 1 year, and X-ray showed ideal bone fusion of proximal and distal fibular lesions (arrows).

OUTCOME AND FOLLOW-UP

During postoperative regular follow-up, strong autogenous fibular bone fused to allogenic fibular bone was observed (Figure 6). No clinical symptoms or signs were observed based on questionnaire survey and visual analog scale.

DISCUSSION

We report a method of treatment for recurrent fibrous dysplasia of the left fibula. As a rare benign bone disease, fibrous dysplasia presents with abnormal arrest in the woven bone stage during bone maturation, including a monostotic or polyostotic distribution[2]. Previous studies have shown that fibroblastic proliferation replaces normal bone matrix, which leads to irregular trabeculae of partially calcified osteoid[5,6]. Some studies have suggested that fibrous dysplasia has age-related self-limiting characteristics and rare malignant transformation, attributed to the number of mutant cells often decreasing with age[7]. Other studies have found that adequate treatment may lead to a favorable prognosis because of local pain and/or fatigue fracture in adolescence and early adulthood[8]. The therapeutic strategies for fibrous dysplasia include conservative surgery, radical excision, and medical treatment with bisphosphonates. We report radical excision with reconstruction of longus fibula allograft combined with fibula bone locking plate and screws for recurrent monostotic fibular fibrous dysplasia with prolonged symptoms, such as local pain and abnormal gait. Choi *et al*[9] suggested that such lesion will continue to grow after various treatments in about 20%-25% of the patients. They also revealed that it is impossible to prognosticate whether the fibrous dysplasia will recur or not, even though it is extirpated radically[9,10]. Our patient previously received lesion removal and allograft bone grafting without internal fixation, even if some investigators found no recurrence of monostotic fibrous dysplasia at the femoral neck[2]. Alves *et al*[4] reported a case of mandibular fibrous dysplasia treated conservatively by excision, and growth of the lesion was observed postoperatively after 1 year. Valentini *et al*[11] reported no recurrence when radical resection of the lesion was applied. Thus, as the only option for eliminating fibrous dysplasia, radical surgery could prevent recurrence of fibrous dysplasia. Our case underwent radical resection for recurrent fibrous dysplasia of the fibular bone. No signs of recurrence and allograft bone fusion in postoperative X-ray were observed during regular postoperative follow-up. One year after operation, internal fixation was removed by surgeon.

Reconstructive methods for defects in the long bones of the extremities have been developed and significantly improved over the last few years, as a result of development of bone graft materials. However, there is still a lack of consensus or solid evidence for reconstructive methods for fibrous dysplasia, although some recommended guidelines have been advocated by Javaid *et al*[12]. For craniomaxillofacial fibrous dysplasia, any reconstructive decision should enhance the aesthetics and function of the patient[11]. There are still aesthetic requirements for therapy of long bones of the extremities with fibrous dysplasia. Patankar *et al*[13] proposed that nonvascularized fibular cortical strut grafting is an effective treatment for fibrous dysplasia of the radius. Majoor *et al*[14] suggested that cortical strut allograft is a viable treatment option for fibrous dysplasia involving the proximal femur in patients who have not already experienced a fracture. Surgeons should pay particular attention to the proximal fixation point of the allograft to decrease the risk of failure. In our case, fusion of strong autogenous fibular bone to allogenic fibular bone was observed at proximal and distal fibular lesions, and the internal fixation was removed after 1 year.

With regard to clinicopathological presentation of monostotic fibrous dysplasia, Özşen *et al*[15] reported small differences but mainly similar characteristics to those reported earlier. In their study of 32 cases diagnosed with fibrous dysplasia, four were accompanied by aneurysmal bone cyst, and recurrence occurred in five treated by curettage. We previously reported a case of fibrous dysplasia associated with aneurysmal-bone-cyst-like changes in proximal femur lesion, which was confirmed by pathological examination[16]. Some authors have found that the tumor tissues scatter within fibrous tissue with various degrees of cellularity, and appear narrow and circular, usually shaped as irregular, immature bone trabeculae under the microscope[15]. It is shown that immature bone trabeculae are not surrounded by osteoblasts, and such trabeculae do not evolve into mature bone. The number, distribution, and maturity of bone trabeculae differ geographically and among cases. Our case underwent curettage of the lesions, and recurrent fibular fibrous dysplasia was observed during follow-up. Prior and later pathological examination of our case supported the diagnosis of fibrous dysplasia.

CONCLUSION

Recurrent fibrous dysplasia of the fibular bone is rare, and appropriate treatment strategies are important. Radical resection of fibrous dysplasia and use of longus fibula allograft combined with fibular bone locking plate with screws for reconstruction are suitable therapeutic methods. After initial treatment of fibrous dysplasia, especially in children, active follow-up and regular reviews should be also carried out for recurrent or malignant tumors.

FOOTNOTES

Author contributions: Xie LL designed, drafted, and revised the manuscript; Yuan X, Zhu HX, and Fu Lei acquired the data and played an important role in interpreting the results; all authors contributed equally to this work, and have read and approved the final

manuscript.

Supported by The Scientific and Technological Innovation Platform of Huaihua, China, No. 2022F2701; and The Science and Technology Planning Project of Huaihua, China, No. 2021R3117.

Informed consent statement: Informed written consent was obtained from the patient for the publication of this report and any accompanying images.

Conflict-of-interest statement: All the authors declare that they have no conflict of interest to disclose.

CARE Checklist (2016) statement: The authors have read the CARE Checklist (2016), and the manuscript was prepared and revised according to the CARE Checklist (2016).

Open-Access: This article is an open-access article that was selected by an in-house editor and fully peer-reviewed by external reviewers. It is distributed in accordance with the Creative Commons Attribution NonCommercial (CC BY-NC 4.0) license, which permits others to distribute, remix, adapt, build upon this work non-commercially, and license their derivative works on different terms, provided the original work is properly cited and the use is non-commercial. See: https://creativecommons.org/Licenses/by-nc/4.0/

Country/Territory of origin: China

ORCID number: Lun-Li Xie 0000-0001-8732-8858; Dan Pu 0000-0003-1618-8354.

S-Editor: Lin C
L-Editor: Wang TQ
P-Editor: Lin C

REFERENCES

1 **Lichtenstein L**, Jaffe HL. Ewing's Sarcoma of Bone. *Am J Pathol* 1947; **23**: 43-77 [PMID: 19970919]
2 **Nishida Y**, Tsukushi S, Hosono K, Nakashima H, Yamada Y, Urakawa H, Ishiguro N. Surgical treatment for fibrous dysplasia of femoral neck with mild but prolonged symptoms: a case series. *J Orthop Surg Res* 2015; **10**: 63 [PMID: 25958111 DOI: 10.1186/s13018-015-0208-6]
3 **Ruggieri P**, Sim FH, Bond JR, Unni KK. Malignancies in fibrous dysplasia. *Cancer* 1994; **73**: 1411-1424 [PMID: 8111708 DOI: 10.1002/1097-0142(19940301)73:5<1411::aid-cncr2820730516>3.0.co;2-t]
4 **Alves N**, de Oliveira RJ, Takehana D, Deana NF. Recurrent Monostotic Fibrous Dysplasia in the Mandible. *Case Rep Dent* 2016; **2016**: 3920850 [PMID: 27340572 DOI: 10.1155/2016/3920850]
5 **Cohen MM Jr**, Howell RE. Etiology of fibrous dysplasia and McCune-Albright syndrome. *Int J Oral Maxillofac Surg* 1999; **28**: 366-371 [PMID: 10535539]
6 **Levine MA**, Modi WS, O'Brien SJ. Mapping of the gene encoding the alpha subunit of the stimulatory G protein of adenylyl cyclase (*GNAS*1) to 20q13.2----q13.3 in human by in situ hybridization. *Genomics* 1991; **11**: 478-479 [PMID: 1769666 DOI: 10.1016/0888-7543(91)90164-a]
7 **Ozek C**, Gundogan H, Bilkay U, Tokat C, Gurler T, Songur E. Craniomaxillofacial fibrous dysplasia. *J Craniofac Surg* 2002; **13**: 382-389 [PMID: 12040205 DOI: 10.1097/00001665-200205000-00004]
8 **Zenn MR**, Zuniga J. Treatment of fibrous dysplasia of the mandible with radical excision and immediate reconstruction: case report. *J Craniofac Surg* 2001; **12**: 259-263 [PMID: 11358100 DOI: 10.1097/00001665-200105000-00012]
9 **Choi JW**, Lee SW, Koh KS. Correction of proptosis and zygomaticomaxillary asymmetry using orbital wall decompression and zygoma reduction in craniofacial fibrous dysplasia. *J Craniofac Surg* 2009; **20**: 326-330 [PMID: 19276831 DOI: 10.1097/SCS.0b013e31819922d3]
10 **Lee JS**, FitzGibbon EJ, Chen YR, Kim HJ, Lustig LR, Akintoye SO, Collins MT, Kaban LB. Clinical guidelines for the management of craniofacial fibrous dysplasia. *Orphanet J Rare Dis* 2012; **7** Suppl 1: S2 [PMID: 22640797 DOI: 10.1186/1750-1172-7-S1-S2]
11 **Valentini V**, Cassoni A, Marianetti TM, Terenzi V, Fadda MT, Iannetti G. Craniomaxillofacial fibrous dysplasia: conservative treatment or radical surgery? A retrospective study on 68 patients. *Plast Reconstr Surg* 2009; **123**: 653-660 [PMID: 19182626 DOI: 10.1097/PRS.0b013e318196bbbe]
12 **Javaid MK**, Boyce A, Appelman-Dijkstra N, Ong J, Defabianis P, Offiah A, Arundel P, Shaw N, Pos VD, Underhil A, Portero D, Heral L, Heegaard AM, Masi L, Monsell F, Stanton R, Dijkstra PDS, Brandi ML, Chapurlat R, Hamdy NAT, Collins MT. Best practice management guidelines for fibrous dysplasia/McCune-Albright syndrome: a consensus statement from the FD/MAS international consortium. *Orphanet J Rare Dis* 2019; **14**: 139 [PMID: 31196103 DOI: 10.1186/s13023-019-1102-9]
13 **Patankar H**, Patankar S, Tandon N, Bairy A. Fibrous Dysplasia of Radius Bone-excision and Fibula Graft: A Case Report. *J Orthop Case Rep* 2022; **12**: 31-34 [PMID: 36660157 DOI: 10.13107/jocr.2022.v12.i05.2804]
14 **Majoor BC**, Peeters-Boef MJ, van de Sande MA, Appelman-Dijkstra NM, Hamdy NA, Dijkstra PD. What Is the Role of Allogeneic Cortical Strut Grafts in the Treatment of Fibrous Dysplasia of the Proximal Femur? *Clin Orthop Relat Res* 2017; **475**: 786-795 [PMID: 27020436 DOI: 10.1007/s11999-016-4806-3]
15 **Özşen M**, Yalçinkaya Ü, Bilgen MS, Yazici Z. Fibrous Dysplasia: Clinicopathologic Presentation of 36 Cases. *Turk Patoloji Derg* 2018; **34**: 234-241 [PMID: 29744853 DOI: 10.5146/tjpath.2018.01428]
16 **Xie LL**, Yuan X, Zhu HX, Pu D. Surgery for fibrous dysplasia associated with aneurysmal-bone-cyst-like changes in right proximal femur: A case report. *World J Clin Cases* 2023; **11**: 6170-6175 [PMID: 37731583 DOI: 10.12998/wjcc.v11.i26.6170]

World Journal of Clinical Cases

Submit a Manuscript: https://www.f6publishing.com

World J Clin Cases 2023 November 26; 11(33): 8058-8064

DOI: 10.12998/wjcc.v11.i33.8058

ISSN 2307-8960 (online)

CASE REPORT

Asian variant intravascular large B-cell lymphoma with highly suspected central nervous system involvement: A case report

Yong-Pyo Lee, Seung-Myoung Son, Jihyun Kwon

Specialty type: Hematology

Provenance and peer review: Unsolicited article; Externally peer reviewed.

Peer-review model: Single blind

Peer-review report's scientific quality classification

Grade A (Excellent): 0
Grade B (Very good): 0
Grade C (Good): C, C
Grade D (Fair): 0
Grade E (Poor): 0

P-Reviewer: Roganovic J, Croatia

Received: September 3, 2023
Peer-review started: September 3, 2023
First decision: October 24, 2023
Revised: November 1, 2023
Accepted: November 10, 2023
Article in press: November 10, 2023
Published online: November 26, 2023

Yong-Pyo Lee, Jihyun Kwon, Department of Internal Medicine, Chungbuk National University Hospital, Cheongju 28644, South Korea

Seung-Myoung Son, Department of Pathology, Chungbuk National University Hospital, Chungbuk National University College of Medicine, Cheongju 28644, South Korea

Corresponding author: Jihyun Kwon, MD, PhD, Associate Professor, Doctor, Department of Internal Medicine, Chungbuk National University Hospital, 776, 1Sunhwan-ro, Seowon-gu, Cheongju 28644, South Korea. marioncrepe@gmail.com

Abstract

BACKGROUND

Intravascular large B-cell lymphoma (IVLBCL) is a rare subtype of extranodal lymphoma. In particular, the Asian variant of IVLBCL is characterized by hemophagocytic lymphohistiocytosis along with bone marrow involvement. However, central nervous system (CNS) involvement is uncommon in this variant compared to the Western variant. Here, we report a case of typical Asian variant IVLBCL with highly suspected CNS involvement and discuss the nature of the disease and its genetic aberration.

CASE SUMMARY

A 67-year-old female patient complained of gradually worsening cognitive impairment. While hospitalized, she developed a high fever and showed marked bicytopenia. Intracranial imaging revealed a suspected leptomeningeal disease. Although no malignant cells were found in the cerebrospinal fluid (CSF), the protein and lactate dehydrogenase levels in CSF were increased. Bone marrow examination revealed an increased number of hemophagocytic histiocytes, and ^{18}F-fluorodeoxyglucose (FDG) positron emission tomography with computerized tomography scan revealed increased FDG uptake in both adrenal glands, the liver, and the right ethmoid sinus. A tissue biopsy showed atypical large lymphoid cells with prominent nucleoli in the vessels, and the tumor cells were positive for CD20, BCL2, BCL6, and IRF4/MUM1. In addition, targeted sequencing identified *MYD88*, *TET2*, and *PIM1* mutations. Consequently, we diagnosed the patient with the Asian variant of IVLBCL with highly suspected CNS involvement.

CONCLUSION

Suspicion of IVLBCL and immediate diagnosis lead to timely treatment. Moreover, careful CNS examination at diagnosis is recommended.

Key Words: Intravascular large B-cell lymphoma; Asian variant; Hemophagocytic lymphohistiocytosis; Central nervous system involvement; Genetic alteration; Case report

©The Author(s) 2023. Published by Baishideng Publishing Group Inc. All rights reserved.

Core Tip: Intravascular large B-cell lymphoma (IVLBCL) is a rare but clinically aggressive lymphoproliferative disease. Given its aggressive nature, immediate diagnosis of IVLBCL and timely treatment are critical for better clinical outcomes. As central nervous system (CNS) involvement adversely affects prognosis if IVLBCL, active CNS examination is required at diagnosis. In addition, along with conventional pathology, targeted sequencing contributes to diagnosis and provides a basis for use of targeted agents. Here, we report a case of Asian variant IVLBCL with highly suspected CNS involvement. We first describe the clinical course of disease and then discuss the genetic aberrations found in the patient.

Citation: Lee YP, Son SM, Kwon J. Asian variant intravascular large B-cell lymphoma with highly suspected central nervous system involvement: A case report. *World J Clin Cases* 2023; 11(33): 8058-8064
URL: https://www.wjgnet.com/2307-8960/full/v11/i33/8058.htm
DOI: https://dx.doi.org/10.12998/wjcc.v11.i33.8058

INTRODUCTION

Intravascular large B-cell lymphoma (IVLBCL), characterized by growth of lymphoma cells within the lumen of blood vessels, is a rare type of lymphoid malignancy[1]. According to the World Health Organization classification, IVLBCL is divided into classic, hemophagocytic syndrome–associated, and isolated cutaneous variants. In addition, classification into Asian and Western variants according to the clinical manifestation and geographic distribution is also practiced[2,3]. The Asian variant of IVLBCL predominantly involves the liver, spleen, and bone marrow and often accompanies hemophagocytic lymphohistiocytosis (HLH), while the Western variant frequently affects the skin and central nervous system (CNS)[3]. Aside from its aggressive nature, IVLBCL patients usually present non-specific symptoms only, which can delay accurate diagnosis and ultimately lead to dismal clinical outcomes. In addition, due to the alterations of various molecules and chemokines that regulate the interaction between lymphoma cells and vascular endothelial cells[1,4], extravascular invasion is unusual, and overt lymphadenopathy is rare compared to other types of lymphoma. Thus, although there has been research on the ^{18}F-fluorodeoxyglucose (FDG) positron emission tomography with computed tomography (PET-CT) features of IVLBCL[5], the definitive role of PET-CT imaging in the diagnosis and staging of IVLBCL remains ambiguous[6]. Here, we report a characteristic Asian variant IVLBCL patient with HLH and highly suspected CNS involvement. We describe the patient's clinical features and the course of disease and discuss observed genetic aberrations.

CASE PRESENTATION

Chief complaints

A 67-year-old female patient visited the department of neurology for deteriorating cognitive function.

History of present illness

The patient was able to walk with a cane and take care of herself. However, upon presentation, her cognitive function had deteriorated, she could not recognize her neighbors, and she had difficulty walking unassisted.

History of past illness

She had been diagnosed with cerebellar ataxia a few years prior and was on the medications such as cilostazol and atorvastatin.

Personal and family history

She had no personal or family history.

Physical examination

At the time of examination, she had a mild fever of 37.8°C, but her other vital signs were stable, and she reported no symptoms other than deteriorated cognitive function. There was no sensory deficit, and motor power was intact, although her coordination was poor.

Table 1 Patient characteristics and laboratory findings at diagnosis

Sex/age (yr)	ECOG	Disease involvement sites	Ann Arbor stage	IPI	Cell of origin	WBC (10^3/μL)	Hb (g/dL)	Plt (10^3/μL)	LDH (IU/L)	CRP (mg/dL)	Ferritin (ng/mL)
F/67	4	Right ethmoid sinus, liver, spleen, bilateral adrenal glands	IV	5	Non-GCB	5.35	8.5	77	891	5.26	835

CRP: C-reactive protein; ECOG: Eastern Cooperative Oncology Group performance status; GCB: Germinal center B-cell; Hb: Hemoglobin; IPI: International Prognostic Index; LDH: Lactate dehydrogenase; Plt: Platelet; WBC: White blood cell.

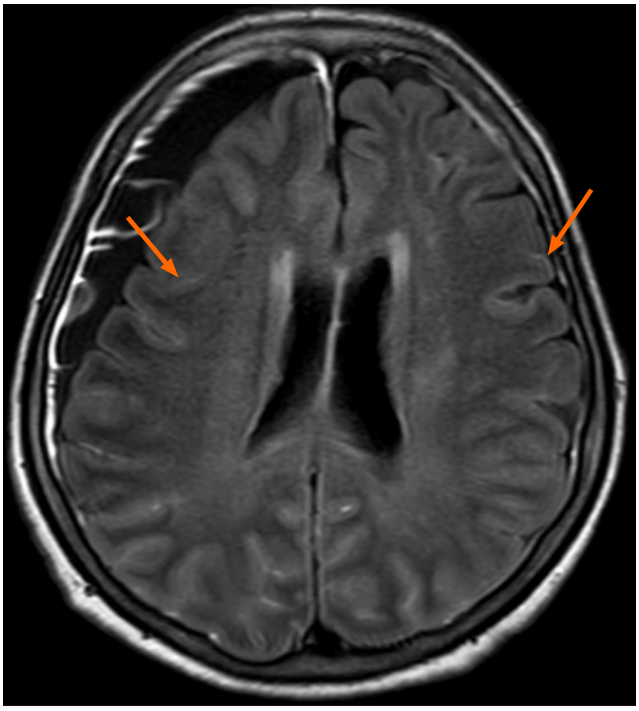

DOI: 10.12998/wjcc.v11.i33.8058 **Copyright** ©The Author(s) 2023.

Figure 1 Axial T2-FLAIR brain magnetic resonance imaging reveals pachymeningeal enhancement in both frontoparietal convexities.

Laboratory examinations

Laboratory testing confirmed bicytopenia (hemoglobin, 8.5 g/dL; platelet count, 77 × 10^3/μL) and elevated C-reactive protein (5.26 mg/dL) and lactate dehydrogenase (LDH) (891 IU/L) levels (Table 1). She was confirmed to have a urinary tract infection caused by *Escherichia coli*.

Imaging examinations

Following brain magnetic resonance imaging (MRI), a focal diffusion restrictive lesion in the left parietal lobe and chronic subdural hemorrhage in the right frontal convexity were observed. In addition, pachymeningeal enhancement of the bilateral frontoparietal convexities was noted, suggesting leptomeningeal disease (Figure 1).

Three consecutive lumbar punctures were performed, and a consistent increase in protein and LDH levels in cerebrospinal fluid (CSF) was observed. No malignant cells were observed and the CSF pressure was within the normal range (7.5 cmH_2O). Abdominal CT showed bilateral enlargement of adrenal glands along with hepatomegaly and splenomegaly. Meanwhile, her cognitive function and the results of blood tests were worsening (*e.g.*, exacerbation of cytopenia, elevation of ferritin and triglyceride levels), and, despite improved urinalysis findings after antibiotic therapy, she developed a high fever up to 39°C. Thus, the patient was referred to a hematologist who performed immediate bone marrow exam. Increased numbers of hemophagocytic histiocytes were found without malignant cells, suggesting secondary HLH. PET-CT was performed to identify the underlying disease. An increased FDG uptake was observed in both adrenal glands, the liver, and the right ethmoid sinus (Figure 2), and a biopsy of the right ethmoid sinus was ordered. Histological examination revealed atypical large lymphoid cells with prominent nucleoli in the vessels (Figure 3A and B). Immunohistochemical analysis showed that the tumor cells were positive for CD20, BCL2, BCL6, and IRF4/MUM1 (Figure 3C-F) but negative for CD3 and CD10. In addition, *MYD88*, *TET2*, and *PIM1* mutations were identified by targeted sequencing using tissues (Table 2).

Table 2 Variants found in next-generation sequencing

Tier 1 variants				Tier 2 variants				Tier 3 variants			
Gene	DNA	Protein	VAF	Gene	DNA	Protein	VAF	Gene	DNA	Protein	VAF
MYD88	c.755T>C	p.Leu252Pro	54.8%	*PIM1*	c.237G>C	p.Glu79Asp	30.77%	*NOTCH1*	c.6283C>T	p.Arg2095Cys	37.7%
								ETV6	c.1123G>A	p.Gly375Arg	14.4%
TET2	c.3280A>T	p.Lys1094Ter	16.0%	*BTG2*	c.97C>T	p.Gln33Ter	19.6%	*HIST1H1E*	c.367G>A	p.Ala123Thr	15.6%
								TBL1XR1	c.848G>A	p.Ser283Asn	16.5%

DNA: Deoxyribonucleic acid; VAF: Variant allele frequency.

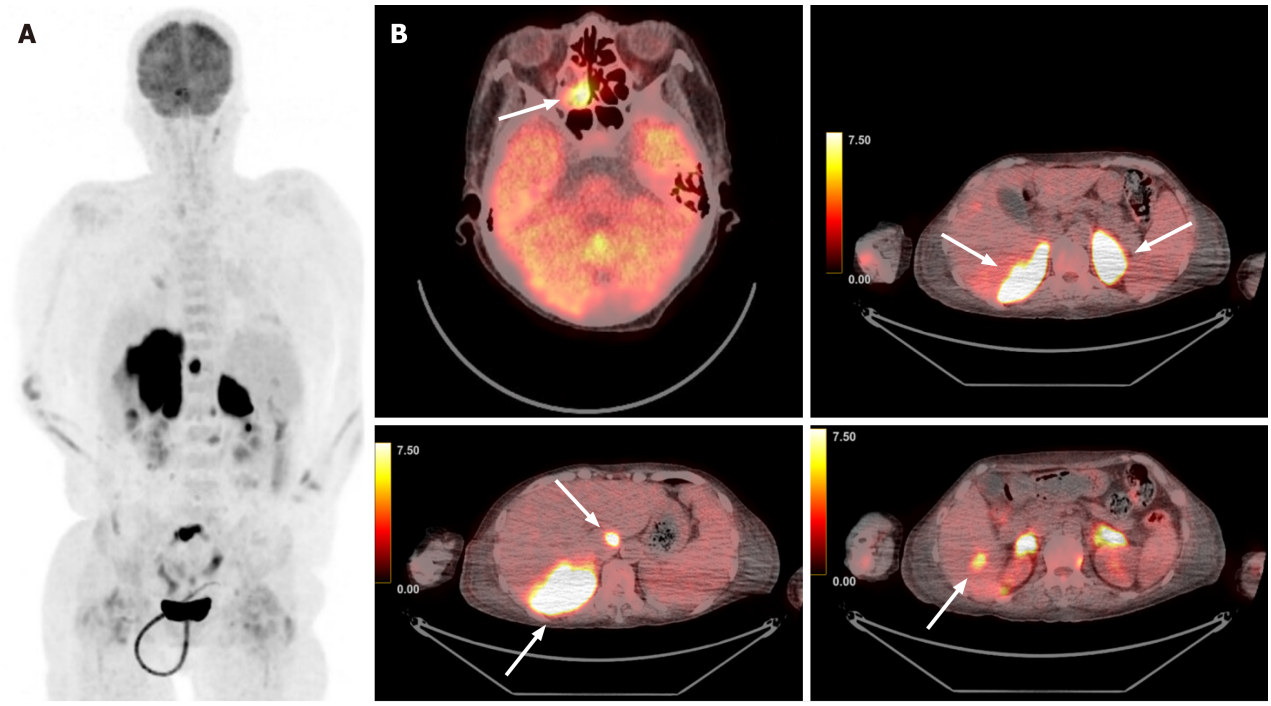

DOI: 10.12998/wjcc.v11.i33.8058 **Copyright** ©The Author(s) 2023.

Figure 2 An ^{18}F-fluorodeoxyglucose (FDG) positron emission tomography with computed tomography scan shows high FDG uptake in the right ethmoid sinus, liver, and both adrenal glands.

FINAL DIAGNOSIS

The Asian variant of IVLBCL was diagnosed. In addition, although there was no cytological confirmation, the IVLBCL was considered to be accompanied by CNS involvement based on the findings of brain MRI and CSF analysis as well as her clinical manifestation.

TREATMENT

Intravenous methylprednisolone administration at a dose of 1 mg/kg was started immediately after the biopsy, and, following the final diagnosis, immunochemotherapy including rituximab and CNS-directed therapy with methotrexate (MTX) was considered. However, due to her poor performance status and economic issues, she decided to receive only steroid therapy and best supportive care.

OUTCOME AND FOLLOW-UP

The patient deteriorated and passed away two weeks after her diagnosis.

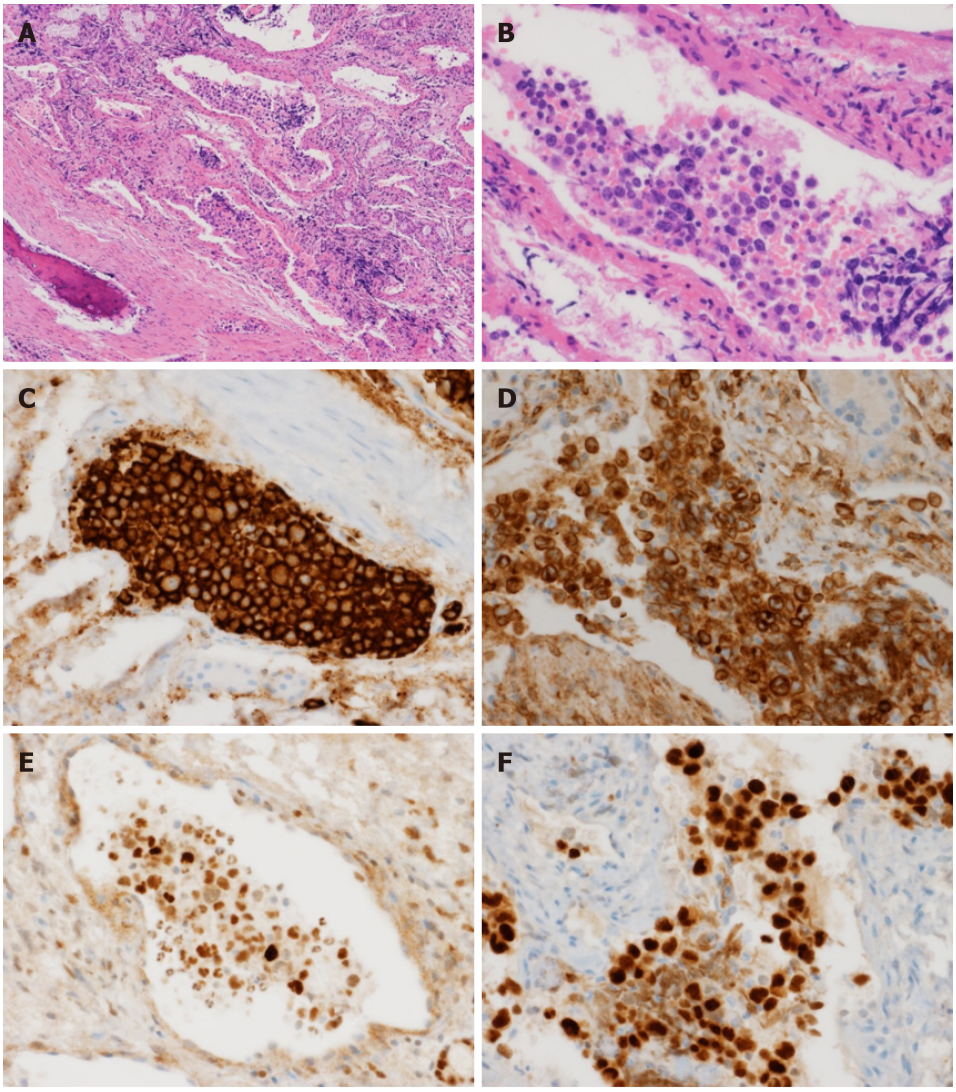

DOI: 10.12998/wjcc.v11.i33.8058 **Copyright** ©The Author(s) 2023.

Figure 3 Haematoxylin and eosin stained section of the biopsy specimen demonstrates atypical large lymphoid cells with prominent nucleoli in the blood vessel. A: Haematoxylin and eosin (H&E) (×100); B: H&E (×400); C: Immunohistochemical staining: CD20 (×400); D: BCL2 (×400); E: BCL6 (×400); F: IRF4/MUM1 (×400).

DISCUSSION

Despite a quantum leap of cancer diagnostic technology, the diagnosis of IVLBCL remains challenging due to the ambiguous signs and symptoms that do not precisely reflect the characteristics of the disease. In particular, approximately 20%-30% of Asian variant IVLBCL cases have CNS involvement at diagnosis[3,7], which is associated with poor prognosis[8]. However, since malignant lymphocytes are rarely found in CSF and there are no previously described pathognomonic findings on MRI[9], auxiliary diagnostic tools may often be required. Recently introduced less-invasive diagnostic methods using peripheral blood or CSF, such as liquid biopsy[10], or mutation detection using circulating tumor DNA[11,12] can play a complementary role in diagnosing IVLBCL. Therefore, when diagnosing IVLBCL, a multidisciplinary approach and an integrated diagnostic process are needed to analyze each symptom according to involved organ, including active CNS examination.

Malignant lymphoma derived from T-cells or natural killer cells is one of the leading causes of HLH in adults[13,14], but B-cell origin lymphoproliferative disease can also provoke HLH[14]. Indeed, the Asian variant of IVLBCL is commonly accompanied by HLH[2,3,6]. Therefore, in adult patients suspected of secondary HLH, systemic evaluation and biopsy based on PET-CT scan should be performed promptly. However, as opposed to the nodal diffuse large B-cell lymphoma (DLBCL), IVLBCL mainly involves extranodal sites and shows various levels (usually mild to moderate) of FDG uptake in PET-CT[5], and in general, the selection of PET-CT-based biopsy lesions may be difficult under these circumstances. Nonetheless, in diagnosing IVLBCL, when infectious or inflammatory diseases are excluded, such findings may help to select the appropriate biopsy site[5]. Therefore, despite some limitations, PET-CT may play an important role in the diagnosis of IVLBCL.

The absence of a prospective study due to the rarity of the disease hindered the establishment of standard of care for IVLBCL. Thus, IVLBCL has been managed by adapting the treatment strategy of DLBCL, where several immunophenotype overlaps[9]. Anthracycline-based chemotherapy with rituximab presented favorable clinical outcomes in both East and West[15,16]. In addition, CNS-directed therapy is an essential part of IVLBCL management. Considering that malignant cells can penetrate the CNS parenchyma through blood vessels[17], intrathecal MTX therapy alone for CNS-involving disease would not be sufficient. Recently, several reports have introduced high-dose IV MTX-based treatment based on the primary CNS lymphoma (PCNSL) treatment strategy[17,18], and this approach seems reasonable given the poor CNS penetration of systemic immunochemotherapy. In several reports of genetic alterations in IVLBCL, mutations in *MYD88* and *CD79B* were frequently detected[19,20], usually in primary testicular DLBCL and PCNSL, where extranodal site involvement is common[21]. With the advances in understanding of the disease and its biology, novel therapeutic approaches to IVLBCL are continuously being attempted. As Bruton's tyrosine kinase inhibitors block the nuclear factor kappa B pathway, patients with B-cell lymphomas harboring *MYD88* and/or *CD79B* mutations are expected to show better treatment responses[22]. Indeed, an interim analysis of a phase II study for treatment-naïve IVLBCL patients using zanubrutinib was recently reported, demonstrating promising efficacy[23]. As such, future studies to improve clinical outcomes with precision treatment for the disease in addition to conventional treatment are required.

CONCLUSION

In conclusion, given the aggressive nature of IVLBCL, suspicion of the disease and subsequent immediate and accurate diagnosis lead to timely treatment, which results in better clinical outcomes. In addition, considering its poor prognosis, careful examination of CNS involvement at diagnosis is recommended. Even if CNS invasion of IVLBCL is not confirmed, active CNS-directed therapy is required when highly suspected.

FOOTNOTES

Author contributions: Lee YP and Son SM contributed to manuscript writing and editing and to data collection; Lee YP and Kwon JH contributed to data analysis; Kwon JH contributed to conceptualization and supervision; All authors have read and approved the final manuscript.

Informed consent statement: The institutional review board of Chungbuk National University Hospital approved this study (approval number. CBNUH 2023-04-024), and informed written consent was obtained from the patient for publication of this report and any accompanying images.

Conflict-of-interest statement: All the authors declare that they have no conflicts of interest to disclose.

CARE Checklist (2016) statement: The authors have read the CARE Checklist (2016), and the manuscript was prepared and revised according to the CARE Checklist (2016).

Open-Access: This article is an open-access article that was selected by an in-house editor and fully peer-reviewed by external reviewers. It is distributed in accordance with the Creative Commons Attribution NonCommercial (CC BY-NC 4.0) license, which permits others to distribute, remix, adapt, build upon this work non-commercially, and license their derivative works on different terms, provided the original work is properly cited and the use is non-commercial. See: https://creativecommons.org/Licenses/by-nc/4.0/

Country/Territory of origin: South Korea

ORCID number: Yong-Pyo Lee 0000-0002-6153-9742; Seung-Myoung Son 0000-0002-1646-4649; Jihyun Kwon 0000-0001-8128-3310.

S-Editor: Liu JH
L-Editor: A
P-Editor: Xu ZH

REFERENCES

1 **Swerdlow SH**, Campo E, Pileri SA, Harris NL, Stein H, Siebert R, Advani R, Ghielmini M, Salles GA, Zelenetz AD, Jaffe ES. The 2016 revision of the World Health Organization classification of lymphoid neoplasms. *Blood* 2016; **127**: 2375-2390 [PMID: 26980727 DOI: 10.1182/blood-2016-01-643569]

2 **Murase T**, Yamaguchi M, Suzuki R, Okamoto M, Sato Y, Tamaru J, Kojima M, Miura I, Mori N, Yoshino T, Nakamura S. Intravascular large B-cell lymphoma (IVLBCL): a clinicopathologic study of 96 cases with special reference to the immunophenotypic heterogeneity of CD5. *Blood* 2007; **109**: 478-485 [PMID: 16985183 DOI: 10.1182/blood-2006-01-021253]

3 **Yoon SE**, Kim WS, Kim SJ. Asian variant of intravascular large B-cell lymphoma: a comparison of clinical features based on involvement of the central nervous system. *Korean J Intern Med* 2020; **35**: 946-956 [PMID: 31752477 DOI: 10.3904/kjim.2018.396]

4 **Ponzoni M**, Arrigoni G, Gould VE, Del Curto B, Maggioni M, Scapinello A, Paolino S, Cassisa A, Patriarca C. Lack of CD 29 (beta1 integrin)

and CD 54 (ICAM-1) adhesion molecules in intravascular lymphomatosis. *Hum Pathol* 2000; **31**: 220-226 [PMID: 10685637 DOI: 10.1016/s0046-8177(00)80223-3]

5 **Lim CH**, Yoon SE, Kim WS, Lee KH, Kim SJ. Imaging Features and Prognostic Value of FDG PET/CT in Patients with Intravascular Large B-Cell Lymphoma. *Cancer Manag Res* 2021; **13**: 7289-7297 [PMID: 34584455 DOI: 10.2147/CMAR.S330308]

6 **Hong JY**, Kim HJ, Ko YH, Choi JY, Jung CW, Kim SJ, Kim WS. Clinical features and treatment outcomes of intravascular large B-cell lymphoma: a single-center experience in Korea. *Acta Haematol* 2014; **131**: 18-27 [PMID: 24021554 DOI: 10.1159/000351060]

7 **Shimada K**, Murase T, Matsue K, Okamoto M, Ichikawa N, Tsukamoto N, Niitsu N, Miwa H, Asaoku H, Kosugi H, Kikuchi A, Matsumoto M, Saburi Y, Masaki Y, Yamamoto K, Yamaguchi M, Nakamura S, Naoe T, Kinoshita T; IVL Study Group in Japan. Central nervous system involvement in intravascular large B-cell lymphoma: a retrospective analysis of 109 patients. *Cancer Sci* 2010; **101**: 1480-1486 [PMID: 20412122 DOI: 10.1111/j.1349-7006.2010.01555.x]

8 **Fonkem E**, Dayawansa S, Stroberg E, Lok E, Bricker PC, Kirmani B, Wong ET, Huang JH. Neurological presentations of intravascular lymphoma (IVL): meta-analysis of 654 patients. *BMC Neurol* 2016; **16**: 9 [PMID: 26849888 DOI: 10.1186/s12883-015-0509-8]

9 **Ponzoni M**, Campo E, Nakamura S. Intravascular large B-cell lymphoma: a chameleon with multiple faces and many masks. *Blood* 2018; **132**: 1561-1567 [PMID: 30111607 DOI: 10.1182/blood-2017-04-737445]

10 **Baraniskin A**, Schroers R. Liquid Biopsy and Other Non-Invasive Diagnostic Measures in PCNSL. *Cancers (Basel)* 2021; **13** [PMID: 34071407 DOI: 10.3390/cancers13112665]

11 **Rimelen V**, Ahle G, Pencreach E, Zinniger N, Debliquis A, Zalmaï L, Harzallah I, Hurstel R, Alamome I, Lamy F, Voirin J, Drénou B. Tumor cell-free DNA detection in CSF for primary CNS lymphoma diagnosis. *Acta Neuropathol Commun* 2019; **7**: 43 [PMID: 30885253 DOI: 10.1186/s40478-019-0692-8]

12 **Yoon SE**, Kim YJ, Shim JH, Park D, Cho J, Ko YH, Park WY, Mun YC, Lee KE, Cho D, Kim WS, Kim SJ. Plasma Circulating Tumor DNA in Patients with Primary Central Nervous System Lymphoma. *Cancer Res Treat* 2022; **54**: 597-612 [PMID: 34325497 DOI: 10.4143/crt.2021.752]

13 **Ramos-Casals M**, Brito-Zerón P, López-Guillermo A, Khamashta MA, Bosch X. Adult haemophagocytic syndrome. *Lancet* 2014; **383**: 1503-1516 [PMID: 24290661 DOI: 10.1016/S0140-6736(13)61048-X]

14 **La Rosée P**, Horne A, Hines M, von Bahr Greenwood T, Machowicz R, Berliner N, Birndt S, Gil-Herrera J, Girschikofsky M, Jordan MB, Kumar A, van Laar JAM, Lachmann G, Nichols KE, Ramanan AV, Wang Y, Wang Z, Janka G, Henter JI. Recommendations for the management of hemophagocytic lymphohistiocytosis in adults. *Blood* 2019; **133**: 2465-2477 [PMID: 30992265 DOI: 10.1182/blood.2018894618]

15 **Ferreri AJ**, Dognini GP, Bairey O, Szomor A, Montalbán C, Horvath B, Demeter J, Uziel L, Soffietti R, Seymour JF, Ambrosetti A, Willemze R, Martelli M, Rossi G, Candoni A, De Renzo A, Doglioni C, Zucca E, Cavalli F, Ponzoni M; International Extranodal Lymphoma Study Group. The addition of rituximab to anthracycline-based chemotherapy significantly improves outcome in 'Western' patients with intravascular large B-cell lymphoma. *Br J Haematol* 2008; **143**: 253-257 [PMID: 18699850 DOI: 10.1111/j.1365-2141.2008.07338.x]

16 **Shimada K**, Matsue K, Yamamoto K, Murase T, Ichikawa N, Okamoto M, Niitsu N, Kosugi H, Tsukamoto N, Miwa H, Asaoku H, Kikuchi A, Matsumoto M, Saburi Y, Masaki Y, Yamaguchi M, Nakamura S, Naoe T, Kinoshita T. Retrospective analysis of intravascular large B-cell lymphoma treated with rituximab-containing chemotherapy as reported by the IVL study group in Japan. *J Clin Oncol* 2008; **26**: 3189-3195 [PMID: 18506023 DOI: 10.1200/JCO.2007.15.4278]

17 **Wang J**, Alhaj Moustafa M, Kuhlman JJ, Seegobin K, Jiang L, Gupta V, Tun HW. Intravascular Large B Cell Lymphoma with CNS Involvement Successfully Treated with High-Dose Methotrexate and High-Dose Ara-C Based CNS-Directed Chemoimmunotherapy Alternating with Anthracycline Based Chemoimmunotherapy. *Blood Lymphat Cancer* 2022; **12**: 47-54 [PMID: 35642208 DOI: 10.2147/BLCTT.S362736]

18 **Takahashi H**, Nishimaki H, Nakanishi Y, Hamada T, Nakagawa M, Iizuka K, Uchino Y, Iriyama N, Miura K, Nakayama T, Masuda S, Hatta Y, Nakamura H. Clinical impact of central nervous system-directed therapies on intravascular large B-cell lymphoma: A single institution's experience. *EJHaem* 2022; **3**: 467-470 [PMID: 35846032 DOI: 10.1002/jha2.380]

19 **Schrader AMR**, Jansen PM, Willemze R, Vermeer MH, Cleton-Jansen AM, Somers SF, Veelken H, van Eijk R, Kraan W, Kersten MJ, van den Brand M, Stevens WBC, de Jong D, Abdul Hamid M, Tanis BC, Posthuma EFM, Nijland M, Diepstra A, Pals ST, Cleven AHG, Vermaat JSP. High prevalence of MYD88 and CD79B mutations in intravascular large B-cell lymphoma. *Blood* 2018; **131**: 2086-2089 [PMID: 29514783 DOI: 10.1182/blood-2017-12-822817]

20 **Somers S**, Jansen P, Veelken H, Vermeer M, Kraan W, Schrader A-R, Posthuma W, Nijland M, Diepstra A, Kersten MJ, Pals S, Cleven A, Vermaat J. High Prevalence of Oncogenic MYD88 and CD79B Mutations in Intravascular Large B-Cell Lymphoma: Implication for Therapy with Bruton's Kinase Inhibitors? *Blood* 2017; **130** Suppl 1: 4000 [DOI: 10.1182/blood.V130.Suppl_1.4000.4000]

21 **Weissinger SE**, Dugge R, Disch M, Barth TF, Bloehdorn J, Zahn M, Marienfeld R, Viardot A, Möller P. Targetable alterations in primary extranodal diffuse large B-cell lymphoma. *EJHaem* 2022; **3**: 688-697 [PMID: 36051079 DOI: 10.1002/jha2.428]

22 **Wilson WH**, Young RM, Schmitz R, Yang Y, Pittaluga S, Wright G, Lih CJ, Williams PM, Shaffer AL, Gerecitano J, de Vos S, Goy A, Kenkre VP, Barr PM, Blum KA, Shustov A, Advani R, Fowler NH, Vose JM, Elstrom RL, Habermann TM, Barrientos JC, McGreivy J, Fardis M, Chang BY, Clow F, Munneke B, Moussa D, Beaupre DM, Staudt LM. Targeting B cell receptor signaling with ibrutinib in diffuse large B cell lymphoma. *Nat Med* 2015; **21**: 922-926 [PMID: 26193343 DOI: 10.1038/nm.3884]

23 **Zhang Y**, Jia C, Wang W, Zhang L, Cao X, Li J, Zhang W, Zhou D. The Interim Analysis from a Prospective Single-Center Phase 2 Study of Zanubrutinib Plus R-CHOP in Treat-Naïve Intravascular Large B Cell Lymphoma. *Blood* 2021; **138** Suppl 1: 3563 [DOI: 10.1182/blood-2021-152417]

World Journal of Clinical Cases

Submit a Manuscript: https://www.f6publishing.com

World J Clin Cases 2023 November 26; 11(33): 8065-8070

DOI: 10.12998/wjcc.v11.i33.8065

ISSN 2307-8960 (online)

CASE REPORT

Treatment of adult congenital anal atresia with rectovestibular fistula: A rare case report

Jun Wang, Xin-Yi Zhang, Ji-Han Chen, Hei-Ying Jin

Specialty type: Surgery

Provenance and peer review: Unsolicited article; Externally peer reviewed.

Peer-review model: Single blind

Peer-review report's scientific quality classification

Grade A (Excellent): 0
Grade B (Very good): 0
Grade C (Good): C
Grade D (Fair): 0
Grade E (Poor): 0

P-Reviewer: Hidaka E, Japan

Received: September 7, 2023
Peer-review started: September 7, 2023
First decision: October 17, 2023
Revised: November 5, 2023
Accepted: November 17, 2023
Article in press: November 17, 2023
Published online: November 26, 2023

Jun Wang, Xin-Yi Zhang, Ji-Han Chen, Hei-Ying Jin, Department of Anorectal Surgery, The Second Affiliated Hospital of Nanjing University of Chinese Medicine, Nanjing 210017, Jiangsu Province, China

Corresponding author: Hei-Ying Jin, MD, Doctor, Professor, Department of Anorectal Surgery, The Second Affiliated Hospital of Nanjing University of Chinese Medicine, No. 23 Nanhu Road, Nanjing 210017, Jiangsu Province, China. jinheiying@hotmail.com

Abstract

BACKGROUND

Female anorectal malformation is a correctable congenital defect. Delayed manifestations in patients with anal deformities are uncommon, especially after adolescence.

CASE SUMMARY

The clinical data of a 19-year-old adult female patient with congenital anal atresia accompanied by rectovestibular fistula as the main manifestation was retrospectively analyzed. Diagnosis was made based on the patient's clinical symptoms, signs, imaging showing the fistula, X-ray and magnetic resonance imaging results. The preoperative examination was improved. Anorectoplasty was performed. The patient exhibited an improvement in quality of life and presented no evidence of fecal incontinence during the 6-mo follow-up.

CONCLUSION

Transfistula anorectoplasty is a reasonable and reliable surgical method for the treatment of adult congenital anal atresia and rectovestibular fistula.

Key Words: Anorectal malformations; Congenital anorectal atresia; Rectovestibular fistula; Transfistula anorectoplasty; Case report

©The Author(s) 2023. Published by Baishideng Publishing Group Inc. All rights reserved.

Core Tip: This paper reports the case of an adult patient with congenital anal atresia combined with rectovestibular fistula who underwent transfistulae anorectoplasty with clear visual field exposure the ability to separate the rectovaginal septum under direct vision, greatly reducing the possibility of vaginal injury, ensuring the integrity of the sphincter, and causing minimal intraoperative damage to normal tissues. It is a reasonable and reliable surgical method for the treatment of congenital anal atresia and rectovestibular fistula.

Citation: Wang J, Zhang XY, Chen JH, Jin HY. Treatment of adult congenital anal atresia with rectovestibular fistula: A rare case report. *World J Clin Cases* 2023; 11(33): 8065-8070
URL: https://www.wjgnet.com/2307-8960/full/v11/i33/8065.htm
DOI: https://dx.doi.org/10.12998/wjcc.v11.i33.8065

INTRODUCTION

Anorectal malformation (ARM) is a common deformity in children, and anal atresia is the main manifestation of it, with a morbidity of 1/5000-1/1500[1,2]; 75%-95% of patients have fistula, which occurs more frequently in women than men. Congenital anal atresia with rectovaginal fistula is most common in females, while congenital anal atresia with rectoperineal fistula is most common in males[3]. At present, the pathology and pathogenesis of ARM are not completely clear, and it is mainly caused by developmental disorders of the enteric nervous system and perianal muscles during the embryonic period. Most children with ARM undergo complete anorectoplasty at preschool age, and the prognosis is generally good. However, it is rarely reported that anoplastic surgery is performed in adulthood, as reported below.

CASE PRESENTATION

Chief complaints

A 19-year-old unmarried Chinese woman presented to the anorectal surgery clinic with a complaint of congenital anal atresia from birth.

History of present illness

Abdominal pain and distension appeared again 6 d prior and could not be relieved.

History of past illness

The patient had a history of abdominal distension caused by constipation, and unformed loose stools were produced during defecation. At the age of 1 year, she was diagnosed but was not treated. Four months before admission, the patient was found to have abnormal bowel habits for 2-4 d a month, and the symptoms of abdominal pain and distension were relieved after resolving a large amount of loose stool. Computed tomography (CT) examination revealed intestinal obstruction, colon and rectum dilation with a large amount of contents, intestinal wall edema and thickening.

Personal and family history

The patient denied any family history of intestinal diseases.

Physical examination

Physical examination on admission: There were no abnormalities in the general examination of skin and mucosa; however, the physical examination of the perineum showed that there was no anus in the normal anal position, but there was an anal incisure, and a red and swollen defecation fistula measuring 10 mm in diameter in the rectovestibular, and no abnormalities in the location or appearance of the labia majora, labia minora, vagina or urethra opening (Figure 1A).

Laboratory examinations

No abnormality was found in routine blood and urine analyses.

Imaging examinations

Auxiliary examination: (1) Abdominal CT: Rectal dilation with intestinal wall thickening, with a maximum diameter of approximately 10 cm (Figure 1B); (2) X-ray imaging: The distal end of the rectum was the blind end and located approximately 6 cm away from the anal notch (Figure 1C); (3) pelvic MRI: A gap was visible in the upper section of the transverse anal canal (Figure 1D), the thickness of the internal sphincter of the anus was approximately 1 mm in the coronal position, some of the internal sphincter was discontinuous, the thickness of the external sphincter was approximately 2 mm in the sagittal position (Figure 1E), the positions of the rectum, vagina and fistula were visible in the sagittal position, and the fistula was adjacent to the posterior wall of the vagina (Figure 1F).

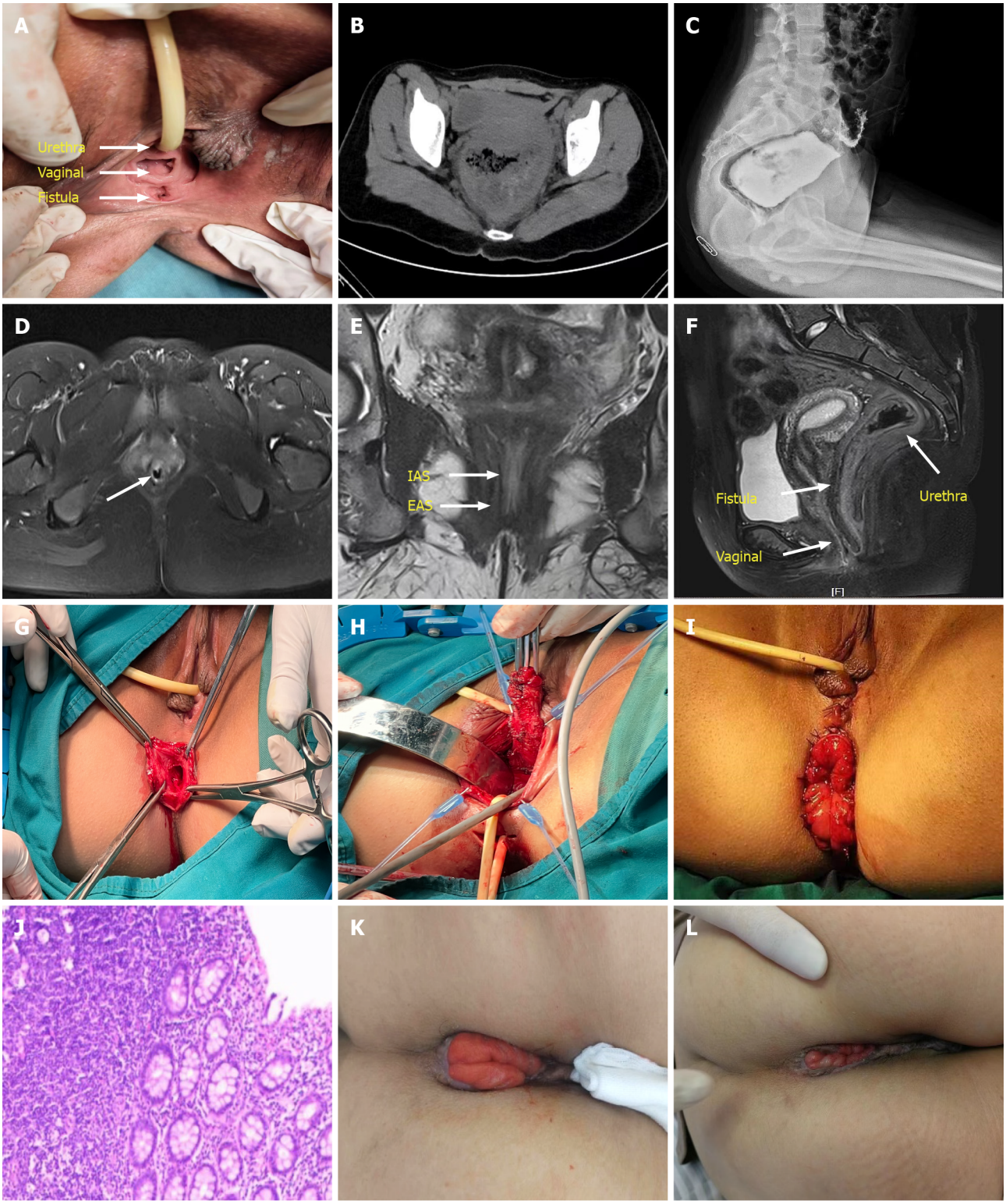

DOI: 10.12998/wjcc.v11.i33.8065 **Copyright** ©The Author(s) 2023.

Figure 1 Preoperative physical examination, imaging examination, operation process and postoperative follow-up were performed in this case. A: The vestibular fossa shows a defecation fistula, the position of the vagina, the urethral opening and the position of the fistula; B: Abdominal computed tomography showed rectal dilation with intestinal wall thickening, with a maximum diameter of approximately 10 cm; C: X-ray: The distal end of the rectum was blind, approximately 6 cm from the anal notch; D: Pelvic magnetic resonance imaging (MRI) cross-section closed the upper segment of the anal canal space, not completely closed; E: Pelvic MRI coronal view showed that the thickness of the internal sphincter was approximately 1 mm, part of the internal sphincter was discontinuous, and the thickness of the external sphincter was approximately 2 mm; F: Pelvic MRI sagittal view shows the position of the rectum, vagina and fistula, and the fistula is adjacent to the posterior wall of the vagina; G: Opening of the atretic anal canal reveals lacunae and muscle fibers; H: Free the fistula and rectum, pay attention to protect the superficial perineal striated muscle and the central tendon of the perineum, and carefully separate it from the posterior wall of the vagina to avoid causing damage to the vagina; I: Reconstruction of the vagina and perineal body, repair of vestibular wounds, intermittent suture of the space between the posterior wall of the vagina and the central tendon of the perineum, intermittent suture of the bulbospongeus muscle, counterposition suture of the vestibular mucosa

and submucosal tissue, repair of the hymen. The whole end of the new rectum was sutured to the subcutaneous dermis of the anus; J: Pathology: Moderate chronic inflammation of the mucosa, loose and swollen submucosa, and congestion of the gut wall; K: At the 2-mo follow-up, the rectal mucosa was slightly retracted; L: At the 4-mo follow-up, the rectal mucosa was almost retracted. IAS: Internal sphincter; EAS: External sphincter.

FINAL DIAGNOSIS

Combined with the patient's medical history, the final diagnosis was congenital anal atresia with a rectovestibular fistula.

TREATMENT

Postoperatively, the patient recovered well. The incision completely healed (Figure 1K) during the 2 mo after the operation. Anorectal manometry showed that the anal tube pressure at rest was low, with an average of 24 mmHg, while the anal tube resting pressure was low when squeezed, the duration was shorter than normal, and the anal stool control ability was weakened. The initial rectal sensation, initial bowel intention and maximum tolerance threshold were high, indicating a decrease in rectal sensitivity.

OUTCOME AND FOLLOW-UP

At the 4-mo follow-up, the rectal mucosa was almost retracted (Figure 1L). The resting pressure of the anal canal reached 48 mmHg after 2 courses of pelvic floor rehabilitation treatment. At present, the patient has undergone stoma closure and defecates 3 to 5 times a day without fecal incontinence.

DISCUSSION

Congenital anal atresia is one of the most common malformations in children, especially newborns. It is most common in female infants. Up to 95% of female cases may be complicated with fistula, among which congenital anorectal combined with rectovaginal fistula or vestibular fistula is more common. Congenital anal atresia occurs more frequently in eastern China than in central and western China, which may be related to environmental pollution[4] and gene mutations[5]. Anal malformation is a correctable congenital malformation that can have a good prognosis. Most of these abnormalities can be easily detected in the clinical examination of newborns, and most patients are surgically treated in infancy. It is rare for this patient to be treated at age 19. The main reason for the delay in surgery is the patient's parents. Moreover, the severity of the deformity increases with age, and its clinical manifestations are mainly constipation. Long-term constipation can be secondary to megacolon, and the operation is more difficult.

On the one hand, whether patients with congenital anal atresia can obtain good anal function after surgery depends on whether the pelvic floor muscles are developed, and more importantly, whether the anatomical structure of the rectal canal is restored through reasonable operation, and whether damage to the pelvic tissue is minimized, which reduces the risk of damage to the defecation receptors so as to ensure a normal defecation reflex after surgery.

Pena *et al*[6] originally proposed that anal atresia should be operated in three stages, namely, first-stage fistulae, second-stage anorectoplasty and third-stage fistula closure. The purpose is to avoid infection during anal reconstruction and subsequent anal retraction, anal stenosis, and fistula recurrence. In recent years, most scholars have advocated that one-stage surgery, despite the high risk of incision infection, can reduce the number of operations, reduce treatment costs, and avoid complications such as skin erosion, wound infection, and ostomy prolapse[7]. However, the patient was admitted to the hospital for emergency ileus, and the problems of difficult defecation and nutritional problems should be solved first. It is necessary to fully evaluate the condition and blindly performing a one-stage operation, which may lead to an increased incidence of anastomotic fistula and an increased chance of infection, leading to the failure of the operation.

The common surgical methods for congenital anal atresia with rectovestibular fistula include anterior and posterior sagittal approach anorectoplasty. The advantages are that the surgical field is wide and the operation is performed under direct vision. However, the surgical injury is large, the operation time is long, and the incision infection rate is high. Incision of the sphincter is needed during the operation, which increases the probability of postoperative fecal incontinence. Patients with poor stool control function are prone to rectal mucosal prolapse. Transfistula anorectoplasty is advantageous in that it causes less trauma, has a short operation time, and is safe. The integrity of the sphincter is not compromised; the procedure does not damage the important nerves or blood vessels on the side or back of the rectum. The fistula was completely resected in the patient, and no fistula recurrence was observed during postoperative follow-up. Therefore, the technical requirements for resection of a free fistula are high, and the fistula must be completely and carefully resected.

The patient was an adult with disuse sphincter atrophy, which may have poor stool control function after surgery. During the operation, the remaining muscle should be protected and utilized as much as possible, and the physiological and anatomical position of the rectum should be restored as much as possible, which is the key to obtaining good

postoperative stool control ability. After fistula resection, vestibular area repair can also achieve good cosmetic results.

The most common complication after anorectoplasty is poor defecation control, with an incontinence rate as high as 10%-75%. Some surgeons have noted that the distal rectum lacks normal innervation and a muscle layer. To ensure good anal function after surgery, it is recommended to remove at least 3 cm of the distal rectum, while some scholars believe that the distal rectum should have an internal sphincter structure[8]. Pathological studies have shown that patients with congenital anal atresia have abnormal changes at the end of the rectum, such as dysplasia of ganglion cells in the intestinal wall, muscle fibrosis in the rectal wall and no relaxation reflex of the internal rectal sphincter, and even postoperative development of intractable constipation secondary to megacolon, requiring surgical treatment. The absence of expression of ganglion cells and Cajal interstitial cells will affect the signal transmission process of the bowel defecation reflex after surgery, thus affecting postoperative defecation dysfunction[9]. In this patient, rectal inflammation and thickening were obvious, and the function was poor. The distal diseased rectum was removed during the operation, and a new rectum was rebuilt.

Because the patient has not defecated in a normal position for many years, the thickness of the sphincter is significantly reduced compared with that of normal people, so there is a high possibility of postoperative anal dysfunction. Anorectal manometry at 2 mo postoperatively showed that the anorectal resting pressure and contraction pressure were both lower than the normal range. The patient was advised to actively perform pelvic floor rehabilitation and anal lift training exercises before the fistula closure procedure to enhance their bowel control ability. After anal lift training, the rectal mucosa was more retracted than before. Some surgeons' excessive aesthetic pursuits lead to postoperative rectal retraction and narrowing. In addition, the patient was an unmarried woman who would later become pregnant and give birth, and cesarean section may be a safer operation for her to prevent damage to the anal sphincter and vagina.

CONCLUSION

In short, treatment of anal atresia is relatively rare after adulthood. The patient underwent transfistulae anorectoplasty with clear visual field exposure and the ability to separate the rectovaginal septum under direct vision, greatly reducing the possibility of vaginal injury and ensuring the integrity of the sphincter. It is a reasonable and reliable surgical method for the treatment of congenital anal atresia and rectovestibular fistula and is worth clinical promotion and application. However, the patient is more likely to experience anal dysfunction in the long term. Regular pelvic floor rehabilitation training is recommended, and further follow-up is needed.

ACKNOWLEDGEMENTS

The authors thank the patient who consented to having her data published in this case report.

FOOTNOTES

Co-first authors: Jun Wang and Xin-Yi Zhang.

Author contributions: Wang J, Zhang XY, and Jin HY designed the study; Wang J and Zhang XY wrote the manuscript and analyzed the data; Wang J and Zhang XY contributed equally to this work; Jin HY and Chen JH supervised coordination and the design of the study; All the authors have read and approved the final manuscript; All authors have consented to the publication of this study.

Informed consent statement: Informed written consent was obtained from the patient for publication of this report and any accompanying images.

Conflict-of-interest statement: All the authors declare that they have no conflicts of interest to disclose.

CARE Checklist (2016) statement: The authors have read the CARE Checklist (2016), and the manuscript was prepared and revised according to the CARE Checklist (2016).

Open-Access: This article is an open-access article that was selected by an in-house editor and fully peer-reviewed by external reviewers. It is distributed in accordance with the Creative Commons Attribution NonCommercial (CC BY-NC 4.0) license, which permits others to distribute, remix, adapt, build upon this work non-commercially, and license their derivative works on different terms, provided the original work is properly cited and the use is non-commercial. See: https://creativecommons.org/Licenses/by-nc/4.0/

Country/Territory of origin: China

ORCID number: Jun Wang 0009-0000-1247-2994; Xin-Yi Zhang 0000-0002-8363-9824; Ji-Han Chen 0009-0000-1934-6878; Hei-Ying Jin 0000-0002-8003-9267.

S-Editor: Liu JH
L-Editor: A

P-Editor: Liu JH

REFERENCES

1 **Rintala RJ**. Congenital anorectal malformations: anything new? *J Pediatr Gastroenterol Nutr* 2009; **48** Suppl 2: S79-S82 [PMID: 19300133 DOI: 10.1097/MPG.0b013e3181a15b5e]

2 **Wang JH**, Zhao XW, Dai CJ. Clinical application of laparoscopic assisted primary arthroplasty of high anal atresia. *Guangdong Med***37**: 876-878 [DOI: 10.13820/j.cnki.gdyx.2016.06.021]

3 **Bhatnagar S**. Anorectal malformations (part 1). *J Neonatal Surg* 2015; **4**: 7 [PMID: 26023531]

4 **Yuan P**, Qiao L, Dai L, Wang YP, Zhou GX, Han Y, Liu XX, Zhang X, Cao Y, Liang J, Zhu J. Spatial distribution patterns of anorectal atresia/stenosis in China: use of two-dimensional graph-theoretical clustering. *World J Gastroenterol* 2009; **15**: 2787-2793 [PMID: 19522031 DOI: 10.3748/wjg.15.2787]

5 **Priyatini T**, Roziana. Transfistula anorectoplasty on adult female anorectal malformation: A rare case report. *Int J Surg Case Rep* 2020; **74**: 182-185 [PMID: 32889246 DOI: 10.1016/j.ijscr.2020.08.014]

6 **deVries PA**, Peña A. Posterior sagittal anorectoplasty. *J Pediatr Surg* 1982; **17**: 638-643 [PMID: 7175658 DOI: 10.1016/s0022-3468(82)80126-7]

7 **Amanollahi O**, Ketabchian S. One-stage vs. three-stage repair in anorectal malformation with rectovestibular fistula. *Afr J Paediatr Surg* 2016; **13**: 20-25 [PMID: 27251519 DOI: 10.4103/0189-6725.181702]

8 **Lombardi L**, Bruder E, Caravaggi F, Del Rossi C, Martucciello G. Abnormalities in "low" anorectal malformations (ARMs) and functional results resecting the distal 3 cm. *J Pediatr Surg* 2013; **48**: 1294-1300 [PMID: 23845621 DOI: 10.1016/j.jpedsurg.2013.03.026]

9 **Zhan JH**, Hu B, Luo X. Clinicopathological study of remote rectal resection of congenital anal atresia. *Zhonghua Xiaoer Waike Zazhi* 2011; **32**: 154-156 [DOI: 10.3760/cma.j.issn.0253-3006.2011.02.019]

World Journal of Clinical Cases

Submit a Manuscript: https://www.f6publishing.com

World J Clin Cases 2023 November 26; 11(33): 8071-8077

DOI: 10.12998/wjcc.v11.i33.8071

ISSN 2307-8960 (online)

CASE REPORT

Cerebral proliferative angiopathy in pediatric age presenting as neurological disorders: A case report

Fu-Ren Luo, Ying Zhou, Zhong Wang, Qi-Yu Liu

Specialty type: Neuroimaging

Provenance and peer review: Unsolicited article; Externally peer reviewed.

Peer-review model: Single blind

Peer-review report's scientific quality classification

Grade A (Excellent): 0
Grade B (Very good): 0
Grade C (Good): C
Grade D (Fair): 0
Grade E (Poor): 0

P-Reviewer: Pavlovic M, Serbia

Received: September 9, 2023
Peer-review started: September 9, 2023
First decision: October 24, 2023
Revised: October 29, 2023
Accepted: November 14, 2023
Article in press: November 14, 2023
Published online: November 26, 2023

Fu-Ren Luo, Qi-Yu Liu, Department of Radiology, The Affiliated Hospital of Southwest Medical University, Luzhou 646000, Sichuan Province, China

Ying Zhou, Zhong Wang, Department of Radiology, Mianyang Central Hospital, Mianyang 621000, Sichuan Province, China

Corresponding author: Qi-Yu Liu, MD, Chief Doctor, Professor, Department of Radiology, The Affiliated Hospital of Southwest Medical University, No. 25 Taiping Street, Luzhou 646000, Sichuan Province, China. lqy2225085@163.com

Abstract

BACKGROUND

Cerebral proliferative angiopathy (CPA) is a rare subtype of arteriovenous malformation. It is extremely rare in pediatric patients and has serious implications for developing children. However, reports of these disorders worldwide are limited, and no uniform reference for diagnosis and treatment options exists. We report the case of a 6-year-old with CPA having predominantly neurological dysfunction and review the literature on pediatric CPA.

CASE SUMMARY

We report the case of a pediatric patient with CPA analyzed using digital subtraction angiography (DSA) who presented initially with a neurological disorder as the main manifestation. This case is the basis for further discussion of the clinical presentation, pathogenesis, diagnosis, and treatment of CPA in children. After the cerebral DSA, the patient was treated conservatively with sedation, fluid replacement, and blood anticoagulation. She could not cooperate with the follow-up magnetic resonance imaging examination because of her young age, and her family declined further treatment because of the surgery's high risk. She was followed up for 3 months; her symptoms did not worsen.

CONCLUSION

This report of rare pediatric CPA can inform and advance clinical research on congenital cerebrovascular diseases.

Key Words: Pediatric cerebral proliferative angiopathy; Pathogenesis; Diagnosis; Treatment; Case report

©The Author(s) 2023. Published by Baishideng Publishing Group Inc. All rights reserved.

Core Tip: Cerebral proliferative angiopathy (CPA) is a type of ischemic cerebrovascular disease that is extremely rare in pediatric patients and has serious implications for developing children. However, reports of these disorders are limited, and no uniform reference for diagnosis and treatment options exists. This article reviews the literature on pediatric CPA from a case of CPA in a child with predominantly neurological dysfunction. We summarize the relevant clinical, diagnostic, therapeutic, and pathogenic explorations and provide suggestions for subsequent research on this disorder.

Citation: Luo FR, Zhou Y, Wang Z, Liu QY. Cerebral proliferative angiopathy in pediatric age presenting as neurological disorders: A case report. *World J Clin Cases* 2023; 11(33): 8071-8077
URL: https://www.wjgnet.com/2307-8960/full/v11/i33/8071.htm
DOI: https://dx.doi.org/10.12998/wjcc.v11.i33.8071

INTRODUCTION

Arteriovenous malformations (AVMs) are diagnosed increasingly as cerebrovascular pathologies because of improved diagnostic techniques. Cerebral proliferative angiopathy (CPA) is a rare variant of AVM that has unique clinical and imaging characteristics; its vascular structures are smaller than the usual blood-supplying arteries and draining veins with the lesion characterized by diffuse proliferating vessels intermixed with the brain parenchyma. CPA lesions often exhibit an epidural blood supply. Patients with CPA commonly present with seizures accompanied by headaches and intracranial hemorrhage[1]; some experience neurological deficits. Unlike AVM, CPA is more likely to be caused by ischemia than hemorrhage. CPA affects young women primarily[1] and is extremely rare in pediatrics.

Based on the histological studies of Chin *et al*[2], CPA vessels have been hypothesized to proliferate in response to unknown signals derived from cortical ischemia. However, the pathogenesis of CPA remains unknown. This study reports the case of a 6-year-old with CPA who presented with predominantly neurological dysfunction. We also review the literature on pediatric CPA, summarize the relevant clinical, diagnostic, therapeutic, and pathogenic explorations, and provide suggestions for subsequent research on this disorder.

CASE PRESENTATION

Chief complaints

The patient was a 6-year-old girl who had experienced transient unsteadiness and slurred speech for 2 years.

History of present illness

The patient was diagnosed with Moyamoya disease using magnetic resonance imaging (MRI) and magnetic resonance angiography (MRA) at another hospital, where she presented with transient unsteadiness and slurred speech lasting several minutes per episode. She complained of the symptoms after eating peppers.

History of past illness

The patient had no previous history of any disease.

Personal and family history

The patient had no known exposure to epidemic areas/water, epidemics, industrial toxins, dust, or radioactive material. The child's uncle had a history of Moyamoya disease; no other family hereditary diseases or tumors were reported.

Physical examination

The positive signs on physical examination included occasional slurred speech and incomplete right eyelid closure.

Laboratory examinations

The patient's liver function, renal function, electrolyte levels, blood coagulation, and urine test results were all negative; blood tests revealed no significant abnormalities.

Imaging examinations

MRI and MRA examinations of the head detected softening foci in the left frontal and parietal lobes and the right parietal lobe. The examinations also revealed localized stenosis of the C2 segment of the left internal carotid artery; bilateral stenosis of the beginning of the middle cerebral artery; segmental stenosis of the M1 segment, small distal middle cerebral artery and branches; thickened and tortuous adjacent meningeal vessels; an unclear lumen at the beginning of the bilateral anterior cerebral artery; and multiple thickened and tortuous surrounding vascular networks (Figure 1).

Cerebral digital subtraction angiography (DSA) showed occlusions in the internal carotid arteries from the posterior communicating artery to the far side of the brain, numerous anomalous hyperplastic capillaries in the area supplied by

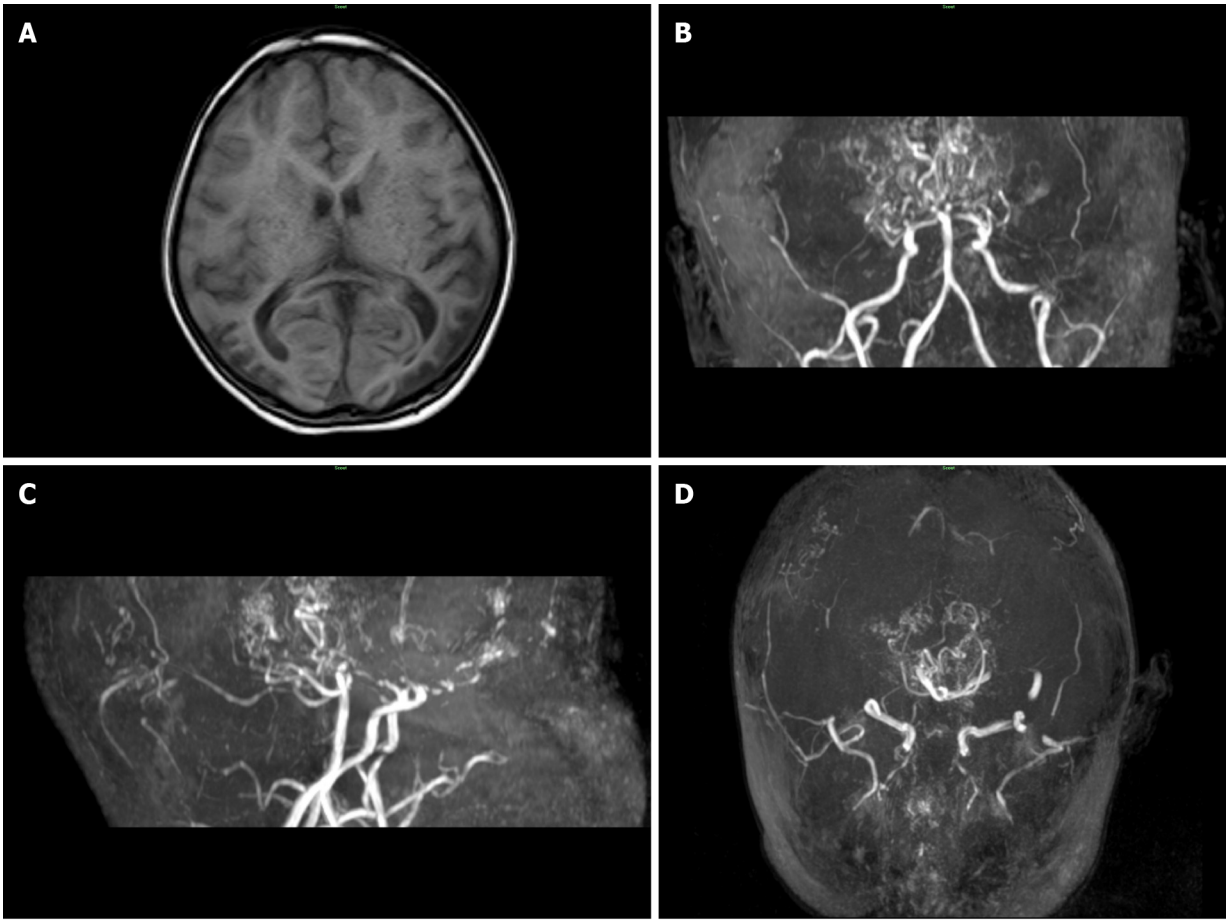

DOI: 10.12998/wjcc.v11.i33.8071 **Copyright** ©The Author(s) 2023.

Figure 1 Head magnetic resonance imaging. A: Head T1 image; B-D: Bilateral stenosis at the beginning of the middle cerebral artery, thickening and tortuosity of adjacent meningeal vessels, and multiple thickening and tortuosity of the surrounding vascular network.

the internal carotid arteries and the posterior cerebral arteries bilaterally, and several branches of the external carotid arteries and dural vessels supplying blood to the intracranial area (Figures 2 and 3).

FINAL DIAGNOSIS

The final diagnosis was pediatric CPA.

TREATMENT

The child showed no obvious signs of intracranial hemorrhage or infarction on imaging examinations for mild neurological symptoms. Cerebral DSA showed clear CPA features. Because of this diagnosis and presentation, no specific treatment was provided; only conservative treatment with sedation, fluid replacement, and blood anticoagulation was administered after the cerebral DSA angiography procedure. The patient could not cooperate with the follow-up MRI examination because of her young age. The patient's family declined further treatment and decided to discharge her because of the surgery's high risk.

OUTCOME AND FOLLOW-UP

The child was followed up for 3 mo; no further worsening of symptoms was observed.

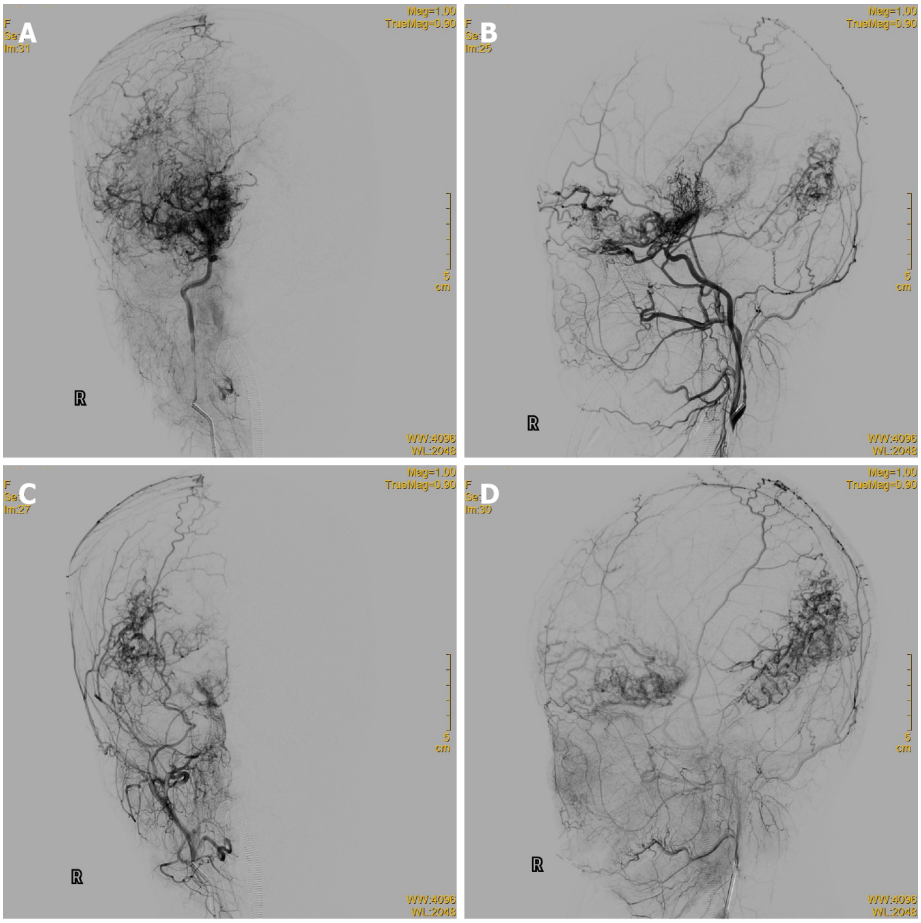

DOI: 10.12998/wjcc.v11.i33.8071 **Copyright** ©The Author(s) 2023.

Figure 2 Brain digital subtraction angiography. A: Anteroposterior view of a right internal carotid artery (ICA) angiogram; B: Lateral view of a right ICA angiogram; C: Anteroposterior view of a right external carotid artery (ECA) angiogram; D: Lateral view of a right ECA angiogram. Diffuse vascular malformations and transmural blood supply can be observed.

DISCUSSION

Lasjaunias *et al*[1] reported case data from 1434 patients with AVM; 49 (3.4%) were screened for CPA in a retrospective study. CPA episodes are predominant in young adult women[1]. This study collected and summarized the clinical, epidemiological, and prognostic follow-up data of pediatric CPA. Includes not only new cases within the last 5 years[3-8] but also older cases[9-18]. The review literature reported 21 pediatric CPA cases, with a mean patient age of 10.4 years and an age range of 2–18 years. Of these 21 children, excluding one case where the authors did not specify the sex, 11 (55%) were female, and 9 (45%) were male, consistent with Lasjaunias's findings. Cerebral hemorrhage was usually the primary presentation in classic pediatric AVM (70%, n = 100)[19]; headache (57%), epilepsy (29%), and limb weakness (24%) were more common in pediatric CPA. Although hemorrhage is rare, the risk of rebleeding is high[20]. In our case, the patient did not experience significant headache or seizure symptoms and had only occasional slurred speech and limb weakness.

CPA is diagnosed based on typical imaging features. Its morphology differs from typical AVMs: MRI shows multiple large vessels entangled and interspersed with brain parenchyma; computed tomography shows a heterogeneous lesion with a densely enhanced vascular meshwork, frequently involving one or more lobes. MRI sequences showed a flowing void effect within the lesion and diffuse enhancement on T1 sequences. DSA imaging revealed a diffusely proliferating capillary network with rapid blood flow, frequent epidural blood supply, and multiple narrowing of the supplying arteries[15]. CPA is characterized by the absence of thick blood-supplying arteries and draining veins, interspersed with brain parenchyma, neurons in the vascular network, and aneurysms in the blood-supplying arteries[7,18]. Vascular lesions in the CPA are unstable; some patients have imaging findings that suggest continued lesion growth[18].

Traditional AVM treatments involve mostly resection, endovascular embolization, or radiation therapy[21]. Pediatric patients with CPA present with headache as the main manifestation; ischemic symptoms manifest more commonly than hemorrhages. Any surgical, interventional, or radiological treatment of pediatric CPA may worsen symptoms because of normal nerve tissue in the vascular network of CPA lesions. In pediatric patients with CPA, conservative treatment aimed at symptom control is preferred, including anticoagulation, antithrombotic, and antiepileptic medications. These treatments are effective in controlling the symptoms of most patients; however, some patients have subsequent cerebral hemorrhaging due to the continued lesion growth[3]. Gamma knife[22] and endovascular embolization[23] relieve

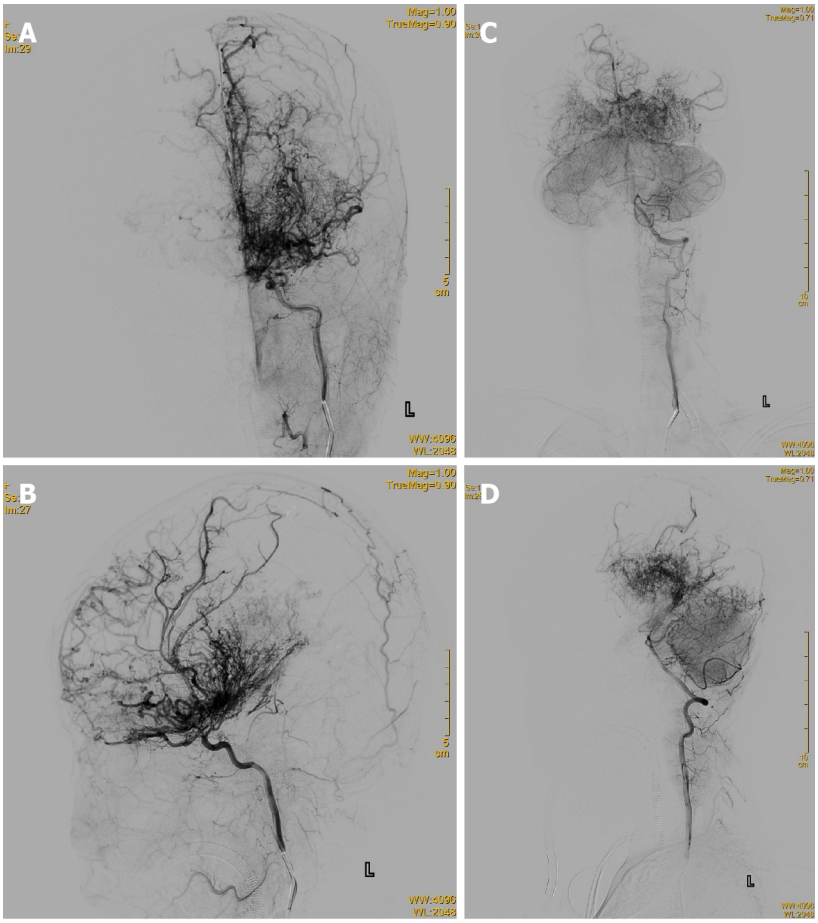

DOI: 10.12998/wjcc.v11.i33.8071 **Copyright** ©The Author(s) 2023.

Figure 3 Brain digital subtraction angiography. A: Anteroposterior view of a left internal carotid artery (ICA) angiogram; B: Lateral view of a left ICA angiogram; C: Anteroposterior view of a right vertebral artery (VA) angiogram; D: Lateral view of VA angiogram.

headaches effectively in patients with CPA, which is difficult to control medically; however, these treatments are less effective for other symptoms of neurological dysfunction, including slurred speech and hemiparesis. Surgical resection has been an option for treating CPA since 2021, when Choi *et al*[6] reported the first successful surgical resection of a CPA lesion despite its extreme risks. Ochoa *et al*[4] in 2022 performed surgical resection on two patients with pediatric CPA. Patients were free of significant recurrence at 3–6 years of follow-up. Other surgical procedures, such as indirect revascularization, have also been proven effective. Kimiwada *et al*[8] and Ellis *et al*[16] used an indirect revascularization procedure to improve patients' symptoms; no worsening of symptoms at a minimum 1-year follow-up was reported.

CPA's pathophysiological type differs from AVM because of its specific vascular configuration. Vargas *et al*[15] demonstrated that patients with CPA have significantly longer mean capillary passage times and multiple segmental arterial stenoses, leading to reduced perfusion of the surrounding brain tissue. Marks *et al*[23] reported a patient with CPA having high levels of vascular endothelial growth factor, thrombin reactive protein, and fibroblast growth factor in the cerebrospinal fluid. This finding suggests CPA may be the body's overreaction to unexplained ischemia, ultimately leading to the proliferation of vascular endothelial cells followed by uncontrolled vascular proliferation. Because CPA and Moyamoya disease have relatively similar pathophysiological mechanisms, they might be confused in clinical diagnosis. However, no direct comparison exists in the literature; further research is required.

CONCLUSION

CPA is a rare ischemic cerebrovascular disease with a much lower incidence in the pediatric population. Most pediatric cases have headaches as the main clinical manifestation; patients achieve good outcomes through medical treatment and observation. Since CPA was introduced as a separate disease category in 2008, research into its pathogenesis, diagnosis, and treatment has advanced; however, the treatment still has no definitive consensus. More high-quality research is required to support the existing studies in developing evidence-based treatment guidelines for CPA.

FOOTNOTES

Author contributions: Luo FR contributed to manuscript writing and editing and data collection; Wang Z contributed to data analysis; Zhou Y contributed to conceptualization and supervision; all authors have read and approved the final manuscript.

Informed consent statement: This report and the accompanying photographs have been published with a waiver of informed consent granted by the Ethical Review Board.

Conflict-of-interest statement: All the authors declare that they have no conflict of interest to disclose.

CARE Checklist (2016) statement: The authors have read the CARE Checklist (2016), and the manuscript was prepared and revised according to the CARE Checklist (2016).

Open-Access: This article is an open-access article that was selected by an in-house editor and fully peer-reviewed by external reviewers. It is distributed in accordance with the Creative Commons Attribution NonCommercial (CC BY-NC 4.0) license, which permits others to distribute, remix, adapt, build upon this work non-commercially, and license their derivative works on different terms, provided the original work is properly cited and the use is non-commercial. See: https://creativecommons.org/Licenses/by-nc/4.0/

Country/Territory of origin: China

ORCID number: Fu-Ren Luo 0009-0008-2964-6020; Ying Zhou 0000-0003-0364-8622; Zhong Wang 0000-0002-6391-9140; Qi-Yu Liu 0000-0002-8166-3134.

S-Editor: Liu JH
L-Editor: A
P-Editor: Liu JH

REFERENCES

1 **Lasjaunias PL**, Landrieu P, Rodesch G, Alvarez H, Ozanne A, Holmin S, Zhao WY, Geibprasert S, Ducreux D, Krings T. Cerebral proliferative angiopathy: clinical and angiographic description of an entity different from cerebral AVMs. *Stroke* 2008; **39**: 878-885 [PMID: 18239181 DOI: 10.1161/STROKEAHA.107.493080]
2 **Chin LS**, Raffel C, Gonzalez-Gomez I, Giannotta SL, McComb JG. Diffuse arteriovenous malformations: a clinical, radiological, and pathological description. *Neurosurgery* 1992; **31**: 863-8; discussion 868 [PMID: 1436409]
3 **Saito T**, Harada K, Kajihara M, Sanbongi C, Fukuyama K. Long-term hemodynamic changes in cerebral proliferative angiopathy presenting with intracranial hemorrhage: illustrative case. *J Neurosurg Case Lessons* 2023; **5** [PMID: 37070681 DOI: 10.3171/CASE22437]
4 **Ochoa A**, Mantese B, Requejo F. Hemorrhagic cerebral proliferative angiopathy in two pediatric patients: case reports. *Childs Nerv Syst* 2022; **38**: 789-794 [PMID: 33956211 DOI: 10.1007/s00381-021-05181-0]
5 **Rebello A**, Ahuja CK, Aleti S, Singh R. Cerebral proliferative angiopathy: a rare cause of stroke and seizures in young. *BMJ Case Rep* 2021; **14** [PMID: 33574046 DOI: 10.1136/bcr-2020-240468]
6 **Choi GY**, Choi HJ, Jeon JP, Yang JS, Kang SH, Cho YJ. Removal of malformation in cerebral proliferative angiopathy: illustrative case. *J Neurosurg Case Lessons* 2021; **1**: CASE2095 [PMID: 35854705 DOI: 10.3171/CASE2095]
7 **Beniwal M**, Kandregula S, Aravind, Rao KVLN, Vikas V, Srinivas D. Pediatric cerebral proliferative angiopathy presenting infratentorial hemorrhage. *Childs Nerv Syst* 2020; **36**: 429-433 [PMID: 31338577 DOI: 10.1007/s00381-019-04313-x]
8 **Kimiwada T**, Hayashi T, Takahashi M, Shirane R, Tominaga T. Progressive Cerebral Ischemia and Intracerebral Hemorrhage after Indirect Revascularization for a Patient with Cerebral Proliferative Angiopathy. *J Stroke Cerebrovasc Dis* 2019; **28**: 853-858 [PMID: 30737070 DOI: 10.1016/j.jstrokecerebrovasdis.2018.11.021]
9 **Maekawa H**, Terada A, Ishiguro T, Komiyama M, Lenck S, Renieri L, Krings T. Recurrent periventricular hemorrhage in cerebral proliferative angiopathy: Case report. *Interv Neuroradiol* 2018; **24**: 713-717 [PMID: 29991310 DOI: 10.1177/1591019918787265]
10 **Zheng WJ**. [Experimental study on the treatment of spinal cord injury with transplantation of the greater omentum]. *Zhonghua Wai Ke Za Zhi* 1989; **27**: 93-95, 125 [PMID: 2776547 DOI: 10.1016/j.pediatrneurol.2016.09.012]
11 **Srivastava T**, Mathur T, Jain R, Sannegowda RB. Cerebral proliferative angiopathy: A rare clinical entity with peculiar angiographic features. *Ann Indian Acad Neurol* 2013; **16**: 674-675 [PMID: 24339605 DOI: 10.4103/0972-2327.120477]
12 **Kimiwada T**, Hayashi T, Shirane R, Tominaga T. 123I-IMP-SPECT in a patient with cerebral proliferative angiopathy: a case report. *J Stroke Cerebrovasc Dis* 2013; **22**: 1432-1435 [PMID: 23830953 DOI: 10.1016/j.jstrokecerebrovasdis.2013.05.038]
13 **Khan A**, Rattihalli R, Beri S, Dickinson F, Hussain N, Gosalakkal J. Cerebral proliferative angiopathy: a rare form of vascular malformation. *J Paediatr Child Health* 2013; **49**: 504-505 [PMID: 23724816 DOI: 10.1111/jpc.12233]
14 **Gold JJ**, Crawford JR. Acute hemiparesis in a child as a presenting symptom of hemispheric cerebral proliferative angiopathy. *Case Rep Neurol Med* 2013; **2013**: 920859 [PMID: 23476841 DOI: 10.1155/2013/920859]
15 **Vargas MC**, Castillo M. Magnetic resonance perfusion imaging in proliferative cerebral angiopathy. *J Comput Assist Tomogr* 2011; **35**: 33-38 [PMID: 21245687 DOI: 10.1097/RCT.0b013e3181ff1e79]
16 **Ellis MJ**, Armstrong D, Dirks PB. Large vascular malformation in a child presenting with vascular steal phenomenon managed with pial synangiosis. *J Neurosurg Pediatr* 2011; **7**: 15-21 [PMID: 21194281 DOI: 10.3171/2010.10.PEDS10388]
17 **Fierstra J**, Spieth S, Tran L, Conklin J, Tymianski M, ter Brugge KG, Fisher JA, Mikulis DJ, Krings T. Severely impaired cerebrovascular reserve in patients with cerebral proliferative angiopathy. *J Neurosurg Pediatr* 2011; **8**: 310-315 [PMID: 21882924 DOI: 10.3171/2011.6.PEDS1170]

18 **Liu P**, Lv X, Lv M, Li Y. Cerebral proliferative angiopathy: Clinical, angiographic features and literature review. *Interv Neuroradiol* 2016; **22**: 101-107 [PMID: 26472638 DOI: 10.1177/1591019915609784]

19 **Nicolato A**, Longhi M, Tommasi N, Ricciardi GK, Spinelli R, Foroni RI, Zivelonghi E, Zironi S, Dall'Oglio S, Beltramello A, Meglio M. Leksell Gamma Knife for pediatric and adolescent cerebral arteriovenous malformations: results of 100 cases followed up for at least 36 mo. *J Neurosurg Pediatr* 2015; **16**: 736-747 [PMID: 26339954 DOI: 10.3171/2015.4.PEDS158]

20 **Yamaki VN**, Solla DJF, Telles JPM, Liem GLJ, da Silva SA, Caldas JGMP, Teixeira MJ, Paschoal EHA, Figueiredo EG. The current clinical picture of cerebral proliferative angiopathy: systematic review. *Acta Neurochir (Wien)* 2020; **162**: 1727-1733 [PMID: 32206904 DOI: 10.1007/s00701-020-04289-7]

21 **Zyck S**, Davidson CL, Sampath R. Arteriovenous Malformations. 2022 Aug 15. In: StatPearls [Internet]. Treasure Island (FL): StatPearls Publishing; 2023 Jan- [PMID: 30285374]

22 **Hong KS**, Lee JI, Hong SC. Neurological picture. Cerebral proliferative angiopathy associated with haemangioma of the face and tongue. *J Neurol Neurosurg Psychiatry* 2010; **81**: 36-37 [PMID: 20019220 DOI: 10.1136/jnnp.2009.183277]

23 **Marks MP**, Steinberg GK. Cerebral proliferative angiopathy. *J Neurointerv Surg* 2012; **4**: e25 [PMID: 21990497 DOI: 10.1136/neurintsurg-2011-010027]

World Journal of Clinical Cases

Submit a Manuscript: https://www.f6publishing.com

World J Clin Cases 2023 November 26; 11(33): 8078-8083

DOI: 10.12998/wjcc.v11.i33.8078

ISSN 2307-8960 (online)

CASE REPORT

Hepatocellular carcinoma presenting as organized liver abscess: A case report

Sung Hyeok Ryou, Hyun Deok Shin, Suk Bae Kim

Specialty type: Medicine, research and experimental

Provenance and peer review: Unsolicited article; Externally peer reviewed.

Peer-review model: Single blind

Peer-review report's scientific quality classification

Grade A (Excellent): 0
Grade B (Very good): B, B
Grade C (Good): C
Grade D (Fair): 0
Grade E (Poor): 0

P-Reviewer: Maslennikov R, Russia; Pan Y, China

Received: October 4, 2023
Peer-review started: October 4, 2023
First decision: October 24, 2023
Revised: November 2, 2023
Accepted: November 17, 2023
Article in press: November 17, 2023
Published online: November 26, 2023

Sung Hyeok Ryou, Hyun Deok Shin, Suk Bae Kim, Department of Internal Medicine, Dankook University College of Medicine, Cheonan 31116, Chungnam, South Korea

Corresponding author: Suk Bae Kim, MD, PhD, Professor, Department of Internal Medicine, Dankook University College of Medicine, 119 Dandae-ro, Dongnam-gu, Cheonan 31116, Chungnam, South Korea. dryakson@hanmail.net

Abstract

BACKGROUND

Hepatocellular carcinoma (HCC) is difficult to treat and has a high mortality rate, emphasizing the importance of early diagnosis and treatment. If characteristic radiologic findings and underlying liver disease are present, a diagnosis can be made without a biopsy. However, when HCC is accompanied by a liver abscess, diagnosis might be delayed by atypical radiologic findings. This case report aims to assist in the diagnosis of HCC, which can manifest in various forms.

CASE SUMMARY

A 75-year-old male presented to the Emergency Department with worsening fever and mental changes. He was diagnosed with liver cirrhosis six months earlier. Abdominal computed tomography (CT) raised our suspicion of an organized liver abscess. A follow-up CT scan after four weeks of antibiotic treatment showed a decrease in the liver lesion size. However, high fever recurred, and C-reactive protein increased to 14 mg/L. Aspiration of the liver lesion was performed, but no bacteria were identified. Blood culture revealed the presence of fungi. The patient received an additional four weeks of antibiotics and antifungal agents before being discharged. Approximately 10 mo later, a CT scan showed an increase in the lesion size, and biopsy was performed. The biopsy revealed an organized abscess with focal carcinomatous changes, for which surgery was performed. Postoperative histopathological examination revealed HCC, clear-cell variant. The nontumor liver tissue showed cirrhosis and an organized abscess.

CONCLUSION

Even if a liver abscess is suspected in a patient with cirrhosis, the possibility of HCC should be considered.

Key Words: Liver abscess; Hepatocellular carcinoma; Infection; Diagnosis; Case report

©The Author(s) 2023. Published by Baishideng Publishing Group Inc. All rights reserved.

Core Tip: Hepatocellular carcinoma (HCC) is more difficult to treat and has a higher mortality rate than other carcinomas, emphasizing the importance of early diagnosis. Radiologic examination is crucial for diagnosing HCC. If characteristic findings and underlying liver disease are present, a diagnosis can be made, but when HCC is accompanied by a liver abscess, diagnosis may be delayed by atypical radiologic findings. The present patient was hospitalized for an organized liver abscess with calcification but was subsequently diagnosed with HCC. This case report aims to assist in the diagnosis of HCC, which can manifest in various forms.

Citation: Ryou SH, Shin HD, Kim SB. Hepatocellular carcinoma presenting as organized liver abscess: A case report. *World J Clin Cases* 2023; 11(33): 8078-8083
URL: https://www.wjgnet.com/2307-8960/full/v11/i33/8078.htm
DOI: https://dx.doi.org/10.12998/wjcc.v11.i33.8078

INTRODUCTION

Liver cancer ranks fifth in global cancer incidence and fourth in cancer-related death[1]. Over 80% of liver cancers are hepatocellular carcinoma (HCC), while intrahepatic cholangiocarcinoma accounts for 10%-15%[2]. The lower survival rate of liver cancer compared to other types of cancer is primarily due to the difficulty of curative treatment in advanced stages. Since HCC is often already advanced at the time of diagnosis, early diagnosis is crucial. This can be challenging when typical radiological findings are absent or when they are accompanied by other conditions. In particular, diagnosing HCC presenting as a liver abscess can be difficult, as the clinician may be unlikely to suspect hidden HCC in the presence of typical abscess symptoms such as fever, pain, and blood test findings. This case report describes a patient who was admitted with fever, sepsis, and acute pyelonephritis and displayed organized liver abscess findings with calcification in the liver. Initially, the liver abscess size decreased during treatment, but it later increased, leading to tissue biopsy and surgery, which confirmed the diagnosis of HCC. This report discusses our process of reaching the final diagnosis of HCC based on the patient's clinical course following the initial diagnosis of liver abscess.

CASE PRESENTATION

Chief complaints

A 75-year-old male visited the Emergency Department with worsening general weakness, loss of appetite, fever, and mental changes for 2-3 d.

History of present illness

General weakness, loss of appetite, and mild fever began 3 d earlier. The mental change that started 2 d prior prompted him visit the Emergency Department.

History of past illness

The patient had been admitted for general weakness six months prior, at which time he was diagnosed with liver cirrhosis (Child-Pugh Class A) based on abdominal ultrasound. The cause of the cirrhosis was unknown.

Personal and family history

There was no history of malignancy or underlying liver disease in the family.

Physical examination

The patient's vital signs were as follows: Blood pressure 89/69 mmHg, respiratory rate 25 breaths/min, heart rate 112 beats/min and body temperature 38.2°C. As patient's consciousness was not clear at the time of admission to the Emergency Department, a proper physical examination could not be conducted. After the patient's consciousness improved, a physical examination was performed, during which the patient complained of discomfort and tenderness in the upper right abdomen.

Laboratory examinations

Laboratory tests revealed white blood cell 13200/μL, hemoglobin 11.5 g/dL, platelet 57000/μL, C-reactive protein (CRP) 14 mg/L, aspartate aminotransferase/alanine aminotransferase 117/89 U/L, total bilirubin 2.3 mg/dL, albumin 3.1 g/dL, prothrombin time 15.7 S, blood urea nitrogen 34 mg/dL, creatinine 2.5 mg/dL, -fetoprotein (AFP) 2.8 ng/mL, protein induced by vitamin K absence II 18 mAU/mL, hepatitis B surface antigen/antibody (-/+), and anti- hepatitis C virus (-). Urinalysis showed nitrite (+) and many bacteria. Urine culture revealed extended-spectrum beta-lactamase-positive *Escherichia coli*.

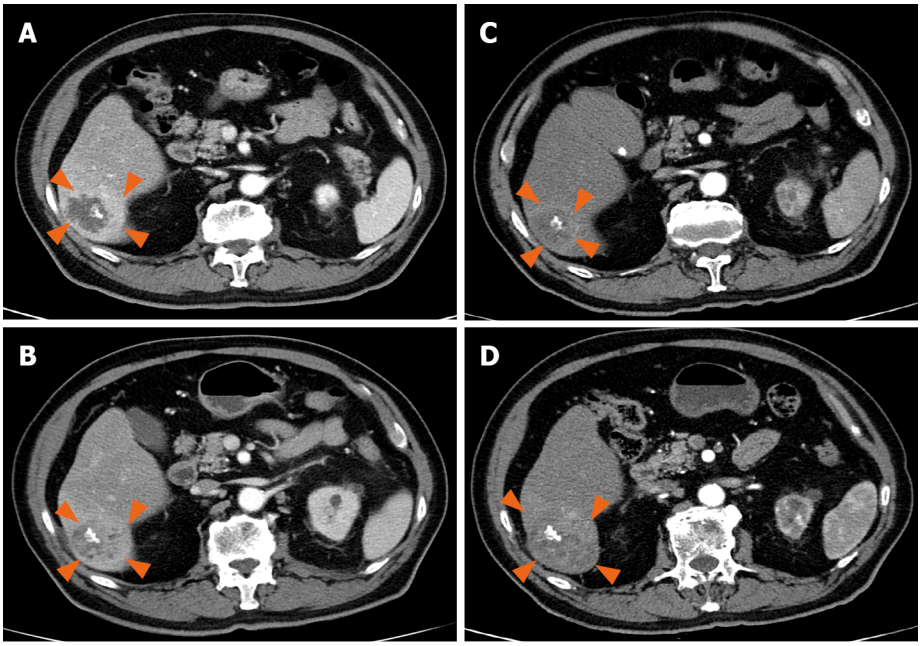

DOI: 10.12998/wjcc.v11.i33.8078 **Copyright** ©The Author(s) 2023.

Figure 1 Liver computed tomography findings. A: On admission day. A lobulated margined multiseptated with central septal calcified 3.9 cm cystic attenuating mass with surrounding prolonged hyperemia in hepatic segment VI; B: Computed tomography (CT) 1 mo later. Still noted was a lobulated margined septated and central calcified cystic attenuating lesion with surrounding high enhancement. The size decreased to 3.3 cm; C: CT at 6 mo. Slightly increased size (from 3.3 cm to 3.6 cm) of the lobulated margined delayed minimal heterogeneous enhancing lesion with surrounding hyperemia, without any interval change in the irregular margined focal central calcification; D: CT at 10 mo. The size of the mass markedly increased to 6 cm.

Imaging examinations

An abdominal CT performed in the Emergency Department revealed a lobulated, margined, multiseptated 3.9 cm cystic attenuating mass with central septal calcification and surrounding prolonged hyperemia in hepatic segment VI, raising our suspicion of an organized liver abscess (Figure 1A).

FURTHER DIAGNOSTIC WORK-UP

A follow-up CT scan four weeks later showed a decrease in the liver lesion size to 3.3 cm (Figure 1B), and CRP dropped to 0.7 mg/L. However, the patient experienced recurrence of high fever, and CRP increased to 14 mg/L. Aspiration of the liver lesion was performed, but no bacteria were identified. Blood culture revealed the presence of *Candida glabrata*. The patient's fever subsided, and CRP decreased following fluconazole administration. The patient received an additional four weeks of antibiotics and antifungal agents (micafungin) before being discharged.

Six months later, the patient returned to the Emergency Department with left upper quadrant pain and decreased urine output. A CT scan revealed a ureter stone and a persistent 3.6 cm liver lesion (Figure 1C). Although biopsy was recommended, the patient's poor condition and lack of size change of the lesion led to a preference for follow-up. Liver magnetic resonance imaging could not be performed due to the patient's pacemaker insertion. Approximately 10 mo later, a CT scan showed an increase in the lesion size to 6 cm (Figure 1D), and biopsy was thus performed. The biopsy revealed an organized abscess with focal carcinomatous changes (Figure 2).

FINAL DIAGNOSIS

HCC presenting as organized liver abscess in patient with cirrhosis of unknown etiology.

TREATMENT

Tumorectomy was performed given the patient’s performance and liver function.

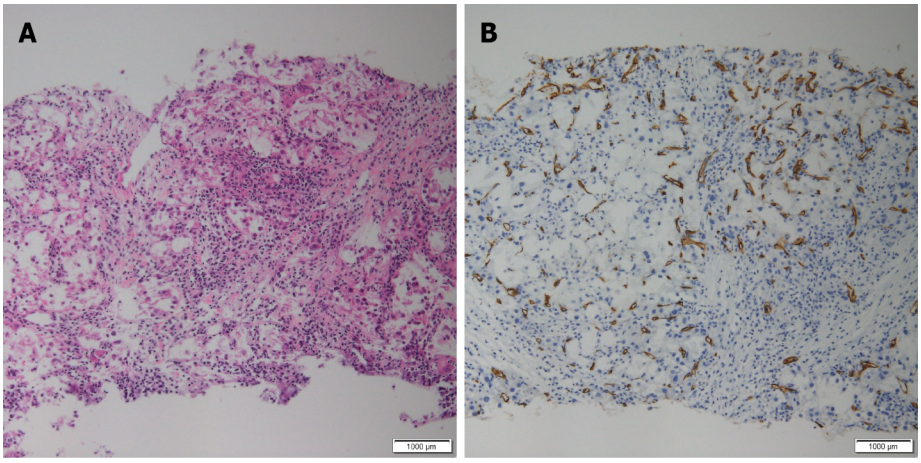

DOI: 10.12998/wjcc.v11.i33.8078 **Copyright** ©The Author(s) 2023.

Figure 2 Liver biopsy histopathological findings. A and B: On H&E staining (A), inflammatory cells and focal carcinomatous changes are observed; some areas show positive staining for CD34 (B).

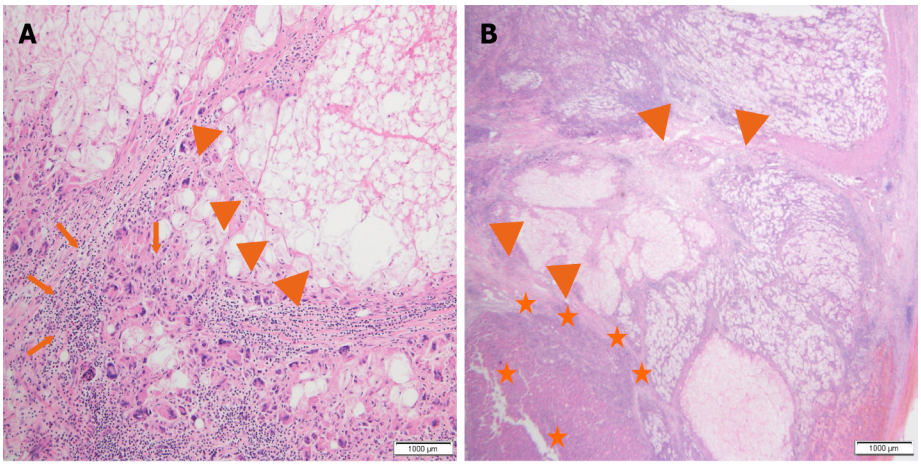

DOI: 10.12998/wjcc.v11.i33.8078 **Copyright** ©The Author(s) 2023.

Figure 3 Postoperative histopathological findings. A and B: A significant portion of the liver parenchyma has undergone necrosis, showing abscess-like features (arrowhead), inflammatory cell infiltration (arrow) and hepatocellular carcinoma tumor cells (star) in the remaining liver parenchyma.

OUTCOME AND FOLLOW-UP

Postoperative histopathological examination revealed a tumor size of 6 cm 5 cm, and the diagnosis was HCC, clear-cell variant. The nontumor liver tissue showed hallmarks of both cirrhosis and abscess. This indicates that the abscess developed in HCC (Figure 3). The patient had multiple intense hypermetabolic enlarged lymph nodes in the common hepatic, portocaval, retrocaval, and SMA root areas on positron emission tomography CT scans performed during surgery. The Barcelona Clinic Liver Cancer stage was C. He is currently undergoing atezolizumab and bevacizumab treatment.

DISCUSSION

HCC is the fifth most common cancer worldwide, though its incidence is higher in countries such as South Korea, where the prevalence of chronic hepatitis B is high[1,2]. HCC ranks second only to lung cancer as a cause of cancer death in Korea, and it has the highest cancer mortality rate among people in their 40s and 50s. The high mortality rate can be attributed to the fact that HCC often occurs in patients with preexisting liver dysfunction, such as cirrhosis, leading to liver failure and death, or because it is diagnosed late because symptoms such as pain are often absent. Therefore, it is recommended that patients with chronic hepatitis or cirrhosis undergo ultrasound and blood tests every six months.

The diagnostic method of HCC varies slightly among countries, but it is mostly performed by radiological examinations. If a liver mass of 1 cm or larger is discovered in patients with chronic hepatitis, cirrhosis, or other underlying liver diseases and if dynamic liver CT or dynamic liver magnetic resonance imaging show arterial enhancement and early

washout in the portal venous or venous phase, a diagnosis can be made without biopsy. In the past, AFP was included in the diagnostic criteria, but it is not included in recent guidelines[3-5]. In this case, the patient had underlying cirrhosis of unknown etiology. However, we did not initially consider HCC, as the findings were more indicative of a liver abscess. Notably, there was calcification inside the tumor in this case. When calcification is identified within a mass, it often leads to the assumption of a benign tumor. Unfortunately, this delayed diagnosis in this patient. It is difficult to find cases in which calcification is present within a mass.

In patients with HCC, fever and increased white blood cell counts can be present in 6%-54% of cases without infection [6-8]. However, the fever is usually low grade, and the increase in white blood cells is not severe. It is more accurate to attribute these symptoms to the tumor itself than to infection. Hypotheses have been put forward to explain these similarities, such as neoplasm-associated granulocytosis resulting from granulopoietin production by tumor cells and pyrogen production by malignant tumor cells or macrophages following tumor necrosis[9,10]. In cases such as this, where sepsis causes low blood pressure, severe leukocytosis, and elevated CRP, it is reasonable to suspect a liver abscess first, even if there is an underlying liver disease such as cirrhosis.

In cases in which a liver abscess is suspected, diagnosis of HCC can be delayed for several reasons. First, the infected necrotic cavities of HCC may appear similar to benign lesions, such as abscesses, on radiological examinations. Second, the presence of calcification in the liver suggests a benign lesion rather than a tumor. Third, if the size of the mass decreases and clinical symptoms improve after antibiotic treatment, the lesion may be a liver abscess, and treatment may continue. Fourth, even if liver biopsy is performed, HCC cells may not be detected due to necrosis or to the abscess, increasing the likelihood of dismissing HCC[11,12].

The mechanism by which HCC with liver abscess arises is thought to be similar to that of liver abscess alone. Bacteria that enter the liver through the blood or bile ducts can form a liver abscess inside the tumor. In cases such as this, where there is a systemic infection caused by urinary tract infection, it is highly likely that bacteria have infiltrated the HCC through the bloodstream. Furthermore, HCC has a rich blood supply and primarily receives blood from the hepatic artery, and thus an infection is more likely to be caused by bacteria from the blood. In such cases, careful attention should be given to the diagnosis of HCC through liver biopsy and other methods while treating liver abscesses. Moreover, even if biopsy results are negative, repeated biopsies may be necessary due to the possibility of false negatives.

Although HCC accompanied by liver abscess is rare, the overall prognosis is known to be poor[6,13]. This is due to both the delay in diagnosis, as in this case, and the fact that treating HCC is complicated when accompanied by a liver abscess. In other words, even if surgery is necessary, the postoperative mortality rate is high because of the accompanying infection, and although RFA and TACE can be performed, a cure is difficult to achieve because the tumor and abscess are mixed, and the risk of postoperative complications increases due to the infection. Therefore, the treatment method must be chosen by considering the patient's overall condition, the size of the tumor, and the state of the liver abscess.

CONCLUSION

When a liver mass is detected in a patient with an underlying liver disease, the possibility of HCC being accompanied by a liver abscess should be considered, even if a liver abscess is suspected or diagnosed. This case report might assist in the diagnosis and treatment of future cases of HCC accompanied by liver abscess.

FOOTNOTES

Author contributions: Kim SB contributed to the study conceptualization; Ryou SH contributed to patient follow-up and monitoring and drafted the original manuscript; Shin HD and Kim SB contributed to reviewing the manuscript and editing; All of the authors critically reviewed the manuscript and approved the final version.

Informed consent statement: Informed written consent was obtained from the patient for publication of this report and any accompanying images.

Conflict-of-interest statement: The authors declare that they have no conflict of interest to disclose.

CARE Checklist (2016) statement: The authors have read the CARE Checklist (2016), and the manuscript was prepared and revised according to the CARE Checklist (2016).

Open-Access: This article is an open-access article that was selected by an in-house editor and fully peer-reviewed by external reviewers. It is distributed in accordance with the Creative Commons Attribution NonCommercial (CC BY-NC 4.0) license, which permits others to distribute, remix, adapt, build upon this work non-commercially, and license their derivative works on different terms, provided the original work is properly cited and the use is non-commercial. See: https://creativecommons.org/Licenses/by-nc/4.0/

Country/Territory of origin: South Korea

ORCID number: Sung Hyeok Ryou 0000-0002-5094-4072; Hyun Deok Shin 0000-0002-2016-4649; Suk Bae Kim 0000-0002-6857-9624.

S-Editor: Lin C

L-Editor: A
P-Editor: Lin C

REFERENCES

1 **Global Burden of Disease Cancer Collaboration**, Fitzmaurice C, Allen C, Barber RM, Barregard L, Bhutta ZA, Brenner H, Dicker DJ, Chimed-Orchir O, Dandona R, Dandona L, Fleming T, Forouzanfar MH, Hancock J, Hay RJ, Hunter-Merrill R, Huynh C, Hosgood HD, Johnson CO, Jonas JB, Khubchandani J, Kumar GA, Kutz M, Lan Q, Larson HJ, Liang X, Lim SS, Lopez AD, MacIntyre MF, Marczak L, Marquez N, Mokdad AH, Pinho C, Pourmalek F, Salomon JA, Sanabria JR, Sandar L, Sartorius B, Schwartz SM, Shackelford KA, Shibuya K, Stanaway J, Steiner C, Sun J, Takahashi K, Vollset SE, Vos T, Wagner JA, Wang H, Westerman R, Zeeb H, Zoeckler L, Abd-Allah F, Ahmed MB, Alabed S, Alam NK, Aldhahri SF, Alem G, Alemayohu MA, Ali R, Al-Raddadi R, Amare A, Amoako Y, Artaman A, Asayesh H, Atnafu N, Awasthi A, Saleem HB, Barac A, Bedi N, Bensenor I, Berhane A, Bernabé E, Betsu B, Binagwaho A, Boneya D, Campos-Nonato I, Castañeda-Orjuela C, Catalá-López F, Chiang P, Chibueze C, Chitheer A, Choi JY, Cowie B, Damtew S, das Neves J, Dey S, Dharmaratne S, Dhillon P, Ding E, Driscoll T, Ekwueme D, Endries AY, Farvid M, Farzadfar F, Fernandes J, Fischer F, G/Hiwot TT, Gebru A, Gopalani S, Hailu A, Horino M, Horita N, Husseini A, Huybrechts I, Inoue M, Islami F, Jakovljevic M, James S, Javanbakht M, Jee SH, Kasaeian A, Kedir MS, Khader YS, Khang YH, Kim D, Leigh J, Linn S, Lunevicius R, El Razek HMA, Malekzadeh R, Malta DC, Marcenes W, Markos D, Melaku YA, Meles KG, Mendoza W, Mengiste DT, Meretoja TJ, Miller TR, Mohammad KA, Mohammadi A, Mohammed S, Moradi-Lakeh M, Nagel G, Nand D, Le Nguyen Q, Nolte S, Ogbo FA, Oladimeji KE, Oren E, Pa M, Park EK, Pereira DM, Plass D, Qorbani M, Radfar A, Rafay A, Rahman M, Rana SM, Søreide K, Satpathy M, Sawhney M, Sepanlou SG, Shaikh MA, She J, Shiue I, Shore HR, Shrime MG, So S, Soneji S, Stathopoulou V, Stroumpoulis K, Sufiyan MB, Sykes BL, Tabarés-Seisdedos R, Tadese F, Tedla BA, Tessema GA, Thakur JS, Tran BX, Ukwaja KN, Uzochukwu BSC, Vlassov VV, Weiderpass E, Wubshet Terefe M, Yebyo HG, Yimam HH, Yonemoto N, Younis MZ, Yu C, Zaidi Z, Zaki MES, Zenebe ZM, Murray CJL, Naghavi M. Global, Regional, and National Cancer Incidence, Mortality, Years of Life Lost, Years Lived With Disability, and Disability-Adjusted Life-years for 32 Cancer Groups, 1990 to 2015: A Systematic Analysis for the Global Burden of Disease Study. *JAMA Oncol* 2017; **3**: 524-548 [PMID: 27918777 DOI: 10.1001/jamaoncol.2016.5688]

2 **Yang JD**, Hainaut P, Gores GJ, Amadou A, Plymoth A, Roberts LR. A global view of hepatocellular carcinoma: trends, risk, prevention and management. *Nat Rev Gastroenterol Hepatol* 2019; **16**: 589-604 [PMID: 31439937 DOI: 10.1038/s41575-019-0186-y]

3 **European Association for the Study of the Liver**. EASL Clinical Practice Guidelines: Management of hepatocellular carcinoma. *J Hepatol* 2018; **69**: 182-236 [PMID: 29628281 DOI: 10.1016/j.jhep.2018.03.019]

4 **Marrero JA**, Kulik LM, Sirlin CB, Zhu AX, Finn RS, Abecassis MM, Roberts LR, Heimbach JK. Diagnosis, Staging, and Management of Hepatocellular Carcinoma: 2018 Practice Guidance by the American Association for the Study of Liver Diseases. *Hepatology* 2018; **68**: 723-750 [PMID: 29624699 DOI: 10.1002/hep.29913]

5 **Korean Association for the Study of the Liver (KASL)**. KASL clinical practice guidelines for management of chronic hepatitis B. *Clin Mol Hepatol* 2022; **28**: 276-331 [PMID: 35430783 DOI: 10.3350/cmh.2022.0084]

6 **Yeh TS**, Jan YY, Jeng LB, Chen TC, Hwang TL, Chen MF. Hepatocellular carcinoma presenting as pyogenic liver abscess: characteristics, diagnosis, and management. *Clin Infect Dis* 1998; **26**: 1224-1226 [PMID: 9597257 DOI: 10.1086/520290]

7 **Kew MC**, Geddes EW. Hepatocellular carcinoma in rural southern African blacks. *Medicine (Baltimore)* 1982; **61**: 98-108 [PMID: 6174843 DOI: 10.1097/00005792-198203000-00004]

8 **Okuda K**, Kondo Y, Nakano M, Kage M, Arakawa M, Kojiro M, Ohtsuki T, Shimokawa Y, Hirata M, Kohno K. Hepatocellular carcinoma presenting with pyrexia and leukocytosis: report of five cases. *Hepatology* 1991; **13**: 695-700 [PMID: 1849115]

9 **Saar B**, Kellner-Weldon F. Radiological diagnosis of hepatocellular carcinoma. *Liver Int* 2008; **28**: 189-199 [PMID: 18251978 DOI: 10.1111/j.1478-3231.2007.01655.x]

10 **Smalley SR**, Moertel CG, Hilton JF, Weiland LH, Weiand HS, Adson MA, Melton LJ 3rd, Batts K. Hepatoma in the noncirrhotic liver. *Cancer* 1988; **62**: 1414-1424 [PMID: 2843280 DOI: 10.1002/1097-0142(19881001)62:7<1414::aid-cncr2820620729>3.0.co;2-7]

11 **Klotz SA**, Penn RL. Clinical differentiation of abscess from neoplasm in newly diagnosed space-occupying lesions of the liver. *South Med J* 1987; **80**: 1537-1541 [PMID: 2827320 DOI: 10.1097/00007611-198712000-00013]

12 **Takayama T**, Makuuchi M, Kojiro M, Lauwers GY, Adams RB, Wilson SR, Jang HJ, Charnsangavej C, Taouli B. Early hepatocellular carcinoma: pathology, imaging, and therapy. *Ann Surg Oncol* 2008; **15**: 972-978 [PMID: 18236118 DOI: 10.1245/s10434-007-9685-0]

13 **Li C**, Li G, Miao R, Lu X, Zhong S, Sang X, Mao Y, Zhao H. Primary liver cancer presenting as pyogenic liver abscess: characteristics, diagnosis, and management. *J Surg Oncol* 2012; **105**: 687-691 [PMID: 21952992 DOI: 10.1002/jso.22103]

World Journal of Clinical Cases

Submit a Manuscript: https://www.f6publishing.com

World J Clin Cases 2023 November 26; 11(33): 8084-8088

DOI: 10.12998/wjcc.v11.i33.8084

ISSN 2307-8960 (online)

CASE REPORT

Generalized granuloma annulare in an infant clinically manifested as papules and atrophic macules: A case report

Dong-Yuan Zhang, Li Zhang, Qin-Yan Yang, Jiazheng Li, Hong-Chao Jiang, Yu-Cheng Xie, Hong Shu

Specialty type: Dermatology

Provenance and peer review: Unsolicited article; Externally peer reviewed.

Peer-review model: Single blind

Peer-review report's scientific quality classification

Grade A (Excellent): 0
Grade B (Very good): B
Grade C (Good): 0
Grade D (Fair): 0
Grade E (Poor): 0

P-Reviewer: Manestar-Blazić T, Croatia

Received: September 14, 2023
Peer-review started: September 14, 2023
First decision: October 17, 2023
Revised: October 28, 2023
Accepted: November 14, 2023
Article in press: November 14, 2023
Published online: November 26, 2023

Dong-Yuan Zhang, Li Zhang, Hong Shu, Department of Dermatology, Kunming Children's Hospital, Kunming 650000, Yunnan Province, China

Qin-Yan Yang, Department of Human Resource, Kunming Children's Hospital, Kunming 650000, Yunnan Province, China

Jiazheng Li, Department of Emergency, The Cooperation of Chinese and Western Medicine Hospital of Yunnan Province, Kunming 650000, Yunnan Province, China

Hong-Chao Jiang, Institute of Pediatric Disease Research in Yunnan, Kunming Children's Hospital, Kunming 650000, Yunnan Province, China

Yu-Cheng Xie, Department of Pathology, Kunming Children's Hospital, Kunming 650000, Yunnan Province, China

Corresponding author: Hong Shu, Doctor, Chief Doctor, Professor, Department of Dermatology, Kunming Children's Hospital, No. 288 Qianxing Road, Xishan District, Kunming 650000, Yunnan Province, China. etyyshuhong@sina.com

Abstract

BACKGROUND

Granuloma annulare (GA) has diverse clinical manifestations including papules, plaques, and nodules on the extremities that are skin-colored, pink, or purple. Approximately 15% of all GA cases are considered generalized GA.

CASE SUMMARY

Herein, we describe the case of a pediatric patient who initially presented with papules and later developed generalized atrophic macules. Upon examination, two different morphologic lesions were histopathologically confirmed: Epithelioid nodular GA and scattered histiocytic infiltrative GA. This patient exhibited rare clinical manifestations that differed throughout the course of the disease. The varying histopathological types and clinical manifestations of GA may be linked to the different stages of the disease.

CONCLUSION

This rare case demonstrates the different histopathological features of different stages and clinical manifestations of granuloma annulare in an infant.

Key Words: Granuloma annulare; infant; Papules; Pitting macule; Epithelioid nodular;

Scattered histiocytic infiltrative; Case report

©The Author(s) 2023. Published by Baishideng Publishing Group Inc. All rights reserved.

Core Tip: Generalized papules were discovered in the early stages of the disease, and the histopathology was epithelioid nodular granuloma annulare (GA). Later in disease progression, the lesions transformed from papules to atrophic macules, and the corresponding histopathology displayed scattered histiocytic infiltrating GA. The clinical manifestations of this case included rare, generalized papules and atrophic maculae. The disease's clinical manifestations varied at different stages, and the corresponding histopathological types differed as well. This suggests that the distinct histopathological types and clinical manifestations of GA may be connected to disease progression.

Citation: Zhang DY, Zhang L, Yang QY, Li J, Jiang HC, Xie YC, Shu H. Generalized granuloma annulare in an infant clinically manifested as papules and atrophic macules: A case report. *World J Clin Cases* 2023; 11(33): 8084-8088
URL: https://www.wjgnet.com/2307-8960/full/v11/i33/8084.htm
DOI: https://dx.doi.org/10.12998/wjcc.v11.i33.8084

INTRODUCTION

Granuloma annulare (GA) is a non-infectious, benign, self-limiting, granulomatous inflammation that typically affects patients aged 3–50 years, with an incidence of approximately 0.04%. Although some small, single-center studies have suggested that GA may be common in children[1-3], the etiology and pathogenesis of this condition are unknown, its clinical manifestations are diverse, and it can present in various forms. GA typically appears as papules, plaques, and nodules on the extremities, with skin-colored, pink, or violaceous hues. However, its diagnosis primarily relies on histopathological examination. The most common form of GA is localized, and generalized GA accounts for only about 15% of all cases[4]. Herein, we describe the case of an infant with the rare primary clinical manifestation of a generalized pitting macule present across the entire body that was histopathologically confirmed as GA.

CASE PRESENTATION

Chief complaints

The patient was a female infant (aged 3 mo and 15 d) who had visited the Department of Dermatology at Kunming Children's Hospital in April 2022 owing to scattered papules and pitting macules on the trunk and limbs that had lasted for more than 10 d.

History of present illness

The child had originally developed papules that ranged in size from approximately 0.1–0.5 cm in diameter with a reddish–light-brown surface and a tough texture on the trunk and limbs without a clear cause. With an absence of subjective symptoms, the number of papules gradually increased and evolved into white pitting macules with a scar-like appearance and normal texture (Figures 1A and B).

History of past illness

No special notes.

Personal and family history

Since the onset of the disease, the child had maintained a normal demeanor and appetite. The patient's history included birth at term, normal postnatal growth and development, normal prenatal examination, and no maternal history of disease during pregnancy. The child had received her first doses of the Bacillus Calmette Guerin (BCG) and hepatitis B vaccines before the onset of GA, following typical vaccination after birth.

Physical examination

There were scattered papules on the limbs and trunk, mostly on the limbs, with a diameter of about 0.1–0.5 cm. These papules had a reddish-light-brown surface and had a tough texture with clear boundaries. The trunk also had pitting macules, which were distributed randomly and appeared as light white scars. The texture of the affected skin appeared normal. (Figures 1A and B).

Laboratory examinations

Tissue samples were obtained from each of the papules and pitting macules for pathological examination. The histopath-

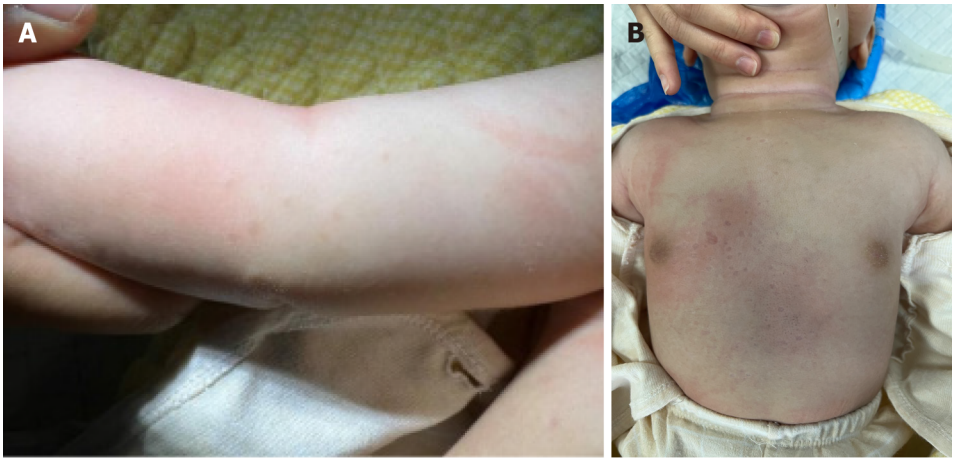

DOI: 10.12998/wjcc.v11.i33.8084 **Copyright** ©The Author(s) 2023.

Figure 1 Clinical manifestation. A: Papules of different sizes scattered on the upper limbs that are reddish and light brown on the surface and firm in texture; B: Scattered pale white pitting macules on the chest and abdomen, resembling scar-like changes in appearance, with normal texture.

ological findings from the papular samples showed focal mild thickening of the epidermis and nested infiltration of lymphocytes, histiocytes, and multinucleated giant cells in the superficial middle dermis. Some collagen was disorganized (Figure 2A). Findings from the pitting macule samples showed approximately normal epidermis; however, the lymphocytes and histiocytes were found to have infiltrated the area between collagen fibers and around blood vessels in the superficial medial dermis, and some collagen fibers were degenerated with widened intervals (Figure 2B). Immunohistochemistry showed the following results: CD1α (+), S-100 (scattered+), langerin (-), Ki-67 (+, 20%), CD163 (+), and CD117 (-). Further, special staining of elastic fibers showed decreased or absent elastic fibers in some areas (Figure 3A and B), and negative alcian blue staining was applied.

Imaging examinations

No special notes.

FINAL DIAGNOSIS

According to their patterns of histiocytic infiltration[2], the papular lesions were histopathologically classified as epithelioid nodular GA, and the scar-like lesions in the depressions as scattered histiocytic infiltrative GA.

TREATMENT

GA is considered to be a self-limiting disease in clinical practice. Therefore, after being fully informed, the parents agreed to observe the progression of the disease for a short term. No treatment was provided, and the patient was advised to return regularly for follow-up.

OUTCOME AND FOLLOW-UP

During follow-up, papular lesions were observed to gradually evolve into pale white, depressed, scar-like lesions that slowly subsided without scarring. On a follow-up visit in September 2022, the skin lesions had largely resolved (Supplementary Figure 1).

DISCUSSION

The etiology of GA is unclear; however, reports suggest a potential association with vaccination[5]. In this case, the previously healthy child had received the BCG and hepatitis B vaccines shortly before disease onset; thus, the relationship between GA and vaccination could not be completely ruled out.

This was a case of generalized GA with the first symptom being scattered papules on the trunk and extremities that gradually evolved into atrophic macules. The untreated skin lesions subsided spontaneously and no scarring remained after healing, which is consistent with the self-limiting nature of this disease.

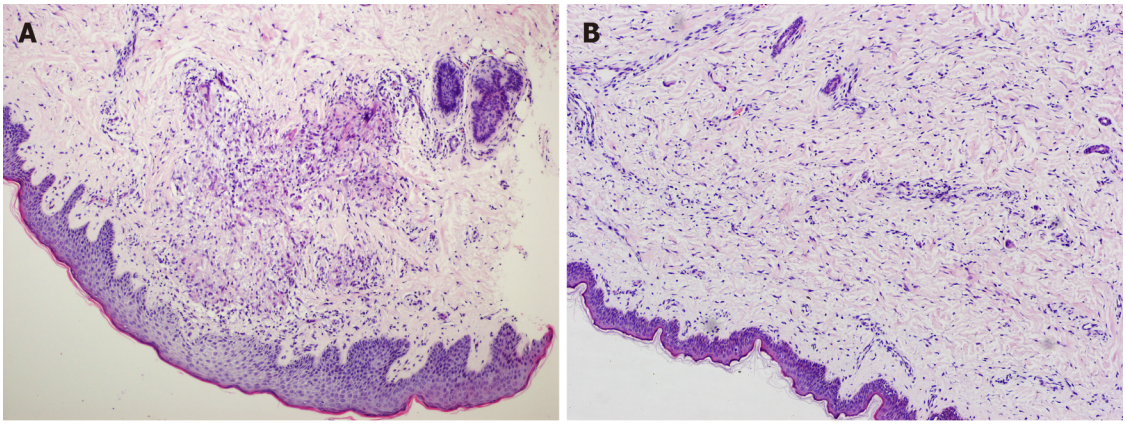

DOI: 10.12998/wjcc.v11.i33.8084 **Copyright** ©The Author(s) 2023.

Figure 2 Images in pathology (hematoxylin and eosin stain). A: Pathological findings of papular lesions (epithelioid nodular granuloma annular (GA); hematoxylin and eosin (HE) ×100): Focal mild thickening of the epidermis and nested infiltration of lymphocytes, histiocytes, and multinucleated giant cells in the superficial and middle dermis, with some collagen disarrangement; B: Pathological findings of scar-like lesions in the depressions (scattered histiocytic infiltrative GA; HE ×100): The epidermis is approximately normal, and lymphocytes and histiocytes have infiltrated between the collagen fibers and around blood vessels in the superficial middle dermis. Some collagen fibers have degenerated, and the intervals are widened.

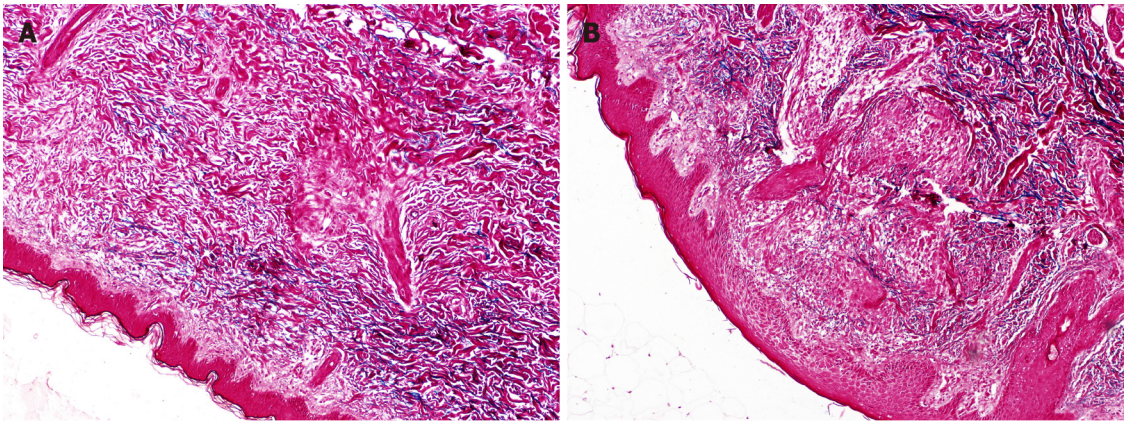

DOI: 10.12998/wjcc.v11.i33.8084 **Copyright** ©The Author(s) 2023.

Figure 3 Images in pathology (elastic fiber stain). A: Elastic fiber staining (×100) in scar-like lesions in the depressions: Elastic fibers have decreased or disappeared; B: Staining of elastic fibers in papular lesions (×100): Elastic fibers have decreased or are absent.

GA has previously been divided into four histopathological types: Scattered histiocytic infiltrative, palisading granuloma, mixed histologic, and epithelioid nodule types[6]. As the patient in this case presented with papules in the early stage of the disease, the type was histopathologically classified as epithelioid nodular GA. While the lesions presented as atrophic macules after resolution of the papules, the child later presented with scattered histiocytic infiltrative GA (with the lesions histopathologically showing decreased cellularity). For this patient, two distinct pathological patterns corresponded to the two lesions, which represented different stages of the disease. Whether the cellular infiltration pattern and pathological type of GA were related to disease stage requires confirmation by future research.

Recent studies have shown that activation of the Th1, Th2, and JAK-STAT pathways are involved in the pathogenesis of GA[7]. In this patient, alcian blue staining was negative in both lesions; however, elastic fibers appeared to dissolve and disappear to approximately the same extent, suggesting there is breakage and phagocytosis of elastic fibers and collagen in the whole disease process of GA. Prospective analysis with larger samples is required to verify this.

However, the analysis and speculation that these events occurred in this particular case require additional prospective and baseline studies.

This suggests that there is breakage and phagocytosis of elastic fibers and collagen in the whole disease process of GA, but the specific mechanism needs more prospective analysis of large samples to verify.

CONCLUSION

The clinical manifestations of GA in children are diverse and vary in different stages of the disease, and GA should be taken into account in children who encounter such generalized and atrophic depression macula in the clinic.

FOOTNOTES

Author contributions: Zhang DY, Zhang L, Jiang HC, and Shu H designed the research; Zhang DY, Zhang L, Yang QY, and Li JZ performed the research; Yang QY, Xie YC, and Jiang HC contributed new reagents/analytic tools; Zhang DY, Yang QY, and Li JZ analyzed the data; Zhang DY and Shu H wrote the paper.

Supported by Spring City Project Famous Doctor Special.

Informed consent statement: The Medical Ethics Committee of Kunming Children's Hospital concluded that the study was ethical and determined that written informed consent was not required.

Conflict-of-interest statement: The authors declare that they have no conflict of interest.

CARE Checklist (2016) statement: The authors have read the CARE Checklist (2016), and the manuscript was prepared and revised according to the CARE Checklist (2016).

Open-Access: This article is an open-access article that was selected by an in-house editor and fully peer-reviewed by external reviewers. It is distributed in accordance with the Creative Commons Attribution NonCommercial (CC BY-NC 4.0) license, which permits others to distribute, remix, adapt, build upon this work non-commercially, and license their derivative works on different terms, provided the original work is properly cited and the use is non-commercial. See: https://creativecommons.org/Licenses/by-nc/4.0/

Country/Territory of origin: China

ORCID number: Dong-Yuan Zhang 0000-0003-2353-5879; Li Zhang 0000-0002-8359-2595; Qin-Yan Yang 0000-0001-8331-0183; Jia-Zheng Li 0009-0002-3089-6170; Hong-Chao Jiang 0000-0003-3900-1556; Yu-Cheng Xie 0009-0005-4813-3915; Hong Shu 0000-0002-0187-2113.

S-Editor: Liu JH
L-Editor: A
P-Editor: Liu JH

REFERENCES

1 **Barbieri JS**, Rodriguez O, Rosenbach M, Margolis D. Incidence and Prevalence of Granuloma Annulare in the United States. *JAMA Dermatol* 2021; **157**: 824-830 [PMID: 34106215 DOI: 10.1001/jamadermatol.2021.1847]

2 **Joshi TP**, Duvic M. Granuloma Annulare: An Updated Review of Epidemiology, Pathogenesis, and Treatment Options. *Am J Clin Dermatol* 2022; **23**: 37-50 [PMID: 34495491 DOI: 10.1007/s40257-021-00636-1]

3 **Leasure AC**, Damsky W, Cohen JM. Prevalence of granuloma annulare in the United States: a cross-sectional study in the All of Us Research Program. *Int J Dermatol* 2022; **61**: e301-e302 [PMID: 34363612 DOI: 10.1111/ijd.15832]

4 **Ehret M**, Lenormand C, Scrivener JN, Gusdorf L, Lipsker D, Cribier B. [Generalized granuloma annulare: A clinicopathological study]. *Ann Dermatol Venereol* 2020; **147**: 271-278 [PMID: 32171551 DOI: 10.1016/j.annder.2019.09.617]

5 **García-Gil MF**, Álvarez-Salafranca M, Martínez García A, Ara-Martín M. Generalized granuloma annulare after pneumococcal vaccination. *An Bras Dermatol* 2021; **96**: 59-63 [PMID: 33267970 DOI: 10.1016/j.abd.2020.05.009]

6 **Friedman-Birnbaum R**, Weltfriend S, Munichor M, Lichtig C. A comparative histopathologic study of generalized and localized granuloma annulare. *Am J Dermatopathol* 1989; **11**: 144-148 [PMID: 2712247 DOI: 10.1097/00000372-198911020-00006]

7 **Min MS**, Wu J, He H, Sanz-Cabanillas JL, Del Duca E, Zhang N, Renert-Yuval Y, Pavel AB, Lebwohl M, Guttman-Yassky E. Granuloma annulare skin profile shows activation of T-helper cell type 1, T-helper cell type 2, and Janus kinase pathways. *J Am Acad Dermatol* 2020; **83**: 63-70 [PMID: 31870914 DOI: 10.1016/j.jaad.2019.12.028]

World Journal of Clinical Cases

Submit a Manuscript: https://www.f6publishing.com

World J Clin Cases 2023 November 26; 11(33): 8089-8093

DOI: 10.12998/wjcc.v11.i33.8089

ISSN 2307-8960 (online)

CASE REPORT

Successful leadless pacemaker implantation in a patient with dextroversion of the heart: A case report

Na Li, Hai-Xiong Wang, Yue-Hui Sun, Yan Shu

Specialty type: Cardiac and cardiovascular systems

Provenance and peer review: Unsolicited article; Externally peer reviewed.

Peer-review model: Single blind

Peer-review report's scientific quality classification

Grade A (Excellent): 0
Grade B (Very good): B
Grade C (Good): 0
Grade D (Fair): 0
Grade E (Poor): 0

P-Reviewer: Sutton R, United Kingdom

Received: September 19, 2023
Peer-review started: September 19, 2023
First decision: October 17, 2023
Revised: October 22, 2023
Accepted: November 14, 2023
Article in press: November 14, 2023
Published online: November 26, 2023

Na Li, Hai-Xiong Wang, Yue-Hui Sun, Yan Shu, Department of Cardiology, Shanxi Cardiovascular Hospital, Taiyuan 030000, Shanxi Province, China

Corresponding author: Yan Shu, Doctor, PhD, Chief Pharmacist, Department of Cardiology, Shanxi Cardiovascular Hospital, No. 18 Yifen Street, Taiyuan 030000, Shanxi Province, China. shuyan20230919@163.com

Abstract

BACKGROUND

Dextroversion is defined as the presence of dextrocardia with situs solitus, dextro-loop ventricles, and normally related great arteries. Dextrocardia can pose technical challenges when interventional treatments are required. However, the challenges posed by dextroversion can be amplified due to the disruption of typical anatomical relationships, the unpredictable positioning and boundaries of cardiac structures resulting from the shift, and the pathological processes influencing rotation.

CASE SUMMARY

A 73-year-old woman with cardiac dextroversion suffered from a recurrence of atrial fibrillation after her radiofrequency catheter ablation and Despite the cessation of antiarrhythmic medications, there were episodes of sinus pauses and symptomatic bradycardia, with heart rates dropping as low as 28 beats per minute.

CONCLUSION

Dextroversion makes the implantation of leadless pacemakers more challenging, and appropriate adjustments in fluoroscope angles may be crucial for intracardiac operations. Additionally, when advancing delivery systems, attention should be paid to rotational direction during valve-crossing procedures; changes in the perspective of posture angle between normal cardiac position and dextroversion can serve as references.

Key Words: Leadless pacemaker; Dextroversion; Pacemaker implantation; Case report

©The Author(s) 2023. Published by Baishideng Publishing Group Inc. All rights reserved.

Core Tip: Dextroversion can be even more challenging given the distortion of normal anatomical relationships and the uncertainty of the accurate location and borders of the cardiac structures caused by the shift and rotation effected by the pathologic process. We present a complicated but successful case of implantation of a leadless pacemaker in a patient with cardiac dextroversion.

Citation: Li N, Wang HX, Sun YH, Shu Y. Successful leadless pacemaker implantation in a patient with dextroversion of the heart: A case report. *World J Clin Cases* 2023; 11(33): 8089-8093
URL: https://www.wjgnet.com/2307-8960/full/v11/i33/8089.htm
DOI: https://dx.doi.org/10.12998/wjcc.v11.i33.8089

INTRODUCTION

Abnormal heart structures complicate cardiac electrophysiology operative treatment, especially the implantation of devices like leadless pacemakers. It is primarily because the tools provided by manufacturers have not been sufficiently designed or tested for rare abnormal structures. Thus, implementing these delivery systems in intricately structured cases can be demanding or necessitate a level of innovation. The literature presents scarce accounts concerning the installation of leadless pacemakers in patients having dextrocardia[1-3]. Dextrocardia, a scarcely occurring inborn anomaly in the general population, is estimated to occur in 1 out of every 12000 live births, and it might be linked with substantial supplementary cardiac deformities[4]. The incidence of dextrocardia is evenly distributed between males and females at a ratio of 1:1. In cases of dextrocardia, the positioning of abdominal organs may be normal (situs solitus), reversed (situs inversus), or indeterminate (situs ambiguous or isomerism) in respective proportions of 32%-35%, 35%-39%, and 26%-28%[4,5]. Dextroversion is characterized by a right-sided cardiac placement with a rightward cardiac apex in the context of situs solitus. Unlike situs inversus, where the arrangement of the visceroatrial mirrors the typical layout, dextroversion features the conventional positioning of the tracheobronchial tree and abdominal organs[6].

The hominine embryonicheart originates from a rudimentary cardiac tube that has the sinus venosus, atrium, ventricle, bulbus cordis, and arterial trunks lined up in sequence. The end of veins and arteries are stationary. The atriums and veins return develop concurrently, thus anchoring the atria in place *via* the inflowing veins. The growth of the bulboventricular loop causes the cardiac tube to bend, creating morphological-biventricular chamber. This process does not impact position of the atria, which continues to correspond with the lacation of te internal organs[7,8]. During the initial phases of fetal development, situs solitus and the establishment of the dextro-loop take place, positioning the heart's apex within the right hemithorax. In the initial four weeks of the newborn's lifetime, the tip of heart transitions from the right thoracic cavity to the left half of the chest. Despite of the auricular positon, every dextro-bulboventricular loop ought to complete their advancement with the heart in the left half of the chest.

Dextroversion can be congenital as well as acquired. The former is due to defeat of the ultimate leftward shift of biventricular chambers duringthe process of embryogenesis. Although the morphologic right atrium and right ventricle are still located on the right side, they are positioned behind the corresponding left atrium. In this case, the right rotation of the heart was caused by mechanical morphological compression of the left diaphragm due to obvious elevation, which was considered to be related to phrenic nerve palsy after previous radiofrequency catheter ablation. Owing to the fact that the apex is towards the right with situs solitus, the cardiac shift in the thoracic cavity to the right causes changes in veinal junctions and also alters the dissecting associations among each vessel, the right heart system.This distortion, coupled with the variations among patients, makes it highly demanding to implement procedures of the heart. Furthermore, literatures provide scant reports on operation of leadless pacemaker in sufferers who have dextrocardia[2,3,9]. At present, this is the first case of leadless pacemaker implantation in a patient with dextroversion of the heart.

CASE PRESENTATION

Chief complaints

A 73-year-old woman was suffered from sinus pauses and symptomatic bradycardia (as low as 28 beats per minute) even after the cessation of antiarrhythmic drugs.

History of present illness

The patient experienced a relapse of atrial fibrillation and subsequently arrived at an external hospital exhibiting episodes of sinus pauses and symptomatic bradycardia (down to 28 beats per minute), even after ceasing the use of antiarrhythmic drugs.

History of past illness

The patient had a history of transient ischemic attack and severely symptomatic paroxysmal atrial fibrillation for 20 years with a history of radiofrequency catheter ablation and left atrial appendage closure in 2019. Initially, the left atrial appendage was occluded, succeeded by the implementation of pulmonary vein isolation (PVI). The placement of the

Watchman device was successfully affirmed with no remaining flow. Subsequently, PVI was executed utilizing radiofrequency ablation. The blockage of both ingress and egress was substantiated in all veins]. And she suffered from dextroversion, which was proved by chest X-ray and Echocardiography.

Personal and family history

This case had no specific personal or family history.

Physical examination

No abnormalities were detected in the physical examination.

Laboratory examinations

All laboratory tests were normal.

Imaging examinations

A chest X-ray verified the presence of a cardiac shadow on the right side, with the apex of the heart orientated towards the right. However, there was no evidence of an expanded cardiac silhouette. The mediastinum was centrally positioned, with the liver's shadow on the right aligning with situs solitus. Furthermore, the left hemidiaphragm displayed at a level higher than its right counterpart. Echocardiography indicated a dextro-loop configuration in ventricular morphology, accompanied by a right-oriented cardiac axis and a ventricular apex directed towards the right.

FINAL DIAGNOSIS

The patient had a history of transient ischemic attack and severely symptomatic paroxysmal atrial fibrillation for 20 years with a history of radiofrequency catheter ablation and left atrial appendage closure in 2019. Then she experienced a relapse of atrial fibrillation and had episodes of sinus pauses and symptomatic bradycardia (down to 28 beats per minute), even after ceasing the use of antiarrhythmic drugs.

TREATMENT

Right femoral venous access was secured under fluoroscopic guidance using a micro-puncture needle. A lengthy Amplatz stiff guidewire was threaded and pushed forward through the micro-puncture sheath, in anticipation of the Micra implantation. Fluoroscopic assessment of the guidewire in the thoracic area revealed the cordis image in the right half of chest (Figure 1A). Owing to the dextroversion, a quadripolar lead wire (F5QD252RT, Biosense Webster, CA, United States) was advanced to the heart to seek an optimal exposure angle (Figure 1B and C). Then, the right anterior oblique view of 45° and left anterior oblique view of 15° were applied by the electrophysiologist to give assistance in order to be more safer and precisein placement of the Medtronic Micra leadless pacemaker. Under fluoroscopic guidance, the pacemaker introducer sheath and delivery system were respectively positioned in the right atrium and right ventricle. Concurrently, the Micra was embedded in the right ventricle septum (Figure 2). Once the stability and electrical thresholds were confirmed, the Micrawas released from the catheter. The pacemaker was functioning properly, and its R wave is 8.0 mV, impedance is 840 ohms, and capture threshold is 0.8 V @0.24 ms.

OUTCOME AND FOLLOW-UP

In the instance, no prolonged complications were noted. The device function was appropriate at 3 mo, 6 mo and 12 mo following Micra leadless pacemaker placement.

DISCUSSION

In the conventional position of the heart, we usually use a right anterior oblique 30° and left anterior oblique 45° to determine the relative position between the delivery system and leadless pacemaker with the interventricular septum. However, due to the dextroversion in this patient, the fluoroscope angle needed to be adjusted accordingly based on anatomical distortion. In this case, a reference was made by placing a quadripolar lead wire in the right ventricular for pre-operation. This helped determine the optimal angle for exposing the delivery system and interventricular septum, which was a right anterior oblique 45° and left anterior oblique 15°. When crossing over the tricuspid valve, an additional counterclockwise rotation angle was required; while after the crossing-over, there was relatively less clockwise rotation compared to when in a normal cardiac position. Owing to the relatively sharp angular torque compared to conventional anatomical structures and the correspondingly reduced coaxiality generated in the delivery system rooting in the complicated anatomical structure, the severed tethers were discovered to be tight. Thus, utmost caution needed to be taken in removing the tethers in order to avoid negative impacts on pacemaker fixation during the release process.

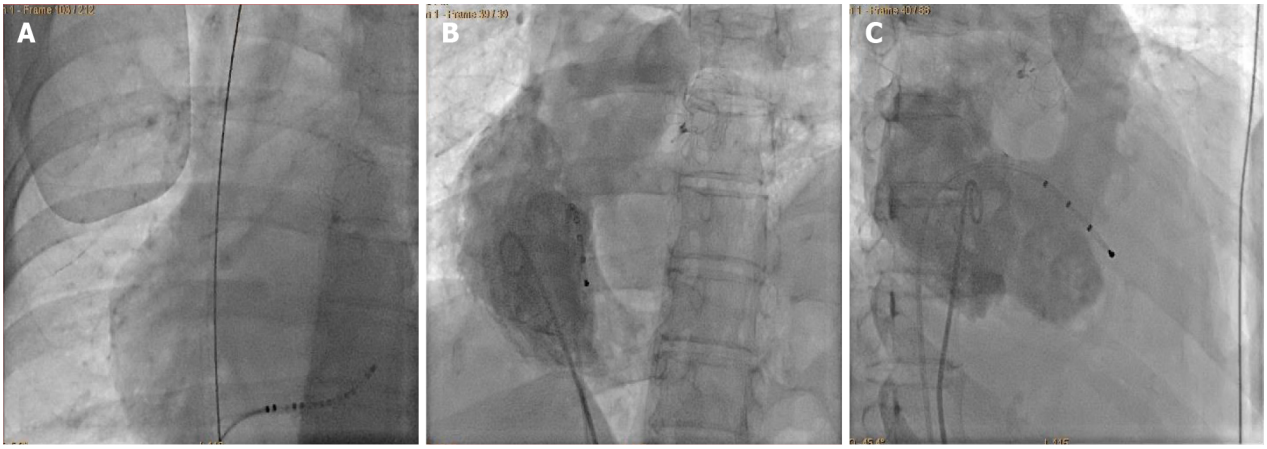

DOI: 10.12998/wjcc.v11.i33.8089 **Copyright** ©The Author(s) 2023.

Figure 1 Fluoroscopy location and optimal exposure angles for treatment. A: The Amplatz stiff guidewire in the right hemithorax, demonstrating the right-sided position of the heart; B: Quadripolar lead wire, left anterior oblique view of 15°; C: Quadripolar lead wire, right anterior oblique view of 45°.

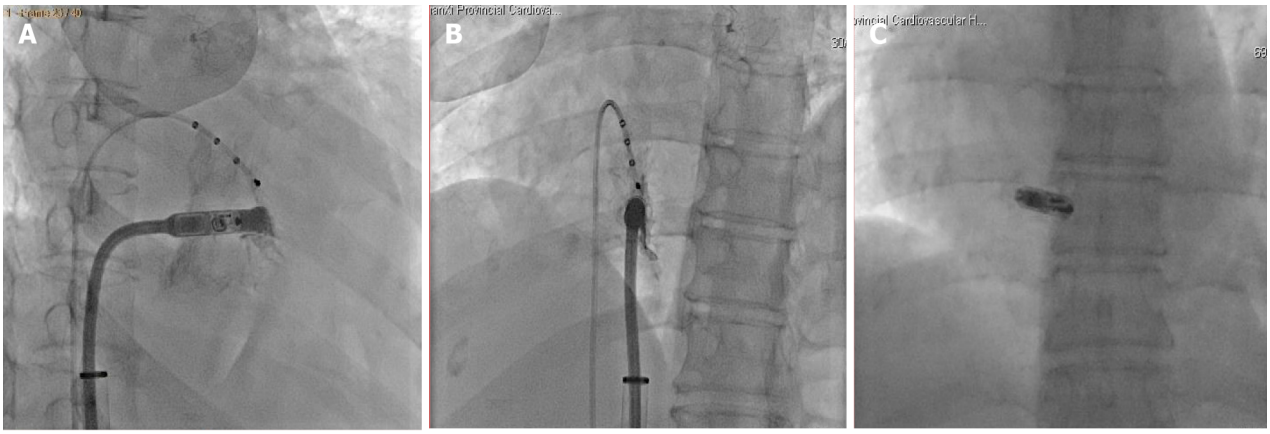

DOI: 10.12998/wjcc.v11.i33.8089 **Copyright** ©The Author(s) 2023.

Figure 2 Fluoroscopy. Implantation of Micra. A: Micra (Medtronic Inc., Minneapolis, MN, United States) sheath injection and septal staining with contrast injection of the right anterior oblique view of 45; B: Micra sheath injection and septal staining with contrast injection of left anterior oblique view of 15; C: Zoomed-in anteroposterior view.

CONCLUSION

Dextroversion makes the implantation of leadless pacemakers more challenging, and appropriate adjustments in fluoroscope angles may be crucial for intracardiac operations. Additionally, when advancing delivery systems, attention should be paid to rotational direction during valve-crossing procedures; changes in the perspective of posture angle between normal cardiac position and dextroversion can serve as references. This case study reports the successful implantation of a leadless pacemaker in a patient with dextroversion and provides invaluable clinical experience for the development of a relevant therapeutic regimen.

FOOTNOTES

Co-first authors: Na Li and Yue-Hui Sun.

Co-corresponding authors: Yan Shu and Hai-Xiong Wang.

Author contributions: Shu Y and Wang HX made an equal contribution to this work, and were responsible for the design of the research study; Li N and Sun YH analyzed the data and wrote the manuscript; Every author has reviewed and given their approval to the final draft of the manuscript.

Supported by Shanxi Provincial Health Commission "Four batch" Science and Technology Innovation Project of Medical Development, No. 2021XM45; Natural Science Foundation of Shanxi Province, No. 20210302123346; Scientific Research Incentive Fund of Shanxi Cardiovascular Hospital, No. XYS20220205; and Traditional Chinese Medicine research project of Shanxi Province, No. 2023ZYYA028.

Informed consent statement: All study participants, or their legal guardian, provided informed written consent prior to study enrollment.

Conflict-of-interest statement: All the authors have no conflicts of interest to declare.

CARE Checklist (2016) statement: The authors have read the CARE Checklist (2016), and the manuscript was prepared and revised according to the CARE Checklist (2016).

Open-Access: This article is an open-access article that was selected by an in-house editor and fully peer-reviewed by external reviewers. It is distributed in accordance with the Creative Commons Attribution NonCommercial (CC BY-NC 4.0) license, which permits others to distribute, remix, adapt, build upon this work non-commercially, and license their derivative works on different terms, provided the original work is properly cited and the use is non-commercial. See: https://creativecommons.org/Licenses/by-nc/4.0/

Country/Territory of origin: China

ORCID number: Na Li 0000-0003-4213-0463; Hai-Xiong Wang 0000-0001-9905-7899; Yue-Hui Sun 0009-0006-6748-9674; Yan Shu 0009-0008-3727-049X.

S-Editor: Liu JH
L-Editor: A
P-Editor: Liu JH

REFERENCES

1 **Buxton AE**, Morganroth J, Josephson ME, Perloff JK, Shelburne JC. Isolated dextroversion of the heart with asymmetric septal hypertrophy. *Am Heart J* 1976; **92**: 785-790 [PMID: 136888 DOI: 10.1016/S0002-8703(76)80017-8]
2 **Shenthar J**, Rai MK, Walia R, Ghanta S, Sreekumar P, Reddy SS. Transvenous permanent pacemaker implantation in dextrocardia: technique, challenges, outcome, and a brief review of literature. *Europace* 2014; **16**: 1327-1333 [PMID: 24591676 DOI: 10.1093/europace/euu024]
3 **De Regibus V**, Pardeo A, Artale P, Petretta A, Filannino P, Iacopino S. Leadless pacemaker implantation after transcatheter lead extraction in complex anatomy patient. *Clin Case Rep* 2018; **6**: 1106-1108 [PMID: 29881575 DOI: 10.1002/ccr3.1532]
4 **Bohun CM**, Potts JE, Casey BM, Sandor GG. A population-based study of cardiac malformations and outcomes associated with dextrocardia. *Am J Cardiol* 2007; **100**: 305-309 [PMID: 17631088 DOI: 10.1016/j.amjcard.2007.02.095]
5 **Garg N**, Agarwal BL, Modi N, Radhakrishnan S, Sinha N. Dextrocardia: an analysis of cardiac structures in 125 patients. *Int J Cardiol* 2003; **88**: 143-55; discussion 155 [PMID: 12714192 DOI: 10.1016/s0167-5273(02)00539-9]
6 **Tripathi S**, Ajit Kumar VK. Comparison of Morphologic Findings in Patients with Dextrocardia with Situs Solitus vs Situs Inversus: a Retrospective Study. *Pediatr Cardiol* 2019; **40**: 302-309 [PMID: 30334087 DOI: 10.1007/s00246-018-2007-4]
7 **Vanpraagh R**, Vanpraagh S, Vlad P, Keith JD. Anatomic types of congenital dextrocardia: Diagnostic and embryologic implications. *Am J Cardiol* 1964; **13**: 510-531 [PMID: 14136294 DOI: 10.1016/0002-9149(64)90159-6]
8 **Applegate KE**, Goske MJ, Pierce G, Murphy D. Situs revisited: imaging of the heterotaxy syndrome. *Radiographics* 1999; **19**: 837-52; discussion 853 [PMID: 10464794 DOI: 10.1148/radiographics.19.4.g99jl31837]
9 **Conti S**, Sgarito G. Leadless pacemaker implantation in postpneumonectomy syndrome. *HeartRhythm Case Rep* 2020; **6**: 124-125 [PMID: 32181128 DOI: 10.1016/j.hrcr.2019.11.005]

Published by **Baishideng Publishing Group Inc**
7041 Koll Center Parkway, Suite 160, Pleasanton, CA 94566, USA
Telephone: +1-925-3991568
E-mail: bpgoffice@wjgnet.com
Help Desk: https://www.f6publishing.com/helpdesk
https://www.wjgnet.com

© 2023 Baishideng Publishing Group Inc. All rights reserved.